Fraunhofer
IBP

FRAUNHOFER-INSTITUT FÜR BAUPHYSIK IBP

Herena Torío Blanco

Comparison and optimization of building energy supply systems through exergy analysis and its perspectives

FORSCHUNGSERGEBNISSE AUS DER BAUPHYSIK BAND 11

Herausgeber:
Prof. Dr.-Ing. Klaus Sedlbauer
Prof. Dr.-Ing. Gerd Hauser

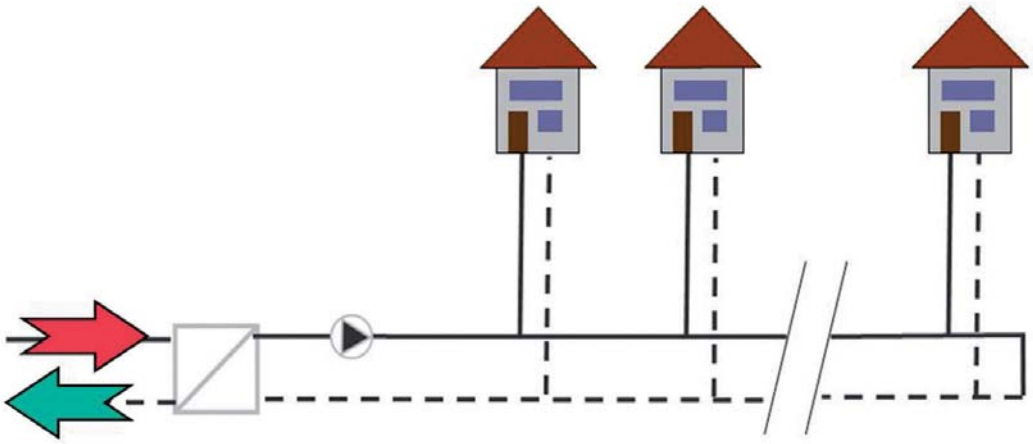

Universität Stuttgart
Lehrstuhl für Bauphysik

Technische Universität München
Lehrstuhl für Bauphysik

FRAUNHOFER VERLAG

Fraunhofer IBP

Universität Stuttgart
Lehrstuhl für Bauphysik

Technische Universität München

FORSCHUNGSERGEBNISSE AUS DER BAUPHYSIK BAND 11
Herausgeber: Prof. Dr.-Ing. Klaus Sedlbauer
Prof. Dr.-Ing. Gerd Hauser

Herena Torío Blanco

Comparison and optimization of building energy supply systems through exergy analysis and its perspectives

FRAUNHOFER VERLAG

Contact:
Fraunhofer-Institut für Bauphysik IBP
Nobelstraße 12
70569 Stuttgart
Phone 0711 970-00
Fax 0711 970-3395
E-Mail info@ibp.fraunhofer.de
URL www.ibp.fraunhofer.de

Bibliographic information published by Die Deutsche Bibliothek
Die Deutsche Bibliothek lists this publication in the Deutsche Nationalbibliografie; detailed bibliografic data is available in the Internet at <http://dnb.d-nb.de>.
ISBN: 978-3-8396-0452-6

D 91

Zugl.: München, TU, Diss., 2012

Printing and Bindery:
Mediendienstleistungen des
Fraunhofer-Informationszentrum Raum und Bau IRB, Stuttgart

Printed on acid-free and chlorine-free bleached paper.

Fraunhofer Information-Centre for Regional Planning and Building Construction IRB
P.O. Box 80 04 69, D-70504 Stuttgart
Nobelstrasse 12, D-70569 Stuttgart
Phone +49 (0) 711 970-2500
Fax +49 (0) 711 970-2508
E-Mail verlag@fraunhofer.de
URL http://verlag.fraunhofer.de

TECHNISCHE UNIVERSITÄT MÜNCHEN
Lehrstuhl für Bauphysik

Comparison and optimization of building energy supply systems through exergy analysis and its perspectives

Herena Torío Blanco

Vollständiger Abdruck der von der Fakultät für Bauingenieur- und Vermessungswesen der Technischen Universität München zur Erlangung des akademischen Grades eines

Doktors-Ingenieur (Dr.-Ing.)

genehmigten Dissertation

Vorsitzender:	Univ.-Prof. Dr.-Ing. Werner Lang
Prüfer der Dissertation:	1. Univ.- Prof. Dr.-Ing. Gerd Hauser
	2. Univ.- Prof. Dr.-Ing. Anton Maas Universität Kassel

Die Dissertation wurde am 07.11.2011 bei der Technischen Universität München eingereicht und durch die Fakultät für Bauingenieur- und Vermessungswesen am 18.06.2012 angenommen.

Abstract

Growing concerns on environmental problems related to current energy use, such as global warming, have emphasized the importance of "energy saving measures" and the necessity for an increased efficiency in all forms of energy utilization. Being responsible for around 40% of the final energy use in Germany, buildings are major contributors to energy related problems and a sector where a more rational and efficient energy use is absolutely necessary.

By showing the thermodynamic efficiency of an energy system, exergy analysis is expected to be a valuable tool for developing and designing more efficient energy supply systems in buildings, similarly as it has contributed to raise the efficiency of power plants. In this thesis, the usability and added value of exergy analysis applied to different building energy systems is investigated. Exergy analysis is, herefore, compared to conventional primary energy assessment and the different results and conclusions obtained from both methods are thoroughly studied and discussed.

The targets of exergy analysis applied to power plants and buildings are very different. In consequence, many of the simplifications and assumptions allowed for power plant analysis are reviewed and adapted here for exergy analysis of building systems. Dynamic exergy and energy analysis are, then, performed on a large solar thermal system and a waste district heating system for space heating and domestic hot water supply. These systems are characterized by different shares of high exergy inputs in their supply. In consequence, it is possible to extrapolate obtained results to other building systems of similar characteristics.

In this thesis it is shown that exergy analysis is strongly dominated by the high-quality fossil fuel input, similarly as conventional (primary) energy analysis. Thus, for energy systems with a great share of high quality energy sources in their supply, such as the solar systems analyzed here, conclusions from exergy analysis are always very similarly to those which can be gained from conventional energy analysis. This can also be extrapolated to other energy systems with the same characteristics, such as heat pumps.

In turn, for energy systems with great shares of low exergy flows in their supply, exergy analysis provides further insight than mere conventional energy assessment. This is the case of waste heat based district heating systems. A combined primary energy and exergy analysis allows highlighting the importance of increasing the use of waste heat for heat supply in buildings, besides that of increasing the electrical efficiency of CHP units. In district energy systems for communities or neighbourhoods where waste heat from different processes at

different temperature levels is available, exergy analysis can help to pinpoint the most efficient supply option by promoting cascaded and multiple use of thermal energy flows.

Acknowledgement

This thesis would not have been possible without the help, patience, guidance and support of many people. It is to them that I owe my deepest gratitude.

First of all, I am truly thankful to my supervisor Tekn. Dr. Dietrich Schmidt for his nice way of giving me support and guidance. Thanks for being always ready to discuss - even at late afterwork hours -, for the competent help and for granting the necessary freedom to carry scientific work on my own.

Thanks to Prof. Gerd Hauser and Prof. Anton Maas for being willing to supervise this thesis and for their valuable remarks and contributions.

I owe sincere thankfulness to the Annex 49 working group for the lively and inspiring discussions. Particularly, I would like to thank Dr. Adriana Angelotti for her insightful and clarifying comments and Prof. Masanori Shukuya for being always ready to answer my questions. I also deeply thank Sabine Jansen for the endless motivating and instructive discussions on thermodynamics.

I would like to thank all my colleagues at the Department of Energy Systems of the Fraunhofer Institute for Building Physics, the ZUB and the University of Kassel for their support and readiness to answer all my questions and for making possible to join fun and work every day. Special thanks go to Dr. Michael Krause, Christina Sager, Jan Kaiser and Andrea Schneider for their useful comments, elucidating discussions and help in technical issues.

Thanks to Iván and my mother for believing in me and for their unconditional support and patience. Thanks to all the friends who always supported and encouraged me to continue in the difficult times. Special thanks to Corry for her careful and patient listening and her advice during this years.

Last but not least, I thank the German Federal Foundation for Environment and the German Federal Ministry of Economy and Technology for their financial support.

Contents

Chapter 1

Introduction

1.1 Background

The built environment is responsible for around 40% of the final energy use in Germany [Hauser, 2008]. Space Heating (SH) and Cooling (SHC) and Domestic Hot Water (DHW) represent the biggest share of energy demands in residential buildings. To satisfy these thermal energy demands, mainly fossil fuels are used [Erhorn et al., 2008], causing large CO_2 emissions and making buildings major contributors to energy related problems. A more rational and efficient energy use in this sector is, thus, absolutely necessary.

Current analysis and optimization methods of energy use in buildings are based on the assessment of primary energy flows [EnEV, 2009; DIN 18599, 2007], where all energy conversion steps from the extraction of energy sources (e.g. fuels) to the final demands to be supplied are assessed. The primary energy approach aims at limiting the use of fossil fuels for providing a given demand, leading to reduce energy demands and maximize the use of renewable energy sources. It is based, thus, on a distinction between renewable and fossil energy sources, being renewable energy flows often not included in the final assessment. Thereby, an assessment of the efficiency of renewable energy use cannot be obtained from such analyses.

Primary energy analyses are based on the first law of thermodynamics, i.e. on balancing the energy quantity. This means that the quantity of energy supplied is matched with the quantity of energy required. Highly efficient condensing boilers, with efficiencies of up to 98% are a straightforward result of such an analysis framework.

The quality of energy is given, in turn, by a combined analysis of the first and second laws of thermodynamics. From these combined analyses, the thermodynamic concept of exergy is derived. Exergy represents the part of an energy flow which can be completely transformed into any other form of energy, thereby depicting the potential of a given energy quantity to perform work. In every energy system, some part of the exergy supplied to the system in question has to be consumed or destroyed during its operation. In the case of highly efficient boilers used to supply low temperature heat, the potential of the fuels fed into the boiler is almost completely lost in the burning process. Exergy efficiencies for such building systems

are lower than 10%, being, from an exergy perspective, a very unappropriate option to supply energy demands in buildings.

Low temperature energy demands have low quality, i.e. low exergy content, as it is shown in the first bars of Figure 1.1[1](labeled as *Demand*). Substituting the fossil fueled boiler by a pellet boiler would allow a greatly renewable supply of SH and DHW energy demands, thereby reducing largely (fossil) primary energy input. In terms of exergy, though, wood is a high quality energy source which is being used to supply low exergy demands. As a result, the exergy efficiency of such a supply system would still be lower than 10%. Exergy analysis shows, thereby, clearly the importance of moving away from direct burning processes for supplying thermal energy demands in buildings, bringing additional information to conventional primary energy analysis.

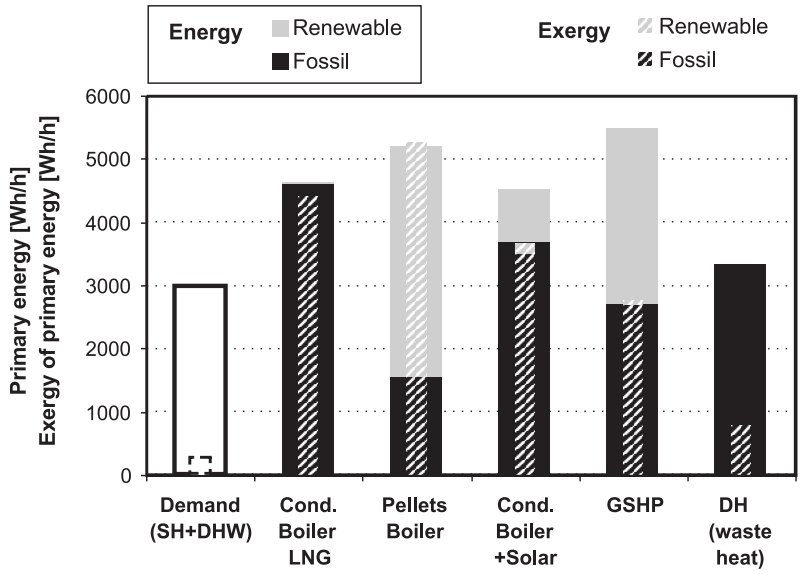

Figure 1.1: Energy (continuous line) and exergy (dashed line) demand of a single family house (first bars labeled as *Demand (SH+DHW)*). Renewable (light grey) and fossil (black) energy (filled bars) and exergy (striped bars) supplied for different building systems. *Cond.* stands for *condensing*, *LNG* stands for *Liquefied Natural Gas*, *GSHP* stands for *Ground Source Heat Pump* and *DH* stands for *District Heat*.

Exergy analysis is a complex thermodynamic method well established and applied since the early 1970s for power plant analysis with the aim of increasing its efficiency. After a period during which most scientific efforts were concentrated on energy analysis and CO_2 emission balances, in the last years exergy has been rediscovered and evenly applied to new scenarios for energy supply both at building and community levels (see for instance the following finished or ongoing international research projects [Annex 37, 2003; Annex 49, 2010; COSTeXergy, 2010]). The aim of exergy analysis of building systems is finding the most rational use of energy, which means at the same time reducing fossil fuels consumption, increasing the

[1]The example in Figure 1.1 corresponds to a steady-state analysis performed with the pre-design Annex 49 MS Excel tool [Annex 49, 2010a] for a single family house with a specific heat transmission coefficient of 0.44 W/(m^{2}K) equipped with floor heating system.

efficiency of energy use and matching the quality levels of the energy supply and demand.

However, the targets of exergy analysis applied to power plants and buildings are very different. The optimization of a power plant aims at increasing the output, i.e. the electricity produced. The reduction of exergy losses in buildings aims, instead, at decreasing the exergy input to maintain the required outputs, i.e. the comfort conditions. Additionally, buildings and power plants are energy systems with very different characteristics in terms of temperature or pressure ranges, dynamic behaviour, etc. In consequence, many of the simplifications and assumptions allowed for power plant analysis need to be reviewed and adapted for exergy analysis of building systems. Results from an extensive literature review [Torío et al., 2009] have shown that no common methodology for exergy analysis of building systems can be found within the scientific community.

1.2 Motivation

By showing the true thermodynamic efficiency of an energy system, exergy analysis is expected to be a valuable tool for developing and designing more efficient energy supply systems in buildings, similarly as it has contributed to raise the efficiency of power plants.

Moreover, renewable energy flows need to be included in the exergy balance, making an assessment of the efficiency of their use possible. Low temperature renewable energy flows, such as solar thermal or ground source heat, have low exergy content (see Figure 1.1), being appropriate energy sources for the supply of thermal energy demands in buildings. Thus, exergy analysis in buildings is also expected to help raising the renewable energy share of energy supply in buildings.

The main motivation of this PhD. thesis is to contribute to a more rational and efficient energy use within the built environment. For this purpose, the contribution and main added value of exergy assessment for the analysis and design of building energy supply systems needs to be thoroughly investigated.

Low temperature renewable energy systems are able to lower significantly the quality of the supplied energy in buildings, thereby increasing the (exergy) efficiency of energy supply. The quality of e.g. solar thermal heat is expected to vary greatly depending on outdoor conditions[2] and on the dynamic behaviour of the solar thermal unit, i.e. on inlet and outlet collector temperatures. Thereby, the exergy performance of such supply systems is expected to vary significantly depending on the solar system design and operation chosen.

Low temperature waste district heat shows the greatest potential of all investigated options in Figure 1.1 for an exergy efficient supply of thermal energy demands in buildings, i.e. the lowest exergy supply of all supply systems presented in the Figure. Its quality is also very sensitive to variations of the outdoor conditions and particular operation of the district heating system.

[2] In this work outdoor air is chosen as reference for exergy analysis, as explained in chapter 2.

A solar thermal supply is often combined with a back up boiler (see Figure 1.1). Herewith, a large part of the energy and exergy is still supplied by means of high-quality energy sources. A similar situation can be found for the Ground Source Heat Pump (GSHP), due to the relatively high share of electricity required for its operation. In turn, the share of high exergy inputs in waste district heat systems is marginal, being nearly completely based on low quality (i.e. low temperature) energy flows. By applying exergy analysis to both supply systems, i.e. solar thermal and waste heat based energy systems, insight can be gained on the usability and potential of exergy analysis to improve different energy supply systems in buildings. Results obtained can be, thereby, extrapolated to other energy supply systems with relatively high and low shares of high exergy inputs, respectively.

1.3 Aim and scope

The main aim of this thesis is to investigate and show the usability and added value of exergy analysis applied to building systems. Exergy analysis is, therefore, compared to conventional primary energy assessment and the different results and conclusions obtained from both methods are thoroughly studied and explained.

Both methods are compared here on a system level, i.e. when applied to the analysis of complete building supply systems. It is at this level at which the environmental impact of a system can be quantified, and thereby, the behaviour of the energy and exergy efficiency of a given system should also be considered at this stage. In this work different operation or design conditions investigated for a given component of the supply systems are always related to their impact on the overall performance of the supply system. A detailed exergy analysis or optimization of different components within the energy supply chain is not the scope of this thesis. Thus, results and conclusions of this work apply only to the comparison of both methods from a system perspective. For a component level, different conclusions might be obtained [Meggers, 2008].

In order to meet the above stated objective, a number of research questions have been formulated:

- **Development of a suitable method:** Which simplifications from the exergy method applied to power plant analysis are suitable for an accurate exergy assessment of building systems? What is a reasonable compromise between accuracy and complexity of a method for exergy analysis of building systems? What additional variables (e.g. pressure, humidity) or heat transfer processes (e.g. thermal radiation) need to be regarded for accurate exergy assessment in building systems?

- **Usability of the method:** Under which circumstances does exergy analysis show additional information or different conclusions than conventional energy assessment on a system level? When are results from both analyses similar? Is that dependent on the

characteristics of the energy system (e.g. share of high quality fuels in the supply) or does it depend on particular assumptions for the operation of the system (e.g. system design, control strategies)?

As part of this thesis and in response to the first research questions mentioned above, a method for dynamic exergy analysis in building systems has been developed. The method has been applied to a solar thermal unit with conventional and high shares of solar heat in energy supply and a waste heat based district heating system. Only SH and DHW demand and supply is regarded. As stated above, these systems show very different shares of high quality energy input in the supply. Thereby, the influence of this parameter on the usability and added value of exergy analysis of building systems is investigated. Additionally, thorough sensitivity analyses are carried out for the two building supply systems studied in order to investigate the influence of the system size, design or control strategy on the additional conclusions that can be gained from exergy analysis.

1.4 Outline

Fundamental concepts related to the exergy method are introduced and applied to building analysis in chapter 2. Based on simplifications obtained from several case studies, a method for (dynamic) exergy analysis of building systems has been developed and is presented in chapter 3. The method is particularly oriented to the heating case, corresponding to German (i.e. central European) climatic conditions. The thermal component of cooling systems, i.e. without humidity treatment, can also be assessed with the equations presented there. In order to compare both assessment methods (i.e. energy and exergy analysis) in detail, dynamic simulations are carried out in the TRNSYS [2007] simulation environment. Models for the simulation of large solar thermal combi-systems and waste heat district heat systems have been arranged. The equations for dynamic simulation of the exergy flows have been implemented in the models.

Main components and particular assumptions used for modeling the systems are described in chapter 4. Results showing the correct operation of the systems and describing the different case studies in detail can be found in chapter 5. Chapters 6 and 7 show the parameters used for characterizing the energy and exergy performance of the systems studied and main results obtained from dynamic analysis, respectively. Additionally, in chapter 7 an exergy based parameter proposed for exergy evaluation of district heatings systems is presented. This parameter could complement conventional primary energy analysis of these systems. Its usability and behaviour are thoroughly discussed. Main conclusions from this work and the conducted investigations are summarized in chapter 8.

Chapter 2

Fundamentals and review of exergy analysis in buildings

2.1 The exergy concept

Expressions like "energy savings", "energy losses" or "energy consumption" are widely used, and appear even in scientific discussions. However, these claims are contradictory to the first law of thermodynamics, which states that energy in a process is conserved, i.e. is transformed from one form of energy into another, but it cannot be destroyed or lost [Shukuya, 2009].

On the light of the first law of thermodynamics, every energy conversion process might happen in both reversible directions. This would mean that, e.g. in an adiabatic system composed of a pot with water and an electrical stove connected to the grid, the energy would be the same before and after heating up the tap water in the pot from tap temperature to, e.g. 80°C. Thermal energy contained in the water after the heating process could, in principle, be transformed back into the electricity originally provided by the stove. This process would not pose any contradiction to the first law of thermodynamics. However, it is by no means possible.

Energy is not being lost in the process. In turn, exergy, which is the thermodynamic magnitude depicting the potential of an energy flow to be completely transformed into any other energy form, is the magnitude being lost in every irreversible energy conversion process.

Exergy is the maximum theoretical work obtainable from the interaction of a system with its environment until the equilibrium state between both is reached [Moran and Shapiro, 1998]. Consequently, it is a measure of the potential of a given energy flow to be transformed into high quality energy, and can also be seen as the departure state of one system from that of the reference environment. Therefore, exergy is a thermodynamic property dependent on the state of the system under analysis and its surrounding environment, so-called *reference environment*.

As stated in [Bejan et al., 1996] if nuclear, magnetic, electric and surface tension effects are neglected the exergy of a system can be divided into four components: physical exergy E_{PH},

kinetic exergy E_{KN}, potential exergy E_{PT} and chemical exergy E_{CH}.

Potential and kinetic exergy components are not relevant for exergy analysis in buildings. Physical exergy is associated to any thermal or mechanical[1] energy flow. In consequence, it is present in most energy processes in the built environment (e.g. heat losses). Chemical exergy, due to a different chemical composition between the given system and the reference environment, plays a significant role in exergy analysis of cooling processes if the humidity ratio of indoor and outdoor air greatly differ from one another [Sakulpipatsin, 2008].

Considering the physical and chemical components, the exergy level of a system is determined by its temperature T, pressure p and chemical potential of the substances comprising it μ_i, as referred to the pressure p_0, temperature T_0, and chemical potentials $\mu_{i,0}$ of the species in the reference environment [Bejan and Mamut, 1999]. Subsequently, for the assessment of the exergy flows, the choice of intensive and extensive properties defining the reference environment is of capital importance. A discussion on the suitable reference environment for dynamic exergy analysis in the built environment can be found in section. 2.2.

2.1.1 Relevant exergy flows for this thesis

Buildings are not in movement or change their position over time. Thus, kinetic and potential exergy do not apply to building systems. In consequence, physical and chemical exergy are the main exergy flows present in the built environment.

Chemical exergy: chemical exergy flows within the building are important if cooling systems with humidity treatment are analyzed. This is not the case in this thesis and thus, chemical exergy flows resulting from different concentration of chemical species between indoor and outdoor air are disregarded. In addition, chemical exergy determines the exergy content of different fuels and sources used as input for energy supply systems in buildings. Values for the chemical exergy potential of fuels have been taken from [Szargut and Styrylska, 1964].

Physical exergy: pressure and temperature are the two physical magnitudes involved in physical exergy. Pressure differences between indoor and outdoor air are the driving force for infiltration losses through the building envelope. In this work, buildings without mechanical ventilation systems are analyzed. Pressure differences between indoor and outdoor air in naturally ventilated buildings are usually low. For wind speeds of 8-10 m/s the pressure difference is about 50 Pa [Fitzner, 2008; Usemann, 2005]. As a result of the low magnitude of this pressure difference, buildings without mechanical ventilation units can be regarded as energy systems at atmospheric pressure and the mechanical contribution to the physical exergy can be disregarded [Schurig, 2010]. Infiltration losses are, thus, regarded here exclusively as a thermal exergy load. With these assumptions only the thermal component of physical exergy is analyzed in this work.

Electrical work: for the operation of energy systems in buildings auxiliary energy in the

[1] Mechanical is here referred to energy processes caused by pressure differences

form of electricity is required (e.g. for pumps, fans, etc.). Electrical work, as any other form of work, is completely convertible in mechanical work or any other energy form [Baehr, 2005]. The exergy of electrical work is also regarded in the analyses within this thesis.

2.2 Definition and discussion on the reference environment

The definition of the reference environment for exergy analysis in buildings is still a controversial issue [Meggers and Leibundgut, 2009]. The reference environment chosen strongly determines results from exergy analysis [Dincer and Rosen, 2007]. However, an extensive literature review on exergy analysis of building systems [Torío et al., 2009] showed that no scientific agreement exists on this issue.

In this section an overview of several definitions of the reference environment found in the literature for exergy analysis on buildings is given. A thermodynamic definition of the reference environment follows. Based on this definition, several proposed reference environments are described and their plausibility and thermodynamic correctness is discussed.

2.2.1 State of the art

Most authors take outdoor air as the reference environment [Shukuya and Hammache, 2002; Angelotti and Caputo, 2007; Alpuche et al., 2005; Nishikawa and Shukuya, 1999; Szargut, 2005; Xiaowu and Ben, 2005; Chow et al., 2009; Wepfer et al., 1979; Boer et al., 2007; Sencan et al., 2005; Khaliq and Kumar, 2007; Izquierdo Millán et al., 1996; Sakulpipatsin, 2008; Hepbasli and Tolga Balta, 2007; Ozgener and Hepbasli, 2007]. Others use indoor air temperature as the reference tempertaure for exergy analysis of thermal energy flows in buildings [Seifert and Hoh, 2009; Henning, 2009; Müller, 2009]. Within the IEA ECBCS Annex 49 group [Annex 49, 2010] discussions on this issue were conducted. To clarify the methodology for exergy analysis in buildings agreement must be reached on this issued. Therefore, here different proposals found and made by the research participants are discussed and analyzed in detail.

2.2.2 Definition

The thermodynamic reference environment for exergy analysis is considered as the ultimate sink of all energy interactions within the analyzed system, and absorbs all generated entropy within the course of the energy conversion processes regarded [Baehr, 2005]. The environment needs to be in thermodynamic equilibrium, i.e. no temperature or pressure differences exist within different parts of it (thermo-mechanical equilibrium). Chemical equilibrium must also be fulfilled. Furthermore, intensive properties of the environment must not change as a result of energy and mass transfer with the regarded energy system [Baehr, 2005; Bejan et al., 1996]. In addition, the reference environment is regarded as a source of heat and materials to be exchanged with the analyzed system [Dincer and Rosen, 2007], i.e. it must be available and

ready to be used by the system under analysis. It can thus act as either an unlimited sink or unlimited source.

As stated in section 2.1.1, only the thermal component of physical exergy is regarded in this work. In consequence, the definition of the reference environment in terms of its temperature is sufficient for the analysis within this thesis.

2.2.3 Discussion: possible choices

Several choices for the reference environment are possible. However, in [Wepfer and Gaggioli, 1980] it is clearly stated that the reference environment for exergy analysis, unlike reference variables for thermodynamic or thermo-chemical tables, cannot be chosen arbitrarily. The reason is that energy analysis is based on a difference between two states and, thus, the chosen reference levels out in the balance. In turn, in exergy analysis the chosen reference does not level out in the balance and values of the e.g. absolute temperature chosen as reference strongly influence results from exergy analysis. In this section the physical and thermodynamic correctness of four following options found in the literature or under discussion in the scientific community is presented.

In order to show the influence of choosing one reference environment or another for exergy analysis, steady-state exergy analyses have been carried out on a building case study. Analyses with the four different options for the reference environment, characterized by means of their respective (reference) temperatures T_0, have been performed with the pre-design Annex 49 MS Excel tool [Annex 49, 2010a]. The building is a simple single family house with a specific heat transmission coefficient of 0.44 W/m^2K equipped with floor heating system and a condensing boiler. Exergy and energy flows obtained with the four different reference environments are shown in Figure 2.1.

Universe, nearly absolute zero (a) The mean temperature of the universe is very low, around 3 K. This allows radiative energy transfer from the earth and, thereby, discarding the entropy produced as a result of energy processes on earth [Shukuya, 1996]. The universe is infinite and undergoes no variation in its intensive properties as a result of heat and mass transfer processes within the building. Thus, it could be regarded as the ultimate sink of energy processes within a building.

However, cool radiation from the universe is not always directly available and ready to be used by the built environment (otherwise no cooling energy would be required).

In addition, regarding the absolute zero as reference environment for thermal energy interactions makes energy and exergy analysis of thermal energy flows equivalent, as shown in Figure 2.1 (a). Differences between the energy and exergy flows in the condensing boiler (i.e."Generation" subsystem in Figure 2.1 (a)) and "Primary energy transformation" subsystem [2] subsystems occur due to quality factors for liquefied natural gas (LNG) used as input in

[2] "Primary energy transformation" and "Generation" referred here corresponds to the modular method for

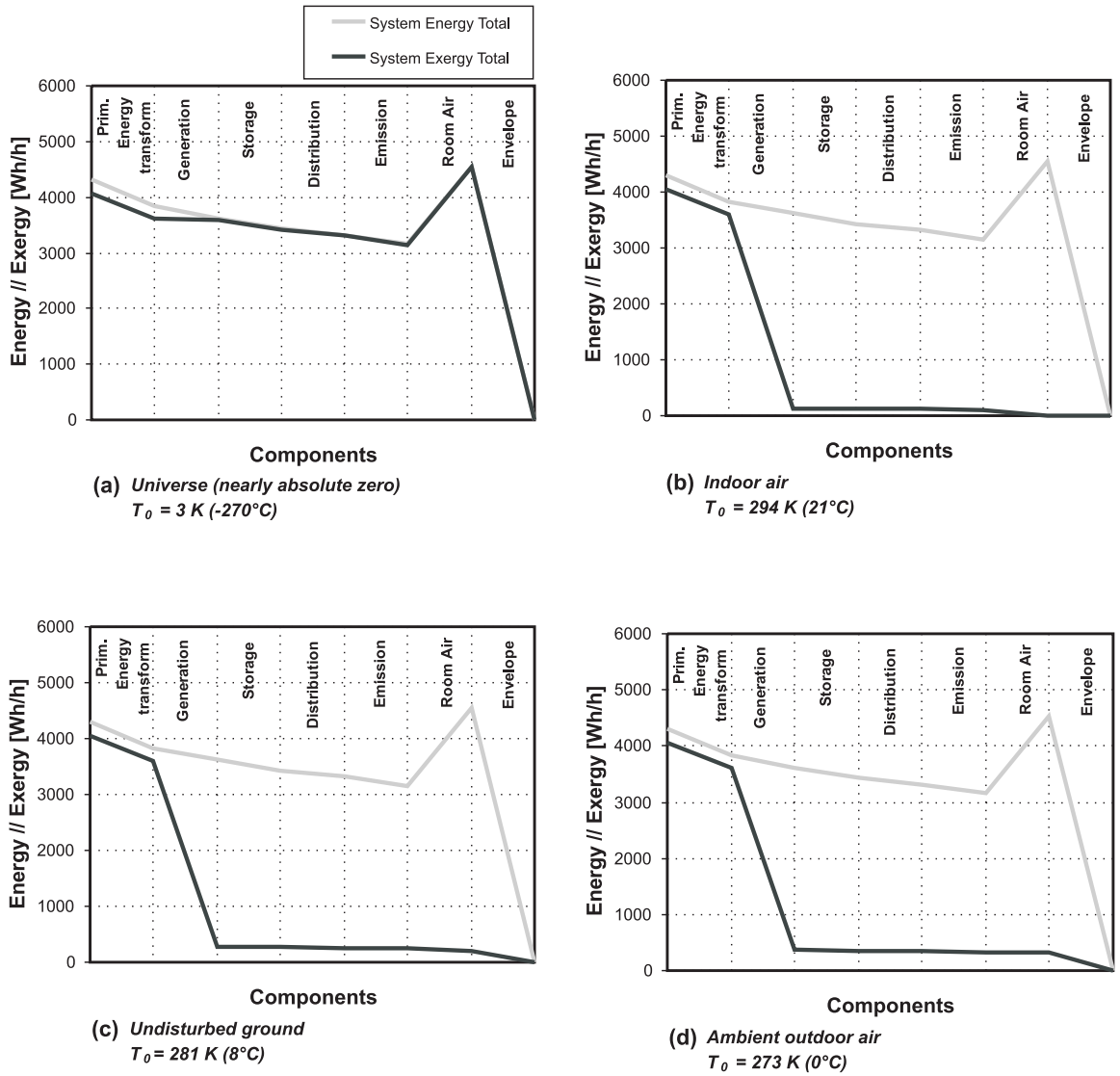

Figure 2.1: Energy and exergy flows for a building case study with the four options introduced for the reference environment; (a): Universe, with an average temperature of 3 K; (b): Indoor air, characterized by a temperature of 20°C; (c): Undisturbed ground with a temperature of 8°C; (d): Ambient outdoor air with a temperature of 0°C.

the condensing boiler and regarded as 0.95 [Szargut and Styrylska, 1964][3].

Indoor air inside the building (b) Building indoor air has also been proposed as reference environment for exergy analysis. However, indoor air is neither an infinite sink nor is it in

exergy analysis developed by Schmidt [2004] and applied in this thesis. The different subsystems are presented in detail in chapter 3

[3]Quality factors in (Szargut and Styrylska, 1964) were derived for a reference temperature of 25°C. It is expected that these quality factors tend to 1 if a reference temperature of nearly zero Kelvin is assumed instead. However, deriving them for 3 K is out of the scope of this thesis. Here, values from [Szargut and Styrylska, 1964] are used to show qualitatively the trend between energy and exergy

thermodynamic equilibrium. In addition, its temperature varies as a result of energy processes within the building. Therefore, it does not fulfill the requirements for being regarded as a thermodynamically correct reference environment.

Results using indoor air as reference environment are shown in Figure 2.1 (b). The exergy demand of the building (input in the "envelope" subsystem) is zero, for it is regarded as reference environment. In consequence, this approach does not allow to derive exergy efficiencies for the overall energy supply in buildings since the desired exergy output is always zero.

Undisturbed ground (c) Undisturbed ground can be regarded as an infinite sink, whose properties remain uninfluenced as a result of interactions with the building. Yet, the main contradiction for regarding it as reference environment, similarly as the universe, is that it is not always directly available and ready to be used by the built environment[4].

Outdoor air surrounding the building (d) Most energy processes in the building sector occur due to temperature or pressure differences to the surrounding air. Thus, the air surrounding the building can be regarded as the ultimate sink for most energy processes occurring in the building. On the other hand, the air volume around the building can be assumed to be big enough (infinite sink) so that no changes in its temperature, pressure or chemical composition occur as a result of the interactions with the building. In addition, outdoor air surrounding the building is naturally available and ready to be used[5].

2.2.4 Conclusions and recommendations

In Figure 2.1 it is clearly shown that main differences arise if the universe and indoor air are regarded as the reference state: regarding the universe as reference environment makes energy and exergy analysis equivalent; regarding indoor air as reference state makes the exergy demands of the building zero, thus making impossible to obtain exergy efficiencies for characterizing the performance of different systems. Results using the undisturbed ground as reference state are very similar to those obtained using outdoor air as reference state. However, from a thermodynamic point of view the last is the only correct option. Particularly indoor air does not fulfill any of the requirements mentioned in the thermodynamic definition.

For all stated above, outdoor air is regarded in this work as the suitable option for reference environment in building exergy analysis.

Thermodynamic equilibrium in the reference environment Outdoor air temperature and pressure do vary with time and space (as it would also be the case of any of the other envi-

[4]Directly available in the sense that if a heating load is present having an undisturbed ground temperature greater than room air temperature would not reduce directly the heating load unless a suitable energy system (e.g. ground heat exchanger) is installed.

[5]On the contrary as the undisturbed ground temperature, if a heating load is present, an outdoor air temperature greater than building air temperature would directly reduce the heating load (by e.g. opening the window).

ronments proposed above as reference states), i.e. external air is not a homogeneous system in thermo-mechanical or chemical equilibrium. As stated in [Dincer and Rosen, 2007] *"the natural environment is not in equilibrium and its intensive properties exhibit spatial and temporal variations. Consequently, models for the reference environment are used which try to achieve a compromise between theoretical requirements and the actual behaviour of the reference environment"*. In order to model the outdoor air surrounding a building as a thermodynamic reference environment, temperature and pressure are assumed to be uniform for the air surrounding the building (thermal and mechanical equilibrium). Concentration of different chemical species in the atmospheric air is also regarded as homogeneous.

2.2.5 Sensitivity of the results

Rosen and Dincer [2004] evaluated the sensitivity of exergy flows as a function of different definitions of the reference environment. The authors show that the sensitivity of exergy assessment to changes in the reference environment is greater when the properties of the system are close to those of the reference environment. This justifies that a constant reference environment has been typically assumed for exergy analysis of power plants and industrial processes involving high quality energy forms as main inputs and outputs. In turn, in the built environment, energy demands happen at conditions close to those of the reference environment and undergo subsequently strong variations for changing conditions of the reference environment. In consequence, for exergy analysis of building systems a dynamic (i.e. time-dependent) definition of the reference environment is required. Weather data can be used for this purpose.

2.3 Thermal exergy

As stated in section 2.1 only the thermal component of physical exergy is regarded in this thesis. In this section an introduction to the concept of thermal exergy, its physical derivation and meaning is given. The behaviour of thermal exergy for different heat transfer mechanisms is explained in detail. Several case studies referred to these issues are also presented. From the results of the case studies some simplifications can be derived and are applied for exergy analysis in the building supply systems investigated in this work. These simplifications are summarized in section 2.5.

2.3.1 Exergy of heat transfer and Quality Factors

Under steady state conditions, the exergy of a heat transfer Q taking place within two temperature levels T and T_0, i.e. the maximum amount of work that could be obtained if a heat engine would operate following the Carnot cycle among the temperature levels given, can be expressed as a function of the Carnot factor as shown in equation 2.1.

$$Ex_Q = Q \underbrace{\left(1 - \frac{T_0}{T}\right)}_{CarnotFactor} \tag{2.1}$$

Carnot factors are valid for analyzing the exergy of an isothermal heat transfer taking place at temperatures both greater and lower than the reference temperature T_0 and are a particular case of the so-called *"quality factors"* introduced later in this section. It is important to remark that in the for obtaining the Carnot factors shown in equation 2.1 the American sign convention has been applied [Moran and Shapiro, 1998]: heat flows into the analyzed system (e.g. heat engine) are regarded as positive and work outputs from the system are regarded as positive.

For temperatures higher than the reference temperature $T > T_0$ Carnot factors have positive values. The natural heat flow Q would be an output from the analyzed system[6], i.e. is negative. In consequence the exergy flow is also negative, i.e. it represents an exergy output

For temperatures lower than the reference temperature $T < T_0$ Carnot factors have negative values. With the sign convention adopted the natural heat flow would be now an input into the analyzed system[7], i.e. Q is positive. The exergy of Q is, thus, negative. Despite the heat flow is an energy input into the building, it represents an exergy output. Negative values of the Carnot factors in equation 2.1 indicate that the exergy flows in the opposite direction to the heat flow.

Exergy associated to the heat transfers in both cases is negative, i.e. those heat flows represent an exergy output from the systems, i.e. they tend to level out the properties of the analyzed system (e.g. building) and those of the environment: as the heat transfers take place, the building temperature would be more similar to the environment temperature in both cases, i.e. the exergy content of the building is decreased.

The heat flows Q can be seen as the net heat losses and gains for the building under heating and cooling conditions, respectively. In order to keep indoor conditions at comfortable levels they need to be compensated by an active heating or cooling system. Active heating would be a heat input into the building, i.e. with a positive value, and active cooling would be an output, i.e. with a negative value. Exergy of active heating would thus be positive as long as the building temperature is higher than that of the environment, i.e. if it cannot be heated up naturally with the environment, and negative otherwise. Active cooling would be positive as long as the building temperature is lower than that of the environment, i.e. if it cannot be cooled naturally with outdoor air, and negative otherwise. In this way, exergy gives information on the available heating or cooling loads, but also on whether they can be directly supplied by means of the reference environment (i.e. outdoor air) or an active system is required for that purpose [Jansen, 2010] .

This shows the importance of calculating exergy values with the appropriate signs. The

[6] e.g. transmission losses from a building during winter conditions.
[7] e.g. heat gains in a building during summer conditions.

equations developed in this work and presented in chapter 3 for exergy assessment follow the American sign convention mentioned above. Exergy inputs are regarded as positive and exergy outputs are regarded as negative.

Quality factors Quality factors are defined as the ratio between the exergy and energy of a given energy system and will be represented in this work as F_Q. The general expression of quality factors is shown in equation 2.2.

$$F_Q = \frac{Ex}{En} \tag{2.2}$$

From a thermodynamic point of view, quality factors represent the proportion of work that can be obtained from an energy conversion process which brings an energy system into equilibrium with its environment as related to the energy present in the system before the conversion process takes place. Carnot factors are a particular case of quality factors applicable when the heat transfer is isothermal. This would be the case of a heat transfer assuming steady state conditions, i.e. the state of the system involved in the heat transfer does not vary over the course of the heat interaction. Thus, it can be argued that exergy in this case is related to the heat flow. Therefore, the exergy of such a process (and its related quality factor) is called *"exergy as a quantity of flow"* [Shukuya, 2009] or *"exergy of heat"* [Jansen, 2009].

In turn, if the temperature of the system changes over the course of the heat transfer, equation 2.1 cannot be applied. The quality factor related to a not isothermal heat transfer, i.e. where the state of the system changes, is shown in equation 2.3. In this case, exergy is said to be *"exergy as a quantity of state"* [Shukuya, 2009] or *"exergy of matter"* [Jansen, 2009].

$$F_Q = 1 - \frac{T_0}{T_{ini} - T_{fin}} ln \frac{T_{ini}}{T_{fin}} \tag{2.3}$$

2.3.2 Exergy of thermal radiation

Radiative heat transfer represents a significant part of the whole energy transfer in radiative heating and cooling systems in buildings. In the case of low temperature heating and high temperature cooling systems radiative heat transfer might represent up to 50% of the overall energy being transmitted to the room air [Olesen, 2002].

Estimating the exergy of thermal radiation has been a controversial issue and is still a matter of discussion in many scientific papers [Candau, 2003; Wright et al., 2002; Petela, 2003; Badescu, 1998]. In the following, the derivation of the formula to assess the exergy of thermal radiation based on [Candau, 2003] is presented. The result is extrapolated and applied to the particular case of radiative heat transfer in buildings.

The maximum work obtainable from the thermal radiant flux between an emitting body of surface A and emissivity ϵ at a temperature T and its environment at a temperature T_0 can be obtained when the hot side of a Carnot engine whose cold side is in equilibrium with the

environment at T_0, absorbs isothermally the thermal radiation, i.e. at a temperature infinitesimally smaller than that of the emitted radiation, *T-dT*. Naturally, the hot side of the Carnot engine would emit also a part of the absorbed thermal radiation at its own temperature level *T-dT*. This could be again used as input for another Carnot engine absorbing the incoming radiation isothermally, at an infinitesimally smaller temperature level, *T-2dT*. Subsequently, the amount of work obtainable in each infinitesimally small and reversible step can be evaluated as a function of the infinitesimally small heat being effectively available to power the Carnot engine ∂Q_{rad}, as shown in equations 2.4 and 2.5.

$$dW_{rev} = \partial Q_{rad} \left(1 - \frac{T_0}{T - dT}\right) \tag{2.4}$$

$$\partial Q_{rad} = \epsilon\, A\, \sigma \left[T^4 - (T - dT)^4\right] \cong \epsilon\, A\, \sigma\, 4\, T^3\, dT \tag{2.5}$$

Integrating the maximum work available in each infinitesimally small step obtained from the reversible conversion steps of thermal radiation into work dW_{rev} the exergy of the initially emitted thermal radiation can be obtained. Equation 2.7 is coherent with that presented by Shukuya and Hammache [2002] for the evaluation of the exergy of thermal radiation being emitted by the surface of a radiant heating system in a building.

$$Ex_{rad} = \int_{T_0}^{T} dW_{rev} = \int_{T_0}^{T} \partial Q \left(1 - \frac{T_0}{T}\right) = \int_{T_0}^{T} \epsilon\, A\, \sigma\, 4\, T^3\, dT \left(1 - \frac{T_0}{T}\right) \tag{2.6}$$

$$Ex_{rad} = W = \epsilon\, A\, \sigma \left[\left(T^4 - T_0^4\right) - \frac{4}{3} T_0 \left(T^3 - T_0^3\right)\right] \tag{2.7}$$

In equation 2.7 two types of irreversibilities are regarded [Petela, 2003]:

- those derived from the conversion of thermal radiation at a temperature T into heat at the same temperature, T
- and irreversibilities derived from the emission of radiation by the absorbing body at its temperature (T_0 in equation 2.7)

As mentioned in the derivation of equation 2.7, this expression can be used for evaluating the exergy of the thermal radiation exchange between a surface A at a temperature T and its environment at a temperature T_0. This result can be generalized for two surfaces at two different temperature levels T_{surf1} and T_{surf2}, in an environment with a temperature T_0. This would be the case of a radiant heating surface inside a building which is in radiative exchange with the other surfaces enclosing the room, emitting radiation at its surface temperature and absorbing radiation at the respective temperature levels from the other surfaces. The general expression of the net radiative exergy transfer between two parallel surfaces with the same area and emissivity is shown in equation 2.8. This is coherent with the conclusions shown in [Wright et al., 2002].

$$Ex_{rad} = W = \epsilon\, A\, \sigma \left[\left(T^4_{surf1} - T^4_{surf2}\right) - \frac{4}{3} T_0 \left(T^3_{surf1} - T^3_{surf2}\right) \right] \tag{2.8}$$

Building surfaces enclosing a building space are not always parallel with each other and view factors between them play a significant role in their radiative heat transfer. The general expression shown in equation 2.8 can be rewritten as a function of the net radiative heat transfer occurring as shown in equation 2.9, where effect of view factors, area and emissivity of the surfaces is already included in the net radiative heat transfer, Q_{rad}.

$$Ex_{rad} = Q_{rad} \left[1 - \frac{4}{3} \frac{T_0}{\left(T^4_{surf1} - T^4_{surf2}\right)} \left(T^3_{surf1} - T^3_{surf2}\right) \right] \tag{2.9}$$

The present work aims at comparing different space heating and cooling systems from an energy and exergy perspective, and not at drawing a detailed exergy balance of each element in the building envelope. Thus for simplicity, the thermal radiant exergy balance between the active surface and the rest of the building, characterized by means of its operative temperature $T_{r,op}$, is regarded. Equation 2.10 can be used for this purpose.

$$Ex_{rad,active} = Q_{rad,active} \underbrace{\left[1 - \frac{4}{3} \frac{T_0}{\left(T^4_{surf,active} - T^4_{r,op}\right)} \left(T^3_{surf,active} - T^3_{r,op}\right) \right]}_{F_{Q,rad}} \tag{2.10}$$

In Figure 2.2 (a) the difference between the absolute values[8] of quality factors, corresponding to a conductive-convective heat exchange, and quality factors associated to a radiative heat exchange are shown. Quality factors associated to radiative heat transfer, $F_{Q,rad}$, are always lower, i.e. losses due to intrinsic irreversibilities associated to the radiative heat transfer process, as explained above, are bigger than for a conductive-convective heat exchange.

2.3.2.1 Case study: Influence of radiant thermal exergy for building systems

In order to study the influence of evaluating the exergy of thermal radiation as such in building applications the multi-family dwelling with radiators described in chapter 4 is taken as case study. Climatic conditions from Meteonorm [2008] for Würzburg are chosen. The building object is simulated dynamically in the software TRNSYS [2007] for January. Radiative and convective heat transfer from the radiators can be obtained separately as an output from the radiator model. According to the energy simulation, 59% of the total energy output from the radiators occurs due to convective heat transfer between the room-air and the floor surface.

[8] Absolute values of the quality factors are used to ease representation. However, as stated above, the sign is very important for the coherence of exergy calculations and thus, for exergy assessment natural values of the quality factor need to be used.

In turn, 41% happens in the form of radiative heat transfer.

In Figure 2.2 (b) results from the exergetic evaluation of the energy output from the radiators into the room-air are shown. The dark grey area shows the exergy output if all energy transfer is regarded as convective (named as *all convective* in the graph), i.e. using the Carnot factor for evaluating the exergy associated to the total heat transfer (equation 2.1). The light grey area shows the exergy output when the corresponding radiative and convective parts of the heat transfer are evaluated as such in exergy terms (named *convective+radiative* in the figure), i.e. using the Carnot factor (equation 2.1) for evaluating the exergy of the convective part and equation 2.10 for the radiative part.

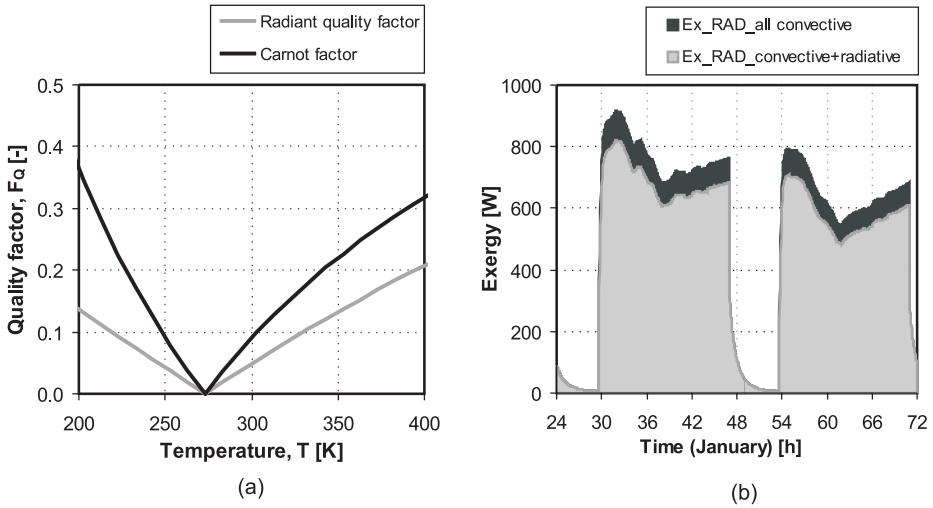

Figure 2.2: (a): Quality factors associated to a radiative and conductive-convective heat transfer process; (b): Exergy from the surface of the radiators if all energy transfer is evaluated as convective (with equation 2.1 (*Ex-RAD-all convective*) and evaluating the radiative and convective parts separately and correctly (with equations 2.1 and 2.10, respectively (*Ex-RAD-convective+radiative*). Results for two days of January are presented.

Exergy input from the radiators and into the room-air[9] is bigger if all energy transfer is regarded as convective, i.e. using the Carnot factor. In turn, exergy input from the radiator surface into the room-air is 8% lower if the exergy from the convective and radiative parts of the heat transfer are evaluated correctly. Obviously, the bigger the radiative part on the whole heat transfer, the greater the difference between both evaluation methods. This allows to conclude that radiative heating and cooling systems may supply the energy demands with lower exergy content, being thus a "LowEx" system. Yet, this lower exergy input only occurs due to bigger irreversibilities associated to the radiative heat transfer, as explained above. Energy input in the radiators happens mainly due to conduction from the heating fluid. Since the graph above represents the same emission system, the same energy and exergy is being

[9] "Room-air" and "emission" subsystems referred here corresponds to the modular method for exergy analysis developed by Schmidt [2004] and applied in this thesis. The different subsystems are presented in detail in section 3.2

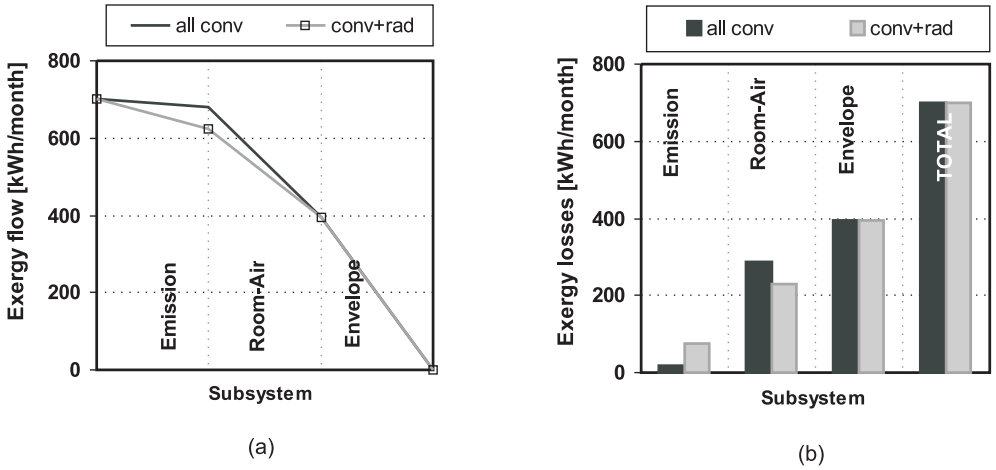

Figure 2.3: (a):Exergy flows from the radiators (emission) to the building envelope regarding all energy transfer as convective (dark grey line) and evaluating the radiative and convective parts separately (light grey line); (b): Exergy losses in the radiators, room-air and envelope subsystems, depending on whether exergy of radiative and convective heat transfer process are regarded separately

.

supplied to the radiators by the heating fluid in the radiator pipes, as shown in Figure 2.3 (a). As this conductive energy flux is converted into thermal radiation in the radiators and regarded as such, higher exergy losses occur within the radiators (*emission subsystem* in Figure 2.3)). Following, the exergy output from the radiators into the room-air is lower.

However, total exergy losses in the emission system as a whole remain the same. Only the allocation of that losses is different, as it is shown in the left diagram on Figure 2.3 (b). In other words, from the perspective of the whole system analysis, exergy losses in the space heating system are the same no matter if the energy transfer to the room happens via convection or radiation.

2.4 Steady state, quasi-steady state and dynamic exergy analysis

Steady-state and quasi-steady state estimations of the energy demands and flows in buildings are proposed and used by building regulations and standards in several European countries [EnEV, 2007; EN ISO 13790, 2008]. Yet, as stated in section 2.2.5 exergy flows in buildings are very sensitive to variations in the properties of the system analyzed or the reference environment [Dincer and Rosen, 2004]. In consequence, an estimation of the error of steady-state exergy assessment as compared to dynamic approaches is mandatory. In this section, results found in the literature comparing both evaluation methods are presented.

Alternatively a quasi-steady state assessment can be performed. Quasi-steady state represents a hybrid between fully dynamic and fully steady-state calculation methods. The exergy flows are evaluated following a steady-state approach, i.e. storage phenomena are disregarded, over discrete and short time-steps. This simplified quasi-steady state evaluation

method is also compared by means of two building case studies to a fully dynamic approach.

2.4.1 Steady state vs. quasi-steady state exergy analysis

Angelotti and Caputo [2007] evaluate the difference between steady state and quasi-steady state analysis for heating and cooling systems in two representative Italian climates, namely Miland and Palermo. Only thermal exergy flows are regarded, i.e. the reference and indoor environments are only defined based on their temperature levels and no considerations on air humidity or pressure are included. For the quasi-steady state assessment a timestep of 1 hour is chosen. Quasi-steady state and steady state exergy efficiencies for a reversible air-source heat pump and a condensing boiler coupled with direct ground cooling are compared for the heating and cooling cases.

Steady state exergy efficiencies for the heating case using average outdoor temperatures are very close to those resulting from quasi-steady state exergy analysis. These results are coherent to findings from Sakulpipatsin [2008] who points out that mismatching between steady-state and quasi-steady state yearly analysis for cold or mild climates are lower than 10%.

However, for the cooling case great differences (of up to 42%) between both assessment methods are found. The authors remark that the difference is larger for cooling rather than heating systems and for Palermo rather than Milan. This is due to the greater sensitivity of the quality factor determining the exergy demand of the building $F_{Q,dem}$ (equation 2.11) to outdoor temperature variations when the outdoor air temperatures (taken as reference for exergy analysis) are closer to room air temperatures in the building. Figure 2.4 shows the greater relative variations experimented by the Carnot factor for summer than for winter conditions in Milan. These results are also in good agreement with findings from [Sakulpipatsin, 2008].

$$F_{Q,dem} = 1 - \frac{T_0}{T_r} \tag{2.11}$$

Thus, it can be concluded that steady-state exergy analysis might be reasonable for a first estimation of the exergy flows in space heating applications, particularly in colder climates. The error is expected to be bigger the milder the climatic conditions are. Yet, exergy flows in cooling applications can often only be assessed by means of quasi-steady state or dynamic analysis, where variations in outdoor reference conditions are taken into account [Torío et al., 2009].

The impact of variable climatic conditions is expected to be different in different energy systems. For example, the exergy input and exergy losses of a condensing boiler are expected to be rather constant even under varying outdoor reference conditions, since high quality fossil fuels with a constant quality factor of 0.95 is being used. In turn, the temperature of the heat output from a solar thermal system varies significantly depending on outdoor conditions and is relatively close to outdoor air temperature. Thus, strong variations in the Carnot factor associated to the exergy flow from the solar thermal system are expected and bigger mis-

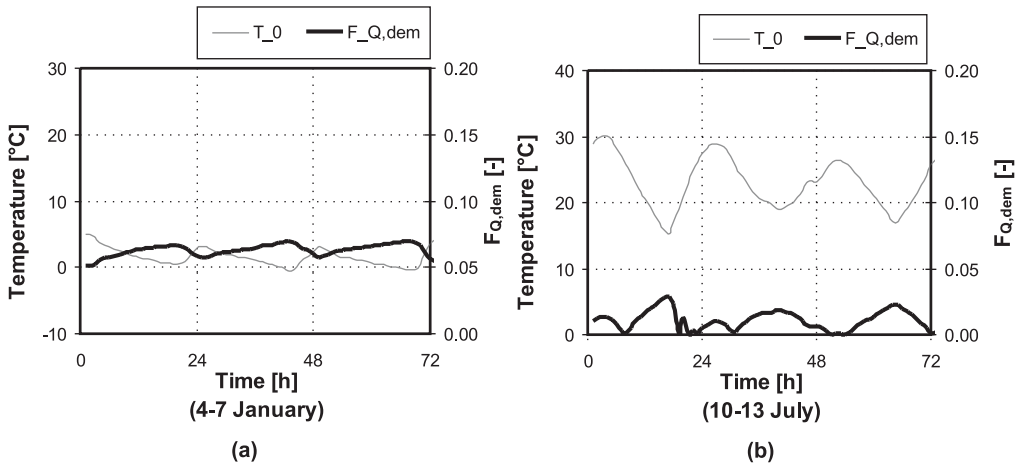

Figure 2.4: Dynamic variation of the outdoor temperature (taken as reference T_0 and Carnot factor for building exergy demands $F_{Q,dem}$ under heating and cooling conditions in Milan.

matching between stationary and dynamic exergy analysis can be presumed. Therefore, if the goal of exergy analysis is to compare different energy systems, quasi-steady state or dynamic exergy analysis is preferable, so that errors arising from the steady-state assessment can be excluded and differences between the energy systems can be solely attributed to improved or optimized performance.

2.4.2 Quasi-steady state vs. dynamic exergy analysis

In this section, equations for quasi-steady state and dynamic approaches for exergy analysis are presented. In order to better understand and clearly explain the differences between both approaches an example of the exergy balance of the subsystem *room air*[10] (see Figure 2.5) within a building is presented.

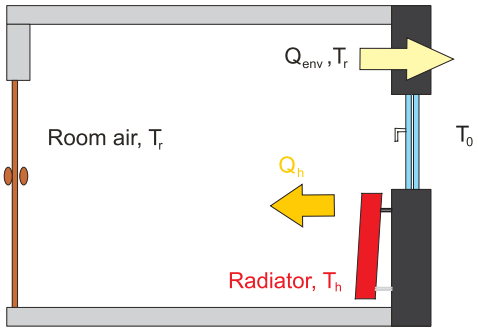

Figure 2.5: Room air as control mass system being heated up by a radiator.

[10] A detailed description of the exergy balances of the *room air* subsystem can be found in section 3.2.3

2.4.2.1 Dynamic approach

A dynamic exergy analysis implies the assessment of all storage processes within the energy systems regarded.

Equation 2.12 is the general expression for a dynamic exergy analysis of the *room-air* subsystem. Exergy consumption in equation 2.12 refers only to the unavoidable irreversibilities arising from the temperature difference between the surface of the radiator T_h and the room air temperature T_r, which is the driving force for the heat transfer.

$$\begin{aligned} \textit{(exergy consumed)}_{dyn} &= \textit{(exergy input) + (exergy output)} \\ &\quad \textit{- (exergy stored in the room-air)} \\ &= Irreversibilities \end{aligned} \tag{2.12}$$

According to the heat flows and temperatures shown in Figure 2.5 the exergy input, output and stored in the room-air can be calculated as shown in equations 2.13, 2.14 and 2.15 respectively. Q_{env}in equation 2.14 represents the net heat losses[11] through the building envelope.

$$Ex_{in} = Q_h(t_k) \cdot \left(1 - \frac{T_0(t_k)}{T_h(t_k)}\right) \tag{2.13}$$

$$Ex_{out} = Q_{env}(t_k) \cdot \left(1 - \frac{T_0(t_k)}{T_r(t_k)}\right) \tag{2.14}$$

$$Ex_{sto,r}(t_k) = m_r \cdot c_{p_a} \cdot \left[(T_r(t_k) - T_r(t_{k-1})) - T_0(t_k) \cdot \ln \frac{T_r(t_k)}{T_r(t_{k-1}))}\right] \tag{2.15}$$

2.4.2.2 Quasi-steady state approach

Alternatively, a quasi-steady state approach for exergy analysis combined with dynamic energy simulations could be applied. In a quasi-steady state methodology, exergy flows are evaluated assuming steady state conditions for every small timestep assumed for the dynamic energy simulation. Exergy analysis can be performed, thus, with relatively simple equations using the results from dynamic energy calculations (i.e. temperature, energy and mass flows).

The general expression for calculating the exergy losses for the *room-air* subsystem following a quasi-steady state approach is shown in equation 2.16.

$$\begin{aligned} \textit{(exergy consumed)}_{q-steady} &= \textit{(exergy input) + (exergy output)} \\ &= \textit{(Irreversibilities)+(exergy stored in room-air)} \end{aligned} \tag{2.16}$$

[11] i.e. the balance of the transmission and ventilation losses with the internal and solar gains inside the building.

The main difference between a dynamic and quasi-steady state approach for exergy analysis is that in the latest storage phenomena are not analyzed separately but implicitly as part of the exergy consumed. On the contrary, in a dynamic approach exergy consumption would only be due to irreversibilities and exergy stored would be regarded separately as a further term (input or output) in the exergy balance (see equations 2.17 and 2.18).

$$Ex_{cons,q-steady}(t_k) = Q_h(t_k) \cdot \left(1 - \frac{T_0(t_k)}{T_h(t_k)}\right) + Q_{env}(t_k) \cdot \left(1 - \frac{T_0(t_k)}{T_r(t_k)}\right) \tag{2.17}$$

$$\begin{aligned} Ex_{cons,dyn}(t_k) =& Q_h(t_k) \cdot \left(1 - \frac{T_0(t)}{T_h(t_k)}\right) + Q_{env}(t_k) \cdot \left(1 - \frac{T_0(t_k)}{T_r(t_k)}\right) \\ & - m_r \cdot c_{p_a} \cdot \left[(T_r(t_k) - T_r(t_{k-1})) - T_0(t_k) \cdot \ln \frac{T_r(t_k)}{T_r(t_{k-1}))}\right] \end{aligned} \tag{2.18}$$

2.4.2.3 Case study: Room air

To show the disagreement between quasi-steady state and dynamic approaches a case study has been dynamically simulated in TRNSYS. The multi-family dwelling with radiators presented in detail in section 4.2.2 and used also as case study in section 2.3.2.1 is used as case study here. Night setback is considered from 23 h to 5 h.

To estimate the net energy losses through the building envelope equation 2.19 is used.

$$Q_{h,r}(t) + Q_{env}(t) = Q_{sto,r}(t) \tag{2.19}$$

Equations for a dynamic (2.18) and quasi-steady (2.17) assessment of the exergy consumption in the room air of the building are implemented in the model. For the dynamic analysis, the energy stored in the room-air has been evaluated as a function of its dynamic temperature change ($T_r(t_k)$-$T_r(t_{k-1})$) following equation 2.15. For the quasi-steady state approach, the exergy of energy stored is not included in the balance (equation 2.17).

In Figure 2.6 the good agreement on the dynamic behaviour of the exergy losses using both approaches is graphically shown. Exergy stored in the room air is very small, as it is in energy terms due to the low specific heat capacity of air. The difference between the exergy consumption following both approaches amounts 0.006% on a monthly balance for January conditions. The net exergy stored in the wall over one month represents 0.0021% of the exergy input into the room-air from the emission system, being thus negligible. Exergy stored in each timestep represents usually less than 0.1% of the exergy input into the room air.

Storage is a periodic phenomenon. To avoid the influence of cancelling out exergy stored and released over a long period of time (such as one month) results from both approaches for a time-scale of 12 hours are compared. For the time between 169h and 180h[12] the exergy stored represents 0.03% of the exergy input in the room air, and the exergy consumed following a

[12]Night setback operation happens between 168-173h.

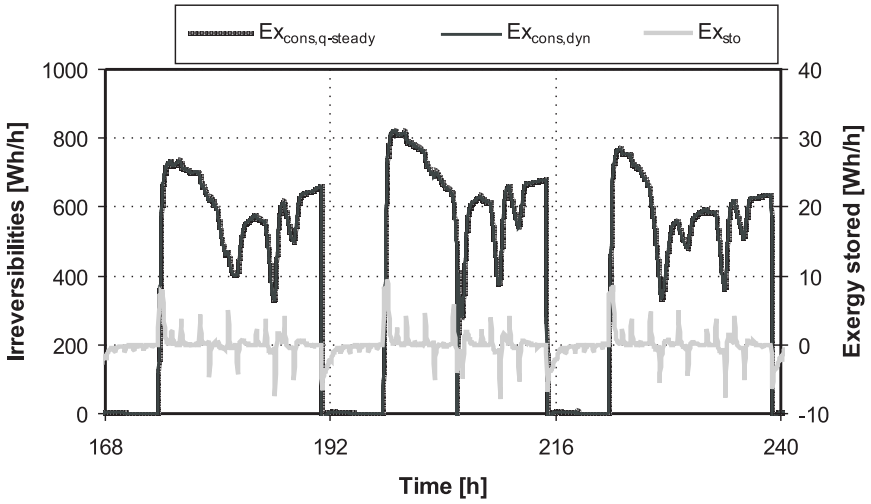

Figure 2.6: Dynamic behaviour of the exergy stored in the room-air (right Y-axis, Ex_{sto}) and the exergy consumption following quasi-steady ($Ex_{cons,q-steady}$) and dynamic ($Ex_{cons,dyn}$) approaches (left Y-axis).

dynamic approach is only 0.088% lower than that estimated following a quasi-steady state approach.

Following it can be concluded that a quasi-steady state approach for systems without great storage capacity is suitable. An analytical demonstration of this statement can be found in [Schmidt and Torío, 2010].

2.4.2.4 Case study: Building wall

Building walls have a much bigger storage capacity than room-air. Therefore, to check the influence of a quasi-steady state assessment on such a building element, a wall of the multi-family dwelling has been taken as case study, see Figure 2.7 (a). In Figure 2.7 (b) results from both approaches can be found.

Exergy stored $Ex_{sto,wall}$ and exergy losses without accounting the stored exergy as a loss $Ex_{cons,dyn}$ (equation 2.21) correspond to the dynamic approach. Exergy losses in the quasi-steady assessment are represented by the curve $Ex_{cons,q-steady}$ (equation 2.22). For completeness, energy stored in the wall is also shown $En_{sto,wall}$.

$$Q_{in,wall}(t_k) + Q_{out,wall}(t_k) = Q_{sto,wall}(t_k) \tag{2.20}$$

$$\begin{aligned} Ex_{cons,dyn}(t_k) = {} & Q_{in,wall}(t_k)\left(1 - \frac{T_0(t_k)}{T_A(t_k)}\right) + Q_{out,wall}(t_k)\left(1 - \frac{T_0(t_k)}{T_B(t_k)}\right) \\ & - \sum_{i=1}^{i=n} m_i c_i \left[(T_{wall}(t_k) - T_{wall}(t_{k-1})) - T_0(t_k)\ln\frac{T_{wall}(t_{k-1})}{T_{wall}(t_{k-1})}\right] \end{aligned} \tag{2.21}$$

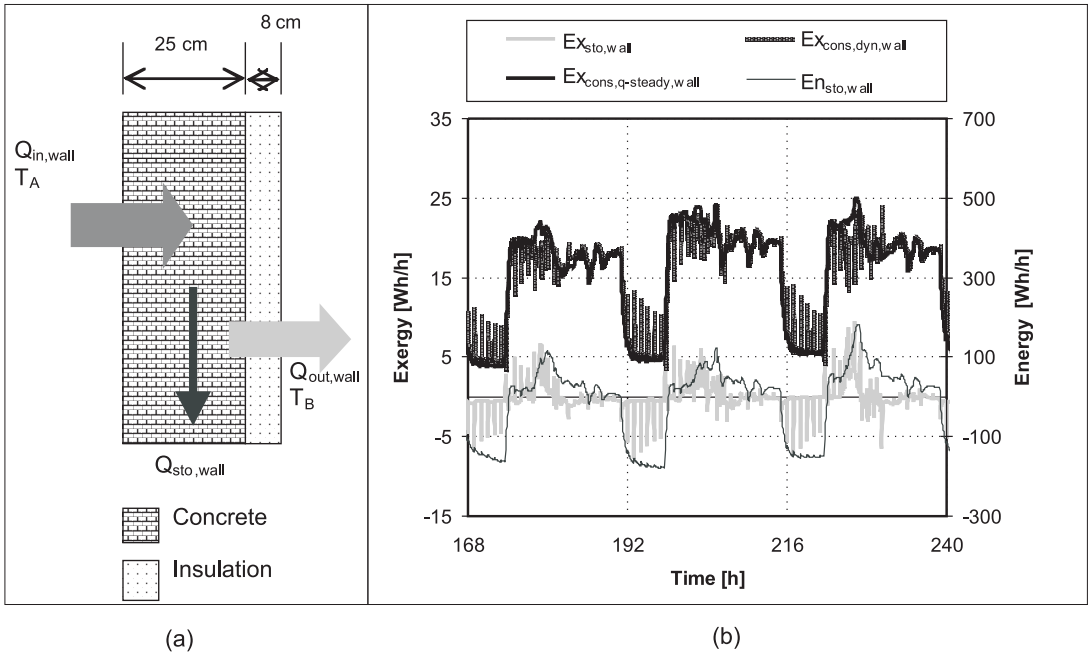

Figure 2.7: (a):Case study of an east facing wall of a building to show the difference between dynamic and quasi-steady state approaches for exergy analysis.(b):Dynamic behaviour of the exergy stored in the building wall and the exergy consumed following quasi-steady ($Ex_{cons,q-steady,wall}$) and dynamic ($Ex_{cons,dyn,wall}$) approaches. The energy ($En_{sto,wall}$) and exergy stored ($Ex_{sto,wall}$) in the wall are also shown.

$$Ex_{cons,q-steady}(t_k) = Q_{in,wall}(t_k)\left(1-\frac{T_0(t_k)}{T_A(t_k)}\right) + Q_{out,wall}(t_k)\left(1-\frac{T_0(t_k)}{T_B(t_k)}\right) \tag{2.22}$$

Energy stored in the wall can be calculated following equation 2.20. Energy inputs and outputs in the wall include convective, conductive and radiative energy inputs in the wall. As shown in equation 2.21, to evaluate the exergy of the energy stored in the wall, the temperatures of each wall layer (i index in the equation) are needed. However, wall models in TRNSYS use the Transfer Functions Method and a discretization of the wall is not directly possible (TRNSYS, 2007). Thus, as an approximation it has been assumed that the temperature of the wall in each timestep is the mean temperature between the inside and outside surface temperatures (T_A and T_B, respectively). Peaks in the dynamic approach are due to the strong influence of temperature variations inside the wall, as a result of the storage phenomena.

Despite the simplification, good agreement can be found for the behaviour of the exergy consumption with both approaches. The difference between the exergy consumption following both approaches amounts 0.32% on a monthly balance (January). The net exergy stored in the wall over one month represents 0.34% of the exergy input into the wall, being about one hundred times bigger than for the case of room-air (see the previous case study). Exergy

stored in each timestep represents a very different share of the exergy input into the wall, with values varying between 1% and 160%.

To avoid the influence of the periodicity of storage processes, both approaches are compared on a 12 hour basis. For the period of time between 168 h and 180 h, the exergy stored represents 0.84% of the exergy input in the room air, and the exergy consumed following a dynamic approach is only 0.85% lower than that estimated following a quasi-steady state approach. For the period of time between 180 h and 192 h, the exergy stored represents 2.37% of the exergy input in the room air, and the exergy consumed following a dynamic approach is 2.38% lower than that estimated following a quasi-steady state approach.

Thus, if the main aim of exergy analysis is to improve, study or optimize a building construction, i.e. the storage system taken as case study in this section, the dynamic behaviour of the exergy stored and consumed needs to be analyzed dynamically. A quasi-steady state approach is not accurate enough as to depict the dynamic behaviour of the exergy flows accurately. However, if the aim is to perform exergy analysis on a system level, the dynamic behaviour is not relevant, but total required exergy input over a certain period of time is enough. A quasi-steady state exergy assessment combined with dynamic energy analysis (including storage phenomena) is suitable in this case.

Additionally, for exergy analysis of building systems a further simplification can be done: exergy input into the building wall can be completely regarded as exergy consumed [Schmidt, 2004] (equation 2.23). This simplification would lead to a mismatch of 0.875% on a monthly basis as compared to the fully dynamic approach.

$$Ex_{cons,q-steady}(t_k) = Q_{in,wall}(t_k)\left(1 - \frac{T_0(t_k)}{T_A(t_k)}\right) \tag{2.23}$$

2.5 Summary on simplifications and assumptions for dynamic exergy analysis

From the general statements and case studies analyzed in the previous sections of this chapter, several simplifications can be derived:

- For heating applications (i.e. without humidity control or humidity treatment) the chemical exergy derived from differences in the humidity ratio between indoor and outdoor air can be disregarded. This is the case of building systems analyzed here.

- The contribution of pressure differences between indoor and outdoor air to the physical exergy of buildings without ventilation units is very small. In consequence, pressure differences can be disregarded. Following, only thermal exergy flows are assessed here.

- Outdoor air surrounding the building is considered as reference environment for exergy analysis. For this, it is considered as an infinite sink in thermo-mechanical equilibrium.

- A detailed assessment of the exergy of thermal radiation for radiant heating systems only leads to a shift in the exergy losses between the components of the energy supply chain (see section 2.3.2). Thus, if the performance of the whole building systems is the main focus of analysis this detailed assessment is not required, for the performance of building systems is the same as with a simpler assessment considering radiative heat transfer as conductive-convective. In consequence, this last simplified assessment is performed for the case studies in this thesis.

- A quasi-steady state approach allows accurate results for exergy analysis of building systems on a system level. Thus, in this work quasi-steady state equations are derived for the building systems analyzed (see chapter 3). Energy storage phenomena in the building structure are modeled dynamically but they are not assessed separately in exergy terms. Storage processes are only modeled in detail in exergy terms for the storage tank in the solar thermal systems. Since a small timestep (3 minutes) is used for all dynamic energy simulations presented here, and due to the small disagreement between fully dynamic and quasi-steady state approaches for exergy evaluation, exergy calculations in this thesis are regarded from here onwards as "dynamic".

These simplifications are applied to the dynamic exergy analysis of all building case studies in this work.

2.6 Review on exergy assessment of building systems

Several authors have applied in recent years the exergy concept to the analysis and optimization of building systems. Extensive scientific literature [Torío et al., 2009] can be found on the topic. However, different frameworks for exergy analysis have been regarded: most of the studies found use steady-state exergy analysis while only few authors perform dynamic assessment [Angelotti and Caputo, 2007; Torío and Schmidt, 2008]. Ambient air surrounding the building is chosen as reference environment in all papers analyzed in [Torío et al., 2009]. For dynamic assessment the dynamic variation of the temperature of ambient air is regarded. In turn, for steady-state analysis the reference state can be chosen upon several criteria: seasonal mean values, annual mean values, design conditions, etc. Due to the great sensitivity of exergy analysis for the particular case of space heating and cooling in buildings, each of these choices significantly influences results from exergy analysis and greatly constrains the comparison among results from different analyses. Furthermore, depending on the chosen definition for the reference environment significant mismatching between the steady-state and dynamic assessment of the exergy values can be found.

To the best of the authors knowledge there is no common agreement for a proper definition of the reference environment for steady state analysis. Therefore, future work in this direction is required [Torío et al., 2009]. These questions are assessed within the case studies analyzed in this doctoral thesis (see section 7.3.6).

In several papers reviewed [Torío et al., 2009] the boundaries for exergy analysis are often not clearly stated by the authors. Ambiguities on the definition of the boundaries are typically found both at the primary energy conversion step and at the heat exchange process within the building: while some authors regard electricity as an energy carrier following an end-energy approach [Dincer and Rosen, 2007; Hepbasli and Akdemir, 2004; Esen et al., 2007; Marletta, 2008] others consider the energy efficiency for its conversion from other energy sources, following a primary-energy approach [Alpuche et al., 2005]; the final output of a building system is regarded as the output from the emission systems or the indoor air energy and exergy demands [Ozgener and Hepbasli, 2007; Esen et al., 2007; Marletta, 2008].

Particularly, for the analysis of direct solar systems, two different approaches can be found for choosing the boundaries for exergy analysis: the first one (also called *technical boundary* [Torío and Schmidt, 2010]) regards the exergy losses from the conversion of solar radiation into the output of the solar system (electricity or heat), while the second one (also called *physical boundary* [Torío and Schmidt, 2010]) disregards this process. A thorough discussion on the physical correctness of the second approach over the first one can be found in [Torío and Schmidt, 2010]. The chosen approach greatly influences results and conclusions obtained from the analysis of solar systems.

The choice of the boundaries for performing exergy analysis significantly influences results and insights gained from it. This is obviously true also for energy analysis, but it is even more for an exergy analysis, due to the fact that exergy destruction would happen at each step of the energy chain even if energy losses were ideally zero (as it is the case of the heat emission system to the room air[13]). Therefore, the boundaries chosen should always be clearly stated.

Chapter 3 of this work describes clearly a method, based on the simplifications mentioned above, that can be followed for performing exergy assessment (dynamic or steady-state) of building systems. In this sense, it represents a contribution towards a unitary method for exergy assessment in buildings.

2.7 Exergy and sustainable development

Several authors [Cornelissen, 1997; Dincer and Rosen, 2007; Wall and Gong, 2001] have linked the exergy concept with insights on "sustainable energy supply" and "sustainable development". This link is based on the fact that exergy is a thermodynamic concept that clearly identifies the improvement potential of an energy system, thus opening up the possibility of increasing its efficiency [Rosen and Tang, 2008]. For this aim, all energy flows involved, fossil and renewable, must be analyzed. This allows showing the thermodynamic efficiency of using different energy sources, independently of their renewable or fossil character, and allows a common basis for the comparison of different energy sources and uses [Schmidt et al., 2007]. Since energy sources, and particularly fossil fuels, are limitedly available, increasing the ef-

[13] In previous examples and in the following chapter this conversion step is regarded in the *room air* subsystem.

ficiency of their utilization leads to increase the time span in which they can be utilized and reduce negative environmental impacts derived from their use (such as CO_2 emissions), thus increasing the “sustainability” of energy systems.

However, it must be clearly stated that systems based on renewable energy sources are more "sustainable" than fossil fuel based ones, even if the exergy efficiency of the first might be lower than that of an equivalent fossil-based alternative. The exergy concept does not distinguish between renewable and not renewable energy sources. This distinction, crucial for finding options towards a more "sustainable" energy supply, must always be regarded additionally to the exergy analysis.

In turn, conventional primary energy analysis is based on the distinction between renewable and fossil energy sources. The primary energy approach aims at limiting the use of fossil fuels for providing a given demand, leading to maximize the use of renewable energy sources. Since fossil primary energy input is the key parameter to be minimized, renewable energy flows are often disregarded in primary energy balances. An assessment of the efficiency of renewable energy use cannot be obtained from such analyses.

From a combined primary energy and exergy assessments advantages of both methods can be joined and their weaknesses leveled out. A combined exergy and primary energy assessment allows obtaining conclusions on the environmental impact AND thermodynamic efficiency of an energy system. Thus, exergy analysis should always be carried out besides primary energy analysis. Exergy is seen in this work as a complementary indicator to primary energy assessment and not as a substitute for it.

For all stated avobe, exergy can NOT be understood as an indicator able to depict sustainability on its own. Exergy performance and sustainability are not equivalent concepts, and exergy analysis can only be seen as a further indicator to complement existing analysis methods in order to develop more "sustainable" energy systems.

Chapter 3

Method for dynamic exergy analysis

3.1 Input-output approach

The aim of this thesis is to show possibilities for improving the energy and exergy performance of the whole energy supply chain in building systems. Thereby, analysis are mainly focused on a system perspective, where the whole supply chain is assessed, instead of on a component level, where the performance of single components of that supply chain is analyzed in detail. Optimization of single components is desirable and required, but the influence of optimizing one component on the performance of the whole supply system should always be regarded [Torío et al., 2009]. In this way, improvement of single components which might have a negative influence on other steps of the energy supply process is avoided.

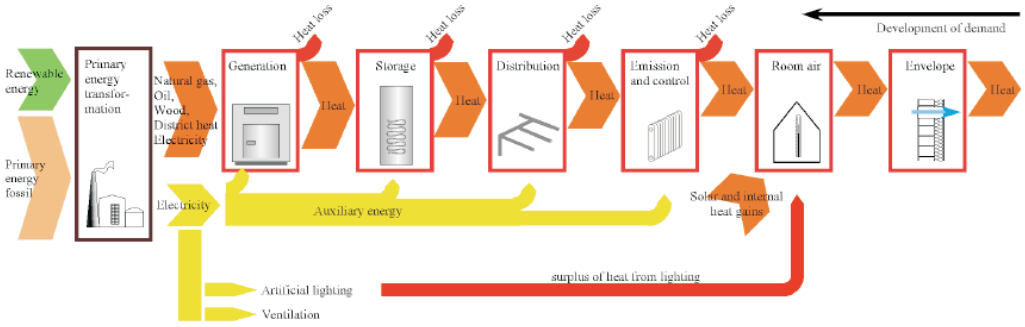

Figure 3.1: Energy supply chain for space heating in buildings, from primary energy transformation to final energy, including all intermediate steps up to the supply of the building demand [Schmidt, 2004; DIN 4701-10, 2001].

Energy and exergy analysis on a system level are performed following the input-output approach found in many building energy regulations [EnEV, 2009; DIN 4701-10, 2001; DIN 18599, 2007], where the supply chain is divided into several subsystems directly related with each other, as shown in Figure 3.1. This input-output approach can be applied both for steady-state [Annex 49, 2010a] and dynamic exergy analysis. Equations for a dynamic analysis based on this input-output scheme are shown in detail in section 3.2 for each of the subsystems in

Figure 3.1.

3.2 Mathematical models for exergy analysis of building systems

In the following subsections the equations and exergy balances for each of the subsystems in Figure 3.1 are presented.

The equations for the subsystems are based on those presented in Schmidt [2004]. However, they have been enhanced for a quasi-steady exergy analysis. Quasi-steady exergy assessment has shown to be a reasonable compromise between accuracy and complexity[1]. Only for storage systems (e.g. storage tanks) equations for fully dynamic assessment are introduced.

The analytical definition of physical exergy is derived applying energy and entropy balances to a combined system that consists of the system to be analyzed and the surrounding environment. The analyzed system can be either a control mass or control volume (i.e. a closed or open system), whereas the combined system is a control mass where only work interactions can take place across the boundary [Moran and Shapiro, 1998]. For each subsystem, a Figure shows the boundaries for the combined system (dashed line) and the system analyzed (dotted line) regarded for the exergy balance.

The equations and subsystems presented here refer to the particular case of DHW and space heating supply in buildings. For sensible cooling systems these equations can be applied as long as the same sign convention is considered.

3.2.1 Exergy demand for DHW supply

The exergy demand for DHW supply $Ex_{dem,DHW}$ can be evaluated as a function of the required setpoint temperature for DHW use and the demanded mass flow, as shown in equation 3.1, where m_{DHW} is the mass flow for DHW demand over a given timestep t_k, $T_{sup,DHW}$ and T_{cw} are the absolute values of the regarded setpoint temperature for DHW supply and the cold water temperature respectively.

$$\begin{aligned} Ex_{dem,DHW}(t_k) =& m_{DHW}(t_k) \cdot c_{p,w} \cdot (T_{sup,DHW}(t_k) - T_{cw}(t_k)) \\ & - m_{DHW}(t_k) \cdot c_{p,w} \cdot T_0(t_k) \cdot \ln \frac{T_{sup,DHW}(t_k)}{T_{cw}(t_k)} \end{aligned} \tag{3.1}$$

3.2.2 Building envelope

$Q_{h,b}$ represents the net active heating demand of the building. Storage phenomena in the building construction are also simulated dynamically and taken into account in the energy

[1] See case studies for the *room air* and *building wall* presented in chapter 2.

balance. It is assumed that the heat flow $Q_{h,b}$ takes place at the indoor operative temperature[2], assumed as constant for each timestep. The exergy of the heat flow out of the building shell $Ex_{out,env}$ is neglected[3].

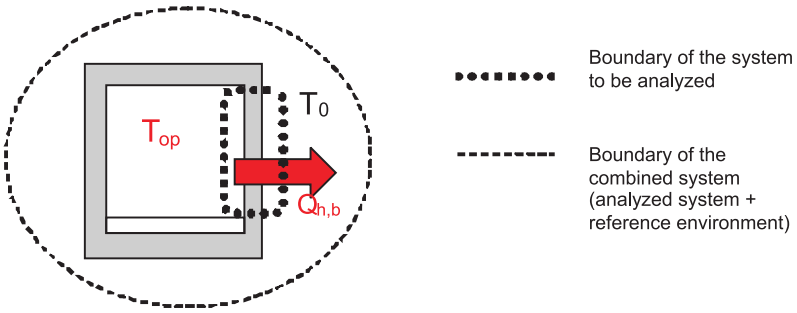

Figure 3.2: Energy flows, temperature levels and boundaries for the building envelope subsystem.

$$Ex_{in,env}(t_k) + \underbrace{Ex_{out,env}(t_k)}_{\approx 0} = Ex_{cons,env}(t_k) \tag{3.2}$$

With this evaluation framework, the net heat demand $Q_{h,b}$ is transferred to the reference environment through the building envelope, i.e. it is consumed during the process as it reaches outdoor air. The corresponding exergy $Ex_{dem,SH}$, which represents the exergy demand for SH supply, is calculated according to equation 3.3.

$$Ex_{in,env}(t_k) = Ex_{cons,env}(t_k) = Q_{h,b}(t_k) \cdot \left(1 - \frac{T_0(t_k)}{T_{op}(t_k)}\right) = Ex_{dem,SH}(t_k) \tag{3.3}$$

3.2.3 Room air subsystem

The *room air* subsystem is introduced to account for the exergy losses between the chosen emission system (at its surface temperature T_h[4]) and the exergy demand of the building $Ex_{dem,SH}$(at its operative temperature T_{op}), since these losses should neither be assigned to the emission system nor to the exergy demand. The energy output from the emission system equals the energy demand, but the exergy is necessarily different due to the difference in temperature allowing the heat transfer process between the heating system and the indoor air to take place.

The surface temperature of the heater θ_h when radiators are used is estimated here by means of the arithmetic mean of the inlet and return temperatures. This is a suitable simplifi-

[2]For the building systems analyzed in this thesis operative temperatures are the controlled variable, i.e. they determine the heat demand. Therefore, for estimating the exergy demand the operative temperature inside the building T_{op} is used in equation 3.3. Alternatively, room air temperatures T_r can be used.

[3]This is a suitable simplification, as shown in the case study (*room-air*) in section 2.4.2.4 of chapter 2.

[4]The subscript *h* stands here for *heater*.

cation [Recknagel et al. 2007][5]. Furthermore, the aim here is not to optimize the radiators, but the whole system performance. Differences between estimations using the logarithmic mean temperature difference and the arithmetic mean are very small [6] and, more importantly, they are irrelevant for the purpose of analysis, since they only shift exergy losses between the room air and emission systems and do not affect the whole exergy performance of the system.

When floor heating systems are used, surface temperatures from the building element with the embedded active layer in TRNSYS [2007] are used.

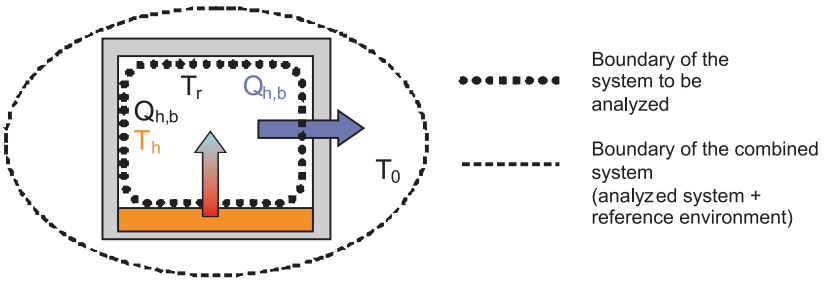

Figure 3.3: Energy flows, temperature levels and boundaries for the room air subsystem.

Equation 3.4 shows the exergy balance for the room air subsystem. Equations 3.5 and 3.6 show the exergy going into and out of the room air, respectively. In equation 3.7 these are used to calculate the exergy consumption occurring during the heat transfer process as a result of the temperature difference between the heater surface and the room air temperature.

$$Ex_{in,r}(t_k) + Ex_{out,r}(t_k) - Ex_{cons,r}(t_k) = 0 \tag{3.4}$$

$$Ex_{in,r}(t_k) = Ex_{h,b,in}(t_k) = Q_{h,b}(t_k) \cdot \left(1 - \frac{T_0(t_k)}{T_h(t_k)}\right) \tag{3.5}$$

$$Ex_{out,r}(t_k) = Ex_{h,b,out}(t_k) = -Q_{h,b}(t_k) \cdot \left(1 - \frac{T_0(t_k)}{T_{op}(t_k)}\right) \tag{3.6}$$

$$Ex_{cons,r}(t_k) = Ex_{h,b,in}(t_k) + Ex_{h,b,out}(t_k) = Q_{h,b}(t_k) \cdot T_0(t_k) \cdot \left(\frac{1}{T_{op}(t_k)} - \frac{1}{T_h(t_k)}\right) \tag{3.7}$$

3.2.4 Emission subsystem

The exergy balance of the emission system is shown in equation 3.8.

[5]The arithmetic mean can be used if the condition $(\theta_{ret,ce} - \theta_r)/(\theta_{in,ce} - \theta_r) \geq 0.7$ is fulfilled. For design conditions in the radiators, i.e. supply/return and room air temperatures of 55/45/20°C, this condition is fulfilled.

[6]on the range of 0.5°C for the surface temperature, yielding differences in the quality factors of around 1%

$$\begin{aligned} Ex_{in,ce}(t_k) + Ex_{ret,ce}(t_k) + (-Ex_{h,b,in}(t_k)) &= Ex_{irrev,ce}(t_k) - Ex_{ls,ce}(t_k) \\ &= Ex_{cons,ce}(t_k) \end{aligned} \tag{3.8}$$

Where the subindex *in* stands for inlet, *ret* for return, *h* for heating , *b* for building, *ls* for energy losses and *ce* for emission system. The additional exergy demand resulting from energy losses on the heat transfer process $Ex_{ls,ce}$ can be added to the exergy consumption resulting from an irreversible heat transfer $Ex_{irrev,ce}$. In this manner, the total exergy consumption in the emission system $Ex_{cons,ce}$ can be obtained.

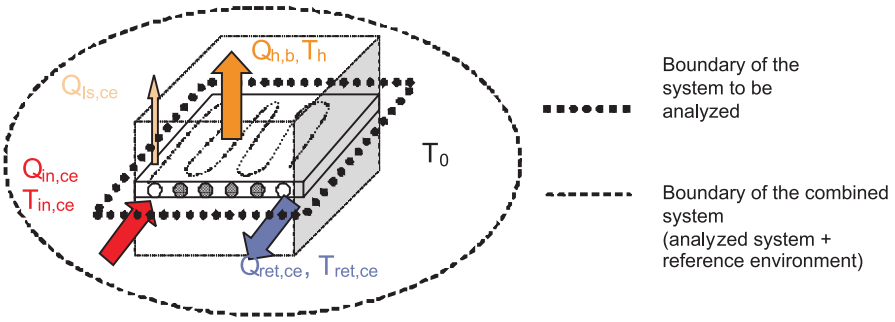

Figure 3.4: Energy flows, temperature levels and boundaries for the emission subsystem.

In equation 3.9 the expression for the exergy consumption is given. Equation 3.10 shows the thermal exergy demand of the emission system[7]

$$Ex_{cons,ce}(t_k) = m_{w,ce}(t_k) \cdot c_{p,w} \left[(T_{in,ce}(t_k) - T_{ret,ce}(t_k)) - T_0(t_k) \cdot \ln \frac{T_{in,ce}(t_k)}{T_{ret,ce}(t_k)} \right] - Ex_{h,b,in}(t_k) \tag{3.9}$$

$$\begin{aligned} Ex_{ce}(t_k) &= Ex_{h,b,in}(t_k) + Ex_{cons,ce}(t_k) = Ex_{in,ce}(t_k) + Ex_{ret,ce}(t_k) \\ &= m_{w,ce}(t_k) \cdot c_{p,w} \left[(T_{in,ce}(t_k) - T_{ret,ce}(t_k)) - T_0(t_k) \cdot \ln \frac{T_{in,ce}(t_k)}{T_{ret,ce}(t_k)} \right] \end{aligned} \tag{3.10}$$

3.2.5 Distribution system

For evaluating distribution pipes Type 31 in TRNSYS [2007] is used. This component models the thermal behavior of a fluid or fluid flow in a pipe using variable size segments of fluid with a plug-flow approach. Entering fluid shifts the position of existing segments. The outlet is then a collection of the elements that are pushed out by the inlet flow. Outlet temperatures are a result of the initial inlet temperatures of each segment and the corresponding thermal

[7] $Q_{ls,ce}$ and Q_{ret} are considered as negative (energy outputs from the emission system).

losses while circulating or being contained in the pipe. To model exactly the exergy losses associated to these thermal losses the dynamic variation of the temperature in each segment within the pipe would be required (see equation 3.12). The exergy of thermal losses would then be evaluated as the change in the exergy content of the fluid in the pipes. Equation 3.12 is written for N segments contained in the pipe, being i the index for each segment, and assuming that water is the fluid circulating in the pipes (subindex w for the specific heat capacity, $c_{p,w}$).

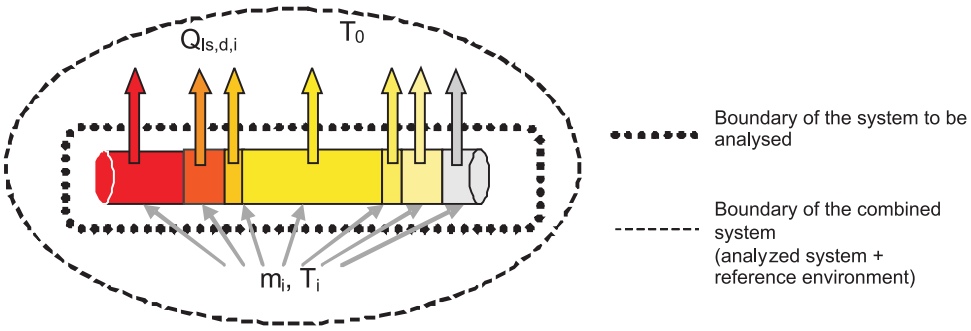

Figure 3.5: Temperature and mass of *i* segments within the plug-flow pipe model used to simulate the distribution subsystem. Boundaries for exergy analysis of the distribution subsystem are also shown.

$$Ex_{in,d}(t_k) + Ex_{ret,d}(t_k) - Ex_{cons,d}(t_k) = 0 \tag{3.11}$$

$$Ex_{cons,d}(t_k) = \sum_{i=1}^{i=N} m_{i,w,d}(t_k) c_{p,w} \left[(T_i(t_k) - T_i(t_{k-1})) - T_0(t_k) \ln \frac{T_i(t_k)}{T_i(t_{k-1})} \right] \tag{3.12}$$

However the temperature in each segment cannot be obtained as output from Type 31. Instead, an average temperature calculated as a mass weighted average of the temperatures of all segments contained in each timestep can be obtained and is used in the calculations.

$$Ex_{cons,d}(t_k) = m_{w,d}(t_k) c_{p,w} \left[(\langle T_d(t_k) \rangle - \langle T_d(t_{k-1}) \rangle) - T_0(t_k) \ln \frac{\langle T_d(t_k) \rangle}{\langle T_d(t_{k-1}) \rangle} \right] \tag{3.13}$$

3.2.6 Mixing from return water from space heating

For supplying space heating demands a mixing valve is foreseen as shown in Figure 3.6. The valve mixes supply water from the boiler or storage tank with return water from the heating system and thereby, the supply temperature demanded by the heating system is achieved.

In the mixing process no energy losses are present. The outlet temperature from the mixing valve $T_{out,mix}$ is a result of the inlet temperatures from the supply and return pipes and their corresponding mass flows. In turn, in the mixing process exergy losses arise. Equation 3.14

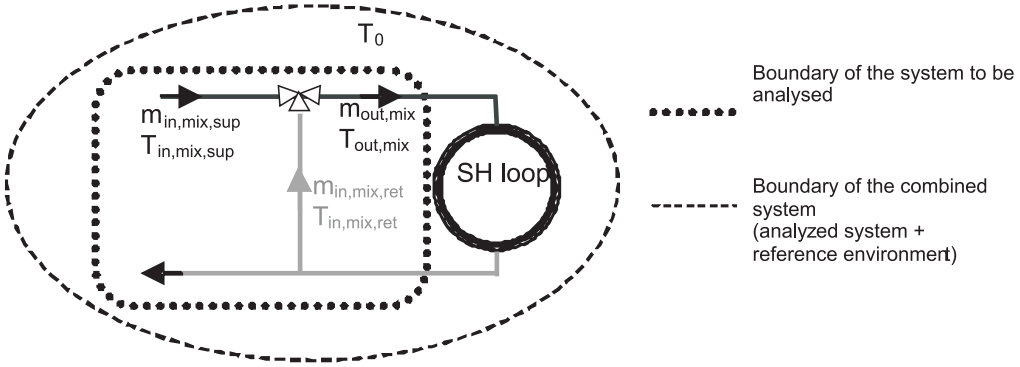

Figure 3.6: Mixing valve used in space heating: temperature levels and mass flows involved in the mixing process. Boundaries used for exergy analysis are also shown.

shows the exergy balance for the mixing valve.

$$Ex_{in,mix,sup}(t_k) + Ex_{in,mix,ret}(t_k) + Ex_{out,mix}(t_k) = Ex_{cons,mix}(t_k) \tag{3.14}$$

Where the single terms in equation 3.14 can be written as follows:

$$\begin{aligned} Ex_{in,mix,sup}(t_k) =& m_{in,mix,sup}(t_k) \cdot c_{p,w} \cdot (T_{in,mix,sup}(t_k) - T_0(t_k)) \\ & - m_{in,mix,sup}(t_k) \cdot c_{p,w} \cdot T_0(t_k) \cdot \ln \frac{T_{in,mix,sup}(t_k)}{T_0(t_k)} \end{aligned} \tag{3.15}$$

$$\begin{aligned} Ex_{in,mix,ret}(t_k) =& m_{in,mix,ret}(t_k) \cdot c_{p,w} \cdot (T_{in,mix,ret}(t_k) - T_0(t_k)) \\ & - m_{in,mix,ret}(t_k) \cdot c_{p,w} \cdot T_0(t_k) \cdot \ln \frac{T_{in,mix,ret}(t_k)}{T_0(t_k)} \end{aligned} \tag{3.16}$$

$$Ex_{out,mix}(t_k) = m_{out,mix}(t_k) c_{p,w} \left[(T_0(t_k) - T_{out,mix}(t_k)) - T_0(t_k) \ln \frac{T_0(t_k)}{T_{out,mix}(t_k)} \right] \tag{3.17}$$

3.2.7 Heat exchanger

Heat exchangers are modeled as adiabatic components in this thesis, i.e. no energy losses are associated to the heat exchange process. Yet, the mass flows and temperature levels at the inlet and outlet of the primary and secondary sides are different. Thereby, exergy consumption during the heat transfer process arises. Equation 3.18 shows the general expression for the exergy balance of a heat exchanger, being $Ex_{in,hx}$ the exergy input from the primary side of the heat exchanger, $Ex_{out,hx}$ the exergy output at the secondary side and $Ex_{cons,hx}$ the exergy consumed in the heat transfer process.

$$Ex_{in,hx}(t_k) + Ex_{out,hx}(t_k) = Ex_{cons,hx}(t_k) \tag{3.18}$$

The exergy input and output at the primary and secondary sides of the heat exchanger (shown in equation 3.18) can be written as follows:

$$\begin{aligned} Ex_{in,hx}(t_k) =& m_{prim,hx}(t_k) \cdot c_{p,w} \cdot (T_{in,prim,hx}(t_k) - T_{out,prim,hx}(t_k)) \\ & - m_{prim,hx}(t_k) \cdot c_{p,w} \cdot T_0(t_k) \cdot \ln \frac{T_{in,prim,hx}(t_k)}{T_{out,prim,hx}(t_k)} \end{aligned} \tag{3.19}$$

$$\begin{aligned} Ex_{out,hx}(t_k) =& m_{sec,hx}(t_k) \cdot c_{p,w} \cdot (T_{in,sec,hx}(t_k) - T_{out,sec,hx}(t_k)) \\ & - m_{sec,hx}(t_k) \cdot c_{p,w} \cdot T_0(t_k) \cdot \ln \frac{T_{in,sec,hx}(t_k)}{T_{out,sec,hx}(t_k)} \end{aligned} \tag{3.20}$$

3.2.8 Storage subsystem

The main purpose of a storage system is to achieve a time delay between the energy supply and energy demand. Correspondingly, the energy stored in the system is the most important variable for the definition of the storage system, and, subsequently, the exergy associated to the storage process cannot be added to the exergy consumption as it is done for other components of energy systems on a quasi-steady state approach.

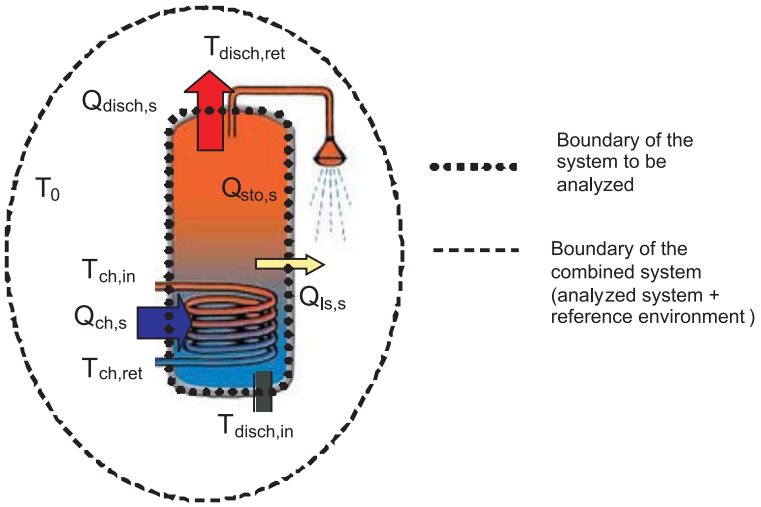

Figure 3.7: Energy flows, temperature levels and boundaries for the storage subsystem.

The general exergy balance for the storage subsystem can be formulated as a function of the charge and discharge processes (equation 3.21). Equations 3.22 and 3.23 show the expressions for calculating the exergy of the charge and discharge processes in the storage tank.

$$Ex_{ch,s}(t_k) + Ex_{disch,s}(t_k) = Ex_{cons,s}(t_k) + Ex_{sto,s}(t_k) \tag{3.21}$$

$$Ex_{ch,s}(t_k) = m_{ch,s}(t_k) \cdot c_{p,w} \cdot \left[(T_{ch,in}(t_k) - T_{ch,ret}(t_k)) - T_0(t_k) \cdot \ln \frac{T_{ch,in}(t_k)}{T_{ch,ret}(t_k)} \right] \tag{3.22}$$

$$\begin{aligned} Ex_{disch,s}(t_k) =& m_{disch,s}(t_k) \cdot c_{p,w} \cdot (T_{disch,in}(t_k) - T_{disch,ret}(t_k)) \\ & - m_{disch,s}(t_k) \cdot c_{p,w} \cdot T_0(t_k) \cdot \ln \frac{T_{disch,in}(t_k)}{T_{disch,ret}(t_k)} \end{aligned} \tag{3.23}$$

The energy losses and storage process in the system are time dependent processes and result in a temperature change of the fluid in the storage tank. Consequently, the dynamic behaviour of the temperature in each storage layer needs to be taken into account for their assessment. For a given storage tank with *n* layers of storage fluid, the exergy stored can be written as shown in equation 3.24 The exergy stored in a well-mixed tank can be calculated with one fluid layer *(n=1)*, whereas that of a stratified tank can be assessed by increasing the number of fluid layers. Following the sign convention stated in chapter 2 the exergy stored is defined as positive if it represents an exergy input in the storage system and negative otherwise (i.e. if it is exergy released from the tank).

$$Ex_{sto,s}(t_k) = \sum_{i=1}^{i=n} m_i(t_k) \cdot c_{p,i} \cdot \left[(T_{i,s}(t_k) - T_{i,s}(t_{k-1})) - T_0(t_k) \cdot \ln \frac{T_{i,s}(t_k)}{T_{i,s}(t_{k-1})} \right] \tag{3.24}$$

As for the emission system, the total exergy consumption can be calculated by adding the exergy consumption associated to thermal energy losses from the storage tank and those corresponding to irreversibilities in the heat storage and transfer processes (equation 3.25)[8].

$$Ex_{cons,s}(t_k) = Ex_{irrev,s}(t_k) - Ex_{ls,s}(t_k) \tag{3.25}$$

The exergy stored in the tank is a function of the initial and final temperatures of each node for a given timestep (see equation 3.24). This depicts the change in the exergy content of the storage tank over a given time period. Instead, the exergy content of the storage gives the actual exergy level of the storage tank at a given moment as compared to the reference temperature at that time. Thus, the latest is a function of the temperature of each tank layer at a given moment and the chosen reference temperature. The expression for evaluating the exergy content of the storage tank is shown in equation 3.26.

$$Ex_{content,s}(t_k) = \sum_{i=1}^{i=n} m_i(t_k) \cdot c_{p,i} \cdot \left[(T_{i,s}(t_k) - T_0(t_k)) - T_0(t_k) \cdot \ln \frac{T_{i,s}(t_k)}{T_0(t_k)} \right] \tag{3.26}$$

[8]The energy $Q_{ls,s}$ and exergy losses $Ex_{ls,s}$ from the storage tank are regarded as negative values, i.e. outputs from the storage tank.

3.2.8.1 Case study

To check the plausibility and correctness of the equations derived for assessing the dynamic exergy behaviour of the storage system a simple case study has been analyzed. Additionally, the influence of thermal stratification on the energy and exergy performance of the storage unit is analyzed.

For this purpose, a 1500 l storage tank is simulated with a 3-minute timestep and with constant mass flows for the charge and discharge processes. Type 340 in TRNSYS [2007] is used for performing the analysis, since it is also the Type implemented in the building case studies analyzed in this thesis. A constant reference temperature of 0°C is assumed for all calculations here. Under this assumption, and considering also an initial temperature equal to the reference temperature, the integral of the exergy stored over a given time period is equal to the exergy content of the storage tank at the end of the time period. This allows crosschecking the correctness of the equations shown above to calculate both variables (equations 3.24 and 3.26). Constant mass flows and temperatures for the charge and discharge of the storage tank are assumed. Main assumptions are summarized in Table 3.1. The charge and discharge profiles are shown in Figure 3.8 .

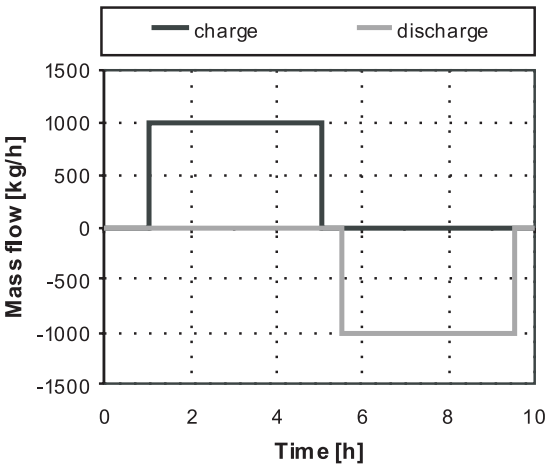

Figure 3.8: Time dependence of the mass flows for charge and discharge processes assumed.

Table 3.1: Main temperatures assumed for the simplified case study studied here.

	[°C]
Initial tank temperature, $\theta_{s,ini}$	0
Inlet charge temperature, $\theta_{ch,in}$	90
Inlet discharge temperature, $\theta_{disch,in}$	10
Surrounding temperature, $\theta_{s,surr}$	0
Reference temperature, θ_0	0

Influence of thermal stratification Stratification in the storage tank influences the performance of energy supply systems coupled with the storage unit, e.g. solar thermal systems. Thermal stratification inside the tank can be varied by changing the number of nodes[9] in the tank model.

[9]Nodes are layers of fluid in the tank assumed to be completely mixed. See section 4.7 for a detailed description of the tank model.

In Figure 3.9 energy and exergy balances for the storage tank over 10 hours, i.e. after completing the charge and discharge processes, are shown for 5, 20 and 100 nodes[10].

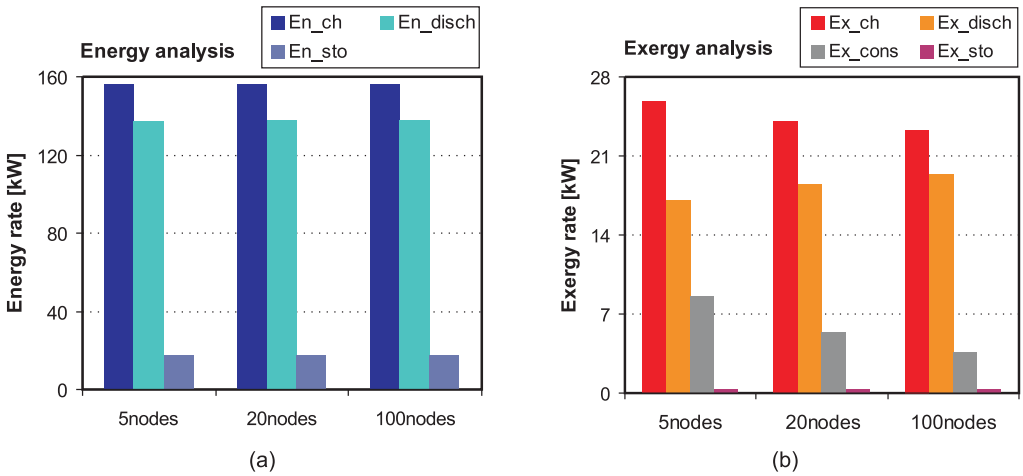

Figure 3.9: Energy (a) and exergy (b) balances over 10 hours for three different numbers of nodes assumed for modelling the storage tank.

The energy charged, discharged and stored is nearly independent from the thermal stratification in the tank, increasing only 0.1% and 0.2% with 20 and 100 nodes as compared to the model with 5 nodes. In turn, the exergy charged and discharged varies significantly with the number of nodes: with 20 and 100 nodes the exergy charged is reduced by 6.7% and 9.8%, respectively. On the contrary, the exergy discharged increases in 8.4% and 13.6%, respectively. Following, A reduction of 34% and 57% in the exergy consumed is found for 20 and 100 nodes respectively, as compared to 5 nodes. In the following paragraphs the reasons for this behaviour of the exergy flows during the charge and discharge of the tank are shown in detail.

Charge process Figure 3.10 (a) shows the top and bottom temperatures inside the storage tank. With increasing number of nodes, mixing is prevented and the temperature at the bottom begins to increase with a delay as compared to the model with 5 nodes. This is coherent with the energy flows shown in Figure 3.10 (c) (thin lines): with 100 and 20 nodes the temperature difference between inlet and outlet of charging flow is greater during the first hour, and so greater energy is being charged in the tank.

At 3 hours the tank with 100 and 20 nodes is almost fully charged, and yet there is a significant charging flow for the model with 5 nodes, due to the lower temperature in the bottom which still allows for energy income from the charging flow. In terms of energy, this just means a slower charging process, i.e. a time shift in the energy flow as shown in the

[10]With the adopted sign convention (see chapter 2) both the energy and exergy discharged represent an output from the storage as energy system, being, thus, negative. However, to ease representation the discharged energy and exergy are depicted as positive values in Figure 3.9.

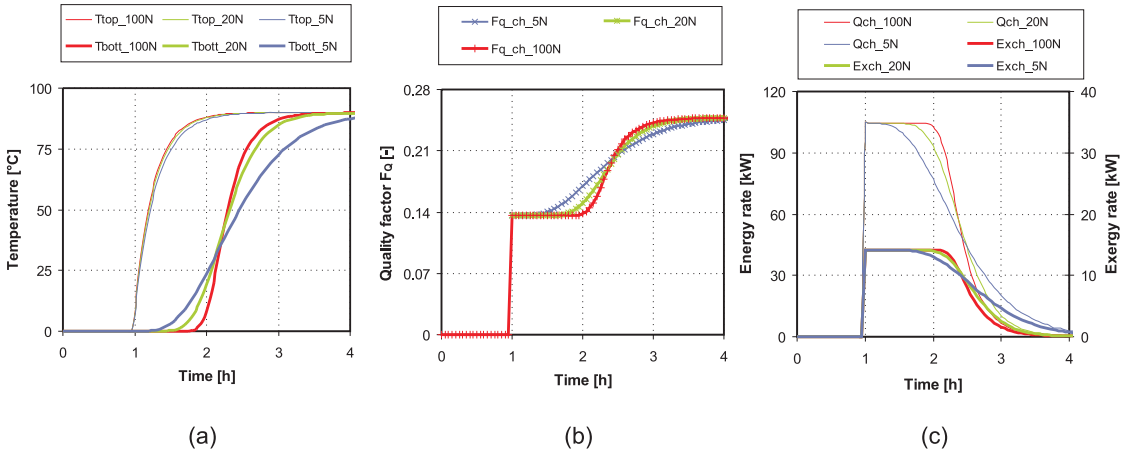

Figure 3.10: Temperature profiles at the top and bottom of the tank (a), quality factors (b) and energy and exergy rates (c) for the charge process with 5, 20 and 100 nodes.

Figure 3.10 (c).

In Figure 3.10 (b) the quality factor for the exergy charged is shown (equation 3.27). As the bottom temperature increases, the quality factor, i.e. the exergy associated to the energy flow, increases. With 20 and 100 nodes the energy flow at the highest quality factor is very low, while the greatest part of the energy charge happens at low quality factors. In turn, with 5 nodes a great part of the charging process takes place at that range of high quality factors, increasing the exergy input from the charge process. This means that higher number of nodes, i.e. stratified charge, allows extracting the same amount of energy from the charge flow with lower exergy content (see Figure 3.9). The exergy charged in the storage tank is thus reduced.

$$F_{Q,ch,s}(t_k) = 1 - \frac{T_0(t_k)}{(T_{ch,in}(t_k) - T_{ch,ret}(t_k))} \ln \frac{T_{ch,in}(t_k)}{T_{ch,ret}(t_k)} \tag{3.27}$$

Discharge process In Figure 3.11 (a) the temperature profile for the top and bottom sensors during the discharge process are shown for 5, 20 and 100 nodes. The temperature at the bottom of the storage tank is quite similar, independently of the number of nodes. However, the temperature at the top layer differs significantly. With increasing number of nodes, mixing is prevented and it takes longer to begin cooling down the top layers with the incoming cold water flow.

Similarly as for the charge process, with 100 nodes the biggest part of the energy is discharged at the range of high quality factors, i.e. at high temperatures (see thin lines in Figure 3.11 (c)). In turn, with 5 nodes cold water mixes more quickly with hot water in the tank, and the discharge happens at lower temperatures, i.e. with lower quality factors.

The energy extracted, i.e. discharged, is similar for 5, 20 and 100 nodes as stated above (and shown in Figure 3.9). However, promoting stratification and preventing mixing in the tank allows extracting that energy more quickly and at higher temperature ranges. Thus, the

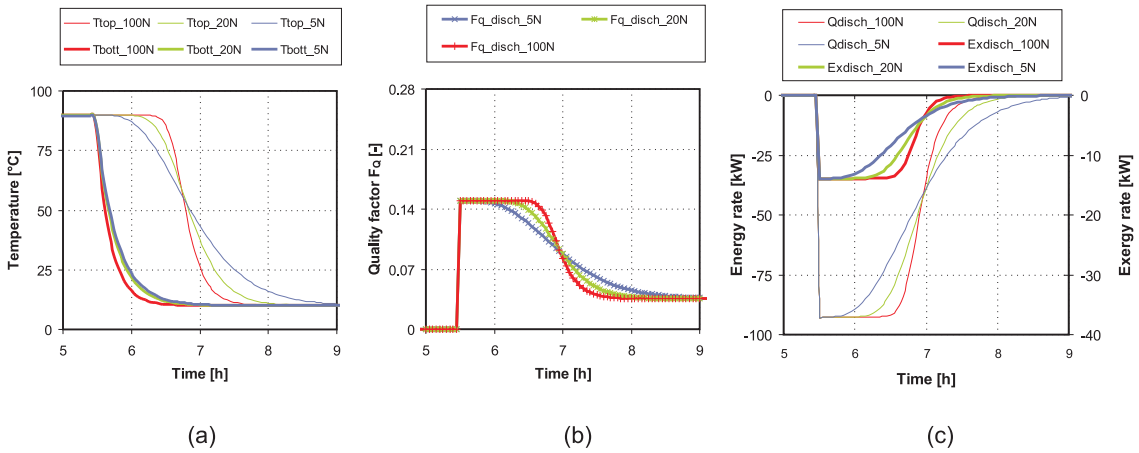

Figure 3.11: (Temperature profiles at the top and bottom of the tank (a), quality factors (b) and energy and exergy flows (c) for the discharge process with 5, 20 and 100 nodes.

exergy extracted increases, as shown in Figure 3.9 (b).

Influence of the reference temperature in the exergy content The exergy content of the storage tank (equation 3.26) represents the exergy level, i.e. potential of the energy stored in the tank, as compared to the given reference temperature at a given moment. If a constant reference temperature is assumed for the analysis of the storage tank, the difference between the exergy content at a given timestep and the next represents the exergy stored in the tank (equation 3.24). In consequence, under this assumption the integral of the exergy stored should be equal to the exergy content of the storage tank for each moment. This is shown in Figure 3.12 (a).

If, in turn, a variable reference temperature is assumed, the exergy content varies as a result of the variation in the reference temperature and not only as a function of a change in the energy stored. In other words, with variable reference temperature the exergy content of the storage tank (i.e. its potential) varies with varying reference temperatures even if no energy store or release occurs. In consequence, no matching can be found between the cumulative of the exergy stored and the exergy content of the storage tank. This is shown graphically in Figure 3.12 (b), where the reference temperature is assumed to increase from 0°C to 15°C at 5 hours.

For analyzing the dynamic exergy performance of storage systems with variable reference temperatures, the exergy content is not relevant. Instead, the exergy stored shall be used.

3.2.9 Generation subsystem

In this subsystem the exergy performance of energy supply units in buildings shall be assessed. In the following sections, the exergy assessment of energy supply components analyzed in this thesis is explained in detail.

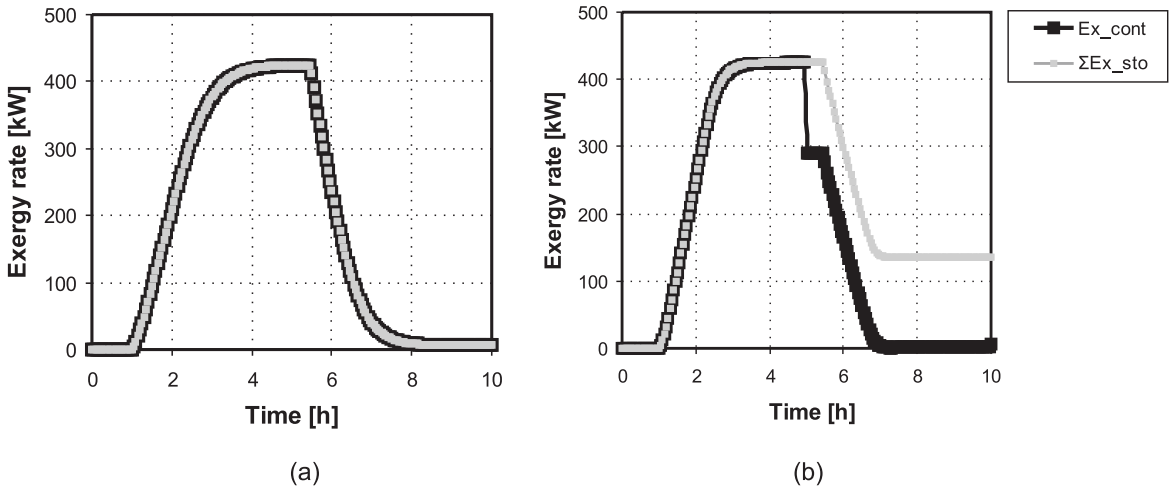

Figure 3.12: (a): Cumulative of the exergy stored $\sum \dot{Ex}_{sto}$ and exergy content $\dot{Ex}_{cont}$ assuming a constant reference temperature of 0°; (b): Summ of the exergy stored $\sum \dot{Ex}_{sto}$ and exergy content $\dot{Ex}_{cont}$ assuming a reference temperature of 0° until 5h and 15°C afterwards.

3.2.9.1 Boiler

The thermal exergy demanded by the boiler can be calculated as a function of the energy content of the fuel used, Q_g, and the corresponding quality factor associated to the energy carrier, $F_{Q,g}$, which is dependent on its chemical properties, as shown in equation 3.28.

$$Ex_g(t_k) = Q_g(t_k) \cdot F_{Q,g} \tag{3.28}$$

In Table 3.2 quality factors found in the literature for different fuels related to their higher heating value (HHV) are shown [Kühler, 2008; Ptasinski et al., 2005; Szargut and Styrylska, 1964].

Table 3.2: Quality factors for different fuels related to their higher heating value (HHV).

Fuel	$F_{Q,HHV}$ [-]	Fuel	$F_{Q,HHV}$ [-]
Brown coal	1.04	Oil	1.00
Wood	1.05	Natural gas	0.95

3.2.9.2 Solar collectors

Solar thermal collectors are energy conversion devices which directly use the energy supplied by incident solar radiation. Direct use of solar radiation instead of degrading other high quality energy resources found in nature is advantageous. Yet, due to physical inconsis-

tencies present in the exergy analysis framework commonly found in literature for assessing direct-solar systems high exergy losses arise in the conversion process of solar radiation in direct-solar systems. In turn, these losses are disregarded in indirect-solar systems.

As part of this thesis a physically consistent boundary for exergy analysis of direct solar systems (called *physical boundary*) has been developed. In the following section this framework is introduced besides the commonly found approach. A more detailed discussion on this issue can be found in [Torío and Schmidt, 2010].

Physical inconsistencies in commonly found framework Considering energy processes on the planet as a whole, the earth is an open system receiving a net energy flux from the sun in the form of short-wave solar radiation and emitting more or less the same energy amount as long-wave thermal radiation [Shukuya and Komuro, 1996]. Other energy forms and processes present on earth are derived to a large extent from incident solar radiation, e.g. potential energy in water masses or the energy content of biomass and crops or fossil fuels, as shown in the energy conversion chains depicted in Figure 3.13 for 12 energy systems [Szargut, 2005; Sorensen, 2004].

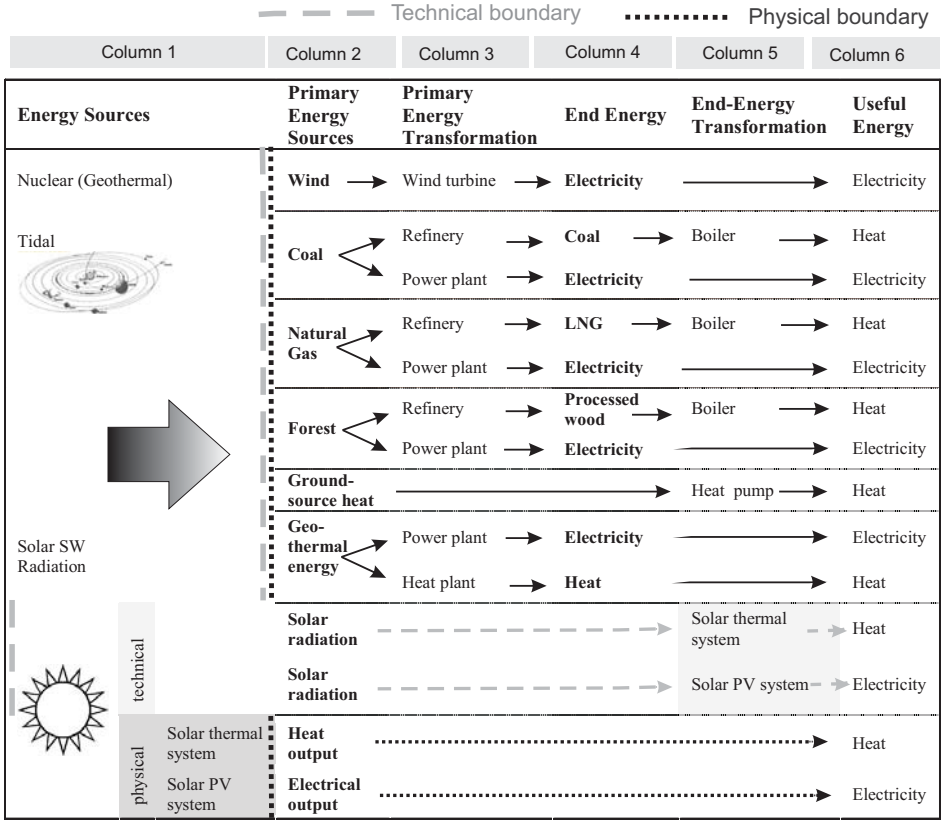

Figure 3.13: Energy chain for 12 energy systems, from *sources* to final uses, including direct-solar systems. The dashed light grey line represents the *technical boundary* typically used for the analysis of energy systems. The dotted dark grey line represents the *physical boundary* proposed here.

When analyzing the energy conversion chain of any certain appliance or usage, the conversion process from the energy inputs into the earth as energy system (*energy sources*, column 1 in Figure 1) into *primary energy sources* (column 2) is often left out of consideration. In other words, the efficiency of the conversion from solar radiation into the kinetic energy in the wind, chemical energy in wood or low-temperature heat in the earth surface (i.e. ground-source heat) is disregarded: the energy content of these *primary energy sources* is considered as existing within the earth-system and ready to be used. Thus, *primary energy sources* are regarded as the first energy input in the primary energy transformation system (column 3).

This boundary is drawn from a *technical* point of view (dashed line in Figure 3.13), i.e. it is place at the first step where some form of technical input is required to make use of the available energy. In the literature, this *technical boundary* is also kept for the analysis of direct solar systems (light grey dashed line in the penultimate row in Figure 3.13), e.g. solar thermal, and photovoltaic (PV) systems.

However, from a physical point of view, an inconsistency arises from this analysis framework: the efficiency of the conversion from solar radiation into other energy forms is included in the analysis of direct solar systems and left out in the rest (i.e. indirect-solar systems). In consequence, efficiencies as well as total energy and exergy losses of indirect- and direct-solar systems are not comparable, since in direct-solar systems a further energy conversion process is being regarded.

Proposed boundary for exergy analysis of direct solar systems In order to withdraw a physically consistent boundary for direct-solar systems, the conversion process from solar radiation into heat or electricity should be disregarded, similarly as it is done for the rest of energy systems. Thus, e.g. thermal energy output of a solar collector field at its corresponding temperature level should be regarded as a primary energy source, as shown graphically in the last row of Figure 3.13 (dotted dark grey line). In this approach, called *physical boundary* [Torío and Schmidt, 2010] the energy efficiency of solar radiation conversion in direct-solar systems is implicitly considered, for it determines the available energy and exergy output from the systems.

$$Ex_{coll}(t_k) = m_{coll}(t_k) \cdot c_{p,coll} \cdot \left[(T_{in,coll}(t_k) - T_{out,coll}(t_k)) - T_0(t_k) \cdot \ln \frac{T_{in,coll}(t_k)}{T_{out,coll}(t_k)} \right] \quad (3.29)$$

Following the *physical boundary*, the exergy input from the collector field into the building systems is evaluated as shown in equation 3.29. Following the sign convention adopted, the exergy output from the system Ex_{coll} has a negative value if heat is being generated in the solar collector field.

3.2.9.3 District heating return line

For the analysis of the district heating return line the relevant magnitude is the exergy input from the district heating network into the primary side of the district heating heat exchanger and not the exergy content of the fluid in the district heating pipe. In consequence, the exergy input from the district heating return line can be characterized similarly as for any other mass flow in the previous subsystems presented above. As for the rest of subsystems, only thermal exergy flows are regarded. Equation 3.30 shows the exergy input from the district heating network into the primary side of the district heating heat exchanger.

$$\begin{aligned} Ex_{in,prim,DH}(t_k) =& m_{DH}(t_k) \cdot c_{p,DH} \cdot (T_{in,prim,DH}(t_k) - T_{out,prim,DH}(t_k)) \\ & - m_{DH}(t_k) \cdot c_{p,DH} \cdot T_0(t_k) \cdot \ln \frac{T_{in,prim,DH}(t_k)}{T_{ret,prim,DH}(t_k)} \end{aligned} \tag{3.30}$$

3.2.10 Primary energy transformation

Energy losses occurring in the conveyance, processing and transport of energy sources used to supply building energy demands are taken into account by means of primary energy factors [DIN 18599-1, 2007]. These are included in the *Primary Energy Transformation* subsystem in Figure 3.1. In this way, a complete energy analysis of the whole energy supply chain in buildings is carried out.

It can be assumed that energy losses occurring in the processes required for providing the given energy sources to the building, i.e. energy losses in the *Primary Energy Transformation* subsystem, are high-quality energy losses. Therefore, exergy assessment of this subsystem can be carried out in a simple manner by multiplying exergy flows entering the generation subsystem in building Ex_g times the primary energy factors.

Chapter 4

Description of the models used for dynamic simulations

In this chapter the program used to model the energy systems studied is briefly introduced followed by a description of the main components used and their more relevant characteristics and behaviour. Sizing criteria or particular assumptions and simplifications met for modeling the energy systems are also described.

4.1 TRNSYS simulation environment

The TRaNsient SYstem Simulation program [TRNSYS, 2007] is a simulation environment which allows the transient simulation of energy systems. The programming language used for developing the program is Fortran 77. In this work, version 16.01 of the program is used. It was originally developed by the University of Winsconsin to perform dynamic simulations of solar thermal systems. Today, even a multi-zone building model allowing the modeling of thermally activated building components is available. Currently, the simulation of several building systems such as ground source heat pumps, photovoltaic systems, complex ventilation systems or solar cooling units is possible.

TRNSYS is based on a modular approach, where the different components in an energy system are interlinked with each other by means of their respective inputs and outputs. Each of these modules or components is called *Type* in TRNSYS and is described by a mathematical model in the TRNSYS simulation engine.

4.2 Definition of the reference buildings

4.2.1 Type 56, the TRNSYS Building Model

Type 56 is used in TRNSYS to model the thermal behaviour of a building divided into different thermal zones. The building model in TRNSYS is a non-geometric balance model [TRNSYS,

2007a]. Each thermal zone is modeled as a single air node in radiative and convective exchange with the enclosing surfaces. Orientation and slope of the exterior surfaces enclosing the thermal zone are regarded to calculate the radiation incident on the surface, influencing thereby their surface temperatures and heat transfer rates. Interior walls are only relevant for energy calculations in terms of thermal mass.

4.2.2 Multi-family dwelling (MFH)

The MFH is used in this thesis to check the improvement and best use possibilities of solar thermal systems based on exergy analysis.

4.2.2.1 Building Geometry

Table 4.1 shows the main geometric details of the multi-family dwelling considered in this work (*MFH Model*), which has been taken from [Heimrath, 2004]. Very good agreement can be found between this building and the building type *MFH_I* [IWU, 2003] which is represents 38% of the constructed habitable surface of multi-family dwellings in Germany [IWU, 2007]. Figure A.1 in the Appendix shows the geometry of the MFH considered.

Table 4.1: Geometric details for the multi-family dwelling taken as reference building here *MFH Model* and building type *MFH_I* according to the German residential building typology from [IWU, 2003].

	A_{net}	**V_{net}**	**A/V**	**Window fraction**	**Nr. storeys**	**Nr. apartments**
	[m^2]	[m^3]	[m^{-1}]	[%]	[-]	[-]
MFH Model [Heimrath, 2004]	929.7	2417.2	0.51	20	3	12
MFH_I [IWU, 2003]	759.0	2971.9	0.49	23	4	12

For all living areas the same user profiles and set points for space heating are regarded. In consequence, all flats in one storey can be regarded as a whole single thermal zone. Yet transmission losses are strongly influenced by the position of the storey, e.g. transmission losses are expected to be higher in the upper floor which has a flat roof in direct contact with outdoor air. Therefore, the building is simulated with three thermal zones, one per each store. Internal walls separating the flats from each other are considered (see Table 4.2).

4.2.2.2 Building Envelope

The building envelope strongly influences the space heating energy demand. It also has a great influence on the type of building systems that can be used (e.g. radiators, floor heating or thermally activated building components) and on the share of space heating and DHW supply in the total energy demand. Currently strong efforts have been done for improving the insulation standard, i.e. the building envelope, of newly erected buildings [EnEV, 2009;

DIN 18599, 2007]. In order to investigate the influence of improving the insulation level of the building envelope, two different building shells are considered:

- Base case with a building shell complying with minimum requirements from German EnEV [2007] Standard (in the following referred as MFH-07).
- Improved building shell corresponding to a *KfW-Effizienzhaus 40*[1] (in the following referred as MFH-KfW-EffH.40).

In Table 4.2 areas and U-values of the building model are shown. For comparison, maximum allowed U-values for each building envelope element according to [EnEV, 2007] are also given. Furthermore, the maximum allowed heat transfer coefficient for the building shell, H_T [EnEV, 2007] and that of the building model used are shown.

Table 4.2: Wall areas and U-values of the building model for the multi-family dwelling (MFH) and minimum U-values according to the German EnEV [2007] Standard.

		MFH-07		MFH-KfW-EffH.40		EnEV [2007]	
	Area [m^2]	U-Value [$W/(Km^2)$]	H_T [W/K]	U-Value [$W/(Km^2)$]	H_T [W/K]	U-Value [$W/(Km^2)$]	H_T [W/K]
External walls	733.2	0.44		0.11		0.45	
Roof	324.6	0.25		0.12		0.25	
Ground	324.6	0.40		0.16		0.40	
Windows	179.5	1.40		0.50		1.70	
Total			0.47		0.16		0.58
Internal walls	58.7	0.65		0.65			

4.2.2.3 Internal loads

Internal loads from people and electrical appliances are defined according to the mean daily load of 100 Wh/m^2d foreseen in [DIN 18599-10, 2007] for multi-family dwellings. This mean daily internal load would correspond to a constant load of 4.2 W/m^2. In this value, internal loads from occupants and appliances are included.

Occupancy factors for weekdays and weekends have been defined as in [Heimrath, 2004] and are shown in Figure 4.1.

Occupancy loads from occupants have been defined in accordance with [ISO 7730, 2005] for a person seated at rest (i.e. 60W sensible heat load and 40W latent heat load per occupant). A total of 29 occupants is assumed [Heimrath, 2004], i.e. an occupancy factor of 1 indicates that full occupancy occurs (i.e. 29 occupants are present in the building). In addition, internal heat loads from appliances inside the building are regarded as a maximum peak load of 9.54 W/m^2 distributed over the day according to the use factor in Figure 4.1 (b).

Daily loads, including appliances and occupants, amount 97.44 and 100.80 Wh/m^2d for weekdays and weekends respectively.

[1] A KfW-Effizienzhaus 40 is a building whose primary energy demand is at most 40% that of the reference building defined in [EnEV, 2009] and its transmission losses are lower than 55% of the reference building.

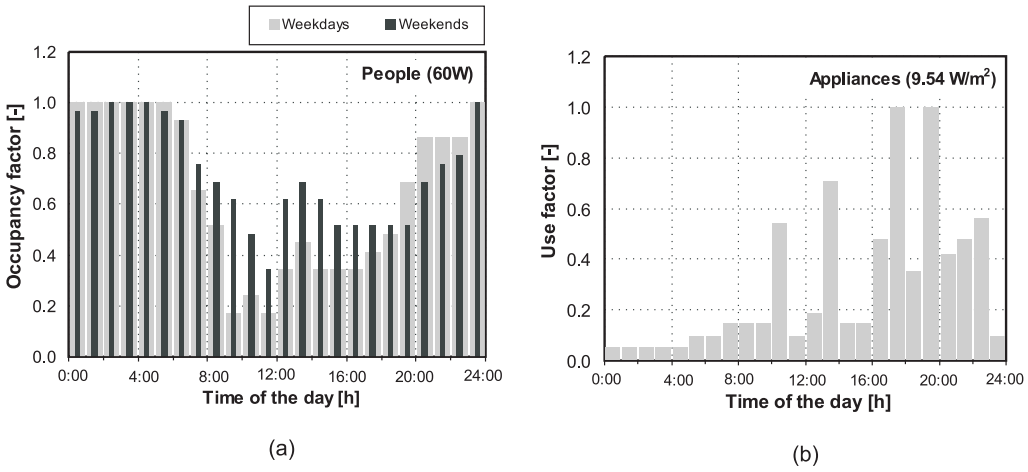

Figure 4.1: Occupancy factors for weekdays and weekends (a) and use factor for appliances in the multifamily dwelling.

4.2.2.4 Ventilation and infiltration rates

Ventilation and infiltration rates for the multi-family dwelling are defined in accordance with the German Standard DIN 18599-10 [2007], which defines a minimum external air exchange due to the occupancy and use of the building as 0.5h^{-1} for residential buildings without mechanical ventilation system. This air exchange rate is to be regarded as dependent on the occupancy profile of the building [DIN 18599-2, 2007]. With these assumptions, the air exchange rate per person amounts about 40 m^3/h.

Additionally, infiltration losses through the building envelope are regarded in dependency of the air exchange rate for 50 Pa overpressure inside the building n_{50}. Here, a value of 3h^{-1} is assumed for n_{50}, corresponding to a newly erected building without ventilation units but with proof of air tightness. The infiltration air exchange is then, assuming a standard value for the wind protection coefficient of 0.07 [DIN 18599-2, 2007], 0.21h^{-1}.

4.2.2.5 Night setback

Disconnecting the heating and cooling systems or allowing lower temperature levels in the occupied zone during the night reduces the energy consumption of buildings. Obviously, the influence of this control strategy is lower for increased thermal insulation level of the building envelope. Oppermann [2003] investigated the influence of different setback strategies on the energy consumption of a single family low energy house, and concluded that savings are on the range of 8-20% depending on the setback and ventilation strategy chosen. However, for passive house level, savings might amount as less as 3% of the energy demand [Bier, 2002].

The night setback has been defined in accordance with the standard DIN 18599-10 [2007]. Here, the night setback for residential buildings is regarded from 23:00h to 6:00h allowing a

temperature drop of 4K during those hours. Thus, minimum setpoint temperature for the indoor air temperature during night operation of the heating system is 16°C, whereas the setpoint for daytime operation should be 20°C.

However, this study intends to compare the energy performance of different heating systems with different radiative and conductive heat transfer rates. Comfort conditions inside the building are better assessed by the operative temperature, as indicated in section 4.12, which is strongly influenced by the type of heat emission system (e.g. radiators or floor heating system). Therefore, in order to compare on an equal basis different emission systems, the operative temperature is regarded here as the setpoint and control variable. Setpoint for the operative temperature during night setback operation is regarded as 16°C and 20.5°C during daytime.

4.2.3 Single family house (SFH)

The SFH is used in this thesis to check the improvement and best use possibilities of a district heating system based on exergy analysis.

4.2.3.1 Building Geometry

The single family house regarded here (*SFH Model* in Table 4.3) has a useful area of 184.44 m^2. Its main geometric details are in good agreement with building type *EFH_J* in the German building typology [IWU, 2003], corresponding to a newly erected single family house estimated to represent 3% of all building living area in Germany [IWU, 2007].

Table 4.3: Geometric details for the SFH considered here and building type *EFH_J* according to the German residential building typology from [IWU, 2003].

	$\mathbf{A}_{net}$	$\mathbf{V}_{net}$	**A/V**	**Window fraction**	**Nr. storeys**
	[m^2]	[m^3]	[m^{-1}]	[%]	[-]
EFH_J [IWU, 2003]	133.2	629.7	0.80	15	2
SFH Model [ZUB, 2009]	184.4	437.9	1.03	16	2

Figure A.2 (in the Appendix) shows the building geometry for the single family house regarded. The ground floor is located above an unheated basement, which is not simulated separately as a thermal zone. Instead, a constant temperature of 10°C has been regarded.

Since transmission losses are strongly influenced by the building elements enclosing the building and their position, space heating demands are expected to be slightly different in the upper and lower floors. The building is simulated with two thermal zones, one per each store. Internal walls, relevant for energy calculations in terms of thermal mass are regarded (see Table 4.4).

4.2.3.2 Building Envelope

The insulation level of the building envelope for the SFH has been chosen in accordance with minimum requirements defined in the German energy saving Standard EnEV [2009]. To compare the influence of improving the building shell on the performance of the district heating system investigated a building shell with better insulation level has also been defined. Table 4.4 shows the heat transfer coefficient for the different building elements in the base case corresponding to the minimum insulation level required [EnEV, 2009] and the improved building shell, corresponding to a *KfW-Effizienzhaus 40* (KfW-EffH.40).

Table 4.4: Wall areas and U-values of the building envelope for the building envelope according to the German standard [EnEV, 2009] (SFH-09) and those corresponding to an improved building shell (SFH-KfW-EffH.40). For completeness maximum values allowed by the EnEV [2009] standard are shown; *Value taken from project data defined by Dipl.-Ing. Michael Ringeler (ZUB).

	Area	SFH-09		SFH-KfW-EffH.40		EnEV [2009]	
		U-Value	$H_T´$	U-Value	$H_T´$	U-Value max.	$H_T´$
	[m^2]	[W/(m^2K)]	[W/K]	[W/(m^2K)]	[W/K]	[W/(m^2K)]	[W/K]
External walls	194.20	0.28		0.11		0.28	
Roof	118.34	0.17		0.12		0.20	
Ground	107.54	0.30		0.16		0.35	
Windows	31.53	1.40		0.5*			
Total	451.60		0.38		0.20		0.40
Internal walls I	97.25	1.81		1.81			
Internal walls II	27.03	2.68		2.68			

4.2.3.3 Internal loads

Internal loads from people and electrical appliances are defined as a constant value of 5 W/m^2 according to the standard DIN 4108-6 (2003) for residential buildings. This corresponds to a mean daily internal load of 120 Wh/m^2d, which is significantly above the value of 50 Wh/m^2d defined in the standard DIN 18599-10 [2007]. The value assumed corresponds to a building with conventional electrical appliances instead of with optimized energy efficient equipment.

4.2.3.4 Ventilation and infiltration rates

The German Standard DIN 18599-2 [2007] defines the minimum value of the external air exchange for residential buildings without mechanical ventilation system as 0.5h^{-1}. This air exchange rate is to be regarded as dependent on the occupancy profile of the building. However, a constant occupancy is regarded here. A total air exchange of 0.6h^{-1}, including infiltration and ventilation, is assumed in accordance with the standard EnEV [2009], corresponding to a building with proof of air tightness and ventilated by windows.

4.2.3.5 Night setback

Night setback operation for space heating systems has shown energy saving potential [Oppermann, 2003]. However, higher peak loads are also required for the reheating phase after the night setback. It can be expected that the users in the single family houses have individual control of their space heating systems. Thus, using the same night setback operation for all SFH would lead to an overestimation of the peak loads for space heating supply.

On the other hand, the energy saving potential of night setback operation is reduced as the insulation level of the building shell increases [Bier, 2002], being for a newly erected building complying with the Standard EnEV [2009] between 3 and 8%. In order to avoid the overestimation of space heating peak loads, no night setback is regarded for the single-family houses.

4.3 Domestic hot water demands

In [VDI 2067, 1999] domestic hot water (DHW) consumption is regarded on a daily basis with values of 15-120 liters of hot water per person at a temperature level of 45°C. The German Standard DIN 4708 [1994] defines the daily hot water consumption per person as 50 liters at the same temperature level of 45°C. Gassel [1997] shows with measurement data that the DHW consumption per person and day varies from 26 to 53 liters at 45°C for different German cities. Heimrath [2004] evaluated measurement data from twelve solar systems for multi-family dwellings located in Austria and Germany, and found that a mean value of the daily draw-off per person of 43 liters at 45°C matched reasonably good the mean value from the measurements.

Here, 40 liters draw-off per person and per day at 45°C are regarded, being a typical value within the range found in the literature.

4.3.1 DHW draw-off profile

Draw off profiles for DHW consumption have a strong influence on the appropriate size of the storage or heat exchanger for the DHW loop. Simplified draw-off profiles are unsuitable for a detailed simulation of DHW supply systems in buildings [Heimrath, 2004]. The great influence of DHW draw-off profiles in the performance of solar thermal systems has been proved by several authors [Sharia and Löf, 1997; Jordan and Vajen, 2001; Knudsen, 2002].Similarly, the draw-off profile is expected to have also a strong influence on the size and performance of heat exchangers for DHW supply in district heating systems.

In this work DHW draw-off profiles are generated using the program *DHWcalc* [Jordan and Vajen, 2005], developed at the University of Kassel (Germany). This tool generates detailed yearly DHW draw-off profiles based on probability distributions of four different types of draw-offs: short and medium draw-offs, bath and shower. For each category a probability function as well as mean, maximum and minimum flow-rates and draw-off duration are de-

fined by the user [Jordan and Vajen, 2005]. The probability function according to [Weiss, 2003] is chosen for the case studies analyzed here.

In the Appendix (Table A.1) main assumptions for the DHW profile are shown. Differences in the DHW consumption patterns between the multi-family and single family buildings arise as a result of different values for the mean daily draw-off volume as well as minimum and maximum flow rates. Values for these parameters are specified on sections 4.3.3 and 4.3.4 for each building case.

4.3.2 Cold water temperature

The seasonal variation of the cold water temperature is defined in accordance with DIN EN 12976-2 [2006], as shown in equation 4.1. Here, the sinusoidal yearly variation of the cold water temperature θ_{cw} is described as a function of the average yearly cold water temperature θ_{ave} (in °C), the average amplitude for seasonal variation $\Delta\theta_{amplit}$, the day of the year DAY, and the time-shift parameter d_s given in days. Following, a constant cold water temperature is derived for each day of the year. According to [DIN 12796-2, 2006] the average yearly cold water temperature θ_{ave} can be assumed as 10°C, the average amplitude for seasonal variation $\Delta\theta_{amplit}$ as 3°C and the time-shift parameter d_s as 137 days for Würzburg. Cold water temperatures calculated with this parameters are in good agreement with values in [Weiss, 2003].

$$\theta_{cw} = \theta_{ave} + \Delta\theta_{amplit} \sin\left(360 \frac{(DAY - d_s)\,24}{8760}\right) \tag{4.1}$$

The yearly seasonal variation of the cold water net temperature with the assumptions mentioned above is shown in the Appendix (Figure A.3).

4.3.3 Particular assumptions for multi-family dwelling

As part of the multi-family dwelling case study, the influence of different hydraulic concepts and DHW supply temperatures on the energy and exergy performance of DHW supply systems is investigated. For this purpose two different supply temperatures of 45°C and 60°C are analyzed and compared. Daily DHW draw-off at a temperature level of 60°C is considered to be lower (28 liters per person and day, instead of 40 liters per person an day at 45°C), so that in both cases the demand is covered by mixing more cold water from the net with the warmer water produced. In this way daily energy consumption per person is constant and the systems can be compared on the basis of the same DHW demand being provided. Hydraulic concepts investigated for DHW supply are introduced in detail in section 5.1.1.2 of chapter 5.

With a supply temperature of 45°C mean daily draw-off amounts 1160 l/day and minimum and maximum flow rates amount 6 l/h and 14400 l/h respectively. With a supply temperature of 60°C mean daily draw-off amounts 812 l/day and minimum and maximum flow rates amount 6 l/h and 8640 l/h respectively. Figure A.4 (in the Appendix) shows the

draw-off profiles generated for the two different supply temperatures regarded in this study, 45°C and 60°C.

The Standard DIN 18599-10 [2007] gives a value for DHW energy demand of 16 kWh/m^{2}a for multi-family dwellings. With the assumptions mentioned here DHW demands from dynamic energy simulations with TRNSYS amount 16.74 kWh/m^{2}a, showing good agreement with values from the Standard.

4.3.4 Particular assumptions for the single family house

According to [AGFW, 2009] in small DHW supply systems such as those in single family houses a constant supply temperature of 50°C at the outlet of the DHW supply element must be ensured at all times.

With a supply temperature of 50°C mean daily draw-off amounts 140 l/day and minimum and maximum flow rates amount 1 l/h and 2400 l/h respectively. DHW demand profiles for each SFH can be seen in Figure A.5 (in the Appendix).

The Standard DIN 18599-10 [2007] gives a value for DHW energy demands of 12 kWh/m^{2}a for single family houses. With the assumptions mentioned here DHW demands from dynamic energy simulations with TRNSYS have a value of 12.9 kWh/m^{2}a, showing good agreement with values from the standard.

4.4 Hydraulic loops

Hydraulic loops represent a part of the thermal losses in building systems, herewith influencing the energy performance of the given building system. Different supply temperature levels, e.g. in DHW supply installations or space heating systems have an influence on that energy losses. Therefore, a correct comparison of the systems analyzed here requires an analysis of the thermal losses in the corresponding hydraulic loops.

Pressure losses in the hydraulic circuits need to be compensated by the installed pump. Thus, they have an influence mainly on the electrical consumption required as auxiliary energy for the operation of the pump. This is explained in detailed in section 4.4.7.

Type 31 from TRNSYS is used to simulate thermal energy losses in the pipe networks. This type is a plug-flow model which simulates the thermal behavior of a fluid flow in a pipe or duct using variable size segments of fluid. Entering fluid shifts the position of existing segments. The temperature of each segment as it reaches the outlet of the pipe depends, thus, on its initial temperature at the pipe inlet and on the time the segment is kept in the pipe, being this last a function of the mass flow. Mixing effect between adjacent segments is not considered. The inside pipe volume must be chosen in such a way that it allows containing the maximum mass of fluid circulating through the pipe in one timestep.

Pressure losses in the pipes are not modeled in Type 31. The electric power consumption of the pumps in the hydraulic loops, which is a function of the pressure losses and mass flow,

is expressed in this work as a function of this last parameter (see section 4.4.7).

4.4.1 Pipes for energy supply in multi-family dwellings

Pipes in hydraulic loops are sized in order to keep pressure losses within a certain acceptable range, i.e. between 100 and 400 Pa/m [Heimrath, 2004]. Further requirements are related to the noise in the circuit. In order to avoid annoyances, the fluid speed for pipes with an inside diameter smaller than 50 mm is limited to 1.2 m/s. In turn, for pipes of bigger diameter pressure losses need to be smaller than 400 Pa/m [Heimrath, 2004; ASHRAE 1993] and the speed might reach values up to 2.5 m/s.

In a multi-family dwelling pipes for DHW and space heating hydraulic loops might have considerable length. In the models developed here length and size of the pipes are calculated in detail. A detailed view of the layout, length and diameter of the pipes for the cases with floor heating and radiators is shown in the Appendix (Figures A.6 and A.7 and Tables A.2 and A.3).

For the floor heating system copper pipes are considered, whereas for the case with radiators steel pipes are regarded. In both cases a two pipe hydraulic configuration is chosen, meaning that each floor heating loop or radiator is connected to a supply and return pipe in parallel with the rest of radiators or floor heating loops [Recknagel et al., 2007]. For the case with floor heating system pipes range from 15x1 to 42x1.5, being the first number the outside diameter and the second the wall thickness. If radiators are regarded instead, pipe sizes range from DN 20 to DN 10.

Thermal insulation thickness is regarded as a function of the pipe diameter according to [EnEV, 2009] as shown in Table 4.5. Heat conductivity of the insulation layer is regarded as 0.035 W/(mK).

Table 4.5: Thermal insulation thickness for the pipes for different inside pipe diameters [EnEV, 2009].

Inside pipe diameter mm	Insulation thickness mm
until 22	20
22-35	30
35-100	equal to inside diameter
above 100	100

4.4.2 Pipes for energy supply in the single family house

Single family houses are modeled here with a district heat supply. In a single family house pipes for DHW and space heating hydraulic loops are relatively short as compared to the distribution pipes from the district heating network. Thus, in the models developed here the length and size of the pipes inside each SFH is not considered or modeled.

4.4.3 Pipes for district heating supply

A common criterium for sizing pipes in local heat networks is a target maximum fluid velocity of 2.5 m/s [AGFW, 2009; UMSICHT, 2010]. This criteria and common sizing method aims on one hand at reducing thermal losses in the pipes and on the other hand at decreasing system costs, since lower pipe diameters are expected to yield considerable money savings for the construction and set up of the network.

From an exergy perspective thermal losses in the pipes, being low temperature heat, represent small exergy losses. In turn, pumping power for operating the local heat network represents a high exergy input to the system. It would, thus, be advisable to reduce the pumping power required to operate the local heat network. This can be achieved by increasing the size of the pipes, i.e reducing the maximum allowed fluid velocity in the network. A target maximum fluid velocity in the pipes of 1 m/s is used for sizing the network following exergy criteria. This allows comparing the energy and exergy performance of a commonly sized network with that of a network sized following exergy considerations.

In the Appendix (Figure A.8) the detailed layout of the pipes in the local district heating network for supplying heat to the single-family houses is shown. Hydraulic balance between the different strings is achieved by means of valves. Nominal diameters and lengths of the pipes in each of the sizing criteria (i.e. with maximum velocities of 1 and 2.5 m/s) and for the different hydraulic configurations investigated in this thesis are shown in Table A.4.

Thermal insulation for pipes up to DN 40 is regarded as 3 cm of an insulation foam with a heat conductivity value λ of 0.042 W/(mK). For pipes with greater diameter the insulation thickness is regarded as 4 cm. In this way a worst-case scenario is modeled, corresponding to e.g. incorrect installation of the insulation or moisture and condensation problems in it. Figure 4.2 shows a comparison between the U-Values obtained for the pipes implemented in the models in this study and values found in the literature [Dötsch and Bargel, 2009] for pipes in district heating networks. It can be seen that criteria chosen here lead to an overestimation of the thermal losses in the pipes.

4.4.4 Simplification: *"equivalent pipes"*

The simulation of detailed hydraulic loops including the description of each pipe diameter and length would be very time-consuming, for it would require the use of a pipe model to simulate every single pipe segment with different diameter in the hydraulic loop.

Instead, a simplification can be made following the approach of the *"equivalent pipes"* [Heimrath, 2004]. In this approach, pipe diameter and size for the *equivalent pipe* are chosen in such a way that the outlet temperature and thermal losses in the *equivalent pipe* are similar to those from the complex detailed hydraulic loop.

The outlet temperature from the complex hydraulic loop can be calculated with equation 4.2. The length of the equivalent pipe can be estimated using equation 4.3. Insulation for the equivalent pipe is assessed using equation 4.4.

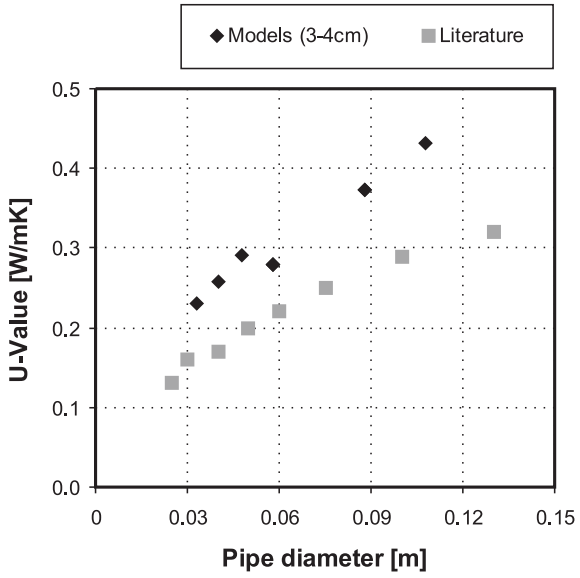

Figure 4.2: U-Values for district heating pipes as a function of pipe diameter found in the literature [Dötsch and Bargel, 2009], labeled as *Literature*, and those considered for the models in this study, labeled as *Models (3-4cm)*.

$$T_{out} = \frac{\sum_{i=1}^{i=n} (T_{out,i} \cdot \dot{m}_i)}{\sum_{i=1}^{i=n} \dot{m}_i} \tag{4.2}$$

$$L_{eq} = \frac{\sum_{i=1}^{i=n} (L_i \cdot \dot{m}_i)}{\sum_{i=1}^{i=n} \dot{m}_i} \tag{4.3}$$

$$U \cdot A_{eq} = \frac{\dot{m} c_p \Delta T}{\Delta T_{LMTD}} \tag{4.4}$$

Setting the diameter for the *equivalent pipe*, the area through which thermal losses to the surrounding environment happen (A_{eq} in equation 4.4) is determined, and so the U-value for the insulation of the pipe can be obtained.

4.4.5 Equivalent pipes for the multi-family dwelling

Inlet and return pipes from the space heating and DHW supply loops have significantly different temperature levels. In consequence, thermal losses in the supply and return pipes are expected to be very different. In order to simulate the temperature drops and thermal losses in the inlet and return pipes separately, equivalent pipes for the inlet and return of these hydraulic loops have been calculated. Table 4.6 shows the equivalent pipes calculated for the radiators, floor heating loops and DHW supply circuits.

Table 4.6: Lenght, diameter and insulation level regarded for the equivalent pipes in the hydraulic circuits for space heating (radiators and floor heating systems) and DHW supply loops.

	Diameter [m]	Lenght, L_{eq} [m]	U-value, U_{eq} [W/(m^{2}K)]
System with radiators			
Supply pipes inside flats	0.097	17.242	5.055
Return pipes inside flats	0.094	18.337	4.003
General supply pipes to flats	0.196	12.571	0.706
General return pipes from flats	0.196	12.571	0.639
System with floor heating loops			
Supply pipes inside flats	0.262	3.833	4.737
Return pipes inside flats	0.149	11.861	1.800
General supply pipes to flats	0.256	12.000	2.068
General return pipes from flats	0.256	12.000	1.548
DHW supply system			
Supply pipes	0.117	22.00	1.89
Recirculation pipes	0.034	22.00	4.27

4.4.6 Equivalent pipes for district heat supply (SFH)

Table 4.7 shows the equivalent pipes calculated for the different investigated options for district heat supply.

Table 4.7: Lenght, diameter and insulation level regarded for the equivalent pipes in the hydraulic circuits for district heat supply. Values for separate domestic hot water (DHW) and space heating supply (SH) and common supply of both demands are shown. Equivalent pipes for cascaded supply of SH and DHW demands is also presented.

	Diameter [m]	Lenght, L_{eq} [m]	U-value, U_{eq} [W/(m^{2}K)]
Separate SH and DHW supply			
SH supply, v_{max} = 1 m/s,	0.106	47.542	1.946
SH return, v_{max} = 1 m/s,	0.106	47.542	6.622
Cascaded SH supply, v_{max} = 1 m/s,	0.227	47.542	1.064
Cascaded SH return,v_{max} = 1 m/s,	0.227	47.542	3.575
DHW supply, v_{max} = 1 m/s,	0.093	47.542	2.105
DHW return, v_{max} = 1 m/s,	0.093	47.542	7.575
Common SH and DHW supply			
Supply pipe, v_{max} = 2.5 m/s,	0.212	47.542	0.880
Return pipe, v_{max} = 2.5 m/s,	0.212	47.542	3.240
Supply pipe, v_{max} = 1 m/s,	0.212	47.542	1.111
Return pipe, v_{max} = 1 m/s,	0.212	47.542	3.730

In the district heating system the single family houses are considered to be connected to the network in parallel. In the supply pipes, the temperature of the circulating water experiences a temperature decrease only dependent on the thermal losses in the pipes. In turn, in the

return pipes, water from the return of the different houses joins the common return pipe and might eventually cool down water circulating in the common return pipe, as would be the case if water has been standing still in the branches. To simulate this, it has been assumed that water from different branches joining the return pipe has the same temperature as incoming water at the joining point. As a result heat transfer coefficients for return pipes are always significantly higher than those for supply pipes.

4.4.7 Pumps in hydraulic circuits

In the models developed in this thesis Type 110 is used to simulate a variable speed pump in TRNSYS. The pump model is able to maintain any mass flow rate between zero and the maximum rated value. Neither pump start and stop behaviour nor pressure drops inside the pump are modeled.

Equation 4.5 shows the expression for calculating the electric power demand of the pump for the given flow conditions in each timestep as a function of the control signal sent to the pump γ and the rated power demand at maximum flow rate $P_{el,pump,max}$. The coefficients of the polynomic function can be entered as parameters in Type 110.

$$P_{el,pump} = P_{el,pump,max} \left(a_1 \cdot \gamma^2 + b_1 \cdot \dot{\gamma} + c_1 \right) \tag{4.5}$$

To determine the coefficients of the polynomial relationship between mass flow or rated power and the actual electric power demanded by the pump the characteristic curve of the hydraulic loop where the pump is installed is determined. The characteristic curve is the relationship between pressure losses in the hydraulic circuit and the mass flow circulating in it. It can be determined calculating the pressure losses occurring in the hydraulic circuit for different mass flow rates. Following, a pump whose characteristic fits with that of the hydraulic loop is chosen. For choosing and sizing an appropriate pump the online tool from Wilo GmbH [Wilo, 2010] is used in this work.

In the space heating and district heat supply loops studied, all users or energy demands (i.e. houses in district heating system and radiators or floor heating loops in the multi-family dwelling) are connected in parallel. Thus, for sizing the pumps only the most unfavorable hydraulic loop is regarded. In district heating supply this corresponds to the supply pipes of house *H-3.5* in *STRING 3* of Figure A.8. For sizing the pump for space heating supply with radiators in the multi-family dwelling pressure losses in the pipes leading to radiator 21 in Figure A.7 are regarded. To size the pumps with floor heating supply pressure losses in the pipes to floor heating circuit 5 in Figure A.6 are considered.

4.5 Heat emission systems

4.5.1 Radiators

To simulate a water based radiator Type 362pro is used. The model is based on Type 162 [Holst, 1996] which simulates the dynamic behavior of a radiator unit as a dynamic first order model, i.e. specific heat capacity of the radiator and its water content is concentrated in one single thermal node. Conductive and radiative parts of the heat emitted are calculated dynamically and separately as a function of the radiator temperature.

The radiator model is connected to a PID controller (Type 23) which calculates the required mass flow as a function of the difference between the set point (20.5°C) and the actual operative temperature of each thermal zone inside the building in each time step.

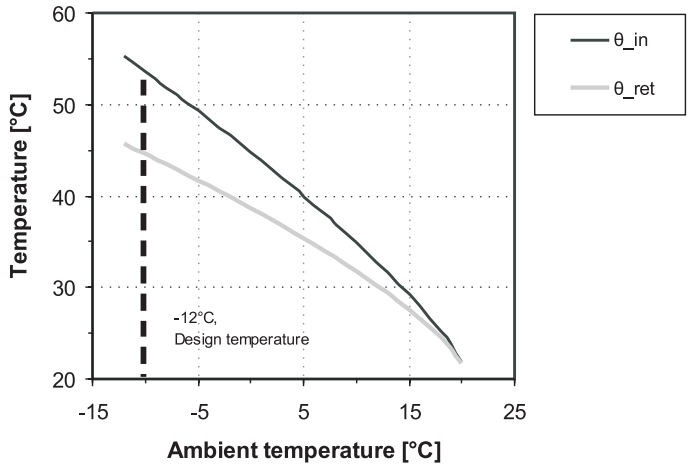

Figure 4.3: Set point for inlet and outlet temperatures in the radiators as a function of the outdoor air temperature.

Radiators need to be sized so as to cover the peak heating load of the building (see section 5.1.1.1 in chapter 5). Nominal inlet and outlet temperatures of 55 and 45°C respectively are regarded for peak load conditions (corresponding to an outdoor design temperature, T_{design} of -12°C, see section 4.11). Yet, required inlet and outlet temperatures are controlled and varied as a function of the outdoor temperature, as shown in Figure 4.3.

In the Appendix (Table A.5) main assumptions for sizing the radiators for the multi-family dwelling with both building envelopes (MFH-07 and MFH-MFH-KfW-EffH.40) are shown. Data related to the design performance of the radiators are taken from [BUDERUS, 2007].

4.5.2 Floor heating system

A floor heating system can be modeled in TRNSYS by adding an *active layer* to the floor construction. An active layer simulates the dynamic behavior of a pipe layer immersed in the building element. Convective heat transfer coefficient between the active surface and building

indoor air is calculated as a function of the surface temperature. The pipe in the active layer is divided in several segments. Heat transfer is calculated for each segment as a function of its particular temperature. The necessary number of segments depends on the minimum allowed mass flow, which needs to be higher than the minimum value acceptable by the model in order to avoid wrong results. This limitation is due to the correlations used in the active layer model, which are based on experimental results.

To define the active layer several geometric parameters such as the distance between pipes, pipe thickness, outside diameter and pipe wall conductivity are required. Table A.6 in the Appendix shows the values assumed for these parameters.

Both in the multi-family and single family houses the floor heating system is connected to a PID controller (Type 23) which calculates the required mass flow as a function of the difference between the set point and the actual operative temperature in the thermal zones of the building for each time step.

The German Standard DIN EN 1264-2 [1997] allows determining the specific heating curve for a given floor heating system, i.e. its power output $\dot{q}$, depending on the constructive details and materials regarded (see equation 4.6). The overtemperature of the heating fluid $\Delta\theta_{overh}$ represents the logarithmic temperature difference between the fluid and the room air temperatures.

$$\dot{q} = B \cdot a_B \cdot a_T^{m_T} \cdot a_u^{m_u} \cdot a_D^{m_D} \Delta\theta_{overh} \tag{4.6}$$

The floor heating systems regarded here consists of a heating layer (pavement) of 7 cm. No covering or coating is regarded over the floor heating pavement layer. Therefore the thermal resistance of the coating R_{cover} required for estimating the coefficients which determine the heating curve of the system in [DIN EN 1264-2, 1997] is regarded as zero. The thermal conductivity of the pavement heating layer λ_E[2] is 1.4 W/(mK). With these assumptions, the coefficients according to [DIN EN 1264-2, 1997] are shown in Table 4.8.

Table 4.8: Coefficients for estimating the heating curve for the floor heating system regarded, in accordance with the Standard DIN EN 1264-2 [1997].

Parameter	Unit	Value	Parameter	Unit	Value
a_B	[-]	1.122	B	[W/(m^{2}K)]	6.70
a_T	[-]	1.230	m_T	[-]	-1.67
a_u	[-]	1.051	m_u	[-]	-1.50
a_D	[-]	1.046	m_D	[-]	0

The heating curve obtained with the parameters in Table 4.8 is shown in Figure 4.4 (a). Required mean overtemperatures for the heating surface in the different building case studies analyzed here are also shown in the Figure. Resulting design inlet temperatures in the floor heating systems as a function of outdoor air temperature are shown in Figure 4.4 (b).

[2] "E"from the German word "Estrich"

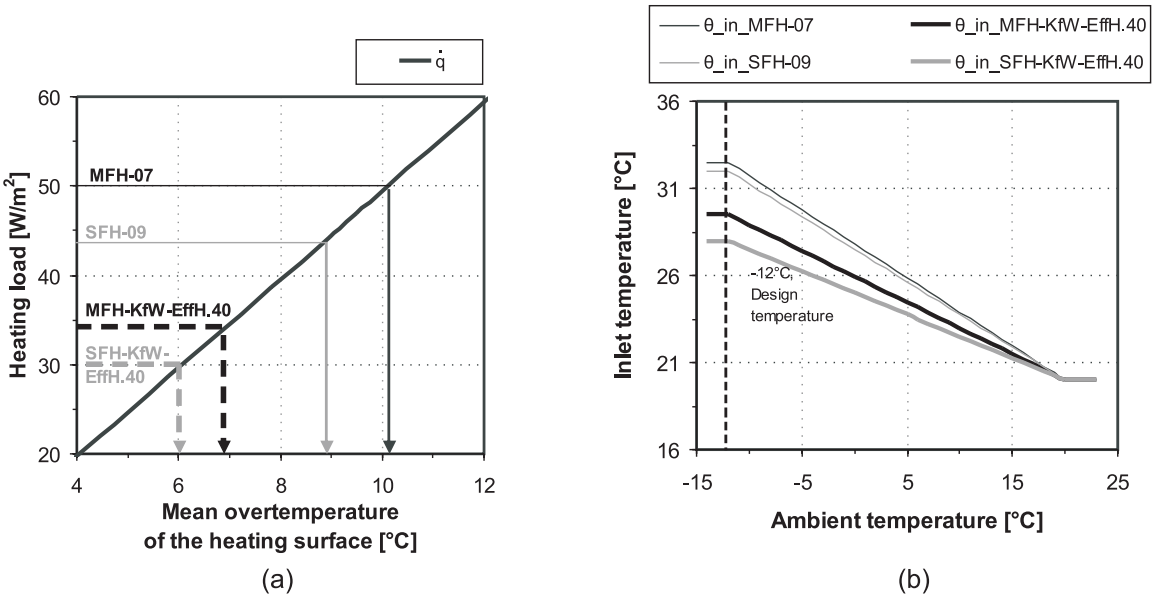

Figure 4.4: (a): Heating curve for the floor heating system regarded as a function of the overtemperature of the heating layer [DIN EN 1264-2, 1997]. Mean overtemperatures for the heating surface required in the different building case studies are also shown; (b): Inlet temperatures required for the floor heating systems in the single- and multi-family buildings as a function of the outdoor air temperature.

4.6 Heat exchangers

Several types of heat exchangers are used in the models developed in this work. To supply DHW demands in the MFH an instantaneous heat exchanger is used. District heating supply to the SFH also succeeds via heat exchangers which decouple the district heating network from the local heat network distributing heat among the buildings. In any of both cases, the heat exchanger is to be operated in such a way that a given outlet temperature is reached at the secondary side (which goes to the demand to be supplied). To model these heat exchangers Type 805 is used in TRNSYS.

Type 805 is a non standard TRNSYS Type developed by Heimrath and Haller [2007]. It models a counter flow heat exchanger where the mass flow of the primary side is controlled depending on the inlet temperatures of both (primary and secondary) sides and the setpoint temperature which needs to be reached at the secondary side. Variable values for the overall heat transfer coefficient (UA) for different regimes of mass flows and temperatures can be defined. The heat transfer is assumed to happen adiabatically and without phase changes on the primary or secondary sides.

Depending on the characteristics of the heat exchanger for each application (i.e. DHW production or district heating supply) UA values have been defined as a function of the secondary mass flow (e.g. see Figure 4.5).

4.6.1 Flow-through heat exchanger for DHW supply

For DHW supply in the multi-family dwelling a flow-through instantaneous heat exchanger is foreseen. In this way, decentralized storage of DHW in each of the apartments is avoided. This supply concept has proved to be more energy efficient than decentralized DHW storage, since thermal losses in the decentralized storage tanks are avoided [Heimrath, 2004]. A recirculation loop aiming at keeping the temperature in the secondary side (i.e. demand side) at 55°C is foreseen[3] [AGFW, 2009].

Data corresponding to the *RATIOFresh 800* heat exchanger from Wagner & Co. have been taken [Wagner, 2007]. Table 4.9 shows the equation for calculating the UA value of the flow-through heat exchanger as a function of the secondary side (i.e. demand) mass flow.

Table 4.9: Type, temperature range and analytical expression of the UA value for the flow-through instantaneous heat exchanger for DHW production in the MFH as a function of the secondary side mass flow.

Demand	Type	Temperature range	UA-Value [kJ/(hK)]
DHW	RATIOfresh 800	$\theta_{in,prim}$ = 70°C	-0.0015·$\dot{m}_{sec}^2$+19.341·$\dot{m}_{sec}$+2872

4.6.2 Heat exchangers for district heat supply

Return temperatures achieved at the primary side of the district heat supply heat exchanger, as well as required primary side mass flows and achievable temperature difference at the secondary side depend on the heat transfer within the supply heat exchanger. Thus, heat exchangers assumed for district heat supply are expected to have a strong influence on the performance of the district heat supply system.

In order to simulate realistic systems, UA values, areas and performance figures from real heat exchangers have been chosen. The program *GEA BRAZED Select 2009.3* [GEA, 2009] is used for sizing the heat exchangers required for each supply configuration investigated, i.e. common supply of DHW and SH demands, separated supply of DHW and SH demands and cascaded supply of SH after DHW supply [4].

Figure 4.5 shows the UA value chosen for the heat exchangers for district heat supply as a function of the secondary mass flow.

In Table 4.10 the equations for calculating the UA value in each timestep as a function of the secondary mass flow are shown. In order to model more accurately the behaviour of the heat exchangers different equations for different ranges of secondary side inlet temperatures are chosen for those heat exchangers whose behaviour varies significantly for different temperature ranges.

[3] see section 5.1.1.2 for further details

[4] see Figure 5.10 in section 5.2.4.2 of chapter 5 for a detailed description of each configuration.

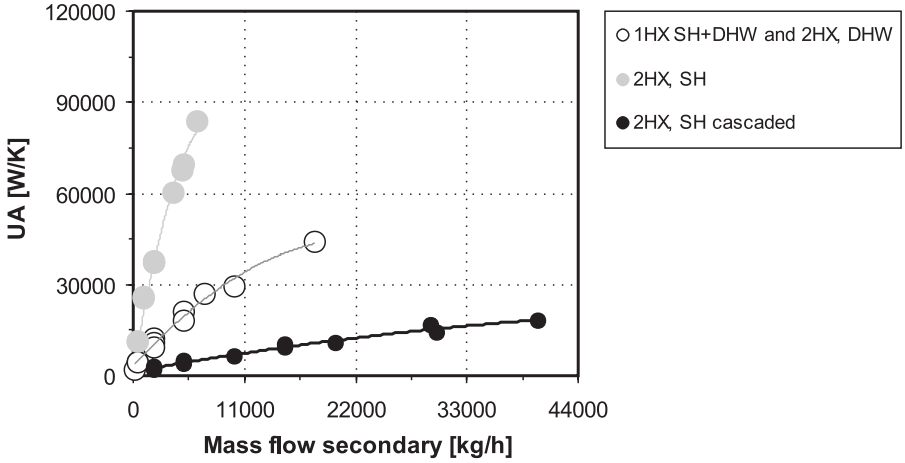

Figure 4.5: UA values for the heat exchangers chosen for the different hydraulic configurations studied for district heat supply as a function of the secondary side mass flow.

Table 4.10: Type and analytical expression of the UA value for the heat exchangers foreseen for DH supply in the SFH as a function of the secondary side mass flow for different ranges of secondary side inlet temperatures.

Demand	Type	Temperature range	UA-Value [kJ/(hK)]
SH+DHW	WP 757 H-90	$\theta_{in,sec} \leq 40°C$	-0.0008·$\dot{m}_{sec}^2$+18.740·$\dot{m}_{sec}$+6572.5
		$\theta_{in,sec} > 40°C$	-0.0001·$\dot{m}_{sec}^2$+10.683·$\dot{m}_{sec}$+14142
DHW	WP 757 H-90	$\theta_{in,sec} \leq 40°C$	-0.0008·$\dot{m}_{sec}^2$+18.740·$\dot{m}_{sec}$+6572.5
		$\theta_{in,sec} > 40°C$	-0.0001·$\dot{m}_{sec}^2$+10.683·$\dot{m}_{sec}$+14142
SH	WP 10U-201	all	-0.0042·$\dot{m}_{sec}^2$+71.892·$\dot{m}_{sec}$+4475.6
SH cascaded	WP 7L-60	$\theta_{in,sec} \leq 20°C$	-0.00001·$\dot{m}_{sec}^2$+2.097·$\dot{m}_{sec}$+4769.2
		$\theta_{in,sec} > 20°C$	-0.00002·$\dot{m}_{sec}^2$+2.445·$\dot{m}_{sec}$+ 5219.4

4.6.3 Heat exchanger for solar loop

A heat exchanger is also used to transfer the thermal energy yield from the solar collector loop into the storage tank. In this work large solar thermal systems with collector areas on the range of 100-300 m^2 and storage tanks ranging from 4000-21000 liters are simulated. For this systems size external heat exchangers are typically used. To model the external heat exchanger Type 5b in TRNSYS is used. This standard Type simulates a zero capacitance sensible counter flow adiabatic heat exchanger. Mass flows at the primary and secondary side are known [5]. For the given mass flows and inlet temperatures at both sides, and for a given overall heat transfer coefficient (UA) Type 5b calculates the outlet temperatures of both (primary and secondary) sides.

In Type 5b variable values of the overall heat exchange coefficient (UA) determining the

[5] i.e. primary-side mass flow is not calculated as a function of a given setpoint as it is the case of Type 805

heat exchange coefficient for different regimes of mass flows and temperature levels could also be defined (similarly as it is done for Type 805). However, the performance of solar thermal systems is very insensitive to variations in the UA value of the solar loop heat exchanger [Heimrath, 2004]. Therefore, in this thesis constant values are taken. Heimrath [2004] showed that a linear relation can be found between the UA values of the solar heat exchanger (in W/K) and the collector area (equation 4.7). In this work for solar systems of different size UA values are chosen according to this equation.

$$UA = 88.561 \cdot A_{coll} + 328.19 \tag{4.7}$$

4.6.4 Internal heat exchanger for decentralized DHW supply

In the district heat system decentralized DHW supply to each SFH is foreseen. Small storage tanks of 200 liters with internal heat exchangers are considered for this purpose. The internal heat exchanger can be directly defined in the storage tank model (Type 340, see section 4.7). Water is regarded as heat transfer fluid inside the heat exchanger. An internal serpentine heat exchanger sized according to [Recknagel et al. 2007] is regarded.

For the decentralized DHW supply a constant mass flow of 200 kg/h is assumed for each single-family house. A constant UA value of 1762.1 W/K is considered for the internal heat exchangers in the decentralized storage tanks.

4.7 Storage tanks

Storage tanks are a key component in solar thermal systems since they allow decoupling in time the available solar energy offer and the demands to be supplied, thereby increasing significantly the solar fraction (i.e. the substituted fossil fuel use). Storage units are also used in district heat supply to accumulate a small amount of DHW, thereby reducing the peak loads that need to be supplied by the district heat network. In both cases, storage tanks in the models in this thesis are simulated using Type 340 in TRNSYS.

Type 340 is a multiport storage model which simulates a stratified fluid storage tank with (at most) four internal heat exchangers and a maximum of 10 doubleports for direct charge or discharge. An internal auxiliary heater is also included in the model and can be activated by the user. Thus, the model has a great flexibility making possible to simulate very different types of storage tanks (in size and configuration).

The model is divided in nodes, which are layers of fluid assumed to be completely mixed. Heat transfer between the nodes happens due to mass flows circulating between the nodes and vertical conductivity of water between nodes at different temperature (which is a function of the heat conductivity of water, the storage wall and, if available, the internal heat exchangers). However, no inversion layers are modeled. Instead, they are simulated by natural mixing

between adjacent nodes. Ideally stratified charge and discharge through the doubleports can also be easily modeled.

For solar systems only direct charge and discharge through doubleports is foreseen. In the small decentralized DHW tanks for each single-family house in the district heating model internal heat exchangers have been considered, so that DHW (drinking water) is hydraulically separated in the tank from water in the local heat network (as stated section 4.6.4).

The number of nodes strongly influences thermal stratification in the tank (as shown in the previous chapter, see section 3.2.8.1). A value of 20 l/node allows a good stratification inside the tank and can be used for big and small tanks indistinctly [Heimrath, 2004]. However, in Type 304 a maximum number of 190 nodes is possible. For solar thermal systems with storages greater than 3.8 m^3 190 nodes are assumed.

The size and control strategy of the storage tank influence, for instance, its storage capacity or thermal energy losses, determining thereby its effectiveness and performance as energy storage system. In the following sections size and operation strategy for the storage tanks regarded in the different models are presented.

4.7.1 Centralized storage tank for MFH

4.7.1.1 Storage tank for DHW supply with condensing boiler

In order to determine several parameters related to the performance of solar thermal systems, a reference model consisting of the same building and DHW demand profiles but being supplied only with a conventional boiler is required. Here, the multi-family dwelling with standard building envelope (i.e. MFH-07) with radiators and a condensing boiler is regarded as reference model. The condensing boiler supplies directly the space heating demand, i.e. no storage is foreseen for this purpose. A centralized storage tank is foreseen for DHW supply. DHW demands of the 12 living units are supplied via the instantaneous heat exchanger described in section 4.6.1.

Size The size of the centralized storage tank for DHW supply is calculated in accordance with [Recknagel et al. 2007]. For a system with instantaneous heat exchanger for supplying DHW demands, i.e. without individual storage units in each apartment, assuming a heating time of 1 hour and a temperature difference within the tank of 40 K, the storage volume is 1325 liters. Here, a storage volume of 1500 liters, corresponding to a storage unit available in the market[6] is considered. The tank has a height of 2.32 m and a diameter of 1 m. Surrounding the storage tank, 15 cm of thermal insulation with a heat conductivity of 0.042 W/(mK) are considered.

Configuration and control The inlet from the boiler is considered to be at 90% of the tank height, i.e. 2.09 m, and the outlet at 5% of its height, i.e at 12 cm from the bottom. Inlet and

[6] Flamco PS/R 1500 [Flamco, 2010]

return from the instantaneous heat exchanger for DHW supply are located at 95% and 10% of the tank height, respectively.

A differential controller connected to a temperature sensor at 50% of the total height of the tank ensures that the temperature in the 50% upper part of the tank is always kept between 65°C and 70°C.

4.7.1.2 Storage tank for SH and DHW supply with condensing boiler and solar thermal system

The height to diameter ratio of a storage tank strongly determines the stratification within the tank, thereby influencing the performance of the solar thermal system. Similarly the position of the temperature sensors or inlets and outlets from the energy demands to be supplied are also crucial factors for the performance of the solar thermal unit. Heimrath [2004] showed that increasing the relative inlet height for the return from space heating supply from 10% to 60% reduces the solar fraction in almost 10%.

In this section, main parameters describing the storage units regarded for the models with solar thermal systems are presented.

Size Storage units in solar thermal systems can be divided in two main parts: the solar volume and the auxiliary volume, which includes the stand-by and switching volumes [Fink and Riva, 2004] and that is heated up by the auxiliary heater.

Solar volume: Heimrath [2004] found that a specific volume of 75-85 $l/m^2{}_{coll}$ per squared meter of collector area yields maximum solar energy savings. In this thesis the influence of different specific storage volume on the exergy and energy performance of solar thermal systems is also investigated. For this aim, the storage volume is varied between 30-300 l/m^2 for a given collector area. For the base case, however, a specific storage volume of 75 l/m^2 is chosen.

Auxiliary volume: The size of the stand-by volume is determined according to [Fink and Riva, 2004] for the building with higher peak loads, i.e the building with radiators. This sizing method follows the heating requirements defined in [DIN 4708, 1994]. In this thesis an auxiliary volume V_{aux} of 1000 litres is considered for all models with a solar thermal system. In Table A.7 (in the Appendix) the the main parameters and variables used for estimating it are shown.

Configuration and control The total size of the storage unit in each model is made up by the auxiliary volume and the solar volume. As stated above, the solar volume is varied resulting in different storage sizes. To describe the height of the storage tank as a function of the total storage volume equations 4.8 and 4.9 taken from [Heimrath, 2004] are used. The storage volume V_s in both equations needs to be stated in m^3.

$$H_s = 4.698 + 0.09302 \cdot V_s, \quad 2m^3 \leq V_s < 20m^3 \tag{4.8}$$

$$H_s = 1.65 + 0.32 \cdot V_s, \quad V_s \geq 20m^3 \tag{4.9}$$

The diameter can be easily obtained as a function of the given height H_s and storage volume V_s. Unless explicitly stated otherwise, a layer of 15 cm of thermal insulation with a heat conductivity of 0.042 W/(mK).

The height of the inlets and outlets for energy charge and discharge as well as the position of the temperature sensors are defined as a function of the relative height of the storage tank (from 0 to 100% in percentage, or from 0 to 1 in absolute value). Relative heights are kept for the different storage sizes investigated. In consequence, absolute height of the inlets and outlets and temperature sensors varies for each storage size. In Figure 4.6 relative heights for the inlets, outlets and temperature sensors used to control the charge of the storage tank with the boiler $z_{T.sens,boil}$ and solar system $z_{T.sens,colls}$ are shown. The temperature at the lower part of the auxiliary volume $z_{T.sens,boil}$ is controlled with a differential controller, to be kept at all times between 65 and 70°C. The charging process from the solar collectors is controlled also by means of a differential controller. Solar charging starts if the outlet collector temperature is 7°C higher than the temperature at the lower part of the tank $z_{T.sens,colls}$. The charging process stops if this temperature difference is lower than 4°C. $z_{T.sens,protect}$ represents the height at which a temperature sensor is located in the storage tank to protect it from too high temperatures from the solar loop in summer.

An ideally stratified return from DHW and space heating supply is foreseen in all cases.

The outlet from the storage tank to the boiler and the inlet from the collector loop are positioned at a relative height dependent on the total volume of the storage tank and the auxiliary volume as shown in equations 4.10 and 4.11. The outlet to the space heating system in the building is positioned right above the outlet to the boiler (equation 4.12), i.e. on the lower part of the auxiliary volume. This ensures that even in periods of low radiation and low energy output from the solar thermal system, space heating demands can be properly supplied.

$$z_{out,boil} = 1 - \frac{V_{aux}}{V_{sto}} \tag{4.10}$$

$$z_{in,coll} = 1 - \frac{V_{aux}}{V_{sto}} - 0.05 \tag{4.11}$$

$$z_{out,SH} = z_{out,boil} + 0.05 \tag{4.12}$$

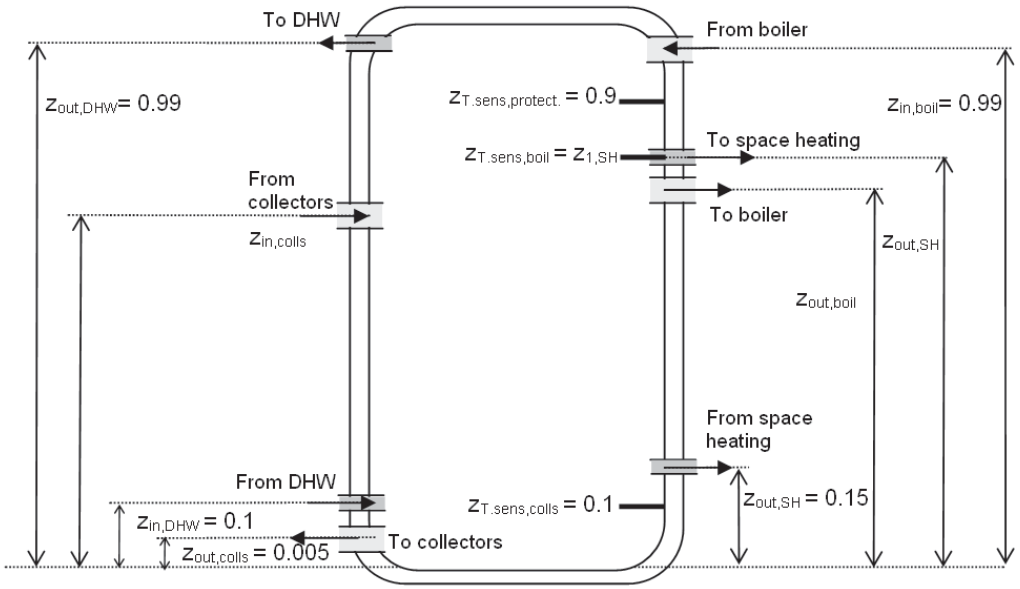

Figure 4.6: Relative heights (from 0 to 1) for the different inlets, outlets and temperature sensors used to control the charging processes in the storage tank.

4.7.2 Decentralized DHW storage tanks for SFH

4.7.2.1 Small storage tanks for DHW supply

In order to reduce peak power demand for DHW production, 200 liters storage tanks are regarded as decentralized DHW storage systems in each single family house (see also section 5.2.1.3 in chapter 5). The charging process succeeds via an internal heat exchanger immersed in the storage volume (see section 4.6.4). In this way, hydraulic detachment is fulfilled between the heat fluid inside the local heat distribution network and the drinking hot water inside the tank.

Size The storage height and diameter are 754 mm and 581 mm, respectively. Around the tank, an insulation layer of 5 cm with a thermal conductivity of 0.042 W/(mK) is regarded.

Configuration and control Charging of the storage units is controlled by a differential controller with a hysteresis of 7°C. The temperature sensor for starting or stopping the charge process is located at 10% of the tank height, so that 90% of the tank volume is kept between 47 and 54°C.

4.8 Condensing boiler

Condensing boilers are simulated as auxiliary heating system to the solar thermal system. Type 700 in TRNSYS is used to simulate this component. Type 700 models an auxiliary heater

of limited capacity (see size of the boiler chosen in Table 4.11). A constant thermal efficiency of 0.95 is regarded in all cases. A changing efficiency for partial load operation of the boilers is not considered. Since the main goal and focus of the investigations within this thesis is the operation and improvement of the solar thermal system, this simplification for modeling the behaviour of the boilers can be regarded as suitable. If, in turn, the operation of the boiler would also be a main goal of this study, its behaviour would need to be described in detail.

Boilers have been sized according to the maximum peak loads for DHW and space heating supply (in chapter 5 peak loads are described in detail). An oversize factor of 10% is regarded. In Table 4.11 maximum peak loads to be supplied in the different cases studied, as well as peak power of the boilers considered in each case are shown. Differences in the peak loads with radiators and floor heating are due to the different reheating time foreseen, corresponding to 1h and 3h respectively[7]. Peak loads for DHW demand are calculated in accordance with the Standard DIN 4708 [1994]. Peak loads for DHW production refer to the power that needs to be supplied by the boiler to the storage tank in order to cover solely DHW demands. Thus, these values are significantly lower than the instantaneous power that needs to be delivered by the DHW flow through heat exchanger (see Table 5.2 of chapter 5).

Table 4.11: Values of the peak loads for DHW and SH supply and rated power of the boilers considered in the buildings with standard (MFH) and improved (MFH-KfW-EffH.40) building envelope.

	Peak loads		Rated power boiler
	SH [kW]	DHW [kW]	[kW]
MFH-07, Radiators (1h)	64	36	110
MFH-07, Floor heating (3h)	47	36	91
MFH-KfW-EffH.40, Radiators (1h)	35	36	78
MFH-KfW-EffH.40, Floor heating (3h)	32	36	75

4.9 Solar thermal collectors

For the simulation of the solar collector field Type 832 in TRNSYS is used. This is a model developed by [Perers and Bales, 2002] and is based on the "Hottel-Whillier-Bliss" equation for flat plate collectors [Duffie and Beckmann, 2006] . The dynamic behaviour of the collector is included in the model.

Main parameters used to describe the performance of the solar collectors used in this work are shown in Table 4.12, where $F(\tau\ \alpha)_{en}$ is the zero loss efficiency, c_1 and c_2 are the coefficients for temperature dependent heat losses, c_5 is the effective thermal capacitance of the collector, b_0 is the incidence angle modifier determined from collector tests and $K_{\varphi diff}$ is the incidence angle modifier for diffuse radiation.

[7] See section 5.1.1.1 for further details

Table 4.12: Values for the parameters used for defining the solar collectors using Type 832 in TRNSYS.

Parameter	$F(\tau\ \alpha)_{en}$	c_1	c_2	c_5	$K_{\varphi diff}$	b_0
Unit	[-]	[W/(m^{2}K^2)]	[W/(m^{2}K^2)]	[J/(m^{2}K^1)]	[-]	[-]
Value	0.8	3.5	0.015	7000	0.9	0.18

Similarly as it is done in [Perers and Bales, 2002] the collectors are modeled without wind or long-wave dependency and with the sky radiation factor set to zero. The data chosen for defining the solar collector correspond to a flat-plate collector with selective surface [Heimrath and Haller, 2007].

4.10 Characterization of district heat return line

In order to characterize the energy available in a district heating return line, the circulating mass flow and its temperature are required. For the simulations performed in this thesis the minimum mass flow is regarded (as constant value in the models), representing, thereby, a worst-case scenario. Minimum mass flow rate available from the district heating pipe is estimated to be 35.3 m^3/h, corresponding to a minimum fluid velocity of 0.2 m/s circulating through a pipe of DN 250. For the dynamic assessment a temperature profile for the district

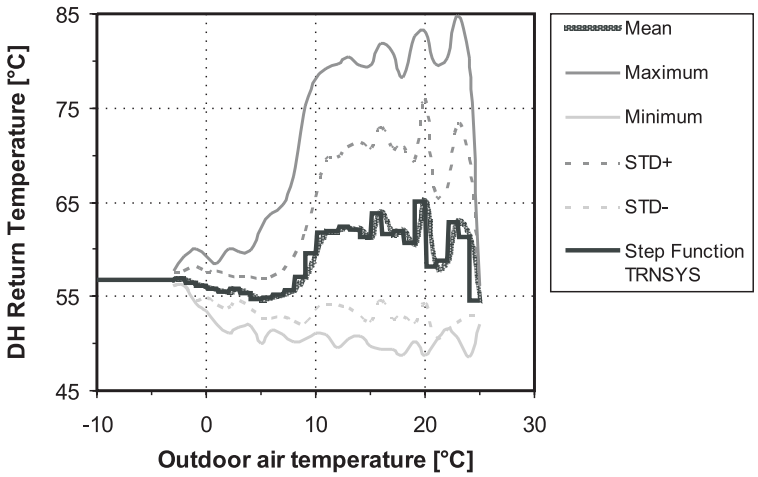

Figure 4.7: Temperature profile for the return district heating line. Profiles for the maximum, minimum and mean values are shown besides the profiles for the higher and lower values of the standard deviation (STD+ and STD-).

heating return temperature (which is the supply of the neighbourhood) has been developed [Kaiser, 2009]. Using this temperature profile allows to get a realistic figure of the utilization potential of low temperature district heating networks for supplying space heating and DHW demands in buildings. In Figure 4.7 maximum, minimum and mean values for the tempera-

ture profile available from the district heating network are plotted as a function of the outdoor air temperature.

The average temperature profile has been considered for dynamic simulations in TRNSYS. The profile has been implemented in the models in TRNSYS as the step function shown in Figure 4.7.

4.11 Weather data

Weather data have a strong influence on the heating load, behaviour and performance of building systems used. Climatic data for Würzburg are considered to be representative for German climatic conditions [DIN 18599, 2007]. In all simulations performed in this work, weather data for Würzburg generated with METEONORM [Meteotest, 2006] are considered.

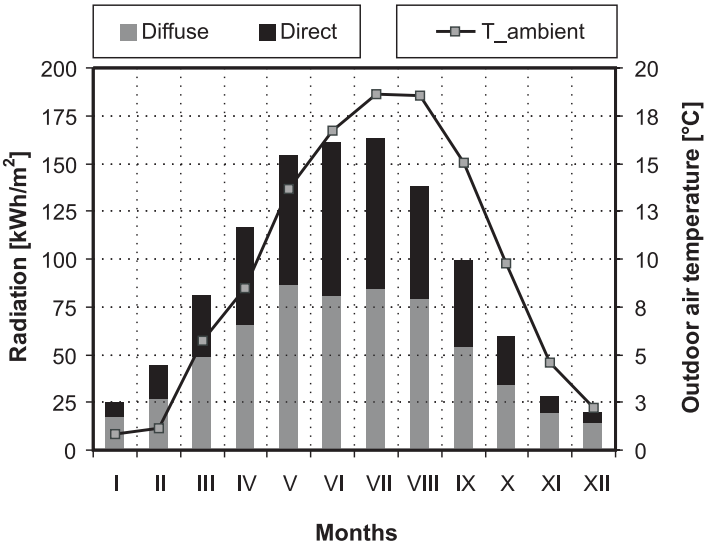

Figure 4.8: Mean monthly outdoor air temperature (right Y-axis) as well as direct and diffuse radiation on horizontal plane (left Y-axis) for Würzburg generated with METEONORM [Meteotest, 2006].

Using the same climatic conditions for the simulation of the solar thermal system used in the multi-family dwellings and the district heating system used for the single family houses means assuming the same reference temperature for exergy analysis in both case studies. In consequence, the exergy performance of the building systems analyzed can be compared with each other.

Figure 4.8 shows graphically monthly values of outdoor air temperature, direct and diffuse radiation for the weather file used in the simulations.

4.12 Comfort criteria in buildings

Buildings are not erected to save energy or to make them more efficient, but to provide a comfortable shelter to their occupants. The energy demand and performance of a building strongly depends on the setpoints and control strategies fixed for its operation, which are based on the comfort level to be provided to the final users. Therefore, any statement of the energy demand or performance of a building needs to come along with the corresponding comfort and indoor environment indicators. Any comparison and optimization of building systems needs to be based on a common basis of thermal comfort conditions kept indoors.

The standard DIN EN 15251 [2007] defines several indicators to evaluate the quality of indoor air environment:

- Thermal criteria for summer and winter: characterized by the operative temperature
- Air quality: characterized by the concentration of several species in indoor air
- Humidity: characterized by the indoor air relative humidity
- Lighting: characterized by the light intensity over a given building area
- Acoustic: characterized by the noise level

In this work different building systems are analyzed and compared based on their thermal performance. Neither humidity treatment units nor lighting equipment are considered and the noise level and air quality inside the studied buildings are out of the scope of this thesis. Therefore, of all criteria mentioned above, only criteria for thermal comfort are relevant.

Thermal comfort: Operative Temperature

In [DIN EN 15251, 2007] ranges for the hourly values of operative temperatures inside the buildings to be used for dynamic energy calculations are defined (see Table 4.13). Mean values for the given ranges should be used as setpoint target value in energy calculations. Yet, variations of the operative temperature within the given range are allowed for energy saving reasons. In this thesis a setpoint of 20.5°C and 21°C has been chosen for the operative temperature in the multi-family dwelling and single-family houses during the heating hours, respectively.

Table 4.13: Recommended values for indoor operative temperatures for hourly energy demand calculation of buildings and building systems according to DIN EN 15251 [2007].

Type of building	Category	Temperature range heating [°C]	Temperature range cooling [°C]
Residential buildings	I	21.0 - 25.0	23.5 - 25.5
	II	20.0 - 25.0	23.0 - 26.0
	III	18.0 - 25.0	22.0 - 27.0

For comparing the energy performance of different building systems the number of hours out of the comfort range needs to be documented. To evaluate thermal comfort conditions within the buildings range II in Table 4.13 is considered. In the following chapter the comfort level is expressed for both buildings with the different building systems considered in each case in terms of the hours outside range II per annum. Additionally, following the concept of *"overtemperature-hours"* introduced by Hauser [1997], the degree-hours under the comfort range for each of the systems analyzed is evaluated and presented.

Chapter 5

Description of case studies

In this chapter the case studies investigated for solar thermal and district heat supply based on the components presented in the chapter before are introduced in detail. Additionally, the correct operation of the building systems studied is shown.

5.1 Solar thermal system for centralized supply of MFH

5.1.1 The multi-family house, MFH

The multi-family building model described in section 4.2.2 is used for performing dynamic simulations of large solar thermal systems. The main aim of such dynamic analyses is to compare the behaviour of the energy and exergy performance of solar systems for different hydraulic configurations and control strategies. By these means, insight on the usability and applicability of the exergy concept for the improvement, sizing or optimization of large solar thermal systems can be obtained.

From the building geometry, orientation and envelope assumed and presented in section 4.2.2 and the DHW consumption profiles obtained as stated in section 4.3.3 energy demands and peak loads of the building can be estimated. The operation of the emission systems used (floor heating and radiators) is also presented.

5.1.1.1 Space heating load - Peak load

According to [DIN V 18599, 2007] a night setback of 7 hours a day can be regarded for energy saving reasons (see section 4.2.2.5), assuming a maximum temperature drop of 4K (from 20°C to 16°C indoor air temperature). Peak heating load for the building is evaluated here following [DIN EN 12831, 2008], which also foresees a factor for estimating the additional power required for reheating the building after a given night setback. Heating loads according to [DIN EN 12831-1, 2008] are used for sizing the heat emission systems inside the building.

The building is assumed to be mid-heavy/heavy (50 Wh/m^3K) and the resulting time constant is 129.5 h. Temperature drops calculated with these assumptions are 2 K for a night

setback of 6 h and a re-heating period of 1 h, corresponding to the control strategy assumed for the radiators, and 1 K for a night setback of 4 h and a re-heating period of 3 h, which corresponds to the control strategy of the floor heating system.

TRNSYS allows a steady-state estimation of the heating load without regarding a night setback. Very good agreement can be found between this simplified stationary approach and peak loads from [DIN EN 12832, 2008] without re-heating factor, as shown in Table 5.1.

Table 5.1: Values of the peak heating load according to [DIN EN 12831, 2008] and calculated using stationary and dynamic methods with TRNSYS. * Values here are referred to useful building area; **_w._ stands for *with* and _wo._ stands for *without*.

Calculation method	Heating load			
	MFH-07		MFH-KfW-EffH.40	
	[kW]	[W/m^2]*	[kW]	[W/m^2]*
DIN EN 12831 wo. additional factor for reheating	36.59	39.35	20.99	22.58
TRNSYS stationary wo. night setback	35.28	37.95	20.49	22.04
DIN EN 12831 w. additional factor for reheating, 1h	63.86	68.68	34.63	37.24
DIN EN 12831 w. additional factor for reheating, 3h	46.33	49.83	31.71	34.10

The use of a night setback implies an increase of 70% and 26% in peak loads for the MFH-07 with re-heating periods of 1h and 3h respectively, and of 65% and 51% for a re-heating period of 1 hour or 3 hours in the building with improved building shell (MFH-KfW-EffH.40).

Monthly energy balances for the multi-family dwelling with the two building shells are shown in Figure B.1 in the Appendix.

5.1.1.2 Configurations for DHW supply

Energy demand for DHW use represents a significant part of the energy requirement in buildings. The importance of DHW energy demands grows as the building shell turns more efficient. Fink and Riva [2004] estimate that the energy demand for DHW applications in central European climates represents between 10% (old buildings) and 50% (low energy houses) of the total energy demand in multi-family dwellings.

Profiles for DHW energy demands are typically calculated with supply temperatures of 45 or 60°C [Heimrath, 2004]. However, the final temperature required for DHW supply is around 30-40°C and is usually achieved by mixing warm water supplied with cold water from the local distribution net. Ideally, exergy losses in the DHW supply process could be reduced by supplying hot water exactly at the requested temperature level (30-40°C). Yet, in order to comply with the technical rule DVGW W 551 [2004] referring to protection against legionella growth, a temperature of at least 60°C must be ensured at the outlet of the drinking water heater system in centralized large DHW systems with a water volume greater than 3 liters in the supply pipes. If the volume in the pipes is smaller than 3 liters supply might occur at temperatures lower than 60°C but heating of the whole water volume up to 60°C must be ensured once a day [DVGW, 2004].

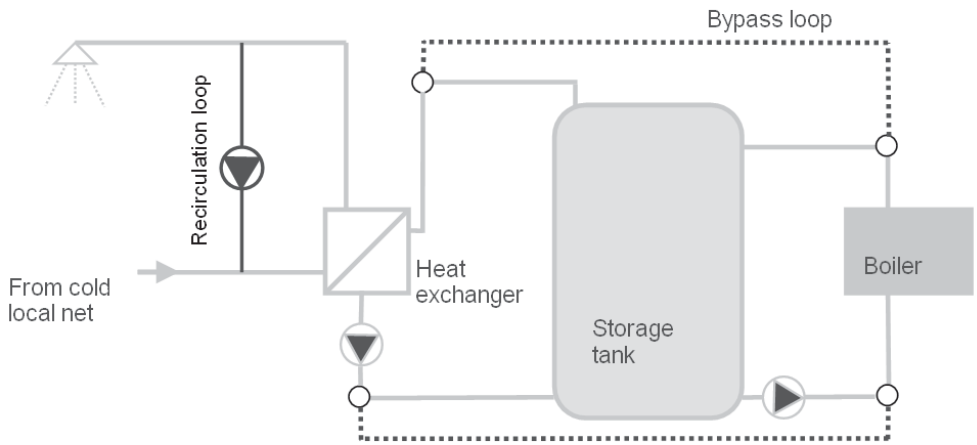

Figure 5.1: Simple schema for the three hydraulic configurations considered for DHW supply side of the multi-family dwelling.

As part of this thesis, and to investigate the influence of lower supply temperatures and different hydraulic configurations for DHW supply on the energy and exergy performance of DHW preparation systems, three different configurations for centralized DHW supply of the multi-family dwelling are studied (see Figure 5.1):

- Option *(i)* is composed of the light grey components in Figure 5.1. It represents a very simple hydraulic loop without recirculation, i.e. instantaneous heating of domestic hot water takes place whenever energy demand is present. The supply temperature for the secondary side of the instantaneous heat exchanger is set constantly to 60°C.

- Option *(ii)* is composed of the recirculation loop (dark grey in Figure 5.1), compulsory for buildings with a useful area greater than 500 m^2 [DIN 4701-10, 2003] and the light grey components in Figure 5.1. The system is sized and operated so that the maximum allowed temperature drop of 5K in the recirculation loop is not exceeded [DVGW, 2004]. For energy saving reasons, the recirculation system is turned off 8 hours a day (from 18pm to 2am), according to [DVGW, 2004]. The set point for the outlet of the secondary side in the heat exchanger was also set constant to 60°C. From the comparison between systems *(i)* and *(ii)* insight on the recirculation losses and the pumping energy required for this purpose can be obtained.

- Option *(iii)* includes all components shown in Figure 5.1. The DHW supply temperature is set to 45°C. The recirculation loop is operated as in (ii), i.e. with 8 hours setback and 5K as maximum temperature drop. However, once a day secondary side water volume must be heated up to 60°C [DVGW, 2004]. To fulfill this aim, the bypass circuit at the primary side has been designed (dotted dark grey lines in Figure 5.1). By this means, the temperature set point of the storage can be lowered to 55°C, since heating of the

secondary circuit to 60°C is done directly by the boiler. This case allows investigating the potential of lowering DHW supply temperatures in the performance of the systems. It is important to remark that case *(iii)* would only be in compliance with the technical rule [DVGW, 2004] if the secondary side water volume would be lower than 3 liters. Therefore, it represents a theoretical analysis of energy and exergy saving potential for planning concepts able to fulfill this aim. Furthermore, it might also help pinpointing the energy saving potential from other forms of protection against legionella such as UV-filters, which prevent the necessity of using higher supply temperatures.

5.1.1.3 DHW Supply - Peak load

The energy demands and peak loads for DHW supply in each configuration are shown in Table 5.2. High values of the peak load for DHW production are due to the use of an instantaneous heat exchanger for heating cold water from the net according to the instantaneous demand.

Table 5.2: Energy demands for supplying DHW consumption for the three different hydraulic configurations analyzed.

Hydraulic configuration	Energy demand		Peak loads
	[kWh/a]	[kWh/(a person)]	[kW]
(i) - T_{supply} = 60°C, without recirculation	17296.6	596.4	187.9
(ii) - T_{supply} = 60°C, with recirculation	22047.9	760.3	187.9
(iii) - T_{supply} = 45°C, with recirculation	20274.9	699.1	150.5

Monthly balances for DHW and SH energy demands with the two building shells and for option *(ii)* are shown in Figure B.2 in the Appendix. DHW energy demands for case *(ii)* represent 33% of the space heating load in the case of a standard building envelope (MFH-07) and 69% of the annual space heating loads in case of improved insulation level (MFH-KfW-EffH.40), being in good agreement with estimations from Fink and Riva [2004] for different building standards.

5.1.2 Emission systems used

5.1.2.1 Radiators

Radiators are sized to cover the heating load of the building in Table 5.1 assuming a re-heating time of 1 hour, i.e. 63.86 kW for the MFH-07 and 34.63 kW for the MFH-KfW-EffH.40. State of the art radiators have moved in the last years from conventional high temperature radiators to low temperature systems. These lower temperature operation allows a reduction of the thermal losses in the distribution pipes and better integration of renewable energy sources. As stated in chapter 4, design supply and return temperatures of 55 and 45°C, respectively, are chosen in this work.

Figure 5.2 shows the good agreement between the set point for inlet and return temperatures and the inlet and return temperatures simulated under dynamic conditions. Simulations in TRNSYS are carried out with a time step of 3 minutes. A display of yearly data for the operation of the radiators would therefore be very comprehensive. Thus, results for the operation during one winter month are presented as an example. Results in Figure 5.2 correspond to 3 minute-wise dynamic conditions in January.

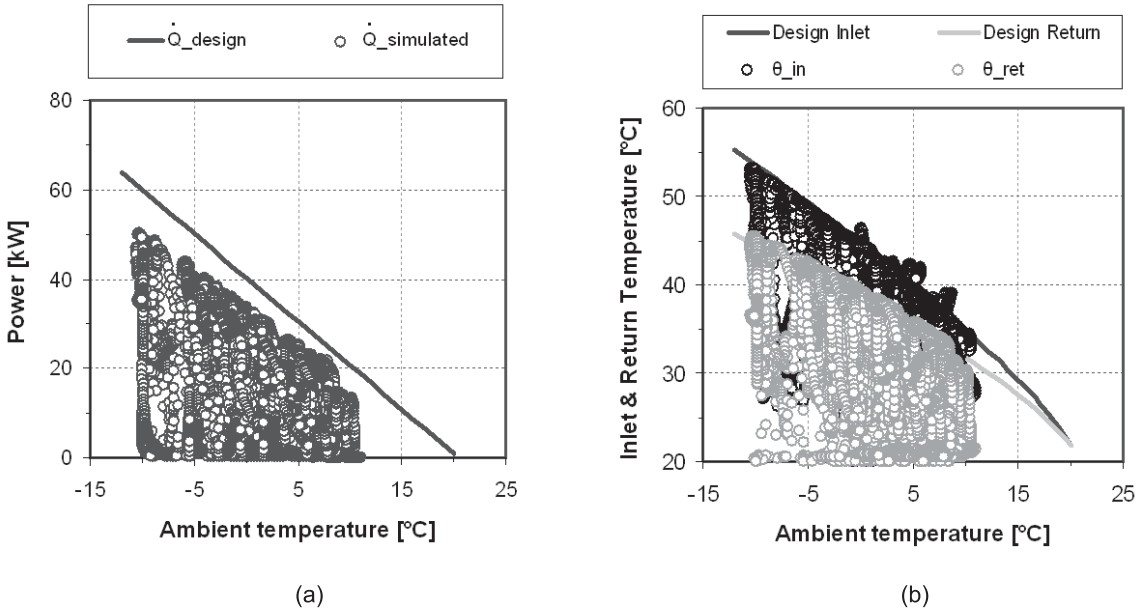

Figure 5.2: (a): Design and simulated heating load as a function of the outdoor temperature in January for the MFH-07 with radiators; (b): Set point and simulated values for the inlet and outlet radiator temperatures of the ground floor in the MFH-07 in January.

Inlet temperatures lower than the demanded set point are due to cooling down of water in the pipes at times where no mass flow, i.e. no heating demand, is present. Return temperatures are always slightly above the given set points. This is due to the overestimation of the heating load required to re-heat the building after the night setback, as shown graphically in Figure 5.2 (a).

5.1.2.2 Floor heating system

The floor heating systems in the multi-family dwelling are sized to cover the heating load of the building in Table 5.1 assuming a re-heating time of 3 hours, i.e. 46.33 kW for the MFH-07 and 31.71 kW for the MFH-LEH.

Figure 5.3 shows the good agreement between the set point inlet temperatures and the inlet temperatures simulated under dynamic conditions. Results in Figure 5.3 correspond to 3 minute-wise dynamic conditions in January. Similarly as with radiators, design peak loads

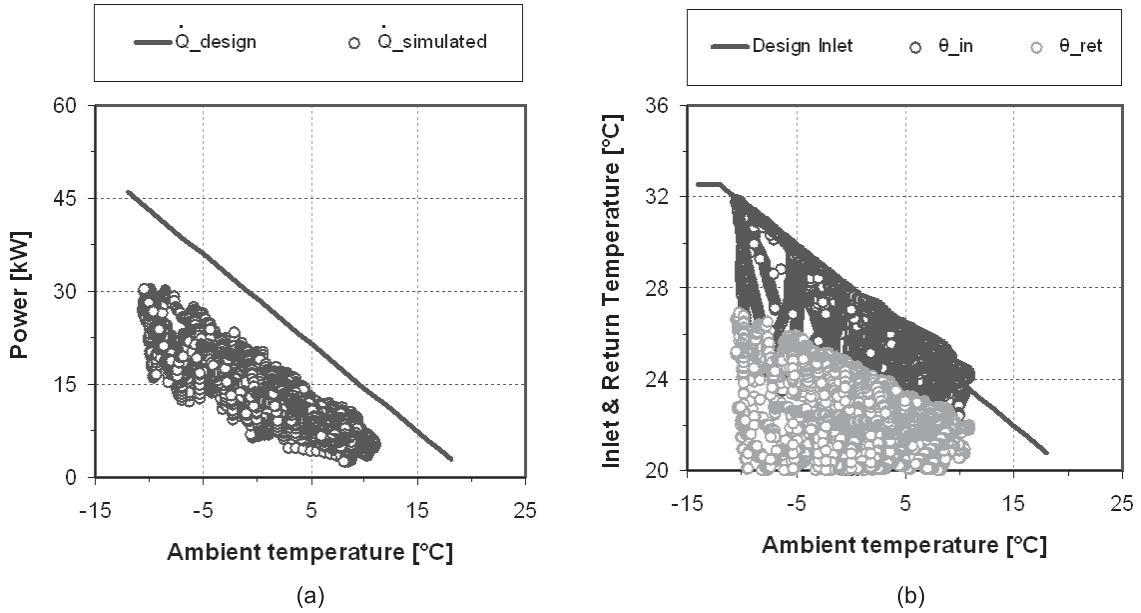

Figure 5.3: Design and simulated heating load as a function of the outdoor temperature in January for the MFH with floor heating system (left); Set point and simulated values for the inlet temperatures for the floor heating system in January (right).

are overestimated as compared to the actual dynamic power supplied in each timestep, as shown in Figure 5.3 (a).

5.1.3 Thermal comfort

Figure 5.4 (a) shows operative temperatures in the three thermal zones used to simulate each storey in the MFH-07 with radiators, named *Ground*, *First* and *Second* in the diagram, as a function of outdoor air temperature. The diagram shows values for each timestep, i.e. 3 minutes, in January. The dynamic behaviour of operative temperatures is shown in Figure 5.4 (b) for the coldest week of the month, which is also the coldest of the year. Operative temperatures for the three thermal zones are between 20 and 21°C during the hours without night setback. This shows the good fulfillment of thermal comfort conditions in the building. A temperature drop of about 2 K can be observed during the night setback.

Figure 5.5 shows the good agreement between the dynamic behaviour of the operative temperatures for the thermal zone *Ground* with both emission systems, i.e. with radiators and floor heating system. For the radiators a re-heating period of 1h between 5:00 and 6:00 is considered. Radiators have lower thermal mass, allowing a much faster increase of the operative temperature after the nigh-setback. In consequence, they are also easier to control, being able to keep almost constantly the required setpoint for the operative temperature (20.5°C). In order to achieve similar operative temperatures with the floor heating system a

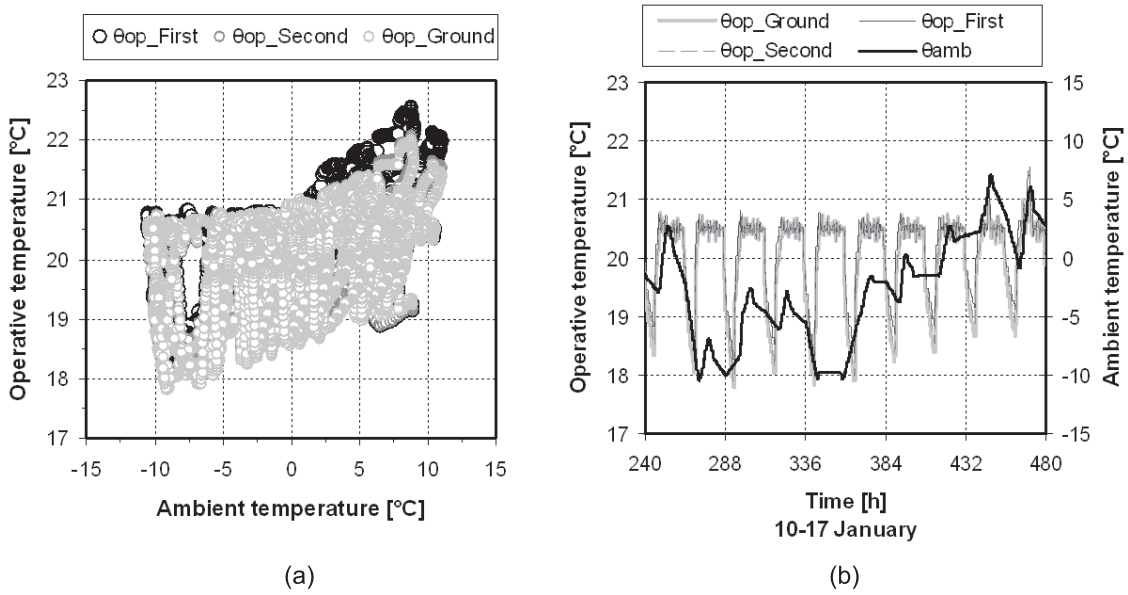

Figure 5.4: (a): Operative temperatures in the three thermal zones of the MFH, named *Ground*, *First* and *Second* in the diagram, as a function of outdoor air temperature in January; (b): Dynamic behaviour of operative temperatures in the three thermal zones and outdoor air temperature for the coldest week of the year.

longer re-heating period is required. Due to the high thermal mass of the floor heating system, re-heating must happen longer before the setpoint for the operative temperature increases to 20.5°C (i.e. at 6:00 am). Here, a re-heating period of 3h between 2:00 and 5:00 is foreseen. This control strategy allows very good agreement in the operative temperatures of both emission systems, as shown in Figure 5.5.

The high thermal inertia of the floor heating system makes this system more difficult to control. In consequence, greater oscillations can be observed in the operative temperature during daytime due to the quick variation of internal and solar gains and the slow response of the floor heating system.

As stated in chapter 4, thermal comfort is evaluated as a function of the hours that the operative temperature is outside the comfort range II [DIN EN 15251, 2007]. Since only heating systems are analyzed here, thermal comfort is only evaluated during the heating period, i.e. from September to May, and only temperature differences below the accepted range are evaluated here. Comfort range II corresponds to operative temperatures between 20 and 25°C for heating conditions. It has been assumed that this temperature range must be kept during daytime (from 6:00 to 23:00). In turn, during night setback operation the minimum the limit for the operative temperature is allowed to drop until 16°C. In Table 5.3 the number of hours that mean hourly values of the operative temperature are out of range II is shown for the different building cases analyzed. Total hours over the heating period amount 6552 h. On the column labelled *Total* the number of hours that the operative temperature in any of the three thermal zones is below the defined comfort range is shown.

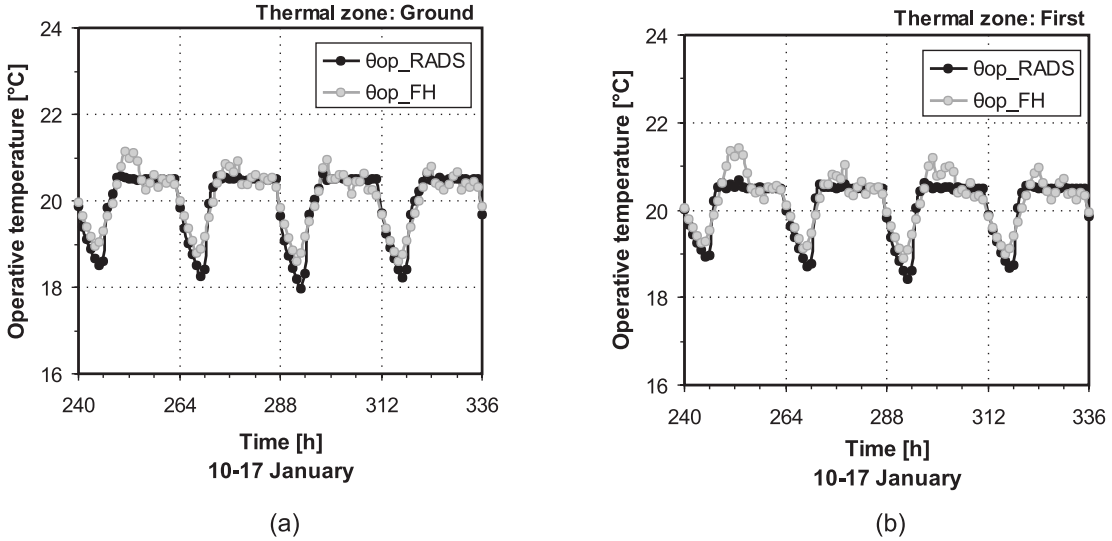

Figure 5.5: Operative temperatures for the building with radiators and with floor heating system for three days in January. Temperatures shown correspond to ground (a) and first floor (b) of the multi-family dwelling, named *Ground* and *First* in the diagrams.

For completeness, in Table 5.3 the degrees-hours below the defined comfort range are also stated. This last indicator joins both considerations on the time out of the comfort range and the temperature difference to the minimum value of the required range. Thus, it is considered to be a clearer indicator of how well comfort criteria are fulfilled.

Table 5.3: Indicators for thermal comfort related to range II [DIN EN 15251, 2007] for the building cases analyzed. The number of hours below the comfort range in a year is stated. For completeness, the degree-hours below the comfort range are also indicated for the three thermal zones. *Rads.* stands for radiators, *FH* for floor heating and *wo.* for without.

	Hours				Degrees-Hours		
	Ground [h]	First [h]	Second [h]	Total [h]	Ground [°Ch]	First [°Ch]	Second [°Ch]
MFH-07, Rads.	322	174	267	325	216.0	117.4	171.5
MFH-07, FH	467	230	489	519	157.9	52.5	187.6
MFH-07, Rads. wo. setback	867	675	786	1088	8.3	3.1	7.2
MFH-07, FH wo. setback	1311	987	1314	1833	154.5	114.8	158.9
MFH-KfW-EffH.40, Rads.	176	134	170	185	90.7	57.9	82.8
MFH-KfW-EffH.40, FH	118	69	129	130	18.4	8.9	26.3

The building with floor heating system shows 51% more hours out of comfort range II than the building with radiators. This is due to the slower re-heating after the night setback achievable with the floor heating system. Despite re-heating with the floor heating system is foreseen from 2:00 to 5:00, often the operative temperature in the building at 6:00 is around 19.9°C, being thus out of the comfort range. However, in terms of degrees-hours the differ-

ence between both emission systems is greatly reduced, being even favourable to the building with floor heating system. Degree-hours below the comfort range for both space heating systems are relatively similar. In consequence, it can be concluded that both systems provide a similar range of thermal comfort. Similar results can be found for the building with improved building shell (MFH-KfW-EffH.40).

5.1.4 Solar thermal systems

For calculating the fractional energy savings[1] achieved by different configurations of a solar system a **reference case** is required. The reference case is taken as the multi-family dwelling with standard building shell (MFH-07) and with radiators operated with night setback. A storage tank of 1500 liters for centralized DHW supply is foreseen. No storage unit is used for space heating supply. All solar systems analyzed in this thesis (and described in the following) are compared with this reference case.

The **base solar thermal system** in this thesis consists of a collector area of 100 m^2 and a storage tank of 8.5 m^3, composed of a specific solar storage volume of 75 l/m^2_{colls} and an additional auxiliary volume of 1 m^3. The annual *utilisation* of the system in this work (also called *Utilisation II*[2]) as defined in [Fink and Riva, 2004; Heimrath, 2004] is 596.5 $kWh/(m^2_{colls}a)$, being significantly high due to the relatively constant DHW demand caused by the recirculation loop regarded for DHW supply (see section 5.1.1.2). Fractional energy savings obtained with such a system are around 30%.

Starting from this base solar system, several hydraulic configurations and system sizes are investigated. The goal is to obtain the influence of different parameters (such as storage or collector field size, connection of the auxiliary boiler to the storage tank, or use of three way valves for discharging the storage tank) on the energy and exergy performance of the solar system. The main case studies and parameters analyzed here are as follows:

- **Storage insulation:** Insulation thicknesses around the storage tank are varied between 10 and 50 cm.

- **Storage size:** The size of the solar storage is varied between 30 and 300 l/m^2_{colls}. Constant insulation thicknesses of 15 cm for the different storage sizes are simulated. Additionally, variable insulation thicknesses[3] for the different tanks were assumed, yielding constant UA values of 14.44 W/K for the different tanks. In this manner, the effect of thermal losses in the tanks on the performance of the solar unit is thoroughly investigated.

[1] This parameter describes the substituted fossil energy as compared to a system without solar unit. See chapter 6 for a detailed definition of this parameter.

[2] This parameter is calculated as the ratio between the annual building energy demands (for DHW and SH) and the collector area.

[3] with values between 9 and 37 cm.

- **Emission system:** Several case studies are simulated in parallel with radiators and floor heating systems. This allows obtaining the influence of using different (low-temperature) emission systems in the performance of the solar unit.

- **Control strategy for space heating systems:** In all cases analyzed, unless explicitly stated otherwise, a night setback strategy for the space heating system is foreseen (see section 4.2.2.5 in chapter 4). Yet, floor heating system and radiators have significantly different thermal inertia. Thus, the influence of night setback operation on their energy and exergy performance is expected to be different.

- **1 and 2 three way valves for space heating discharge:** The impact of using one and two three way valves for enabling as stratified discharge from the storage tank for space heating supply is investigated. The three way valves are located at a relative storage heights of 0.7 and 0.5.

- **Building shell:** Several case studies, e.g. the systems with three way valves or with different emission systems, are simulated additionally for the building with improved building shell (i.e. KfW-EffH.40). This allows studying the energy and exergy performances for increased solar fractions (due to the lower building energy demands).

- **Series connection of auxiliary boilers for space heating and DHW supply:** In all solar systems described above, the auxiliary boiler heats up directly the *auxiliary volume* (see section 4.7.1.2), keeping it at temperatures between 65 and 70°C, as stated in chapter 4, and causing, thereby, significant thermal losses. Furthermore, although the auxiliary volume is located at the top of the storage tank, a slight heating up of the upper part of the solar volume by the auxiliary boiler is expected due to mixing and conduction inside the tank. These processes can be avoided if the auxiliary heater is connected in series with the solar storage tank. To check the improvement achievable with such a hydraulic connection between the boiler and the storage unit, a system with two separate boilers for supplying DHW and space heating demands connected in series with the solar volume has been simulated. This connection is applied to both emission systems studied, i.e. floor heating system and radiators.

5.2 District heat supply for a neighbourhood of SFH

5.2.1 The single-family houses, SFH

The single-family house described in section 4.2.3 is used for performing dynamic simulations of different configurations of district heat supply in a neighbourhood in order to compare their energy and exergy performances. From the building geometry, orientation and envelope assumed and the DHW consumption profiles obtained as stated in section 4.3.4 the energy

demands and peak loads required to supply the buildings can be estimated. In the following sections, peak loads used for sizing energy supply systems are presented. Additionally, several aspects showing the correct performance of the simulated systems are also shown.

5.2.1.1 Space heating load - Peak load

Similarly as for the multi-family dwelling, peak heating load for the single family houses is evaluated here following DIN EN 12831 [2008] without additional factor for reheating, since no night setback is foreseen. Very good agreement can be found between peak loads calculated with the standard and those from the stationary simplified assessment in TRNSYS, as shown in Table 5.4.

Table 5.4: Values of the peak heating load of the SFH with the two building shells (EnEV 09 and KfW-EffH.40) according to DIN EN 12831 [2008] and calculated using stationary and dynamic methods with TRNSYS. * Values here are referred to useful building area.

Calculation method	EnEV 09 Heating load		KfW-EffH.40 Heating load	
	[kW]	[W/m^2]*	[kW]	[W/m^2]*
DIN EN 12831	7.89	42.75	5.52	29.91
TRNSYS stationary	7.72	41.86	5.61	30.42

Monthly energy balances for each of the 24 SFH studied are shown in Figure B.3 in the Appendix for both building shells.

5.2.1.2 Configuration for DHW supply

The neighbourhood to be supplied with the district heating return pipe consists of 24 single family houses. A DHW draw off profile has been derived for each house (see Figure A.5 in the Appendix). A recirculation loop inside the houses is not necessary [DIN 4701-10, 2001]. In addition to DHW demand profiles for each house, a reasonable combination of the consumption profiles must be found. A simultaneity factor of 0.39 can be found for centralized district heat supply systems with small storage units in each house [Recknagel et al., 2007].

DHW profiles for the SFH are combined here with the help of the simultaneity factor to obtain a reasonable DHW consumption pattern for the whole neighbourhood. For this purpose, it is assumed that 39% of the SFH, i.e. 9.36 houses, demand DHW at the same time and with the same consumption profile (Figure A.5). Another 9.36 houses demand have simultaneously the same DHW demand pattern one hour later than the first ones, i.e. with one hour time delay. The rest, i.e. 22% of the houses (5.28 houses) demand DHW one hour before the first ones also with the same consumption pattern. The total DHW draw-off profile for the whole neighbourhood, results from the time-shifted combination of the single draw-off profiles as explained above.

5.2.1.3 DHW supply - Peak load

Instantaneous peak loads for DHW supply amount 84 kW per house. Power supply available from the district heating network is limited by the mass flow and temperature level available. In order to avoid such big power demands to the district heating network a small storage unit is considered in each house. For systems with storage units hourly peak power demands for a single family house are calculated assuming a bath (200l/h) at 40°C, resulting in a peak power of 7kW. Assuming a heating time of one hour for the storage units a minimum storage volume of 172.25 liters is required. A 200 liters storage tank is assumed for each SFH.

Monthly energy demands for SH and DHW supply can be found in Figure B.4 in the Appendix. DHW energy demand represents 30.5% of the space heating load in the SFH with EnEV 2009 building shell and 52.9% of the space heating loads in case of the building with KfW-EffH.40 envelope, being in good agreement with values in [Fink and Riva, 2004].

5.2.2 Emission systems used: Floor heating system

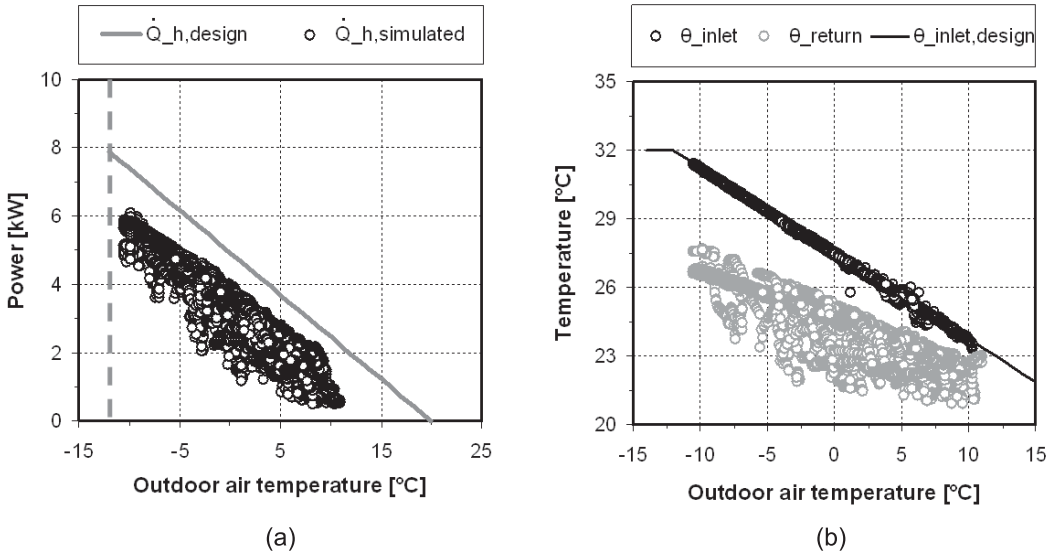

Figure 5.6: (a): Design heat loads to be supplied to the building (*Q_h,design*, grey line) and actual power supplied to the FH systems (*Q_h,simulated*, black unfilled dots) as a function of outdoor air temperature in January; (b): Setpoint for inlet temperatures in the floor heating systems *θ_inlet,design* and simulated values for the inlet *θ_inlet* and return *θ_return* temperatures from the FH system as a function of outdoor air temperature in January.

In Figure 5.6 (a) design heat loads as a function of outdoor air temperatures are shown in addition to the real power supplied to the floor heating system. Design heat loads are oversized as compared to real power demanded in dynamic conditions.

Figure 5.6 (b) shows design setpoint for inlet temperatures of the floor heating system in the SFH *θ_inlet,design* as a function of outdoor air temperatures. Values from dynamic analysis

θ_inlet for each timestep in January are shown also on the diagram. As stated in section 4.4.2 no pipes are regarded inside the single family houses. Additionally, the mixing valve for providing the desired inlet temperature to the floor heating system is located at the entrance of every house, i.e. after the district heat network and the subsequent thermal losses in its pipes. In consequence, very good agreement can be found between design and simulated values, since after the mixing process no thermal losses occur.

5.2.3 Thermal comfort

Figure 5.7 (a) shows operative temperatures in the two thermal zones used to simulate the SFH corresponding to the ground floor and upper first floor, named *θ_Ground* and *θ_First* in the diagram, as a function of outdoor air temperature. The diagram shows values for each timestep, i.e. 3 minutes, in January. The dynamic behaviour of the operative temperatures is shown in Figure 5.7 (b) for the coldest week of the month, which is also the coldest of the year. Operative temperatures for the two thermal zones are always between 20 and 21°C, showing good fulfillment of thermal comfort conditions inside the buildings.

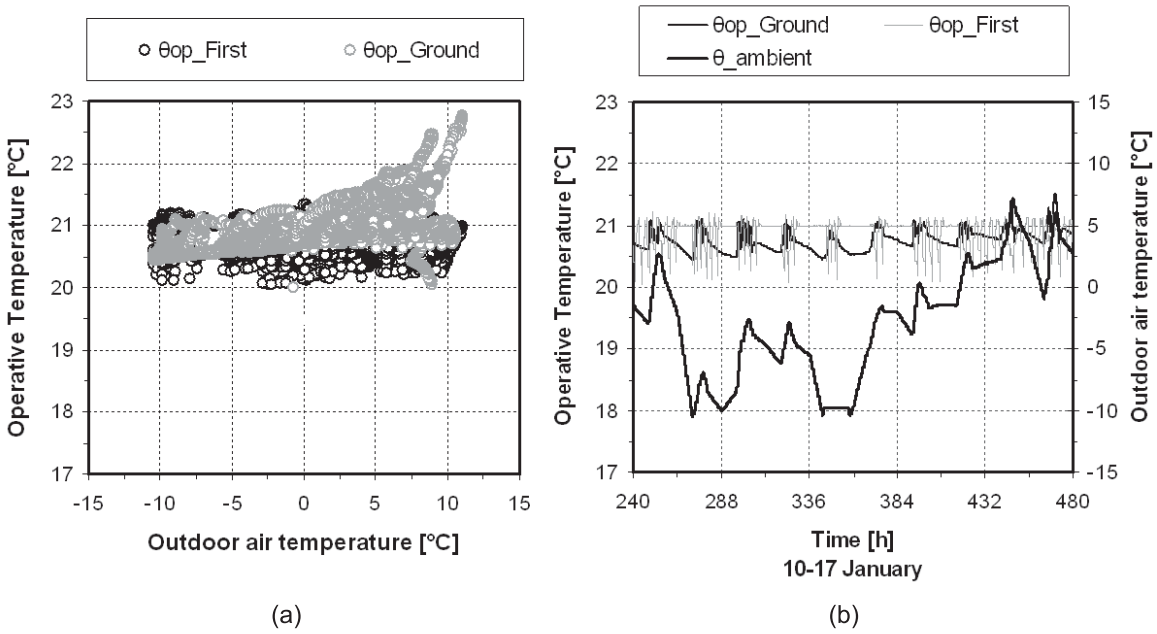

Figure 5.7: (a): Operative temperatues in the two thermal zones of the SFH, named *θ_Ground* and *θ_First* in the diagram, as a function of outdoor air temperatures in January; (b): Dynamic behaviour of operative temperatures in the two thermal zones and outdoor air temperature for the coldest week of the year.

Operative temperatures for the two thermal zones are always between 20 and 21°C. Thereby, thermal comfort conditions are always fulfilled and an evaluation of the hours or degree-hours out of the comfort range is superfluous, i.e. both amount to zero.

5.2.4 District heat supply

In the district heating system studied here district heat supply to the neighborhood occurs via a centralized heat exchanger (Figure 5.8). In this way, the district heating network from the local utility company is decoupled from the building appliances and systems installed, i.e. mass flow and temperature drop in the district heating network are not directly determined by the mass flows and temperature drops in the building systems (e.g. floor heating systems).

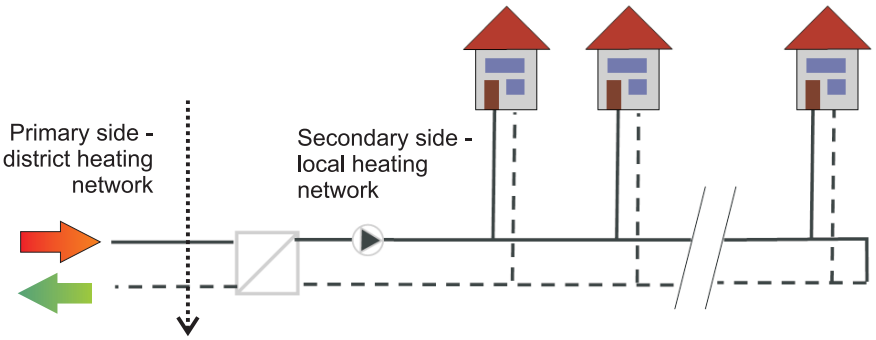

Figure 5.8: Simplified scheme showing the hydraulic configuration for supplying district heat to the neighborhood. Local utility network is decoupled from the building services by means of a centralized heat exchanger.

5.2.4.1 Preliminary steady-state analysis

With the configuration shown in Figure 5.8 the main energy and exergy inputs into the district heating system are the heat flow from the primary side of the heat exchanger, i.e. from the district heating network, and the pumping energy both in the primary and secondary sides. As it is shown in chapter 7, pumping energy for the secondary side (i.e. for the local heat distribution within the neighbourhood) represents a marginal part of the energy and exergy supply. Having much shorter pipes and less pressure losses in the primary side, it can be expected that pumping energy in the primary side is even smaller. Thus, pumping energy for the primary side is not regarded here.

Preliminary steady state analyses have been carried out in order to understand the exergetic behaviour of the district heating supply. As a first simplification, it is assumed that the secondary side operates under given conditions, i.e. pumping energy, which depends on the mass flows and temperature levels chosen, remains unchanged. The main variable is, then, the thermal energy input from the primary side district heating pipe (see dotted arrow in Figure 5.8). In Figure 5.9 exergy efficiencies achieved when supplying the space heating and domestic hot water (DHW) loads at different primary side inlet and return temperatures and mass flows are shown. The reference temperature is assumed as the mean outdoor air temperature over the heating period (4.8°C) and mean total load for SH and DHW supply is considered (85.97 kW).

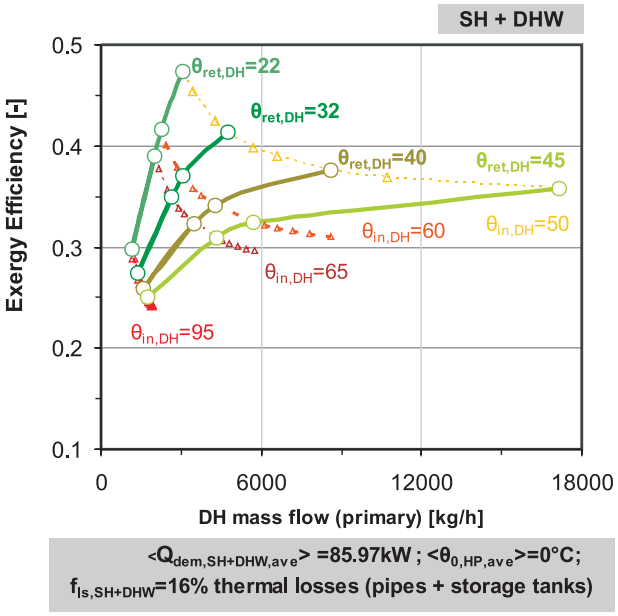

Figure 5.9: Exergy efficiency for different supply and return temperatures and mass flows (primary side). Continuous lines represent constant return temperatures $\theta_{ret,DH}$, while dashed lines represent constant supply temperatures $\theta_{in,DH}$. Only thermal mass flows are regarded here. Energy losses in the pipes have been assumed as constant.

Lower supply temperatures (dashed lines) increase the exergy efficiency of the heat supply, i.e. lower the quality at which the heat flow is supplied to the single family houses allowing a better matching of the energy supply and demand. Lower return temperatures (continuous lines) also increase significantly the exergy efficiency of heat supply. For a given supply temperature, lower return temperatures lead to an increase in the exergy efficiency. In other words, maximizing the degradation of the thermal potential of the primary mass flow increases the exergy efficiency. These trends and strategies for improved operation of district heating networks are coherent with those found by Dötsch and Bargel [2009].

From this graph, two main strategies to increase the exergy efficiency of district heating supply can be derived:

1. **Minimize return temperature to the district heating network:** this can be achieved by proper sizing of the heat exchanger between the district heat and the local heat distribution networks. However, minimum achievable return temperatures to the district heating pipe strongly depend on the building systems, e.g. low temperature space heating systems allow lower return temperatures. Therefore, the use of appropriate building systems is of great importance for promoting this strategy.

2. **Minimize supply temperature from the district heating network:** supply temperatures are determined by temperature profile available from the district heating pipe and cannot be directly influenced. However, for DHW preparation a supply temperature of

50°C must be always ensured [AGFW, 2009]. In turn, maximum required inlet temperature for space heating is 32°C. Thus, a way to reduce the supply temperature the low temperature uses (i.e. space heating demand) is by cascading the energy demands according to their required temperature level.

5.2.4.2 Hydraulic configurations studied

Two different hydraulic configurations have been developed to achieve each of the improved strategies mentioned above. In Figure 5.10 improved options (1) and (2) are shown besides the reference option (0).

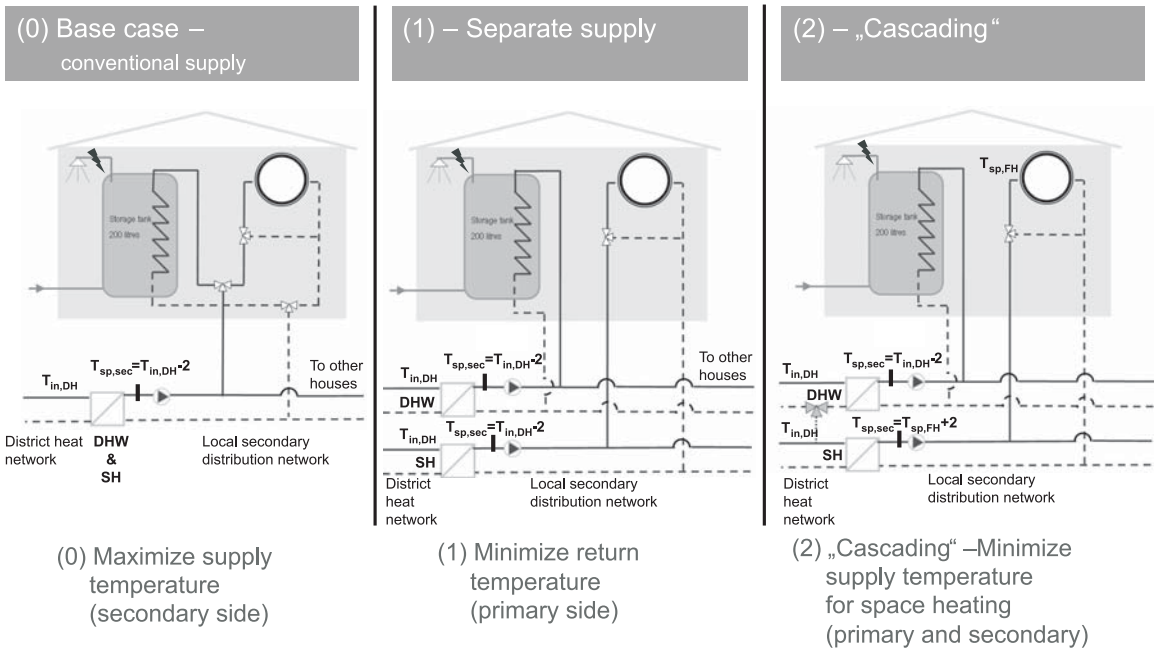

Figure 5.10: Hydraulic configurations investigated for the low temperature district heating supply.

Case (0) is a typical configuration of district heating supply [StWerke, 2009]. DHW and SH demands are supplied by a common heat exchanger. To minimize pumping power in the secondary side (i.e. in the local heating network) outlet temperature at the secondary side of the heat exchanger is maximized at all times. Setpoint for the outlet temperature is calculated as a function of the inlet temperature available from the district heating network (see equation 5.1), i.e. temperature difference in the secondary side is maximized, leading to reduced mass flows.

$$T_{sp,sec} = T_{in,prim,DH} - 2 \tag{5.1}$$

In case (1) DHW and SH demands are supplied by two separate heat exchangers. In this configuration each of the heat exchangers can be sized separately for minimizing primary side

return temperatures at its specific operation conditions. Following, lower outlet temperatures at the primary side of the heat exchanger are expected. The setpoint for the secondary sides of DHW and SH supply is also defined following equation 5.1.

In case (2) a three way valve connects the primary side return from DHW supply with the primary side for SH supply. If the return temperature and mass flow from DHW are high enough to supply SH demands, mass flow from DHW supply circulates also through the SH heat exchanger. Otherwise, mass flow is withdrawn directly from the main district heating pipe. In this way, cascading of DHW and SH demands is achieved. The setpoint for DHW supply has been kept as in the previous cases (equation 5.1). However, primary side mass flow from the DHW heat exchanger can only be used for supplying space heating demands (i.e. cascaded) if its temperature is higher than the required setpoint. Thus, secondary side setpoint for SH supply has been minimized. It is defined as a function of the required inlet temperature in the floor heating systems, as shown in equation 5.2.

$$T_{sp,sec,SH} = T_{sp,FH} + 2 \tag{5.2}$$

The three cases in Figure 5.10 have been dynamically simulated in TRNSYS. In chapter 7, results from this detailed dynamic assessment are presented.

Instantaneous electric heater for DHW supply The temperature profile assumed for the district heating return pipe oscillates between 50 and 65°C (see Figure 4.7). As stated in chapter 4 (see section 4.3.4), the required temperature for safe DHW supply (due to legionella protection) in the single family houses is 50°C [AGFW, 2009]. Thus, the district heat supply alone might not be able to guarantee the required supply temperatures of 50°C at the outlet of the storage tanks at all times. To ensure a safe DHW supply, an instantaneous electric heater is foreseen at the outlet of the storage unit, as shown by the black flash in Figure 5.10. This electric unit operates only if outlet temperatures from the storage tank (i.e. from DH supply) are below the required level of 50°C. In this manner, supply temperatures of 50°C are guaranteed. The series connection between the electric heater and the storage tank ensures maximum use of the district heat supply to pre-heat and supply DHW demands.

Chapter 6

Benchmarking parameters

6.1 Parameters for characterizing the performance of solar thermal systems

6.1.1 Thermal fractional energy savings, $f_{sav,th}$

The thermal fractional energy savings characterize the energy from conventional fuels that is substituted by a solar thermal system as compared to a reference scenario without solar thermal energy use. The use of a *reference case* (see chapter 5) consisting of the same building, i.e. the same space heating and DHW demands, but supplied with a conventional boiler, i.e. without solar thermal system, is required. Equation 6.1 shows the expression of the thermal fractional energy savings.

$$f_{sav,th} = 1 - \frac{\frac{Q_{boil,out,sol}}{\eta_{aux,sol}} + P_{el,coll} \cdot f_{PE,el}}{\frac{Q_{boil,ref,out}}{\eta_{aux,ref}}} \tag{6.1}$$

6.1.2 Extended fractional energy savings, $f_{sav,ext}$

The extended fractional energy savings characterize the energy substituted by the use of the solar thermal system, including all auxiliary energy required for the pumps in both the solar combi-system and the reference cases. Equation 6.2 shows the analytical expression of this parameter.

$$f_{sav,ext} = 1 - \frac{\frac{Q_{boil,out,sol}}{\eta_{aux,sol}} + (P_{el,coll} + P_{el,boil,sol} + P_{el,SH} + P_{el,DHW}) \cdot f_{PE,el}}{\frac{Q_{boil,ref,out}}{\eta_{aux,ref}} + (P_{el,boil,ref} + P_{el,SH} + P_{el,DHW}) \cdot f_{PE,el}} \tag{6.2}$$

6.2 Parameters for exergy performance

A great number of parameters to depict the exergy performance of an energy system can be found in the literature [Cornelissen, 1997; Dincer and Rosen, 2007; Tsatsaronis, 1993]. In

this chapter the set of parameters considered as most relevant for characterizing the exergy performance of the case studies analyzed are presented. These parameters are applied in chapter 7 to the different building case studies shown.

6.2.1 Annual final and primary specific exergy input

Similarly as in terms of energy, the performance of a given system increases if the required exergy input for supplying the given demands is reduced. The aim of optimizing or improving the performance of a system is, therefore, to reduce the required input. Thus, the performance of different system configurations in this thesis is also depicted in terms of the annual required exergy input.

Final exergy input represents the final exergy that needs to be supplied to the building in order to cover its demands (i.e. represents the input in the *Generation subsystem* in Figure 3.1). The exergy of primary energy represents the exergy required as input for the whole energy supply chain of the building, i.e. including transport and transformation losses in the supply chain of the used energy carrier (i.e. input in the *Primary energy transformation subsystem* in Figure 3.1).

In buildings, the energy demanded and supplied is often stated in specific terms, i.e. as energy required per squared meter useful building area. Similarly, yearly final and primary exergy inputs are stated in this thesis also in specific terms.

6.2.2 Exergy efficiency

Exergy efficiencies are a suitable and appropriate base for comparing the performance of different heating and cooling systems. As any other efficiency, exergy efficiencies are defined as the ratio between the obtained output and the input required to supply it. Exergy efficiencies help identifying the magnitude of exergy destruction within an energy system [Cornelissen, 1997], i.e. how suitable the chosen supply is for covering a particular demand. Exergy efficiencies, on the contrary to energy efficiencies (e.g. COP of heat pumps), have always values between 0 and 1.

6.2.2.1 Simple and rational exergy efficiency

Different definitions of exergy efficiency parameters can be found in the literature. At least two types of exergy efficiencies can be identified and differentiated: *"simple"* or *"universal"* and *"rational"* or *"functional"* [Cornelissen, 1997; Tsatsaronis, 1993]. The general mathematical expressions of the simple and rational exergy efficiencies are shown in equations 6.3 and 6.4.

$$\psi_{simple} = \frac{Ex_{out}}{Ex_{in}} \tag{6.3}$$

$$\psi_{rat} = \frac{Ex_{des,out}}{Ex_{in}} \tag{6.4}$$

Although the simple exergy efficiency is an unambiguous definition for the exergy performance of a system, it works better when all components of the incoming exergy flow are transformed into some kind of useful output [Cornelissen, 1997]. In most of the building systems analyzed in this work this is not the case, since some part of the exergy input is fed back again to the energy system and does not constitute a useful output strictly speaking, e.g. in a hydronic heat or cold emission system in a building outlet water flows back via return pipes into the heat/cold generation system. The rational exergy efficiency, in turn, accounts for this difference between *"desired output"* and any other kind of outflow from the system. Therefore, it is a much more accurate definition of the performance of a system. It is, in consequence, a term that can be better used without taking to misleading conclusions. An example illustrating in detail the difference between both exergy efficiencies can be found in [Torío et al., 2009]. It shows the greater appropriateness of the rational exergy efficiency for building systems.

In this work the rational exergy efficiency is considered as relevant, i.e. undesired output is regarded also as an exergy consumption within the system that could and should be reduced. All exergy efficiencies presented here correspond to rational exergy efficiencies.

6.2.2.2 Single and overall exergy efficiency

Depending on whether the exergy efficiency is referred to a single component or process of a whole energy system, or to all processes and components integrating the system, so-called *"single"* and *"overall"* exergy efficiencies can be defined [Marletta, 2008; Esen et al., 2007; Hepbasli and Tolga Balta, 2007]. An example of single and overall efficiencies for the room air subsystem and complete energy chain in Figure 3.1 is given in equations 6.5 and 6.6. Overall efficiencies are derived from an input/output approach for the analysis of a given energy system and are derived from the product of the single efficiencies of the single processes or components encomprised in the energy system analyzed.

$$\psi_{single,r} = \frac{Ex_{in,env}}{Ex_{in,r}} \tag{6.5}$$

$$\psi_{ove} = \frac{Ex_{in,env}}{Ex_{in,prim}} \tag{6.6}$$

In this work mainly overall exergy efficiencies, characterizing the total performance of a complete energy system, are presented. Overall exergy efficiencies of different supply systems studied, e.g. different hydraulic configurations of district heat supply or of the solar thermal systems, can be directly compared with each other, since the same reference temperature has been used for exergy anaylsis of both building supply systems (see section 4.11).

6.2.2.3 Primary and final exergy efficiency

In this work the exergy peformance of a system is stated in terms of its final and primary exergy efficiency. The general expression for both parameters is shown in equations 6.7 and

6.8. As any other efficiency, the general definition of *use* over *effort* applies. Both are defined as rational efficiencies, i.e. only the desired output of the system (i.e. exergy demand, $Ex_{dem(SH+DHW)}$) is regarded as *use*. The *effort* is considered as the final exergy input or the exergy of primary energy required by the system to supply the given use. In this sense, both are overall exergy efficiencies since the performance of the complete energy system into analysis (in the final exergy efficiency) or the whole supply chain (in the primary exergy efficiency) are analyzed.

$$\psi_{fin} = \frac{Ex_{dem(SH+DHW)}}{Ex_{fin}} \tag{6.7}$$

$$\psi_{PE} = \frac{Ex_{dem(SH+DHW)}}{Ex_{PE}} \tag{6.8}$$

Equations 6.9 and 6.10 show the expression for calculating final and primary exergy efficiencies from dynamic exergy analysis with n timesteps. In this thesis annual exergy efficiencies are presented, i.e. the ratio between annual exergy demands for SH and DHW and annual final or primary exergy input, respectively.

$$\psi_{fin} = \frac{\sum_{k=1}^{k=n} Ex_{dem(SH+DHW)}(t_k)}{\sum_{k=1}^{k=n} Ex_{fin}(t_k)} \tag{6.9}$$

$$\psi_{PE} = \frac{\sum_{k=1}^{k=n} Ex_{dem(SH+DHW)}(t_k)}{\sum_{k=1}^{k=n} Ex_{PE}(t_k)} \tag{6.10}$$

Similarly as energy performance parameters such as the seasonal performance factor[1], annual final and primary exergy efficiencies can be seen as a measure of the exergy performance over the analyzed period.

6.2.3 Exergy expenditure figure

Schmidt et al. [2007] developed and introduced a new parameter for characterizing the exergy supply in buildings called *exergy expenditure figure*. In equation 6.11 the exergy expenditure figure is defined for a general component *i* of an energy system.

$$\varepsilon_i = \frac{Effort}{Use} = \frac{Ex_{in,i}}{En_{out,i}} = \frac{F_{Q,i}}{\eta_i} \tag{6.11}$$

The exergy expenditure figure is calculated as the ratio of the exergy input required to supply a given energy demand *(effort)* and the provided energy demand *(use)*. Therefore, it represents a sort of quality factor (exergy to energy ratio, see chapter 2) of the energy processes occurring in the given component. Energy and exergy losses happening in the component are

[1] e.g. $f_{sav,ext}$ for solar thermal systems or so-called *JAZ, Jahresarbeitszahlen* in German for characterizing the performance of heat pumps.

implicitly taken into account by the ratio of provided output to required input. In consequence, if the energy losses in the component are high, i.e. energy efficiency is low, the exergy expenditure figure might reach values higher than 1 (see equation 6.11).

This parameter needs to be compared to the exergy to energy ratio of the energy demand to be provided, i.e. to the quality factor of the energy demand. Values close to the exergy to energy ratio of the energy demand indicate a good matching between quality levels (i.e. exergy) of the energy supplied and demanded. In turn, values diverging from the exergy to energy ratio of the demand indicate bad matching and, in consequence, lead to conclude that other energy sources shall be used for providing that specific use and/or energy losses need to be reduced.

For the particular application of space heating and cooling of buildings, quality factors of the energy demanded are very low[2]. Subsequently, in space heating and cooling applications, lower exergy expenditure figures indicate more optimized energy supply systems.

Exergy expenditure figures can be derived for any subsystem shown in Figure 3.1 of an energy supply system within a building. However, the chosen generation system influences more strongly than any other component the overall exergy performance of energy supply. Thus, in chapter 7 for the building cases analyzed in this thesis only exergy expenditure figures for the generation subsystem are presented.

[2]For space heating applications and reference and indoor air temperatures of 0 and 20°C respectively, the quality factor of energy demand is 7%.

Chapter 7

Results and discussion

7.1 Configurations for DHW supply

In this section results from the different hydraulic configurations presented in section 5.2.4.2 for DHW supply in the multi-family dwelling (MFH) considered are analyzed. The focus of this section is to study the performance of the different DHW system configurations, disregarding the energy generation system they might be coupled with (e.g. boiler, solar thermal system). Therefore, the energy and exergy flows are analyzed from the storage system onwards, i.e. energy and exergy flows in the generation system are not regarded at this stage. Renewable energy sources and low-temperature environmental heat available have low exergy content (due to its relatively low temperature level). Thus, it can be expected that those DHW system configurations which require lower exergy input to supply the given demands, can be coupled more efficiently with low exergy sources.

Energy and exergy inputs required for DHW supply in each of the three configurations proposed, as well as energy and exergy losses in each component of the DHW supply system are analyzed. By these means, insight can be gained on the optimization potential of the different components of DHW supply.

Figure 7.1 shows the annual energy and exergy flows through the different components of the DHW supply systems following the input-output approach described in chapter 3.

The DHW demand represents the final energy demand to be provided to the users, once the warm water has been mixed to a lower temperature level. For estimating this theoretical DHW demand which could be provided ideally to the users a supply temperature of 40°C has been regarded. The difference between the input and output in each of the components labelled on the X-axis in Figure 7.1 shows the energy and exergy losses in each component of the supply system. Thermal energy losses in the supply pipes represent the greatest energy losses of the system and one of the greatest exergy consumption in the supply chain. The difference in the energy and exergy levels between the theoretical energy and exergy demands (right end of the lines in Figure 7.1) and the previous point (i.e. outlet from the supply pipes) shows the energy and exergy losses associated to the mixing process from the supply temperature in

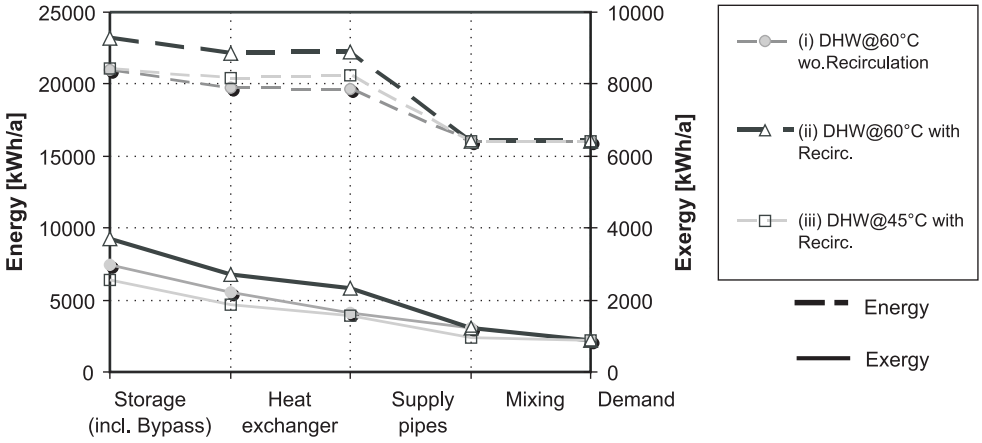

Figure 7.1: Energy and exergy flows through the different components of the three hydraulic configurations investigated.

each case (45 or 60°C) to the final demand temperature of 40°C. The mixing process does not imply any energy loss. However, in terms of exergy this mixing process has associated exergy consumption.

Case (ii) shows the highest required energy and exergy input, being therefore the system where greatest energy and exergy losses happen on the supply process. Yet, it also has the highest safety conditions regarding thermal protection against legionella. Case (i), with the same supply temperature but without recirculation system, shows energy and exergy inputs which are 10 and 25% lower than in case (ii) respectively. Energy and exergy required in case (iii) is 9 and 30% lower, respectively.

In Figure 7.2 the energy and exergy losses for the different components of the three hydraulic systems are shown. Thermal energy losses and electrical energy input for the operation of the pumps are shown separately. Electrical energy, which might be considered as a loss in the corresponding component, is evaluated here as final energy, i.e. primary energy factors for electricity have not been regarded.

Thermal energy losses in the recirculation pipes might amount between 10 and 100% of the final DHW demand [Heimrath, 2004]. In cases (ii) and (iii) they amount 38% and 25% of the total DHW energy demand, respectively, thus representing medium to well insulated systems. Yet, they represent the greatest energy losses in Figure 7.2. In terms of exergy thermal losses in the supply pipes represent a great part of the total losses present, namely 19%, 33% and 26% of the total losses for cases (i), (ii) and (iii), respectively. They are the third greatest exergy consumption in case (i) and the second in cases (ii) and (iii). This shows the importance of insulating well the DHW supply and recirculation pipes.

Exergy consumption due to mixing the supply hot water with cold water from the net to obtain the final demand temperature of 40°C are plotted separately in Figure 7.2 (see *"demand mixing"*). Thermal exergy consumption due to this mixing process is reduced by 77%

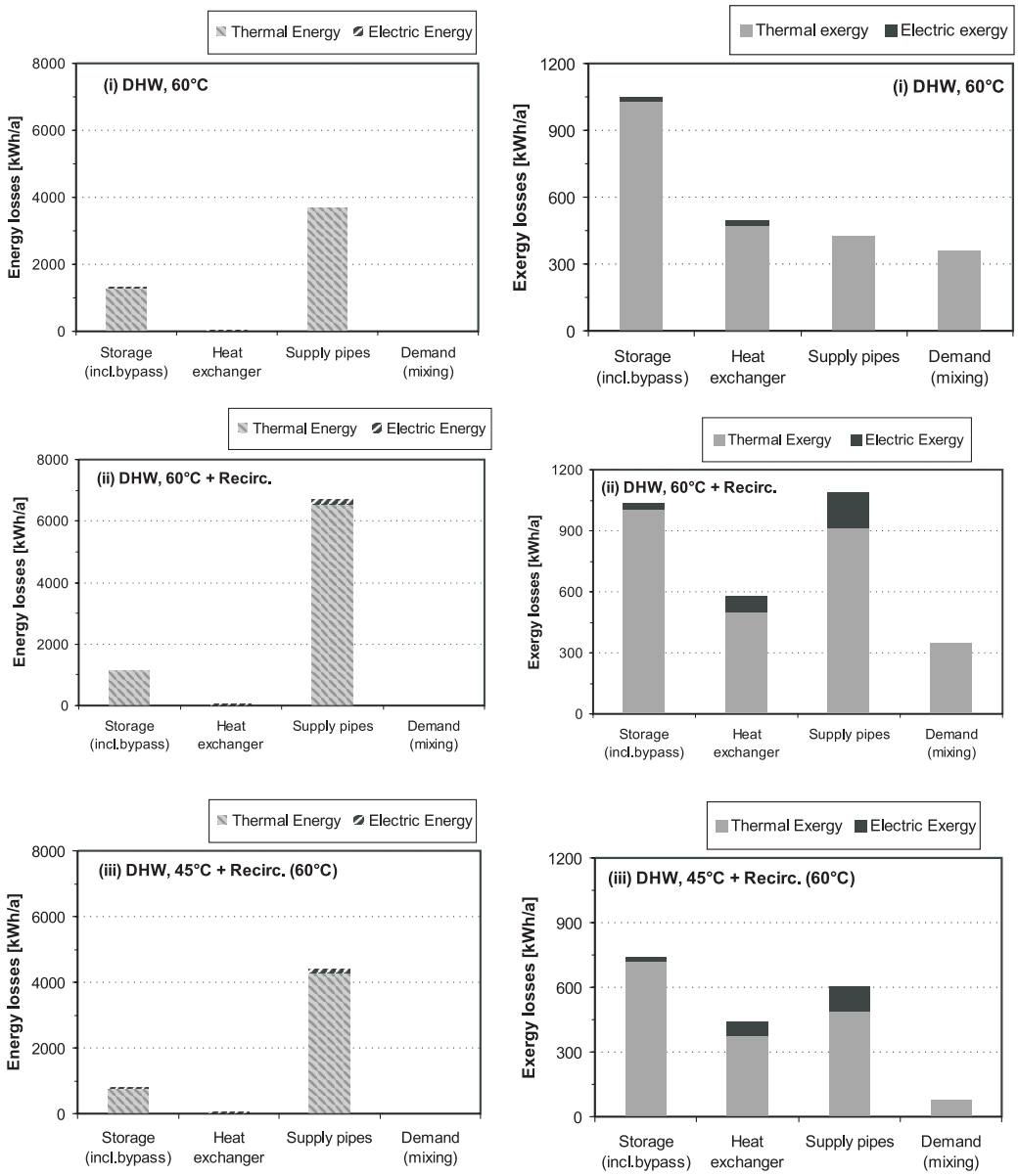

Figure 7.2: Energy and exergy losses by components of the three different hydraulic configurations investigated. For clearness, thermal and electrical energy and exergy inputs are plotted separately.

by lowering the supply temperatures from 60°C to 45°C (cases (ii) and (iii)). This shows the importance of systems supplying the required temperature level and avoiding mixing at the end of the supply process. Substituting thermal protection against legionella growth by other systems available would be of great advantage for this purpose.

Pumping energy for the operation of the heat exchanger is similar in cases (ii) and (iii), namely 3.66 Wh_{el}/kWh_{th} and 3.08 Wh_{el}/kWh_{th} respectively. In case (i) (i.e. without recirculation) the electrical input required amounts 1.30 Wh_{el}/kWh_{th}. The great difference with

cases (ii) and (iii) shows the pumping energy required for the recirculation pump. However, the electrical input required for the operation of the systems does not represent a relevant share of the total exergy input, thus not being critical for the choice of the systems. This indicates that the additional pumping energy required due to higher mass flows when lowering supply temperatures does not represent a threshold for the more efficient operation of the systems. From an exergy perspective the heat exchanger operation might also be improved. Thermal exergy losses in the heat exchanger represent about 20% of the total exergy losses. They are reduced by 20% and 25% by using lower temperature levels (case iii) as compared to cases (i) and (iii) respectively.

Thermal energy losses in the storage tank do not seem to be very relevant as compared to thermal losses in the pipes. However, in terms of exergy they represent the greatest share of all exergy consumption in the components shown in Figure 7.2. Exergy consumption in the storage tank is strongly influenced by stratification during the charge and discharge processes, as shown in section 3.2.8.1 of chapter 3. In the models analyzed here ideal stratification during charge or discharge process has not been regarded. In consequence, exergy losses happen when the inlet temperatures of the charge and discharge mass flows are at different temperatures than the water layer in the tank where the mass flow enters. The return temperature from DHW supply might reach values as low as 10-15°C, being significantly lower than the temperature in lower part of the tank (around 58-32°C for cases (i) and (ii)). This temperature difference is significantly reduced in case (iii), where the temperature in the lower part of the tank is around 47-28°C. In consequence, exergy losses in the storage tank are reduced by 28% if lower supply temperatures are chosen, i.e. for case (iii).

Energy analysis highlights the importance of reducing thermal energy losses in the pipes. In turn, exergy analysis shows clearly the advantages of supplying DHW demands at temperatures closer to that of the final energy demand (here assumed as 40°C): with supply at lower temperatures exergy losses in the storage tank and mixing process are reduced additionally to the exergy losses in the supply pipes. Energy input required for a supply at 60°C without recirculation loop (i) and at 45°C with recirculation loop (iii) are nearly the same. In turn, exergy supply is reduced by 14%.

However, of all hydraulic options analyzed in this section only case (ii) complies with current German standards and regulations for DHW supply. Therefore, despite being the worst performing option, only system (ii) is regarded in the following section for DHW supply with large solar thermal systems. Yet, insight gained from the analysis introduced in the present section is applied to the investigated configurations of the solar thermal system, i.e. strategies to minimize mixing processes and to avoid unstratified charge and discharge of the storage tank are analyzed.

7.2 Solar thermal system for centralized supply of a MFH

In this section, results from energy and exergy analysis of the solar thermal system for providing a part of the SH and DHW demands in the multi-family dwelling are presented.

As shown in chapter 6, a reference building case without solar thermal unit is required to calculate the fractional energy savings $f_{sav,ext}$ and $f_{sav,therm}$. As stated in chapter 5, for all cases analyzed here, the multi-family dwelling with standard building shell (MFH-07) and with radiators operated with night setback is taken as reference. A 1500 l storage tank for centralized DHW supply is foreseen. No storage unit is used for space heating supply.

7.2.1 Insulation of the storage tank

Energy losses in the storage tanks of solar thermal system greatly influence their energy performance [Fink et al., 2007]. In this section, the influence of increasing the insulation thickness around the storage tank on the energy and exergy performance of the solar system is studied.

Figure 7.3 shows the behaviour of the fractional energy savings and exergy efficiencies for insulation thicknesses between 10 and 50 cm.

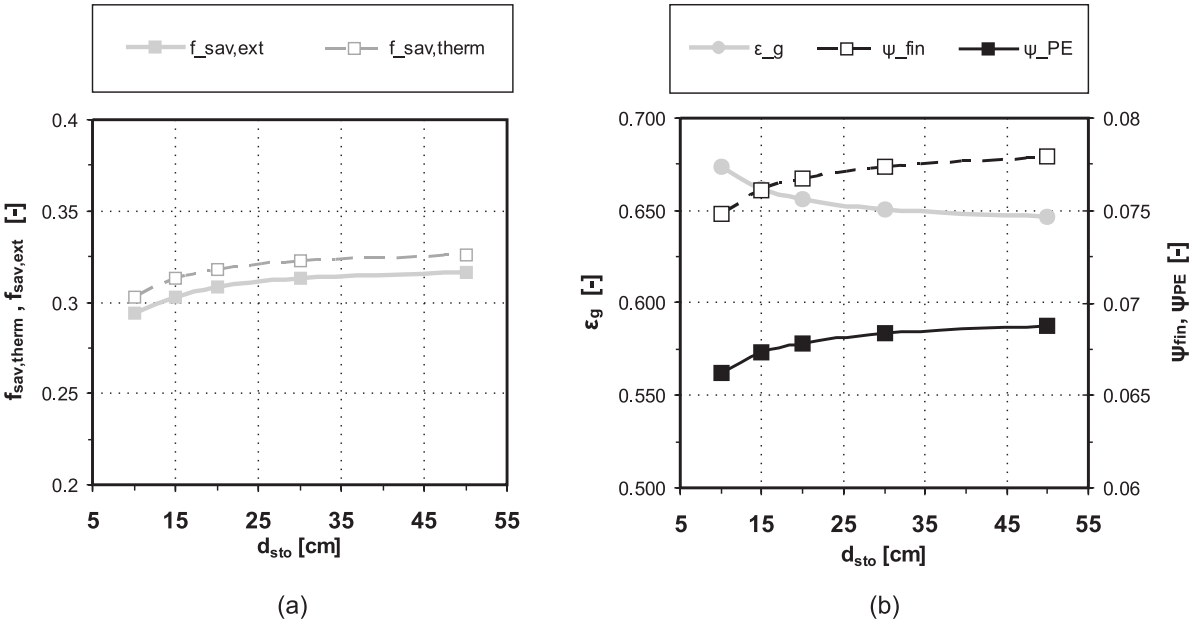

Figure 7.3: Thermal and extended fractional energy savings (left Y-axis), primary and final exergy efficiencies (right Y-axis) for the solar thermal system as a function of the storage insulation thickness.

With an insulation thickness of 50 cm thermal energy losses are reduced by 71% as compared to an insulation of 10 cm. In consequence, the energy input from the boiler is reduced, thereby increasing the share of solar heat in the supply and extended fractional energy savings increase by 2.2%. Herewith, the quality of the supplied energy, i.e. the exergy expenditure fig-

ure for the generation system ε_g, is reduced almost by the same amount (2.8%).

As stated above, the main effect of an increased insulation is the reduction of the energy input from the boiler. Since this represents a high exergy input, proportional to the energy input[1] and which amounts for 90% of the total exergy input, the exergy efficiency is strongly influenced by the variation of the fossil fuel input. Any changes in the quality of the solar thermal heat supplied cause only marginal changes in the exergy efficiency. In consequence, exergy efficiencies show the same behaviour as the energy performance figures.

It is remarkable that changes in the exergy expenditure figure are on the same range than those found for fractional energy savings. In turn, the change in the exergy efficiency amounts only 0.26%. This is due to the low exergy demands for SH and DHW in buildings. In consequence, supplying them with a great share of high-quality fossil fuels (amounting to 90% of the total exergy input) leads to very low values of this paramter and only small changes can be observed as the share of fossil fuels in the supply is slightly reduced.

7.2.2 Storage size

The energy performance of solar thermal systems strongly depends on the storage tank size. Heimrath [2004] determined an optimum specific storage size between 50 and 100 $\mathrm{l/m^2_{colls}}$ for a combi-solar thermal system supplying a multi-family dwelling. Fink and Riva [2004] use a specific storage volume of 50 $\mathrm{l/m^2_{colls}}$ for sizing different large solar thermal systems and solar supported heating networks for space heating and DHW supply in residential buildings.

In this section the influence of the storage size in the energy and exergy performance of the solar thermal system studied is investigated. For this purpose, the specific storage volume in the *base solar system*[2] is varied between 30 and 300 $\mathrm{l/m^2_{colls}}$.

Figure 7.4 (a) shows the behaviour of the main parameters for characterizing the energy and exergy performance of the solar thermal system as a function of the specific storage volume. Extended and thermal fractional energy savings are shown on the left Y-axis. Primary and final exergy efficiencies are shown on the right Y-axis. For comparison, primary exergy efficiency of the reference case, i.e. conventional supply with a condensing boiler and without solar thermal unit $\Psi\_prim,boiler$, is also shown in the diagram.

The behaviour of the energy and exergy performance of the system is very similar. Curves for energy and exergy performance show the same conclusions: until a specific storage size of 100 $\mathrm{l/m^2_{colls}}$ fractional energy savings and exergy efficiency of the systems increases. Bigger storage units do not yield a significant increase in the energy or exergy performances. With a specific storage volume of 300 $\mathrm{l/m^2_{colls}}$ a slight decrease in the energy and exergy performance of the system can be observed.

A similar trend for the fractional energy savings of a solar thermal system can be found in [Heimrath, 2004]. Heimrath [2004] states that this behaviour is due to the increase in the

[1] The proportionality constant is the quality factor for LNG, here assumed as 0.95.

[2] i.e. the multi-family dwelling with standard building envelope (MFH-07), with radiators operated with night-bac a 8.5[3] storage tank and a solar thermal collector field of 100 $\mathrm{m^2_{colls}}$ (see section 5.1.4 in chapter 5).

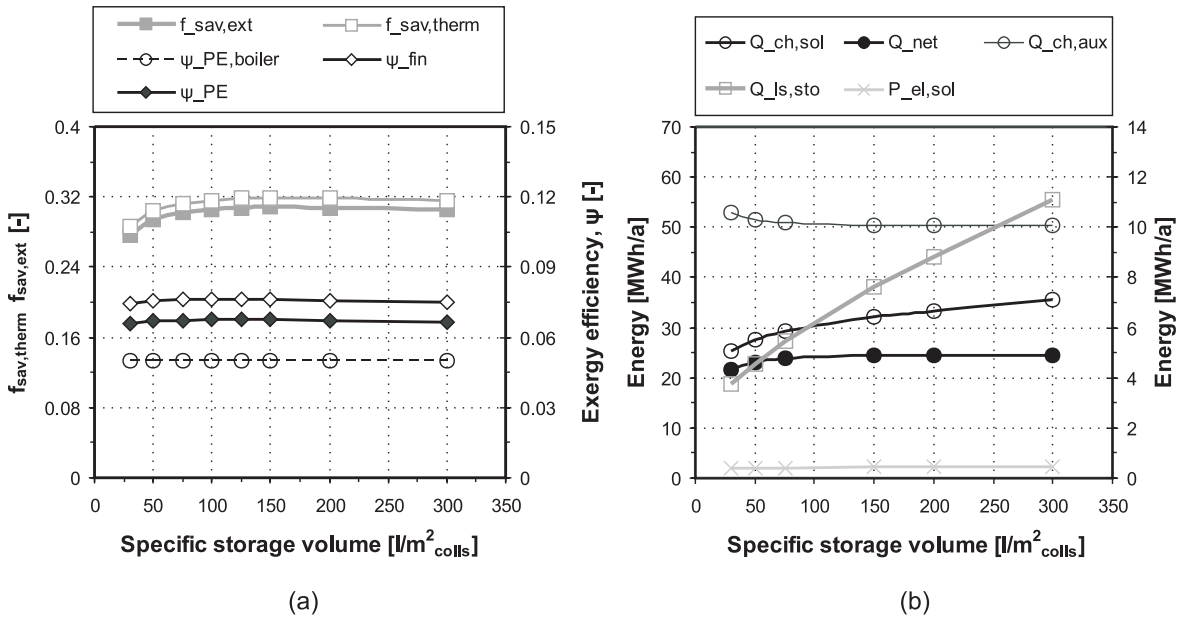

Figure 7.4: (a): Thermal and extended fractional energy savings, primary and final exergy efficiencies for the solar thermal system as a function of the storage size. A constant thickness of 15 cm for the thermal insulation is foreseen in all tanks; (b): Energy charged in the storage tank by the boiler (*Q_ch,aux*) and solar thermal system (*Q_ch,sol*), as well as electric power required for operating the pumps in the solar loops *P_el,sol* and thermal losses in the storage tank (*Q_ls,sto*). The variable *Q_net* represents the net additional output obtained from the solar thermal system, calculated as *Q_ch,sol-Q_ls,sto*.

pumping energy required for operating the solar thermal loops (primary and secondary) with greater storage volumes. Pumping energy increases by 21% for the system with specific storage volume of 300 l/m^2_{colls} as compared to 30 l/m^2_{colls} . Yet, being around 0.5% and 0.7% of the total energy and exergy supplied to the system, it represents a marginal input and does not affect its energy or exergy performance, as it is shown in Figure 7.4.

Larger specific storage volumes increase the energy yield from the collector field *Q_ch,sol*, as shown in Figure 7.4 (b). However, due to the constant insulation thickness of 15 cm regarded in all cases, thermal energy losses in bigger storage tanks *Q_ls,sto* increase steeply for bigger volumes. The increase in the thermal losses levels out the increase in the energy yield as it is shown by the trend of the net additional output *Q_net*[3] obtained from the solar thermal system.

Results from exergy analysis are strongly influenced by the high exergy inputs present, i.e. natural gas for the condensing boiler and pumping energy. Being pumping energy for the operation of the solar system a marginal input, its increase does not influence significantly the exergy performance of the solar thermal systems. Following, it can be concluded that the behaviour of the energy and exergy efficiency of the solar thermal system with greater

[3]The net additional output *Q_net* in the diagrams is calculated as the solar energy charged in the storage tank *Q_ch,sol* minus the storage tank losses *Q_sto,ls*

specific storage sizes is solely due to the increase in the thermal losses with greater storage tanks. Since thermal losses represent a low exergy input, the behaviour of the energy and exergy parameters is similar. In turn, if the difference would be due to an increase in the pumping energy, different conclusions could have been obtained from both analyses.

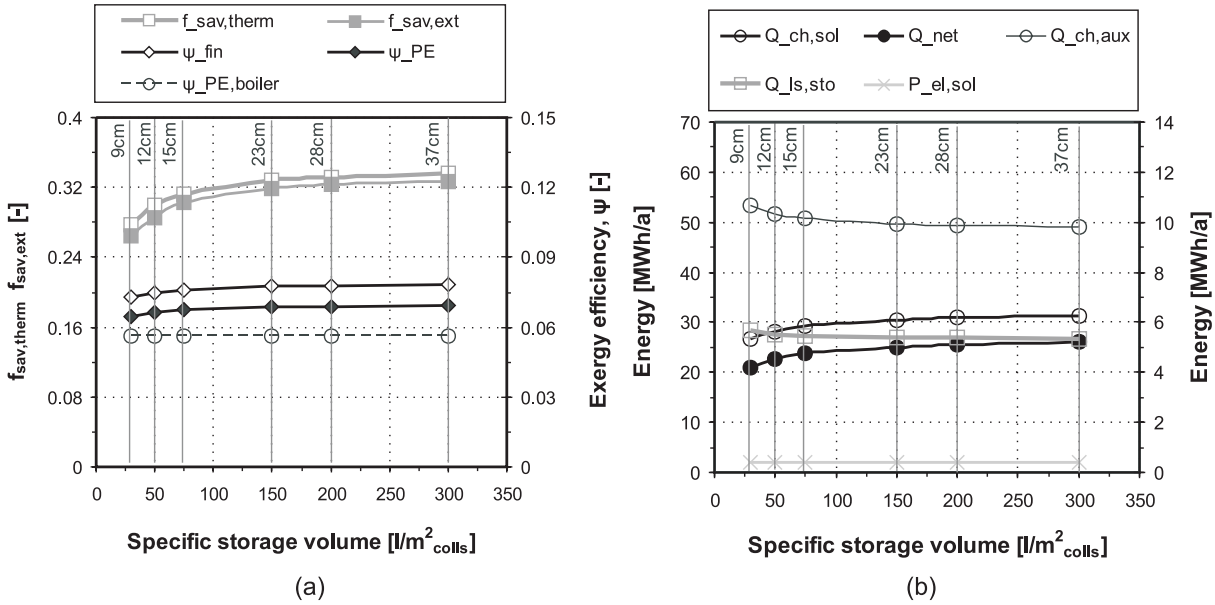

Figure 7.5: (a): Thermal and extended fractional energy savings, primary and final exergy efficiencies for the solar thermal system as a function of the storage size. A constant UA value of 14.44 W/K is kept in all cases, i.e. insulation thickness varies as a function of the storage size. The insulation thickness regarded in each case is expressed in cm at the top of the diagrams; (b): Energy charged in the storage tank by the boiler *Q_ch,aux* and solar thermal system *Q_ch,sol*, as well as electric power required for operating the pumps in the solar loops *P_el,sol* and thermal losses from the storage tank *Q_ls,sto*. The variable *Q_net* represents the net additional output obtained from the solar thermal system, calculated as *Q_ch,sol*-*Q_ls,sto*.

Figure 7.5 shows the behaviour of the energy and exergy performance of the same solar thermal system as a function of the specific storage size assuming a variable insulation thickness. Insulation thicknesses vary between 9 cm for a specific storage size of 30 l/m^2_{colls} and 37 cm for a specific storage size of 300 l/m^2_{colls} and have been chosen so that the UA value of the storage tank is kept at a constant value of 14.44 W/K for all cases. In consequence thermal losses in the tanks are nearly the same in all cases (see Figure 7.5 (b)). The slight decrease in the thermal losses for higher specific storage volumes is due to the lower temperatures inside the tank for higher tank volumes.

In Figure 7.5 it is clearly shown that if the insulation thickness is increased as a function of the storage size, the energy and exergy performance of the solar thermal system increases with greater storage tanks. In other words, the thermal losses and not the pumping energy are responsible for the stagnation and decrease in the performance of the systems shown in Figure 7.4.

7.2.3 Different emission systems

The emission system used for space heating also influences the energy performance of solar thermal systems [Zaß et al., 2008]. It is expected that space heating systems requiring lower supply and return temperatures lead to an increase in the fractional energy savings obtained from the solar unit. Following, the exergy performance of the solar system is also expected to increase. Additionally, the use of emission systems with low supply and return temperatures is expected to decrease the temperature of the provided solar heat, i.e. its exergy content. Thereby, greater increase in the exergy performance is also awaited.

In this section the influence of using emission systems with lower supply and return temperatures on the energy and exergy performance of the solar thermal system studied is investigated. For this purpose, a space heating supply with radiators (with design inlet and return temperatures of 55 and 45°C, respectively) is compared to a supply by means of a floor heating system (with design inlet and return temperatures of 32.5 and 27.5°C, respectively). The multi-family dwelling with standard building envelope (MFH-07), i.e. corresponding to requirements in the standard EnEV [2007], is assumed in both cases.

To ensure the comparability of both emission systems, it is required that both provide the same level of thermal comfort inside the building. Thermal comfort conditions with both systems were extensively discussed in section 5.1.3. Results show that the degree-hours under comfort range II as defined in [DIN EN 15251, 2007] are similar for both systems.

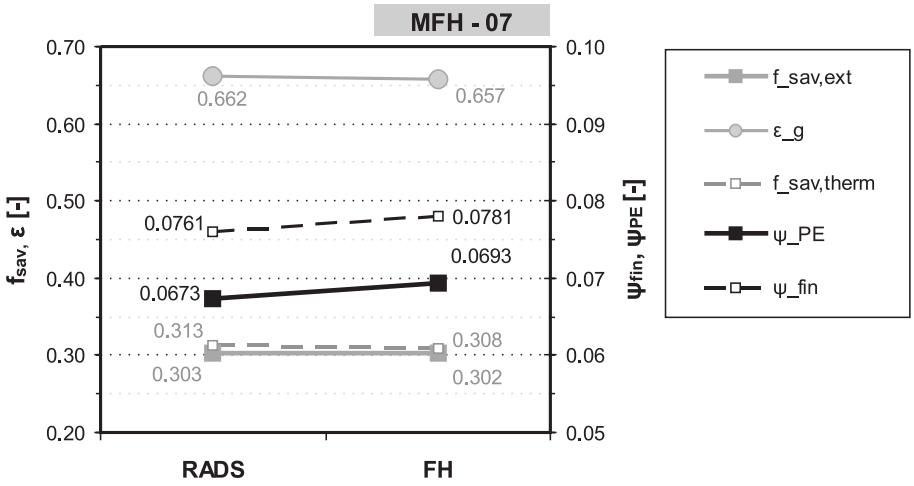

Figure 7.6: Thermal and extended fractional energy savings, exergy expenditure figure for the generation subsystem as well as primary and final exergy efficiencies for the solar thermal system with radiators (*RADS*) and floor heating (*FH*) systems.

Figure 7.6 shows the main parameters describing the energy and exergy performance of the solar unit with both emission systems. Thermal and extended fractional energy savings are very similar in both cases. Due to the lower return temperatures from the floor heating system, lower temperatures can be found in the lower part of the solar storage volume. This

leads to an increase of 3% in the solar thermal energy output from the collector field, as compared to the system with radiators. However, due to thermal energy losses in the floor heating system, the energy that needs to be supplied to the floor heating is also 2% higher than in the case of radiators. This results in a similar energy performance of both systems: extended fractional energy savings are just 0.1% higher for the system with radiators.

As expected, the quality factor of solar thermal energy output is 3% lower, i.e. has lower exergy content due to its lower temperature level, if the floor heating system is used. The energy from the solar collectors represents around 35% of the total energy input in the systems. However, due to its low exergy content, the solar thermal output represents only around 8% of the exergy supplied in both cases. Thus, the differences in the quality level of the supplied solar heat become irrelevant and are not able to influence visibly the exergy performance.

Figure 7.7 shows the energy and exergy input required from the boiler and solar thermal system extrapolated for different extended fractional energy savings. Only with extended fractional energy savings higher than 0.9 the exergy input from the solar thermal unit starts dominating the total exergy input into the system (representing 60% of the total exergy input for $f_{sav,ext}$ = 0.9), and the quality of the delivered solar heat might become relevant for exergy analysis. Otherwise, for conventional solar fractions the exergy performance, as the energy performance, is strongly influenced by the high-quality energy required, i.e. the fossil fuel input in the system.

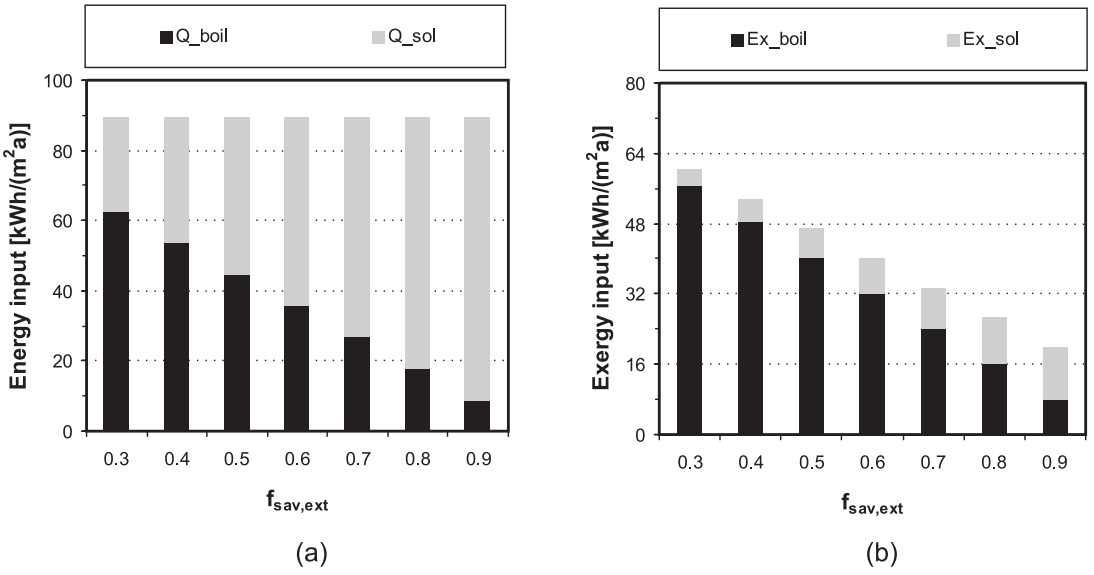

Figure 7.7: Energy (a) and exergy (b) input from the boiler and solar thermal unit for different extended fractional energy savings $f_{sav,ext}$.

For all stated above, exergy expenditure figures for the generation system (i.e. boiler and solar collectors) in both cases are very similar. However, on the contrary to the fractional

energy savings, this parameter shows a favourable trend for the floor heating system. This is due to the higher share of solar heat supplied if the floor heating system is used[4].

Exergy efficiencies show the same trend as exergy expenditure figures, being favorable for the floor heating system. The 0.2% increase in the primary and final exergy efficiencies for the case with floor heating is due to a 4% increase in the exergy demand[5] of the building.

The exergy efficiency is the only investigated parameter directly influenced by the exergy demand of the building: variations in the exergy demand might significantly change its value. In consequence, it represents a suitable parameter for comparing the performance of systems with different emission units, since the energy output from each emission system is thereby also taken into account.

7.2.3.1 Space heating operation without night setback

A continuous operation without steep changes in the control strategy[6] allows a better controllability for systems with high thermal inertia, as it is the case of the floor heating system. Thus, it is expected that the emission losses[7] in the floor heating system are reduced if no night setback operation is used. To check the influence of the control strategy of the emission systems in the energy and exergy performance of the solar thermal system, a continuous operation has been assumed for the MFH-07 with radiators and floor heating system. In order to obtain similar levels of thermal comfort (in terms of degree-hours under the comfort range) as with night setback operation the setpoint is considered as 20°C. Results for thermal comfort conditions for both emission systems with both control strategies can be found in Table 5.3.

As show in Figure 7.8, without night setback operation emission losses in the floor heating system are reduced by 23%, from 3.1 kWh/m^{2}a to 2.4 kWh/m^{2}a. They represent around 5 and 4% of the energy supplied to the emission system. Emission losses in the radiators amount only 1% of the energy supplied to the radiators, and do not experience a significant reduction without night setback.

Due to the lower emission losses, the difference in the energy that needs to be supplied to the space heating system (including pipe and emission losses) is reduced if no night setback is used. Additionally, lower return temperatures from the space heating loop allow lower temperatures in the storage tank and, thereby, higher solar thermal output from the collector field is achieved. As a result, extended fractional energy savings increase by 0.8% if the floor heating system is used without night setback operation as compared to the radiators (see Figure 7.9). These results are in very good agreement with those obtained by Zaß et al. [2008].

[4]The share of solar heat supplied amounts 34.8% and 35.7% in the cases with radiators and floor heating, respectively.

[5]The exergy demand is defined in chapter 3, section 3.2.2. It represents the exergy of the energy supplied actively to the room once it reaches indoor air, i.e. at the indoor operative temperature.

[6]On the contrary to night setback operation, where the operative temperature must be raised significantly in relatively short periods of time.

[7]Emission losses in the floor heating system referred here are mainly due to heat transfer to the lower part of the active building element, i.e. beyond the insulation layer underneath the water pipes.

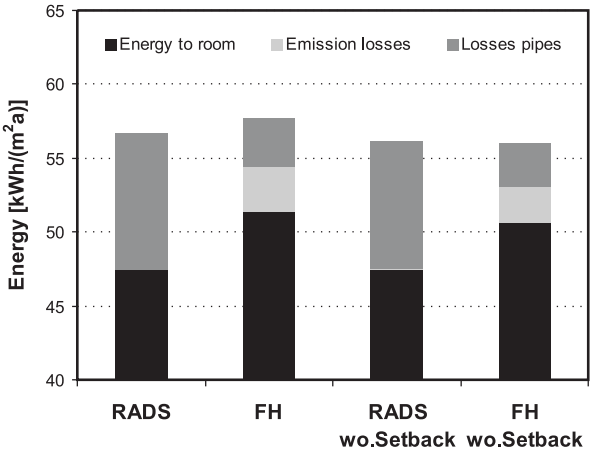

Figure 7.8: Energy losses in the pipes, emission losses and energy supplied to the floor heating system and radiators for an operation with and without night setback (*wo. setback*).

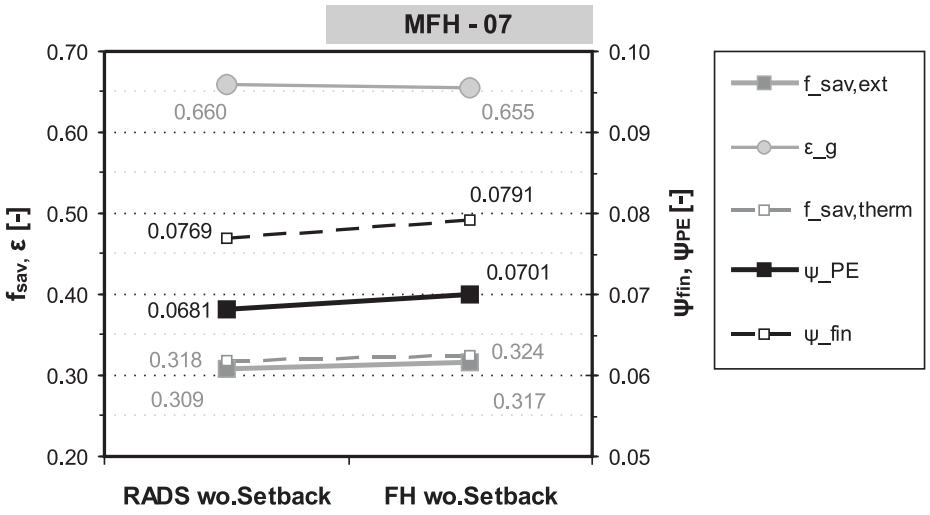

Figure 7.9: Thermal and extended fractional energy savings, exergy expenditure figure as well as primary and final exergy efficiencies for the solar thermal system with radiators (*RADS*) and floor heating (*FH*) systems operated without night setback (*wo. setback*).

The differences in the final and primary exergy efficiencies are on the same range as with night setback (0.2%) and show the same trend (increase for the floor heating system). This is again, due to the slightly higher exergy demand that is supplied to the room with floor heating[8].

[8]The difference can be seen in terms of energy in the black bars in Figure 7.8

7.2.3.2 Improved building shell

In order to check the influence of using each emission system with higher solar fractions, the use of both emission systems in the multi-family dwelling with improved building envelope (MFH-KfW-EffH.40) is investigated.

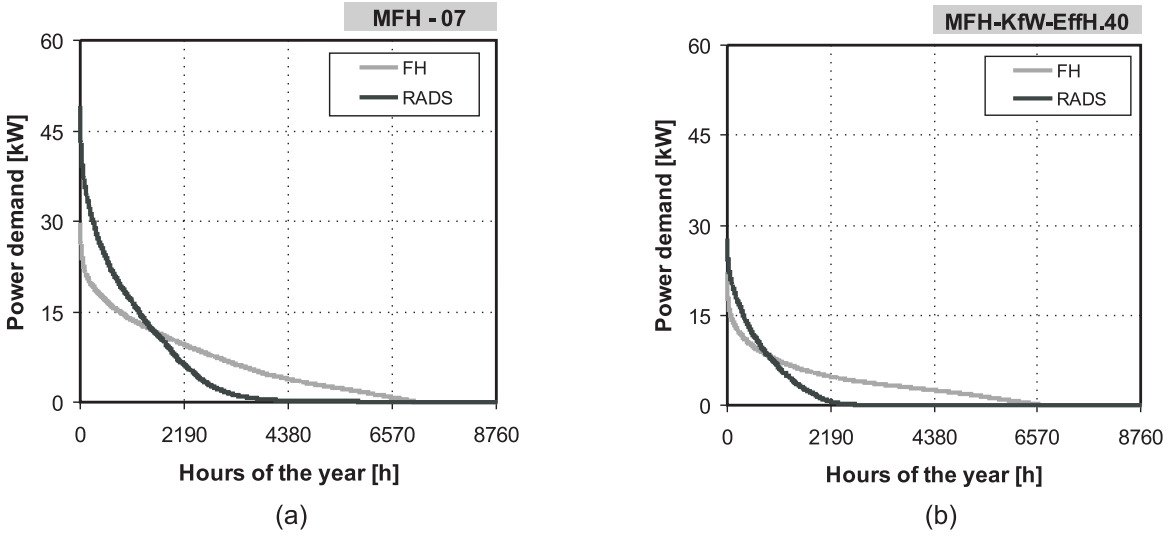

Figure 7.10: Duration curves for the space heating loads supplied in the case of MFH-07 (a) and MFH-KfW-EffH.40 (b) if radiators and floor heating systems are used.

A comparable level of thermal comfort is provided by both systems (see Table 5.3). The duration curves (Figure 7.10) for the heating loads in the multi-family dwelling with radiators and floor heating for the two building shell standards (EnEV 2007 and KfW-EffH.40) show that no great reduction in the number of hours with low space heating loads could be achieved for the MFH-KfW-EffH.40 with floor heating system (as compared to the building with EnEV 2007 standard and with floor heating). This reduction, however, can be found if radiators are used. In other words, low space heating loads remain despite the improved building shell if the floor heating is used.

However, for the floor heating system in the low energy house lower design supply and return temperatures (28 and 23°C, respectively) as in the MFH-07 case (32.5 and 27.5°C, respectively) are considered and a higher insulation level is foreseen under the floor heating in the ground floor. In consequence, emission losses in the floor heating system are reduced from 5.7% of the energy supplied in the MFH-07 case, to 3.5% in the MFH-KfW-EffH.40 case. Inspite of this, the energy required for space heating (including pipe and emission losses) is 5% higher in the case with floor heating.

Due to the lower return temperatures from the floor heating system, lower temperatures in the storage tank occur, allowing for a 3% increase in the solar energy yield. However, with

an absolute value of 786.9 kWh/a this increase is lower than the increase in the demand from the space heating system (1399.5 kWh/a). In consequence, the energy provided by the boiler increases by 2% for the building with floor heating, causing the slight decrease of 0.4% in the extended fractional energy savings.

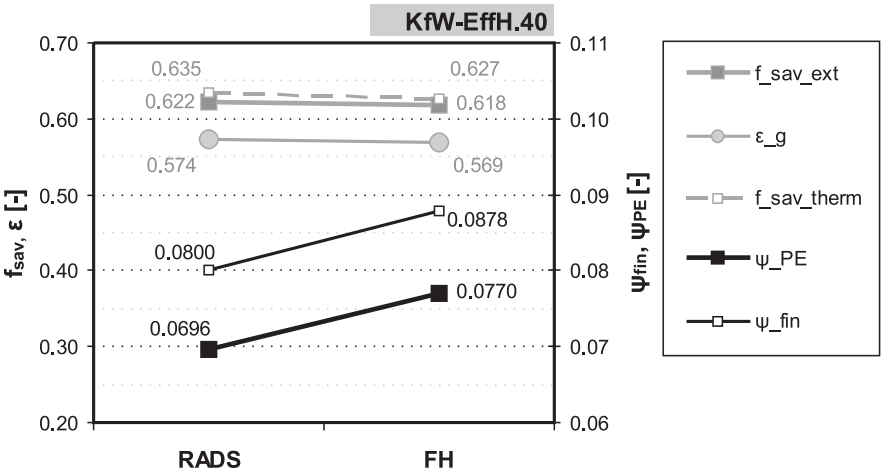

Figure 7.11: Thermal and extended fractional energy savings, exergy expenditure figure as well as primary and final exergy efficiencies for the solar thermal system with radiators (*RADS*) and floor heating (*FH*) in the multi-family dwelling in low energy standard (MFH-KfW-EffH.40).

In turn, as it happened in section 7.2.3, the exergy expenditure figure is 0.5% lower for the system with floor heating. This is again due to the higher share of solar heat in the supply.

The increase in the exergy demand for space heating supply with the floor heating system is responsible for the 0.8% and 0.4% increase in the final and primary exergy efficiencies, respectively. Again, despite a slightly higher fossil fuel input for the boiler in the case with floor heating system (and the subsequently lower fractional energy savings), the exergy-based paramters show this emission system as preferrable.

Fractional energy savings show that more fossil fuel is being used as compared to the reference case (without solar thermal unit). In turn, exergy-based parameters show that the share of solar energy in the supply is increased and the demands (despite being higher) are supplied more efficiently if a floor heating system is used.

7.2.4 Stratification in the storage tank

Strategies for promoting good thermal stratification inside the storage tank increase the achievable fractional energy savings [Heimrath, 2004; Furbo et al., 2005; Zaß et al., 2008]. As shown in chapter 3 and being coherent with results in [Rosen, 2001], stratification in the storage tank allows reducing also the exergy losses in the storage unit. In this section, the influence of measures for promoting a stratified charge of the storage tank on the energy and exergy performance of the solar thermal system is discussed.

The MFH-07 with radiators and floor heating system are taken as case studies here. In this way, the influence of stratification in the tank for space heating systems with different temperature demands can also be studied. As base cases for both emission systems ideal stratification is assumed for the inlets of the solar thermal system, i.e. solar charging process, as well as for the return from DHW and SH supply[9]. For the system without ideal stratification, the inlet from the solar thermal system is assumed at a relative storage height of 0.05, and the inlets from DHW and space heating are assumed at relative heights of 0.1 and 0.15, respectively. No stratification is assumed in any case for the charging process with the auxiliary boiler.

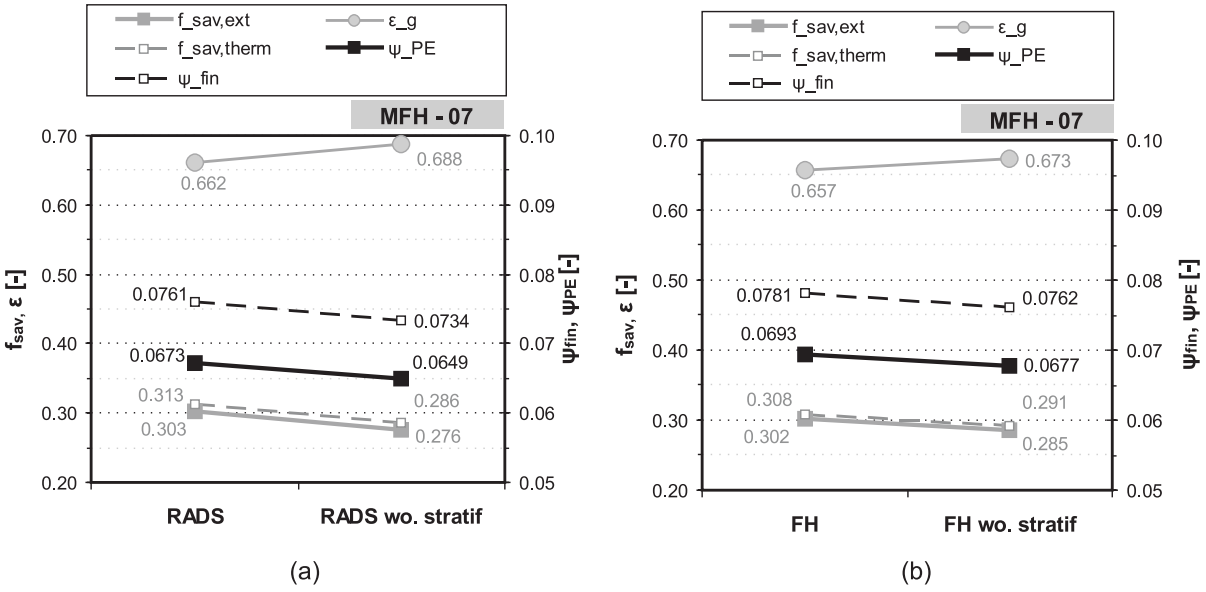

Figure 7.12: Thermal and extended fractional energy savings, exergy expenditure figure as well as primary and final exergy efficiencies for the solar thermal system with radiators (a) and floor heating (b) systems with and without stratified inlets in the storage tank.

A reduction in the extended and thermal fractional energy savings can be observed for the systems without stratification, as shown in Figure 7.12. This reduction amounts 2.7% and 1.7% for the system with radiators and floor heating, respectively. The difference is due to the higher temperatures found in the lower part of the fully mixed tank with radiators, due to higher return temperatures from the space heating system. In consequence, lower energy output can be obtained from the solar thermal collectors. In other words, the use of strategies promoting a stratified return is more important if space heating systems operating at high temperatures are used. These results are coherent with those found in [Zaß et al., 2008].

The behaviour of the exergy efficiencies and expenditure figures is similar to the fractional energy savings: the exergy expenditure figure for the generation subsystem increases by 2.6% and 1.6% for each system and exergy efficiencies decrease in 0.24% and 0.16% for the systems

[9]Ideal stratification in these inlets is also assumed in all cases presented in all other sections.

with radiators and floor heating, respectively.

The decrease in the exergy efficiency, however, is significantly lower than the decrease in fractional energy savings. This is due to the fact that the energy input from the boiler represents 63 and 65% of the total energy input in the systems with and without stratification, respectively. In terms of exergy, the input from the boiler represents 90.1% and 90.3% of the total exergy input in each case. In other words, the exergy input, and herewith the exergy efficiency, is again dominated by the fossil fuel input from the boiler.

7.2.5 Three way valves for discharge of storage tank

As stated in the previous section, stratified inlets are assumed for the solar loop as well as the DHW and SH demands. In turn, the outlets for providing both demands are considered at a given fixed position in the tank: the outlet to DHW supply is located approximately at the top of the tank, at a relative height of 0.99; the outlet for SH supply is located at 0.05 above the outlet to the boiler[10]. Both outlets are, therefore, located within the auxiliary volume, which is always kept at temperatures between 65 and 70°C by the boiler. This is done in order to guarantee the supply even if no solar radiation is available.

The setpoint for DHW supply is 70°C, being similar to the setpoint for the auxiliary boiler. In turn, the setpoint for SH supply varies between 55 and 20°C if radiators are used and between 32.5 and 20°C if the floor heating system is used. Warm water from the auxiliary volume in the tank is mixed with cold return water from SH supply in order to achieve the relatively lower setpoint temperatures required by the radiators and floor heating. This mixing process implies significant exergy losses, as shown in Figure 7.13. After exergy losses in the energy transformation (i.e. primary energy) and boiler, exergy losses in the storage tank, and mixing process represent the biggest shares.

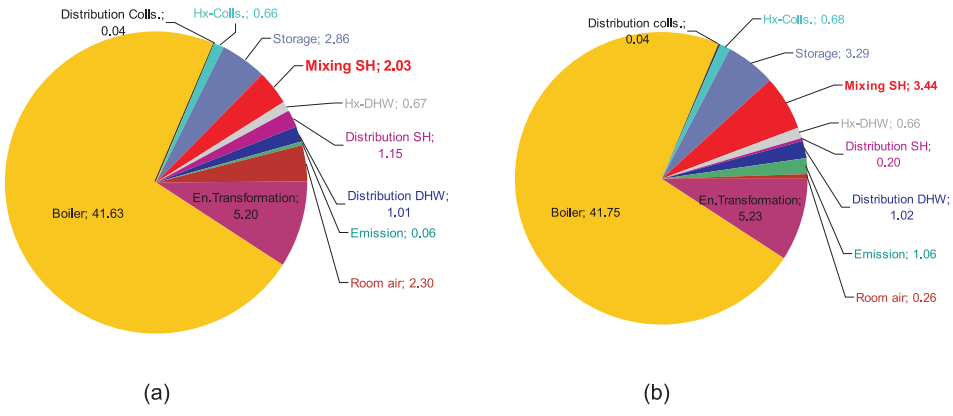

Figure 7.13: Exergy losses, in kWh/(m^{2}a), in the different subsystems regarded for energy supply with the solar thermal system in the case of space heating by means of radiators (a) and floor heating (b).

It is expected that the solar volume is often at a temperature level high enough to supply

[10] see equation 4.12.

SH demands directly, avoiding firstly a further heating with the boiler and, secondly, reducing the mixing process. To realize this, SH outlets at lower tank heights are required.

In this section the influence of using one and two three-way valves for enabling the outlet for SH supply from the solar volume on the energy and exergy performance of the systems is studied. The three way valves are located at a relative storage height of 0.7 and 0.5, respectively. Whenever the temperature at one of these heights in the solar volume is 5°C higher than the required setpoint for SH supply, water is taken from that layer of the tank[11]. Otherwise, water is withdrawn conventionally from the lower part of the auxiliary volume.

Figure 7.14 shows the behaviour of the extended fractional energy savings (a), exergy expenditure figure (b) and primary exergy efficiency (c) for the systems with one and two valves as compared to without any additional valve for SH supply.

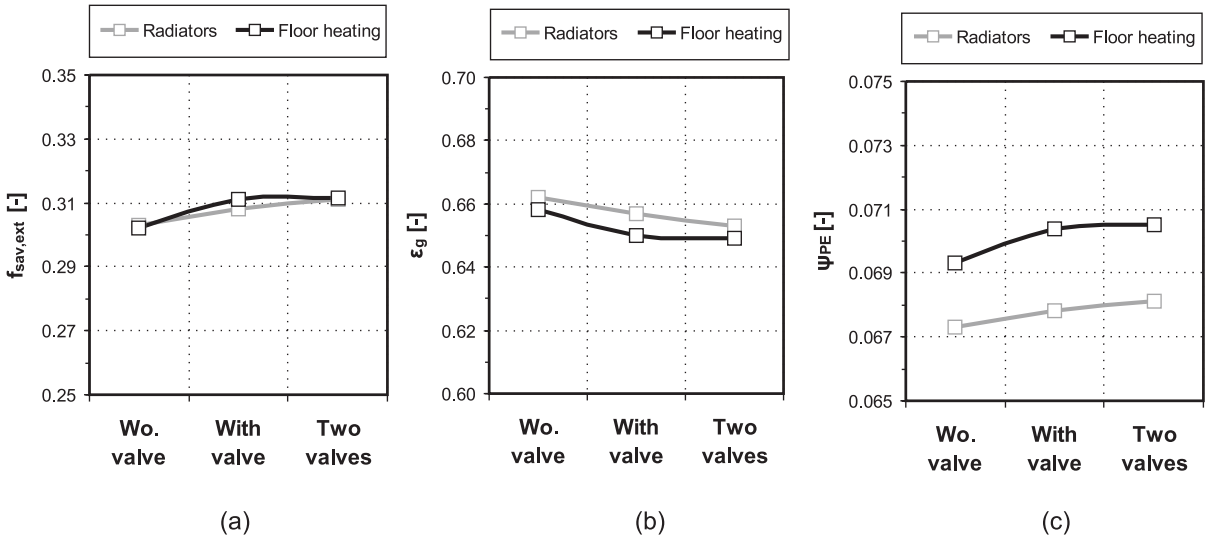

Figure 7.14: Extended fractional energy savings (a), exergy expenditure figures for the generation system (b) and primary exergy efficiency (c) for systems without, with one and two three-way valves for SH supply. Results are shown for the systems with radiators and floor heating.

The use of a single three-way valve for SH supply yields a 0.9% increase in the extended fractional energy savings for the system with floor heating. A similar increase could be achieved by increasing the thermal insulation in the storage tank, from 15 cm to 30 cm[12]. If, instead, radiators are used a lower increase can be found (0.5%). The use of two three way-valves for space heating supply does not show any relevant increase in the fractional energy savings for the system with floor heating (0.1%), but causes a further 0.3% increase if radiators

[11]The discharge is kept at this height until the temperature in the storage layer is 1°C above the SH setpoint, i.e. a hysteresis of 4°C is allowed.

[12]With this measure the same increase in the energy (0.9%) and exergy (0.1%) performance as with one valve and floor heating is achieved.

are used. These trends are due to the higher temperatures that can be found in the solar tank if radiators are used (due to the higher return temperatures from space heating supply), making the second valve more often usable than if the floor heating system is considered. These trends are coherent with results in section 7.2.4.

As stated in the previous sections for such low solar fractions, results from exergy analysis are completely dominated by the high exergy input represented by the auxiliary boiler. In consequence, the behaviour shown by the parameters characterizing the exergy performance of the systems with and without valves and the conclusions obtained from them, are similar to those from conventional energy analysis.

Differences in the energy and exergy performance with each of both emission systems are coherent with those presented in section 7.2.3: with the use of a floor heating system a more (exergy) efficient energy supply can be achieved, despite slightly higher input of fossil fuels is required.

7.2.5.1 Larger solar thermal system

In this section the influence of using one and two three-way valves on the energy and exergy performance of a larger solar thermal system is studied. The solar thermal system investigated here is twice as big as the *base solar system*, i.e. a 200 m^2 collector field and 16 m^3 storage tank are regarded. The building with standard building shell (MFH-07) is regarded here.

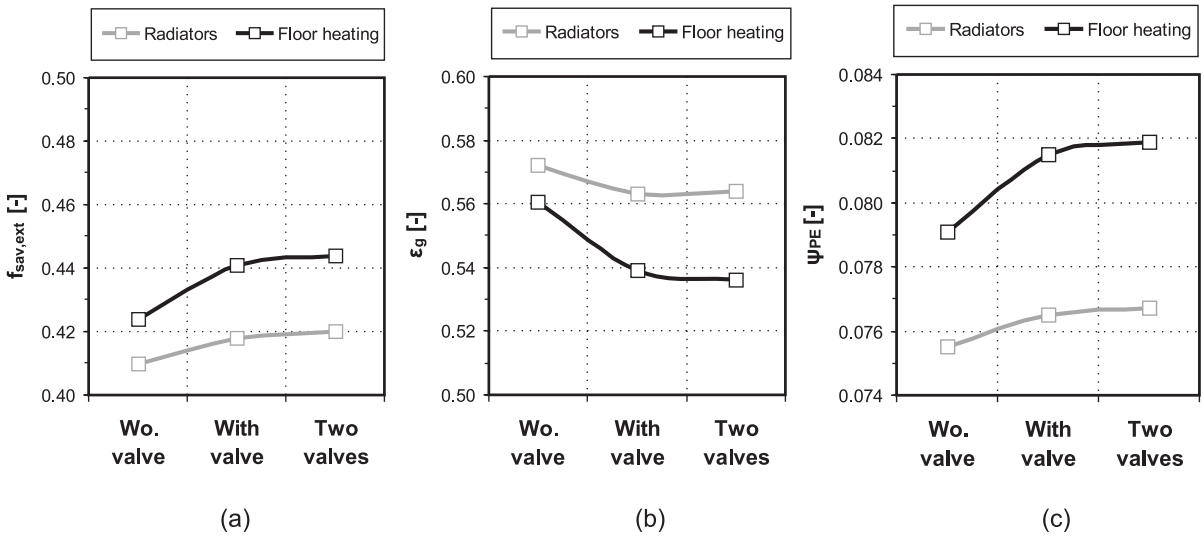

Figure 7.15: Extended fractional energy savings (a), exergy expenditure figures for the generation system (b) and primary exergy efficiency (c) for systems without, with one and two three-way valves for SH supply. Results are shown for the systems with radiators and floor heating and a solar system with 200 m^2 collector field and 16 m^3 storage tank.

It is remarkable that the energy performance with radiators and floor heating without using any three-way valve is inverted as compared to the smaller sized solar thermal system: fractional energy savings increase by 1.4% if the floor heating system is used instead of radiators. This is due to the higher increase in the solar energy yield (1887.9 kWh/a) with a floor heating system[13] as compared to the increase in the energy demand for space heating (1194.3 kWh/a) and shows that the importance of using low temperature heating system increases for bigger solar thermal systems.

The use of a single three-way valve for SH supply allows a 1.7% increase in the extended fractional energy savings for the system with floor heating. If, instead, radiators are used a lower increase can be found (0.8%). This is due to the lower setpoint temperatures required by the floor heating system, making possible the use of direct solar heating more often.

The use of two three way-valves for space heating supply causes a further 0.3% increase with both emission systems. This increase could also be found for the smaller solar thermal system if radiators are used. In the case of floor heating, the increase is now due to the larger solar thermal system, which is able to heat up to higher temperatures lower parts of the tank even if the floor heating system is used.

Despite the relatively high fractional energy savings achieved, in terms of exergy the fossil fuel input into the boiler still represents 83% of the exergy supplied, thereby dominating the exergy input into the system. In consequence, the exergy performance of the systems without and with valves is completely paralell to the energy performance. No further conclussion can be obtained about the use of three-way valves from exergy analysis.

7.2.5.2 Improved building envelope

In this section the influence of using one and two three-way valves on the energy and exergy performance of a system with reduced space heating loads is studied. For this purpose, the base solar thermal system and the building with improved building shell (MFH-KfW-EffH.40) is considered. Figure 7.16 shows the behaviour of the energy and exergy-based parameters for the system with and without three-way valves.

The trends for both energy- and exergy-based parameters are similar and coherent to those found in the case of a standard building envelope (MFH-07), presented in section 7.2.5.

However, the use of a three-way valve causes a 2.6% and 1.3% increase in the extended fractional energy savings for the system with floor heating and radiators, respectively. These are the greatest improvements found as compared to systems operating without three-way valves and show that the importance of proper stratified discharge for space heating increases as the solar fraction increases (either due to a bigger solar unit, as it was the case in section 7.2.5.1, or to a reduction of the loads).

Again, the same trends and conclusions can be found for the energy- and exergy-based parameters. No additional information is delivered by exergy analysis regarding the use of

[13] Due to lower temperatures in the solar volume of the storage tank.

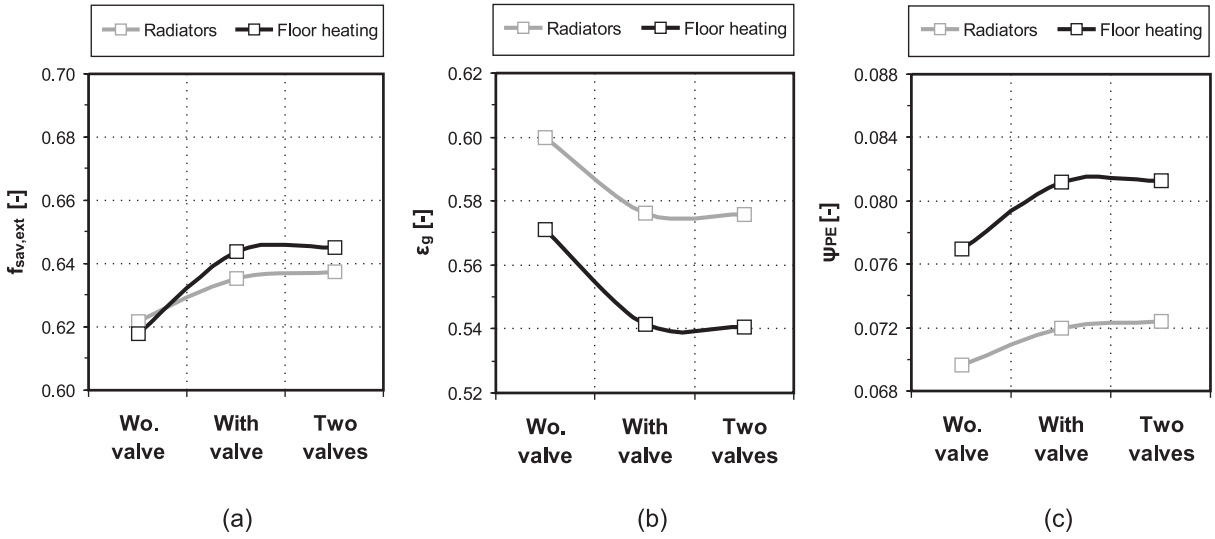

Figure 7.16: Extended fractional energy savings (a), exergy expenditure figures for the generation system (b) and primary exergy efficiency (c) for systems without, with one and two three-way valves for SH supply. Results are shown for the systems with radiators and floor heating and the multi-family dwelling with improved building envelope (MFH-KfW-EffH.40).

three-way valves for lower space heating demands.

7.2.6 Connection between auxiliary boiler and storage tank

In all systems studied up to here, the auxiliary boiler heats up the auxiliary volume located at the top of the storage tank. Since a temperature of 70°C is required for instantaneous DHW supply, the auxiliary volume is kept between 65 an 70°C at all times. High thermal losses in the auxiliary volume follow. These thermal energy losses need to be covered by the boiler, increasing the fossil fuel input and reducing the fractional energy savings and exergy performance of the system. On the other hand, those are relatively high temperatures for a solar thermal system. In consequence, the solar thermal unit often only manages to pre-heat the water, which needs to be further heated up by the boiler. Additionally, heating up of the solar volume with the auxiliary boiler (due to internal conduction and convection processes inside the tank) might occur. These disadvantages are avoided if the boiler is connected in series with the solar storage unit.

In this section the influence of using two separated boilers for SH and DHW supply in series with the solar storage volume is investigated.

An effective thermal conductivity of 2 W/(mK) is assumed between the tank nodes. This value was obtained from measurements in small storage tanks [Drück and Hahne, 1998]. For larger tanks with lower area to volume ratios it can be expected to be lower. With this as-

sumption, a very good level of thermal stratification is achieved inside the tank, as shown exemplary in Figure 7.17 for the storage tanks with conventional connection with the boiler (i.e. with auxiliary volume) in case of using radiators (a) and floor heating (b). In consequence, marginal heating of the solar volume with the boiler follows.

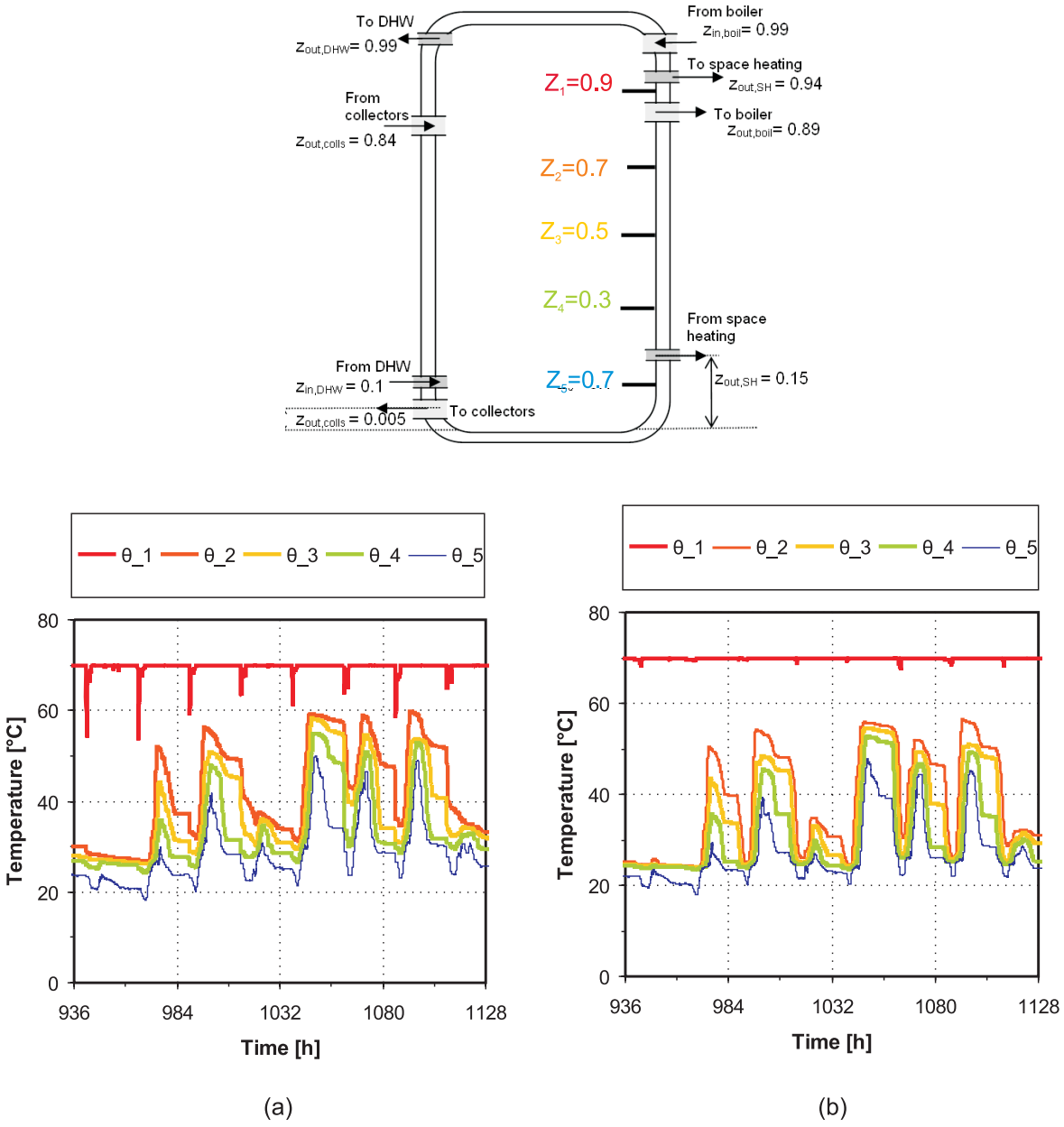

Figure 7.17: Temperatures at five temperature sensors evenly distributed over the storage height for the case of parallel connection between the boiler and the storage tank (i.e. conventional configuration with auxiliary volume in the tank) for radiators (a) and floor heating (b) systems. For completeness, the relative height of the sensors z_1-$z_5$is shown at the top of the diagrams.

Connecting the boilers for SH and DHW supply in series with the storage tank reduces thermal energy losses in the storage units by 20% and 17% for the cases with radiators and floor heating, respectively. The output from the solar collector field increases by 0.7% and 2% in each case[14]. As a result, the energy input into the boilers is reduced by 4% and 3%, respectively. The increase in the fractional energy savings shown in Figure 7.18 (by 2.9% and 3.2%, respectively) is, therefore, due to both the reduction in the thermal losses in the storage tank and the increase in the solar energy yield.

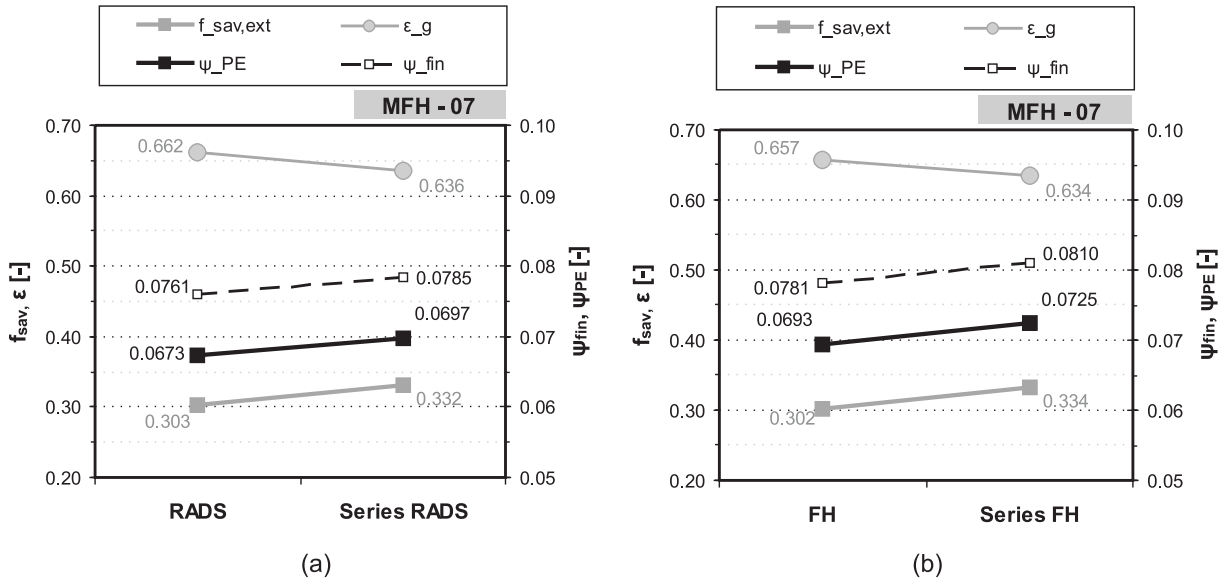

Figure 7.18: Thermal and extended fractional energy savings, exergy expenditure figure as well as primary and final exergy efficiencies for the solar thermal system with radiators (*RADS*) and floor heating (*FH*) systems in case of conventional and series connection of the boiler(s) with the storage tank.

As it happened in the previous sections, the behaviour of the exergy parameters is strongly determined by the fossil fuel input. In consequence, the same behaviour and conclusions can be obtained from exergy analysis as from conventional analysis of the systems by means of the fractional energy savings.

7.2.7 Overview of some investigated options

Results in the sections above show that, for the range of solar fractions investigated, the exergy performance of the systems is strongly dependent on the fossil energy input into the systems. Following, similar results as with conventional energy analysis can be achieved and no added value for the exergy approach can be found. This conclusion is supported by the diagrams

[14]The higher increase in the solar yield with FH system is due to the lower achievable SH return temperatures, allowing lower temperatures in the storage tank (see Figure 7.17) and a more often operation of the solar loop.

in Figure 7.19, where the behaviour of energy- and exergy-based parameters for some of the investigated cases is presented graphically.

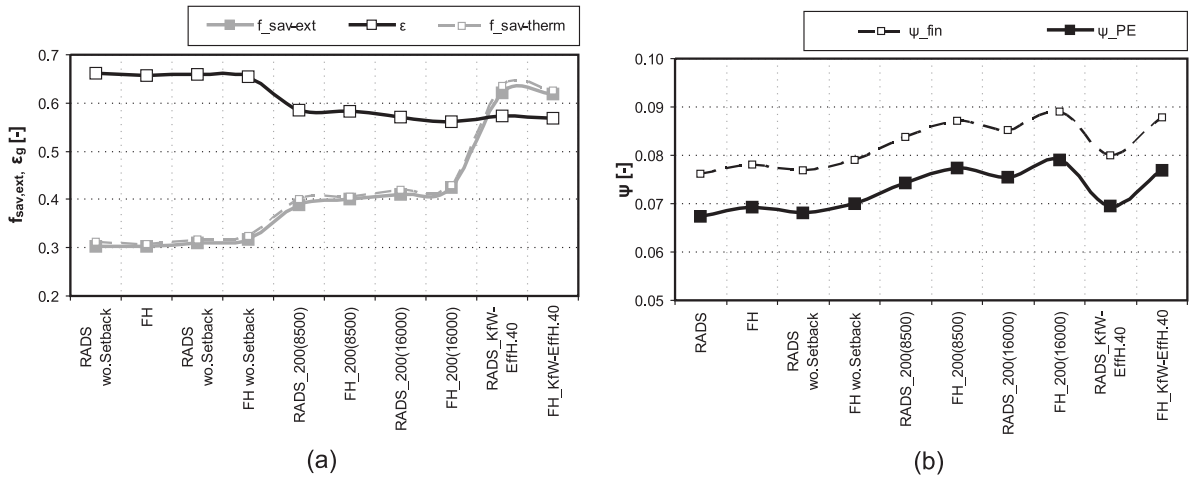

Figure 7.19: (a): Extended and fractional energy savings and exergy expenditure figures for selected cases of solar thermal supply; (b): Final and primary exergy efficiencies for the same cases shown in (a).

Trends for the fractional energy savings and exergy expenditure figures are very similar. Small differences arise in the comparison of different emission systems due to the different shares of solar heat in the supply, as explained in detail in section 7.2.3. Differences in the behaviour of the exergy efficiency arise particularly for the comparison of different emission system due to the fact that exergy demands provided by each emission system directly and greatly influence this parameter (see section 7.2.3 for a detailed explanation on this issue).

A different energy and exergy behaviour can also be observed for the *KfW-EffH.40* building envelope as compared to the rest of options: exergy expenditure figures are not significantly reduced for these cases despite the great increase in fractional energy savings. This is due to the definition of the parameters: fractional energy savings increase drastically due to the reduction in fossil fuel supply as compared to a reference case consisting of a building with worst building shell (MFH-07). Exergy expenditure figures do not decrease significantly, since the reduction in fossil fuel input is mainly due to a similar reduction in the energy demands, i.e. the share of solar heat in the overall supply as compared to a building with standard building shell and with a bigger solar thermal unit, e.g. *FH_200(16000)*[15], is nearly the same. Exergy efficiencies are greatly influenced by the reduction in the exergy demands if a better building envelope is used, and, in consequence, do not show significant improvement as compared to other options investigated.

[15]In Table A.8 (Appendix) a description of the main parameters for each case study in Figure 7.19 can be found.

7.2.8 Economics of favourable options

In this section the economics of three selected options are briefly introduced. In this way, besides the energy and exergy performance of the systems, insight on their economic behaviour can be gained. The cases analyzed from an economic perspective are the base case with floor heating system (*FH* in Figure 7.19), the system with a twice as big solar thermal collector area (*FH_200(8500)* in Figure 7.19) and the system with the base solar thermal system but with improved building shell (*FH_KfW-EffH.40* in Figure 7.19). Economic analysis are carried out here in accordance with VDI 2067 [2000] for an observation period of 20 years. Table 7.1 shows the costs of energy savings for the last two cases as compared to the base case (*FH*), as well as the annuity in each case.

Table 7.1: Annuity and cost of energy savings for three selected cases of solar thermal systems investigated.

	Annuity	Costs of energy savings	
	[€]	[€/kWh$_{PE}$]	[€/kWh$_{end}$]
FH	19719	-	-
FH_200(8500)	22496	262.9	370.2
FH_KfW-EffH.40	25520	86.8	99.8

Results show clearly the cost effectiveness of increasing the insulation level of the building envelope as compared to the installation of higher solar thermal collector fields.

7.2.9 Main differences between energy- and exergy-based parameters

From the comparison of the energy and exergy performance of the solar thermal systems investigated, some conclusions can be obtained about the behaviour and usability of the energy- and exergy-based parameters introduced:

- Fractional energy savings indicate the share of saved fossil fuel for a given solar thermal system as compared to the fossil fuel demand of a conventional system without solar unit (i.e. with a condensing boiler as supply system). Thus, they are sensitive to variations in the fossil fuel input from the boiler. In turn, they do not give any information on the behaviour of the energy demands of the building (see the comparison between different emission systems in section 7.2.3). Changes in their values for the systems investigated range from 0.1% to 3.2%.

- Exergy-based parameters presented give insight into the share of solar energy in the total supply, thereby characterizing how efficiently a given load is being provided. These parameters are influenced by small changes in the energy demands of the building (e.g. raising from using different emission systems). Following, they are suitable parameters for comparing the performance of solar thermal systems coupled with different emission systems.

- Primary and final exergy efficiencies and exergy expenditure figures for the generation subsystem, i.e. exergy-based parameters analyzed, always behave coherently and give the same conclusions.
- The behaviour of the exergy-based parameters is strongly dominated by the high-exergy input from fossil fuels required by the auxiliary boiler (which represents between 80 and 90% of the total exergy input in all cases investigated). In consequence, conclussions from exergy analysis are similar to those obtained from conventional energy analysis for most of the systems studied. Only in the comparison between the performance with different emission systems conclussions from energy and exergy analysis differ from each other[16].
- Exergy demands in buildings are very low. For the range of solar fractions studied, the high exergy input from the auxiliary boiler dominates the exergy input in the systems. Thus, values for the exergy efficiencies are low. Additionally, their values vary only slightly (between 0.1 and 0.4%) for the different cases investigated.
- Exergy expenditure figures for the generation subsystem ε_g show the quality of the energy being provided. The sensitivity of this parameter to changes in the share of solar energy supplied (i.e. solar energy yield) is higher than for exergy efficiencies. Variations in this parameter for the systems studied range from 0.5% to 3%. Changes in the energy demands influence this parameter indirectly.

The exergy method is a scientifically correct approach for analyzing solar thermal units. However, since exergy analysis is strongly dominated by the high-quality fossil fuel input, similarly as energy analysis, conclusions from exergy analysis are always very similarly to those which can be gained from conventional energy analysis of the systems. Thus, it can be concluded that exergy analysis and exergy-based parameters do not supply relevant further information for the analysis of solar thermal systems as compared to conventional energy analysis.

7.3 Waste heat district heating system

In this section, results from energy and exergy analysis of the district heat system for SH and DHW supply in the single-family houses are presented.

7.3.1 Exergy-based vs. conventional sizing criteria for DH net

As stated in chapter 4 (see section 4.4.3), from an exergy perspective low-temperature thermal energy losses in the pipes of the DH network are expected to represent a minor exergy consumption in the district heating supply system. In turn, pumping energy for operating the

[16]This is due to the sensitivity of these parameters to variations in the energy demands to be supplied.

secondary side local heat distribution network is expected to represent a major exergy input. Consequently, from an exergy point of view, pumping exergy shall be minimized. To accomplish this aim, target maximum fluid velocities in the local heat distribution network can be reduced from the conventional value of 2.5 m/s [Dötsch and Bargel, 2009; AGFW, 2009] to lower values. Following, greater diameter for the pipes are allowed, increasing thermal energy losses in the network, but reducing pumping power required for the operation of the network.

In order to check the impact of the thermal energy losses and pumping energy in differently sized networks, three cases have been dynamically simulated in TRNSYS, corresponding to target maximum fluid velocities of 2.5, 1.0 and 0.4 m/s respectively. Figure 7.20 shows the required energy (a) and exergy (b) inputs to cover pumping energy and thermal energy losses in the three cases as a function of the target maximum velocities chosen in each case.

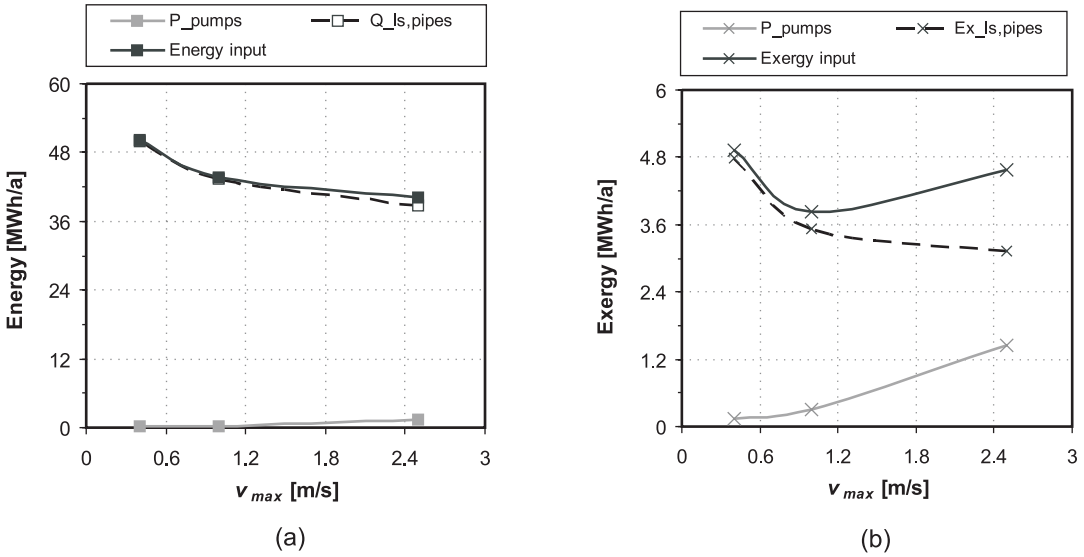

Figure 7.20: (a): Pumping energy *P_pumps*, thermal losses in the distribution pipes *Q_ls,pipes* and resulting required energy input to supply both magnitudes *Energy input*, as a function of the target maximum fluid velocities chosen for sizing the pipes in the network; (b): Pumping energy *P_pumps*, exergy of thermal losses in the distribution pipes *Ex_ls,pipes* and resulting required exergy input to supply both magnitudes *Exergy input* as a function of the target maximum fluid velocities chosen for sizing the pipes in the network.

Thermal energy losses in the distribution network clearly dominate the required energy input. Pumping energy represents, in terms of energy, a marginal input in the system. In turn, in terms of exergy pumping power and thermal losses in the distribution pipes represent comparable inputs, being of the same order of magnitude. Conventional sizing criteria, i.e. target maximum fluid velocities of v_{max}=2.5 m/s, yield the lowest energy input being the most advisable configuration in terms of energy performance. In terms of exergy, however, the lowest input can be found as a threshold between both concurrent magnitudes for target maximum fluid velocities of v_{max}=1.0 m/s.

In the following sections the energy and exergy peformances of the conventionally sized network (v_{max}=2.5 m/s) and the exergy optimized one (v_{max}=1.0 m/s) are evaluated in detail and compared with each other.

7.3.1.1 Energy and exergy performance

Figure 7.21 shows the energy demands for space heating and DHW supply in the two district heating systems sized with a maximum target fluid velocity of 2.5 m/s (a) and 1.0 m/s (b), respectively. Sizing criteria for the local district heat network do not vary the energy demands to be provided. Thermal losses in the storage tanks are also the same. However, as expected, thermal energy losses in the local distribution network increase if lower maximum target fluid velocities are used. Yet, representing around 11% of the thermal energy supplied losses in the distribution pipes are within typical ranges for conventional networks [Olsen et al., 2009; UMSICHT, 2010; Manderfeld et al., 2008].

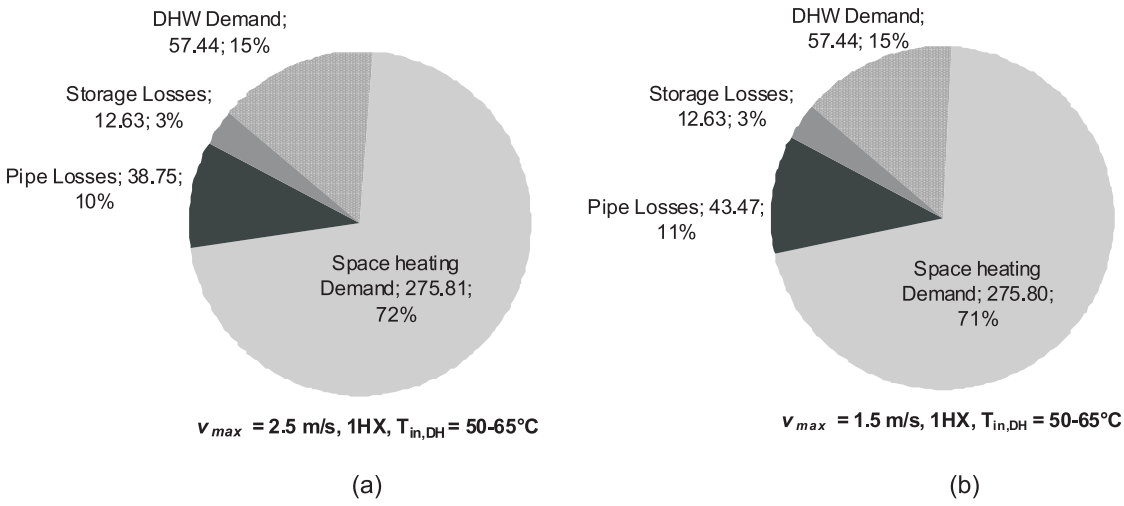

Figure 7.21: Energy demand and losses for district heat supply sized with v_{max}=2.5 m/s and for the network sized with v_{max}=1.0 m/s. In both cases space heating and DHW supply succeed with one single heat exchanger, option (0) in Figure 4.16 (chapter 4). Absolute values of the energy demands and losses are shown in [MWh/a].

Figure 7.22 shows the annual specific final energy (a) and exergy (b) demands for the two options. Additionally, final energy and exergy efficiencies for both district heating systems are shown (c).

Greater heat input into the local heat network is required to compensate for the higher thermal energy losses in the network sized with maximum fluid velocities of v_{max}=1.0 m/s. The difference in the heat input in both cases amounts 1.015 kWh/m^{2}a, i.e. 4.5 MWh/a. Pumping energy in the conventionally sized network represents 0.4% of the thermal energy input, being in good agreement with values found in the literature (Dötsch and Bargel, 2009;

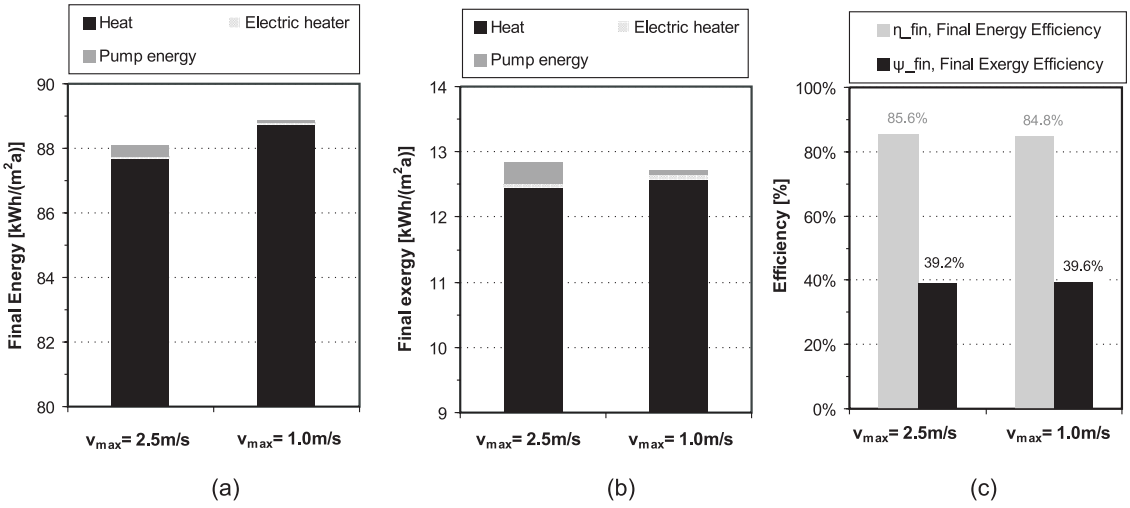

Figure 7.22: Annual specific final energy (a) and exergy (b) supply for the district heat networks sized with maximum velocities of v_{max}=2.5 m/s and v_{max}=1.0 m/s. Final energy and exergy efficiencies for both systems are also shown (c).

Olsen et al., 2009). As a result of the greater diameter of the pipes for the system sized with v_{max}=1.0 m/s, pumping energy is reduced by 79.5% as compared to the conventional one (with v_{max}=2.5 m/s). The absolute reduction in pumping energy required, however, is with 0.26 kWh/m^{2}a (1.15 MWh/a) significantly lower than the increase in thermal losses. Total final energy input increases by 0.9% and final energy efficiency is reduced by 0.8% for the system with larger pipe diameters, being coherent with Figure 7.20.

In terms of exergy, greater thermal losses in the pipes cause an increase of 0.13 kWh/m^{2}a (566 kWh/a) in the exergy supply.The decrease in pumping power, however, amounts 0.26 kWh/m^{2}a, being higher than the increase in the exergy input caused by the higher thermal losses. In consequence, final exergy input is reduced by 1% for the network sized with maximum velocities of v_{max}=1.0 m/s and final exergy efficiency increases by 0.4%.

The difference in the performance of both options becomes larger in terms of primary energy and its associated exergy, as shown in Figure 7.23.

Due to the primary energy factor for electricity production[17], the increase in pumping power required for the conventionally sized network (v_{max}=2.5 m/s) makes the two systems nearly equivalent in terms of total primary energy input[18]. The exergy associated to primary energy, however, is 6.8% lower for the network sized with v_{max}=1.0 m/s. This results in an increase of the primary exergy efficiency by 3.7%.

Results from energy analysis show that the system with bigger pipes (v_{max}=1.0 m/s) is

[17]Primary energy factors for district heating and electricity have been assumed as 0.7 and 2.7, respectively [DIN 18599-1, 2007]. In turn, the total primary energy factor (fossil and renewable) in [DIN 18599-1, 2007], i.e. 3, has been considered for primary exergy analysis of electricity.

[18]The system sized following exergy criteria has a primary energy input 0.4% higher than the conventionally sized one

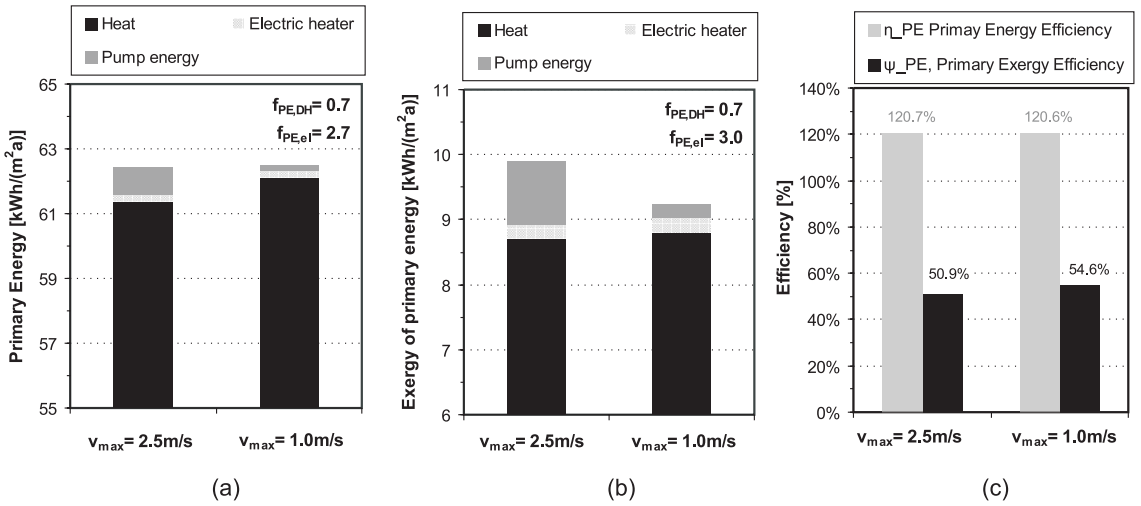

Figure 7.23: Annual specific primary energy (a) and its associated exergy (b) supply for the district heat networks sized with maximum velocities of v_{max}=2.5 m/s and v_{max}=1.0 m/s. Primary energy and exergy efficiencies for both systems are also shown (c). Primary energy factors used for calculating the primary energy and its associated exergy are shown on the diagrams.

almost equivalent to the conventional one (v_{max}=2.5 m/s) in terms of primary energy performance. However, due to greater thermal energy losses in the pipes, the final energy performance of the first system is worst. Exergy analysis, in turn, shows clearly the importance of reducing pumping power. The better performance of the system with bigger pipes can be seen both in terms of final exergy and exergy associated to primary energy.

7.3.1.2 Economic considerations

Pipes of greater diameter are significantly more expensive than smaller pipes. Common sizing criteria aim at an optimum cost-benefit ratio, thereby trying to maximize the energy sold (i.e. reducing thermal losses in the pipes) while keeping investment and operation costs (including those for pumping energy) of the network at a minimum. Table 7.2 shows the estimated investment costs for the two differently sized networks studied.

Table 7.2: Investment costs for the pipes and pumps in the local district heat networks sized with conventional criteria (v_{max}=2.5 m/s) and following exergy considerations (v_{max}=1.0 m/s).Costs for DH pipes are taken from [Uponor, 2010]; **Costs for pumps are taken from [Wilo, 2010]

	Costs v_{max}=2.5 m/s [€]	Costs v_{max}=1.0 m/s [€]
Pipes*	18066	25046
Pumps**	8822	4531
Total costs	26888	29577

Electricity consumption for operating the pumps in both networks amounts 1.44 MWh/a

and 0.333 MWh/a in the cases of v_{max}=2.5 m/s and v_{max}=1.0 m/s respectively. Assuming an electricity price of 0.2294 €/kWh, the saved operation costs resulting from the lower electricity demand for the network sized following exergy criteria (v_{max}=1.0 m/s) amount 262.5 €/a. Assuming that all other investment and operation costs not listed in Table 7.2 are the same in both cases, the payback time of the additional investment costs for the network with bigger pipes amounts 10 years.

7.3.2 Use of district heating return line against conventional supply systems

District heating is a flexible way of supplying energy demands in buildings. With adequate control and storage strategies it can allow a time shift between the energy supply and demand and, thereby, enhances the combination of different renewable energy supply systems, e.g. solar thermal systems. However, typically high temperature levels are used for district heating systems [Dötsch and Bargel, 2009], reducing the potential use of renewable energy sources.

In this section advantages of low supply temperatures for district heating systems supplying SH and DHW energy demands in buildings are shown. All results presented from here onwards correspond to secondary networks sized following exergy criteria, i.e. with a maximum fluid velocity of 1 m/s.

7.3.2.1 Option (0): single heat exchanger

In this section the performance of low temperature district heat supply is compared to conventional high temperature district heating supply. In addition, a more conventional supply with individual condensing boilers in each house is included as reference case. For low temperature district heat the step function representing the average temperature profile as a function of the outdoor air temperature in Figure 4.7 (chapter 4) is considered. For high temperature district heating supply a constant temperature of 95°C is assumed. The hydraulic configuration from case (0)[19] in Figure 5.10 is considered for both temperature levels.

In the low temperature DH system the secondary side setpoint temperature for the local distribution network is a function of the inlet primary side temperature (see equation 5.1). A constant setpoint of 55°C has been chosen for the secondary side of the high temperature district heating supply at 95°C. Higher setpoint temperatures lead to higher temperatures in the upper layers of the DHW tanks, causing higher thermal losses in the storage tanks. In turn, with 55°C as setpoint the energy supplied by both systems is nearly the same and the systems can thereby be better compared with each other.

Figure 7.24 shows the specific final energy and exergy supply for the three supply systems considered in this section. A supply with individual boilers allows avoiding thermal losses in the supply network, which amount 11% of the total energy supplied. Thereby, final energy demands are reduced nearly in the same amount.

[19] This configuration corresponds to a common supply of SH and DHW demands with a single heat exchanger and a single local heat distribution network.

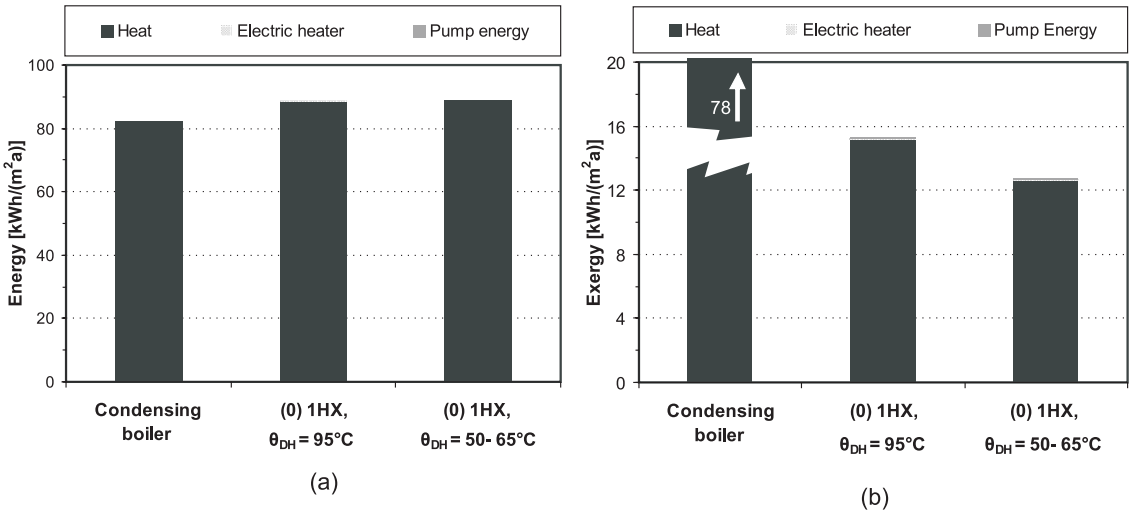

Figure 7.24: Annual specific final energy (a) and exergy (b) supply for three different supply systems: condensing boiler, high temperature district heating (95°C) and low temperature district heating (50-65°C), from left to right in the diagrams.

In turn, final exergy supply is greatly reduced if low temperature waste heat is used to supply the energy demands instead of using high quality fossil fuels (LNG) for SH and DHW supply. Reductions in the final exergy supplied amount 79% and 83% for the high and low temperature district heating options respectively. The difference between both district heating systems is solely due to the lower, and thus more suitable, temperature level chosen for the supply of the energy demands in the case of low temperature supply.

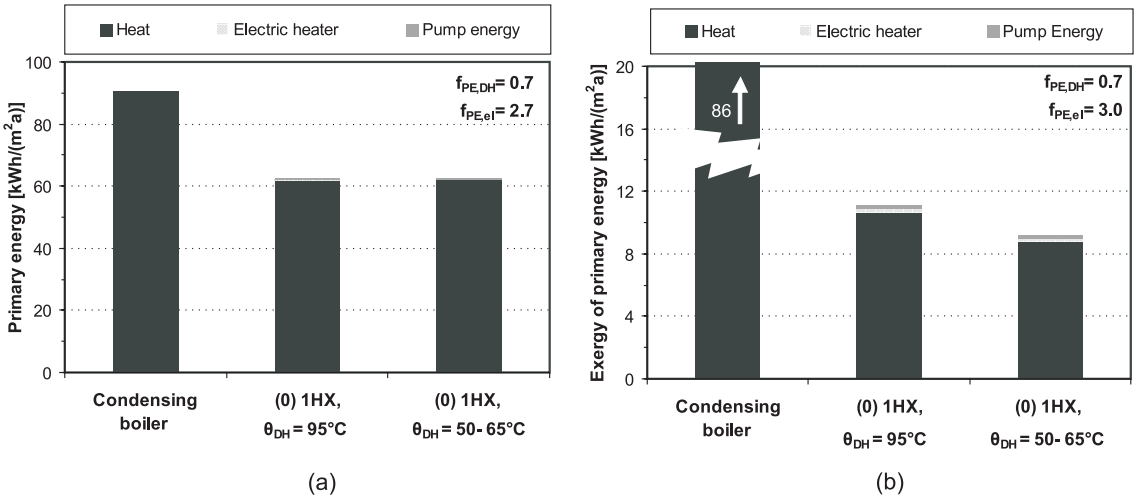

Figure 7.25: Annual specific primary energy (a) and exergy (b) supply for three different supply systems: condensing boiler, high temperature district heating (95°C) and low temperature district heating (50-65°C), from left to right in the diagrams.

Figure 7.25 shows the specific annual primary energy and exergy supply for the three options. The advantage of using waste heat for providing SH and DHW demands can now be clearly seen both from an energy and exergy perspective. In terms of energy the better performance is due to the lower primary energy factor for district heat and the primary energy factor of 1.1 for liquefied natural gas (LNG), resulting also in primary energy efficiencies higher than 100% as shown in Figure . Thermal losses in the pipes amount 11% of the thermal energy supplied by the district heating heat exchangers, being thus lower than the 30% primary energy reduction caused by the primary energy factor of 0.7. If thermal losses would be higher results from primary energy analysis might show a completely different trend.

In turn, primary exergy input is reduced by 86% and 89% respectively if available waste district heat is used instead of firing fossil fuels directly in a condensing boiler. This great reduction is due to the use of low valued energy (i.e. heat at 95 or 50-65°C) to supply low quality energy demands in buildings. Furthermore, thermal energy losses in the district heating network represent a low-quality loss in terms of exergy. Thus, exergy analysis is less sensitive to thermal losses as energy analysis is (see section 7.3.4). Even if thermal energy losses would be several times bigger, exergy analysis would favour district heating supply. This is of particular importance for evaluating low temperature district heating supply of an area with low energy demand density.

Primary energy input in the district heating system is nearly the same[20], independently of the supply temperature used. In turn, primary exergy input is reduced by 17% if a low temperature district heating network is used to supply the equally low temperature heat demands in buildings as compared to a conventional high temperature district heating system.

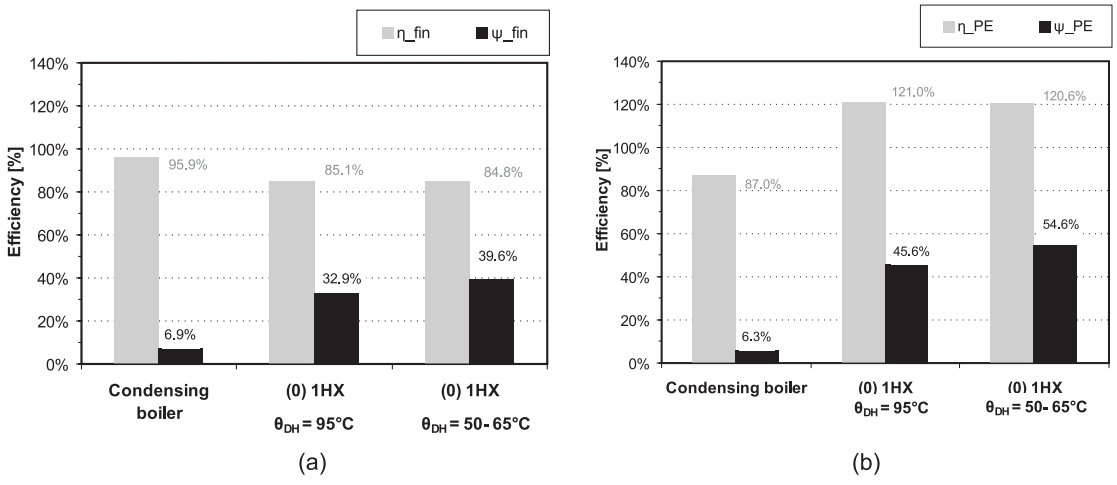

Figure 7.26: Final energy and exergy efficiencies (a) and primary energy and exergy efficiencies (b) for three different supply systems: condensing boiler, high temperature district heating (95°C) and low temperature district heating (50-65°C), from left to right in the diagrams.

[20]It is only 0.1% lower for the low temperature supply option

Figure 7.26 shows primary and final energy and exergy efficiencies for the three options mentioned above. While primary and final energy efficiencies are nearly the same for both district heating options, exergy efficiencies significantly increase if the district heat is supplied at lower temperatures.

7.3.3 Favourable hydraulic configurations

In this section a detailed analysis of the energy and exergy performance of the three hydraulic options shown in Figure 5.10 (section 5.2.4.2) is presented. Results from annual dynamic analysis for the three cases are compared with each other. The conventional hydraulic configuration based on a single heat exchanger for providing DHW and space heating demands, i.e. option (0) in Figure 5.10 is taken as base case.

7.3.3.1 Option (1): two independent heat exchangers

Figure 7.27 shows the specific final energy (a) and exergy (b) supplied for options (0) and (1).Electricity input for operating the pumps in the secondary network and the instantaneous electric heater for DHW supply represent marginal energy and exergy inputs in both systems. Due to the higher thermal energy losses in the distribution network final energy input is 2.5% higher for option (1). In consequence, final exergy efficiency is about 2% lower for option (1).

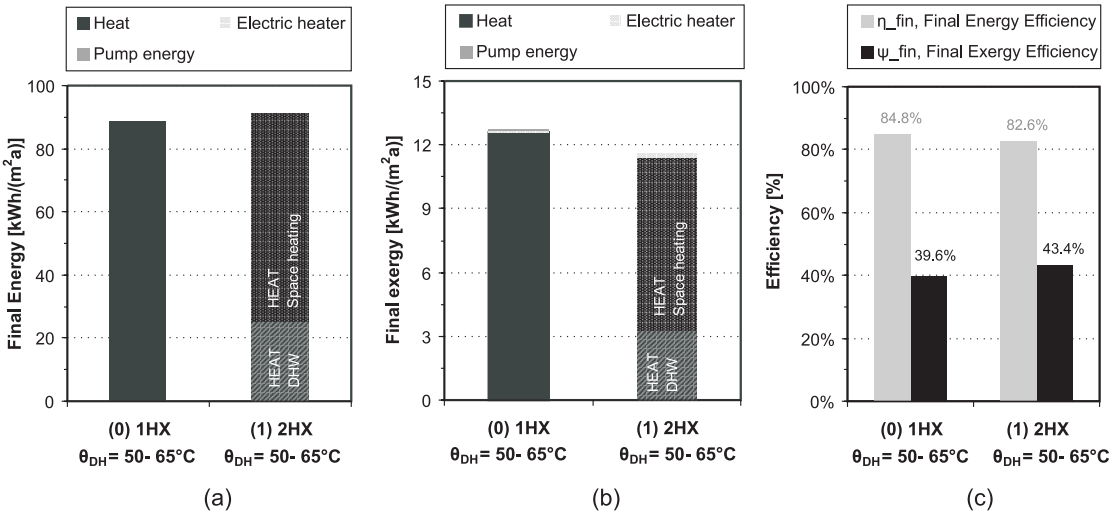

Figure 7.27: Specific annual final energy (a) and exergy (b) supply for low temperature district heating supply with one and two heat exchangers, i.e. options (0) and (1), respectively.

However, despite higher thermal losses in the distribution network, final exergy input is 9% lower for option (1). This reduction is due to the lower return temperaures at the primary side that can be achieved in the configuration with two separate heat exchangers. The quality of the energy supplied is thereby significantly reduced, being able to compensate for the

additional energy that needs to be supplied to the network due to higher thermal losses. The exergy efficiency of option (1) is, hereby, almost 4% higher than for option (0).

In Figure 7.28 the dynamic behaviour of the two options is shown. For case (1), i.e. with two heat exchangers, thermal energy transfer corresponds to the sum of the heat flows at the two heat exchangers. Similarly, mass flow rate $\dot{m}\_2hx$ is the total primary side flow rate through the two heat exchangers. Return temperatures, θ_2hx, are the average of the return temperatures for each single heat exchanger weighted with their corresponding mass flow rates (equation 7.1). In this way, instantaneous temperatures, heat and mass flows for the two options can be directly compared.

$$\theta_{ret,prim,tot} = \frac{\theta_{ret,prim,SH} \cdot \dot{m}_{prim,SH} + \theta_{ret,prim,DHW} \cdot \dot{m}_{prim,DHW}}{\dot{m}_{prim,SH} + \dot{m}_{prim,DHW}} \tag{7.1}$$

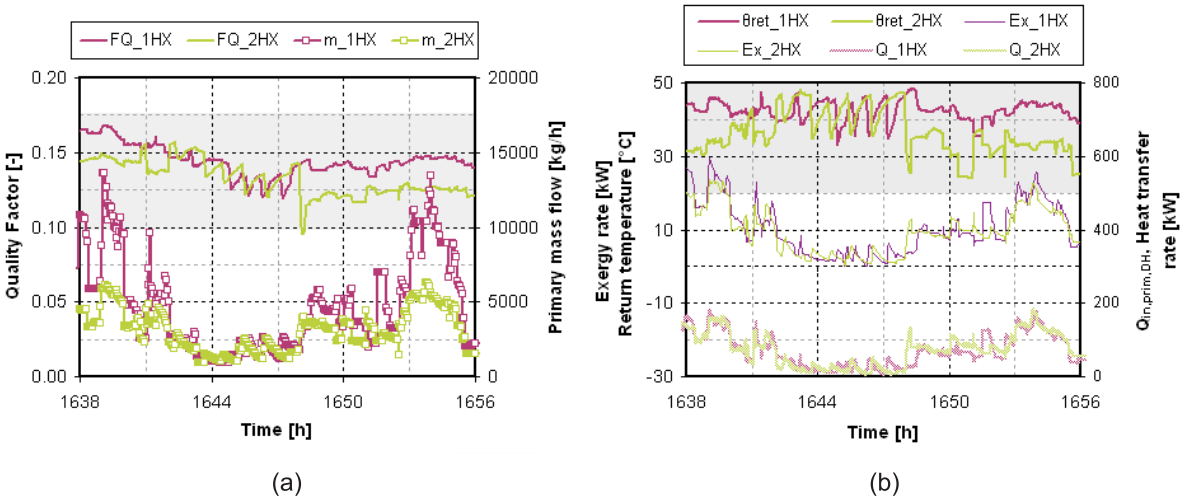

Figure 7.28: Dynamic behaviour of the system with one (*1HX*) and two (*2HX*) heat exchangers. (a): Quality factors for thermal heat transfer through the heat exchangers and total primary side mass flows; (b): Primary side return temperatures, total heat transfer and exergy transfer (input) from the primary side.

Total heat transfer rate through the heat exchangers $\dot{Q}$ is very similar in both cases. However, primary side mass flow is significantly higher with only one heat exchanger ($\dot{m}\_1HX$), reaching values of 200% that of case (1), i.e. $\dot{m}\_2HX$, as shown in Figure 7.28 (a). In turn, primary side return temperatures θ_{ret} are often up to 10°C lower for the system with two heat exchangers as compared to the system with only one.

The grey shadowed areas in the diagrams of Figure 7.28 highlight the strong correlation between return temperatures and quality factors of the energy provided (*FQ*): whenever return temperatures are higher for a given system, so are quality factors associated to the heat transfer, i.e. the energy is being provided with higher exergy. In other words, a greater part of the thermal potential available in the primary side mass flow remains unexploited and, herewith, greater mismatching arises between the exergy demanded and supplied, i.e. higher

exergy losses occur.

For completeness, in Table 7.3 annual average values of inlet and return temperatures at the primary and secondary sides of the district heat exchangers for the systems with one (0) and two (1) heat exchangers are shown. Secondary side return temperatures and mass flow rates for case (1) are obtained as the average of return temperatures for each heat exchanger weighted with the corresponding mass flow, as shown exemplary for the primary side in equation 7.1.

The operation of the secondary side is very similar for both cases (0) and (1). In turn, weighted average of the primary side return temperature is lower for case (1), showing that lower return temperatures are representative for this case as compared to case (0).

Table 7.3: Annual average values of primary and secondary sides total mass flows, inlet and return temperatures for space heating and DHW supply in cases (0) and (1).

	Units	(0) 1HX	(1) 2HX
$\langle\theta_{in,prim,tot}\rangle$	[°C]	57.7	57.7
$\langle\theta_{ret,prim,tot}\rangle$	[°C]	42.8	37.9
$\langle\dot{m}_{prim,tot}\rangle$	[kg/h]	3928.5	2809.9
$\langle\theta_{in,sec,tot}\rangle$	[°C]	32.9	33.0
$\langle\theta_{ret,sec,tot}\rangle$	[°C]	55.7	55.7
$\langle\dot{m}_{sec,tot}\rangle$	[kg/h]	2322.1	2504.4

Lower return temperatures are partly due to the sizing of the heat exchangers [21], but might also be due to lower return temperatures achieved on the secondary side due to separating DHW and space heating supply circuits. The importance of each factor is analyzed in detailed as part of the sensitivity analysis (see section 7.3.4).

In Figure 7.29 specific annual primary energy (a) and exergy (b) supplied is shown for the low temperature district heating supply with one and two heat exchangers respectively. The increase in the primary energy input for option (1) is mainly due to the higher thermal losses in the secondary network, causing a 3% decrease in the energy efficiency of the system.

The decrease in the primary exergy input system (1) is due to the lower return temperatures achieved in the supply with two separate heat exchangers as shown in Table 7.3 and Figure 7.28.

The lower exergy input results in an increase of nearly 5% in the exergy efficiency, as shown in Figure 7.29 (c).

Economic issues

The use of two separated pipe networks for supplying SH and DHW demands is expected to increase the costs of the district heating system. Table 7.4 shows the costs for the different components in the local district heat network in the case of combined and separated supply of

[21] Higher heat exchanger area on case (1) leads to higher temperature drops at the primary side.

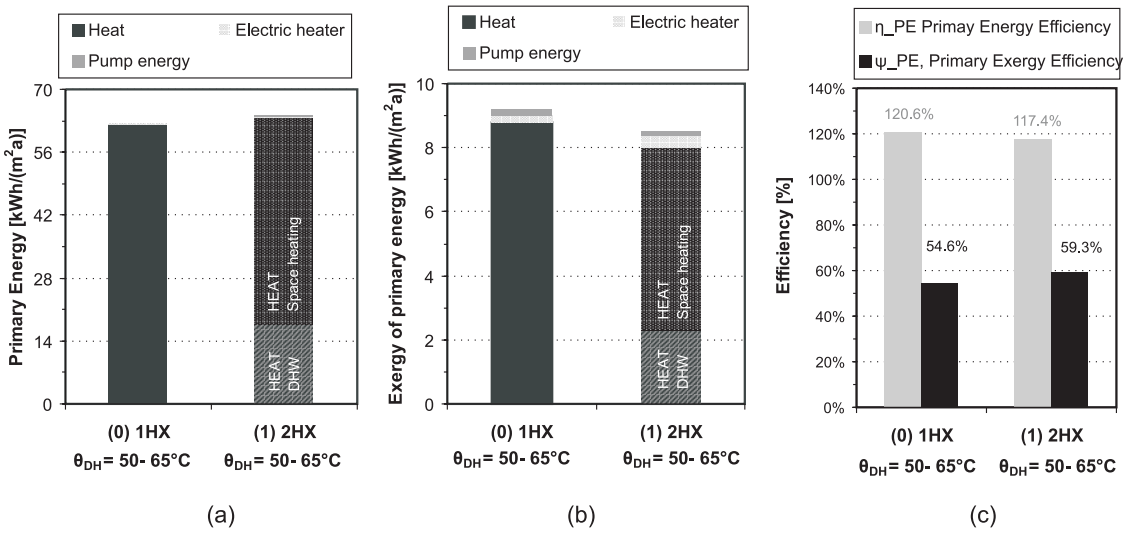

Figure 7.29: Specific annual primary energy (a) and exergy (b) supply for low temperature district heating supply with one and two heat exchangers, options (0) and (1), respectively. ($f_{PE,DH}$=0.7; $f_{PE,el}$=2.7 for energy analysis and $f_{PE,el}$=3.0 for exergy analysis).

both energy demands. The greatest increase in the costs is found for the heat exchanger. This

Table 7.4: Investment costs for the pipes, pumps and heat exchangers for a supply with one and two separated heat exchangers.*Costs for DH pipes are taken from [Uponor, 2010]; **Costs for pumps are taken from [Wilo, 2010];***Costs for the heat exchangers are taken from [GEA, 2010].

	(0) 1 HX Costs [€]	(1) 2HX Costs [€]
Pipes*	25046	30489
Pumps**	4531	3611
Heat exchangers***	1750	10080
Total costs	31953	46021

is due to the bigger heat exchanger (with greater heat exchange area) used for space heating supply in the case of separated supply (2HX) in order to ensure maximum temperature differences at its primary side, i.e. reduce return temperatures to the district heat network. Total costs for separated supply are 44% higher than those from a conventional separated supply.

Alternatively, a smaller heat exchanger for space heating supply still yielding a good exergy performance could be used. A good example of such a heat exchanger unit is shown in Table 7.6, whose use would only reduce the exergy efficiency in 0.7%. With that unit costs for the heat exchangers in the separated supply would amount 6400 € and total cost could be reduced to 40501 €, representing only a 27% increase as compared to a combined supply. Further details comparing the costs of options (0) and (1) for differently sized SH heat exchangers can be found in section 7.3.4.2.

7.3.3.2 Option (2): cascaded supply

In this section results from the optimized configuration with two separated heat exchangers without and with cascaded supply of domestic hot water and space heating demands, i.e. options (1) and (2) in Figure 5.10 are compared. The performance of option (2) with cascaded supply of space heating demand is closely analyzed.

In order to maximize the cascading between DHW and SH supply, the temperature set-point for the secondary side of space heating has been minimized (see equation 5.2 in chapter 5). Thus, higher mass flows are required for the secondary side of the space heating supply, making the use of pipes with greater diameter necessary for the secondary network in option (2). However, despite greater surface of the pipes, thermal losses are not higher in option (2) due to the lower water temperatures circulating at the secondary side of SH supply.

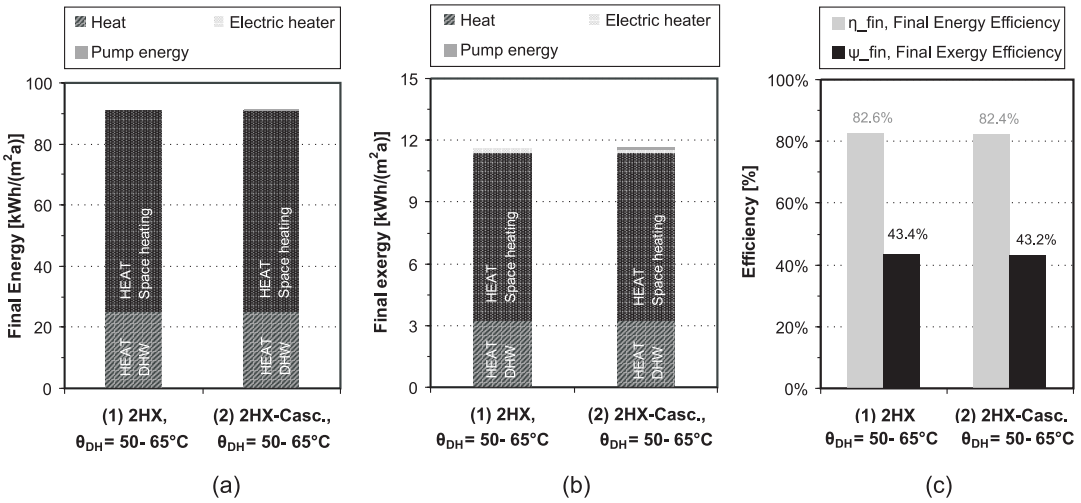

Figure 7.30: Annual final energy (a) and exergy (b) supply for low temperature district heat supply with two heat exchangers without and with cascaded supply of DHW and SH energy demands, options (1) and (2), respectively. (c): Final energy and exergy efficiencies for the two hydraulic options.

Final energy and exergy input are very similar for both systems, being only 0.1% and 0.4% lower for option (1) respectively. In consequence, very similar final energy and exergy efficiencies are obtained.

Option (2) with cascaded supply allows providing the space heating demand at lower temperatures, whenever cascading of mass flow from the DHW heat exchanger is possible[22], as shown in Figures 7.31 (a) and (b). At the times when cascading is possible, lower inlet temperatures for supplying space heating demands in option (2) can be found. As a result, higher mass flows are required at those times and, in consequence, higher return temperatures can be found at the primary side. Instantaneous heat transfer to the space heating supply network is nearly the same in both options, showing also the same dynamic behaviour. Despite greater mass flows and higher return temperatures for the cascaded option, lower quality factors for

[22] i.e. when mass flow rate and temperature level from DHW return are high enough for SH supply.

the energy supplied can be achieved for the times when cascading succeeds, see Figure 7.31 (a). This shows the greater impact of reducing supply temperatures for reducing thermal exergy supply. The strong correlation between supply temperatures and the quality factor of the energy supplied is highlighted in the shadowed areas in Figure 7.31.

However, cascading between DHW and SH heat exchangers succeeds only 536 h/a of the 3618 h/a when space heating energy demand exists and it represents only 1.6% of the total energy and exergy supplied to space heating. Therefore, the benefit of this improved exergy performance due to cascading represents a very small amount of the total energy and exergy supplied.

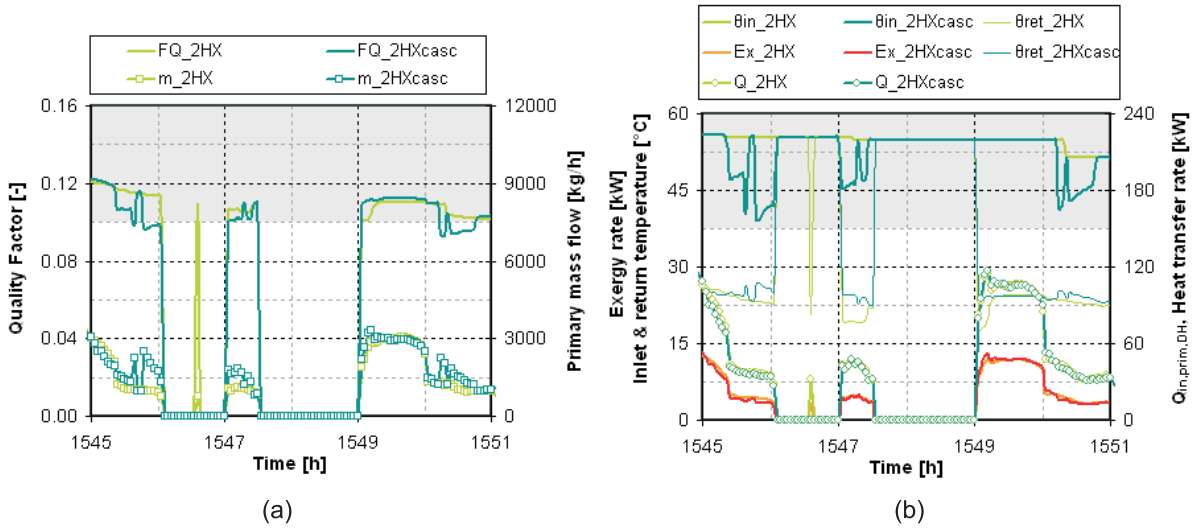

Figure 7.31: Dynamic behaviour of the system with two heat exchangers without cascading (*2HX*) and with cascaded supply of energy demands (*2HX_casc.*). (a): Quality factors for thermal heat transfer through the heat exchangers and total primary side mass flows; (b): Primary side inlet and return temperatures, total heat transfer and exergy transfer (input) from the primary side in both supply options.

Results from statistic analysis show that the operation of the primary side of both options (1) and (2) is very similar (see Table 7.5). In turn, the operation of the secondary side is very different: outlet temperatures at the secondary side for space heating are much lower in option (2) in order to allow a supply by means of the return from the DHW heat exchanger. Mean temperature drop at the secondary side is nearly two times lower. In consequence, mean mass flow required for space heating supply is greater. This results in higher pumping power which amounts 0.116 kWh/m^{2}a (as compared to 0.046 kWh/m^{2}a for case (1)), i.e. an increase of 151.0%.

Annual specific primary energy and exergy supplied to both systems (1) and (2) are shown in Figure 7.32 (a) and (b). Thermal primary energy and exergy supplied by the heat exchangers for providing DHW demands are nearly the same in both cases.

In energy terms pumping energy is not relevant, representing 0.2% and 0.5% of the total

Table 7.5: Mean values of the primary and secondary sides inlet, return temperatures and mass flow rates. Values for the space heating heat exchangers (*SH*) and domestic hot water heat exchangers (*DHW*) are shown. Besides, total mass flow rates and inlet temperatures as well as weighted average for return temperature combining the supply of both energy demands (*tot*) are shown.

	Units	(1) 2HX	(2) 2HX+Cascading
$\langle\theta_{in,prim,SH}\rangle$	[°C]	55.7	55.0
$\langle\theta_{ret,prim,SH}\rangle$	[°C]	25.0	25.1
$\langle\dot{m}_{prim,SH}\rangle$	[kg/h]	2343.1	2407.0
$\langle\theta_{in,prim,DHW}\rangle$	[°C]	58.1	58.1
$\langle\theta_{ret,prim,DHW}\rangle$	[°C]	44.6	44.1
$\langle\dot{m}_{prim,DHW}\rangle$	[kg/h]	1919.2	1914.9
$\langle\theta_{in,prim,tot}\rangle$	[°C]	57.7	57.5
$\langle\theta_{ret,prim,tot}\rangle$	[°C]	37.9	37.9
$\langle\dot{m}_{prim,tot}\rangle$	[kg/h]	2809.9	2834.9
$\langle\theta_{in,sec,SH}\rangle$	[°C]	22.9	23.8
$\langle\theta_{ret,sec,SH}\rangle$	[°C]	53.7	28.5
$\langle\dot{m}_{p,SH}\rangle$	[kg/h]	2332.6	15028.2
$\langle\theta_{in,sec,DHW}\rangle$	[°C]	38.6	38.8
$\langle\theta_{ret,sec,DHW}\rangle$	[°C]	56.1	56.1
$\langle\dot{m}_{sec,DHW}\rangle$	[kg/h]	1559.7	1560.5
$\langle\theta_{in,sec,tot}\rangle$	[°C]	33.0	31.7
$\langle\theta_{ret,sec,tot}\rangle$	[°C]	55.7	43.7
$\langle\dot{m}_{sec,tot}\rangle$	[kg/h]	2504.4	9040.5

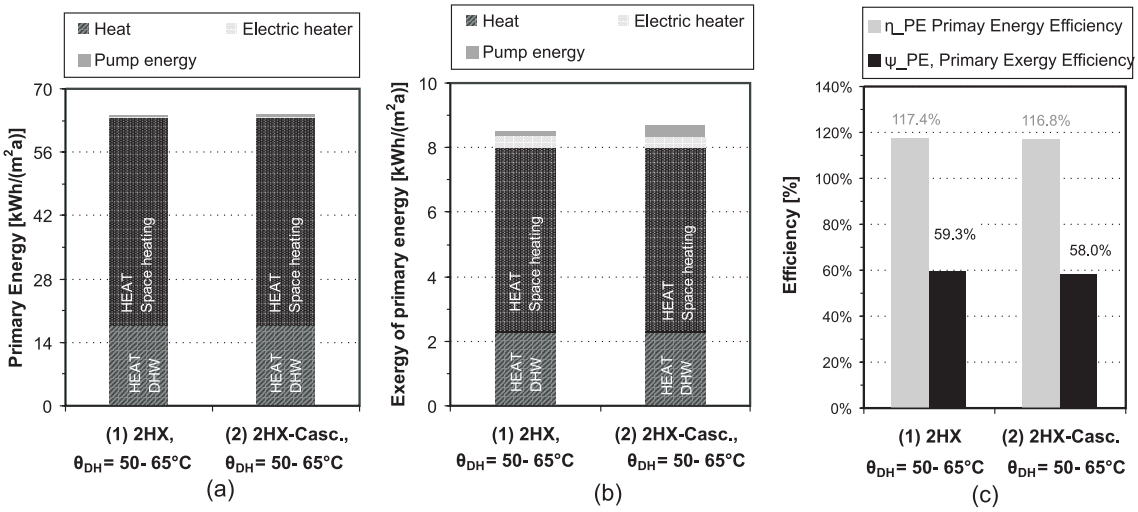

Figure 7.32: Annual primary energy (a) and exergy (b) supply for low temperature district heating supply with two heat exchangers without and with cascaded supply of DHW and space heating energy demands, options (1) and (2), respectively. (c): Primary energy and exergy efficiencies for the two hydraulic options. ($f_{PE,DH}$=0.7; $f_{PE,el}$=2.7 for energy analysis and $f_{PE,el}$=3.0 for exergy analysis).

primary energy supply. In terms of exergy, thermal energy flows represent a smaller input, due to their low quality, and electricity input becomes more relevant. Pumping energy repre-

sents 1.6% and 4.2% of the total primary exergy input in cases (1) and (2), respectively, being responsible for the differences in the behaviour of both options.

7.3.4 Sensitivity analysis

Several parameters might strongly influence the dynamic behaviour of the systems analyzed. A sensitivity analysis has been performed in order to show to which extend different parameters determine the energy and exergy performance of the district heat system studied. The three hydraulic configurations investigated, i.e. options (0), (1) and (2), (Figure 5.10) behave in a similar way to the variation of a given parameter. Results from sensitivity analysis for the best case, i.e. option (1), are shown here.

The sensitiveness of the model to different sizes of the heat exchangers and thermal losses in the pipes is analyzed. To avoid the influence of primary energy factors results showing the sensitivity of the model to a given parameter are expressed in terms of final energy or exergy demands and final energy or exergy efficiencies. Only in the last section, devoted to the influence of primary energy factors, results from primary energy analysis are shown.

7.3.4.1 Thermal energy losses in supply pipes

In this section the sensitivity of the results for case (1) to thermal losses in the supply pipes is studied. For this, heat transfer coefficients determining the thermal losses in the pipes have been stepwise reduced. Figure 7.33 shows final energy and exergy input for different heat transfer coefficients in the pipes U_{pipes} as percentage of those assumed in the base case (100%).

Thermal energy losses in the pipes amount 13% of the thermal energy supplied to the network in the base case (both for DHW and SH demand together). If these thermal losses could be completely avoided, final energy efficiency would increase by 11.8%. However, a much smaller can be observed for the final exergy efficiency under the same situation: from 43.4% to 49.6%, i.e. an increase by 6%. This is due to the fact that thermal energy losses in terms of exergy have low quality and, thus, do not represent savings of the same magnitude as in energy terms. This is shown also in Figure 7.33 (a): a much steeper reduction in the final energy input than in the final exergy input into the system can be observed.

The improved hydraulic configuration of option (1) showed an increase of nearly 5% in the final exergy efficiency as compared to the conventional case with a single heat exchanger, i.e. option (0). A similar increase could be obtained if thermal energy losses in the pipes are reduced by 80%, i.e. if the heat loss coefficient of the pipes is reduced to 20% of the reference value. This shows the importance of minimizing thermal energy losses even in low temperature district heating systems.

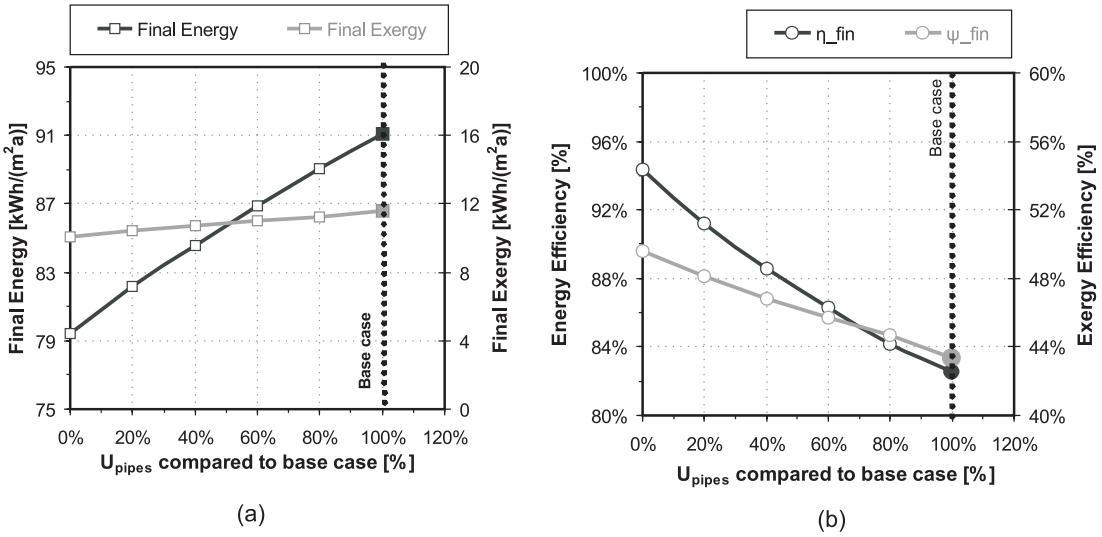

Figure 7.33: Final energy and exergy supply (a) and final energy and exergy efficiencies (b) for case (1) with different heat transfer coefficients chosen for the pipes in the secondary hydraulic networks. U values in the X-axis are referred in percentage to the U value assumed for the base case (100%).

7.3.4.2 Sizing of space heating heat exchanger

Return temperatures at the primary side of the heat exchangers have a strong impact on the exergy efficiency of the systems analyzed, as shown in section 7.3.3.1. The size of the heat exchanger is expected have a great influence on the achievable primary side return temperatures. To investigate the impact of the heat exchanger size in the performance of the system, several heat exchanger sizes for SH supply have been simulated.

The size of the space heating heat exchanger is characterized here by means of its UA value. In Figure 7.34 UA values of the cases investigated for the sensitivity analysis as a function of the primary mass flow are shown. Table 7.6 shows the physical characteristics of real heat exchangers, sized with a free available software from the company GEA Group [GEA, 2009], corresponding to those shown in Figure 7.34.

Table 7.6: Area, Type and UA values of the heat exchangers regarded for the sensitivity analysis as percentage of UA value from the base case.

Case	UA compared to base case [%]	Area [m^2]	Heat exchanger type
Base case (1)	100	59.70	WP10-U201
Sensitivity.1	67	14.10	WP10-U49
Sensitivity.2	43	9.05	WP7M-U69
Sensitivity.3	32	8.16	WP757M-U53
Sensitivity.4	20	7.68	WP757M-50

Figure 7.35 (a) shows the behaviour of total final energy and exergy supplied as a function

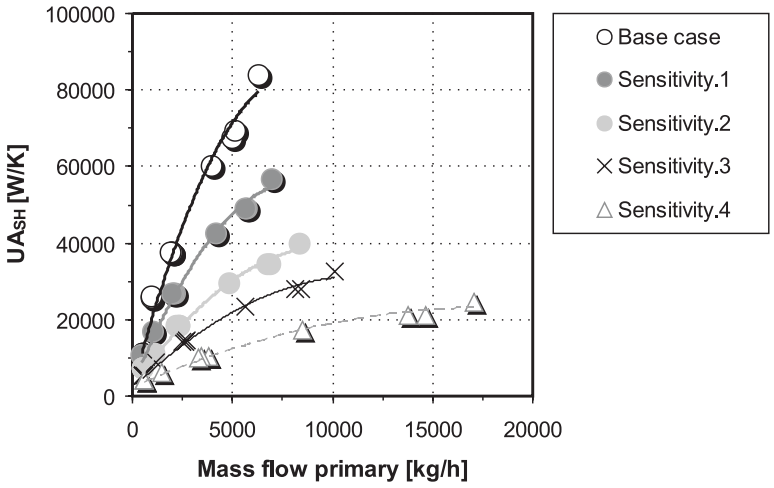

Figure 7.34: UA values assumed as a function of the primary mass flow for the space heating heat exchangers in case (1).

of the UA value assumed for the space heating heat exchanger. The energy supplied is not influenced by the size of the heat exchanger. A total final energy input of 91.08 kWh/m^{2}a can be found for all cases. In turn, final exergy values are sensitive to variations in the UA value: decreasing the UA value of the heat exchanger to 20% of the chosen reference case would increase the total final exergy input in the system by 14%, from 11.65 kWh/m^{2}a to 13.25 kWh/m^{2}a.

Similar trends can be found for the final energy and exergy efficiencies. A decrease of 80% in the UA value of the space heating heat exchanger of the reference case (i.e. *Sensitivity.4* in Table 7.6) causes a reduction of 5% in the final exergy efficiency, as it is shown in Figure 7.35 (b).

Higher UA values of the heat exchanger allow achieving higher temperature differences between the inlet and outlet at the primary side. Thus, the required heat transfer succeeds with lower mass flows, as shown in Table 7.7. In other words, higher UA values allow exploiting better the thermal potential of a given mass flow thereby increasing the exergy efficiency of the heat transfer. Average values of the thermal exergy efficiency for supplying space heating demands and final exergy efficiencies shown in Table 7.7 confirm this trend.

Having two different heat exchangers allows sizing them accordingly to the particular operation conditions for each use (e.g., secondary side return temperatures from DHW supply might be much higher than those from space heating supply), thereby facilitating improved operation of the system. A single heat exchanger must be able to supply both demands but it will not be able to operate on the optimum range for both uses. However, separate supply alone (i.e. without appropriate sizing of the heat exchangers) does not guarantee a better performance, as it is shown here.

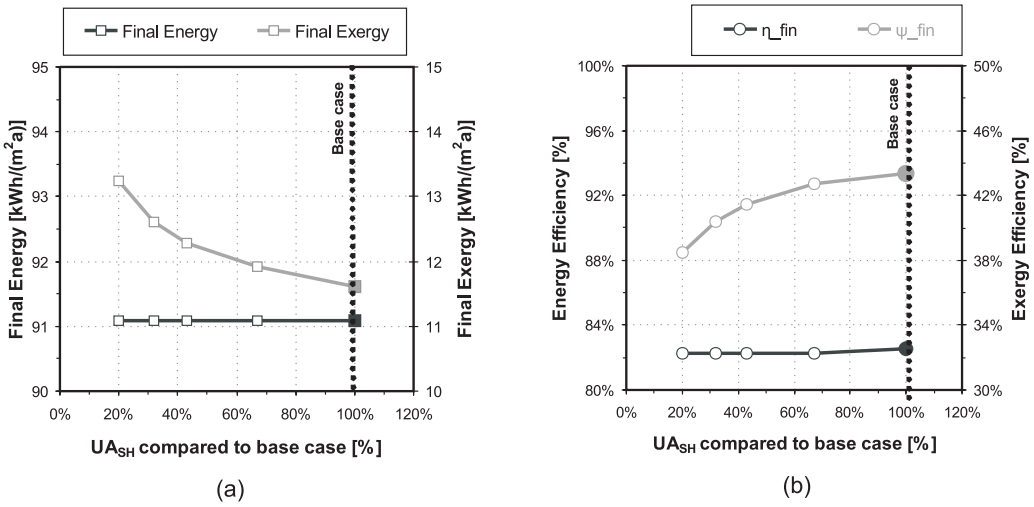

Figure 7.35: Final energy and exergy supply (a) and final energy and exergy efficiencies (b) for case (1) with different UA values chosen for the space heating heat exchanger. UA values in the X-axis are referred in percentage to the UA value of the space heating heat exchanger in the base case (100%).

Table 7.7: Mean values of the primary side inlet, return temperatures and required mass flow rates for the different UA values of the space heating heat exchanger analyzed in this section. Average values of the thermal exergy efficiency for space heating supply, $\langle \Psi_{th,SH} \rangle$, are also shown.

Case	$\langle \theta_{ret,prim,SH} \rangle$ [°C]	$\langle \theta_{in,prim,SH} \rangle$ [°C]	$\langle \dot{m}_{prim,SH} \rangle$ [kg/h]	$\langle \Psi_{th,SH} \rangle$ [-]	Ψ_{fin} [-]
Base case (1)	24.98	55.70	2343.11	0.48	0.434
Sensitivity.1	26.73	55.70	2499.81	0.47	0.427
Sensitivity.2	30.34	55.70	2893.97	0.45	0.415
Sensitivity.3	33.69	55.70	3365.54	0.43	0.404
Sensitivity.4	40.57	55.70	4427.19	0.40	0.384

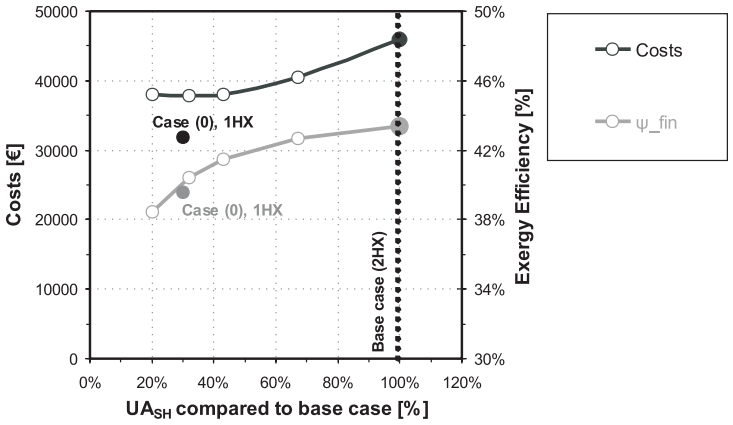

Figure 7.36: Final exergy efficiencies and investment costs for the cases with the different SH heat exchangers investigated in this section. For comparison, exergy effciency and costs for option (0) are also shown.

Figure 7.36 shows the total investment costs[23] for the cases with different SH heat exchangers investigated in this section as a function of their UA value UA_{SH}. Investment costs are reduced for lower UA values. For comparison, investment costs and exergy efficiency for case (0), i.e. with a common heat exchanger and network for SH and DHW demands, are shown. Case *Sensitivity.3* shows similar exergy performance as case (0). However, costs for *Sensitivity.3* are still 18% higher than for case (0), due to the additional costs for the two separated heat exchangers and distribution networks.

7.3.4.3 Sizing of DHW heat exchanger

Domestic hot water demands represent 17% of the total energy demands (for SH and DHW). In consequence, the sensitivity of the results to different sizing criteria for the DHW heat exchanger is expected to be lower than to space heating heat exchangers.

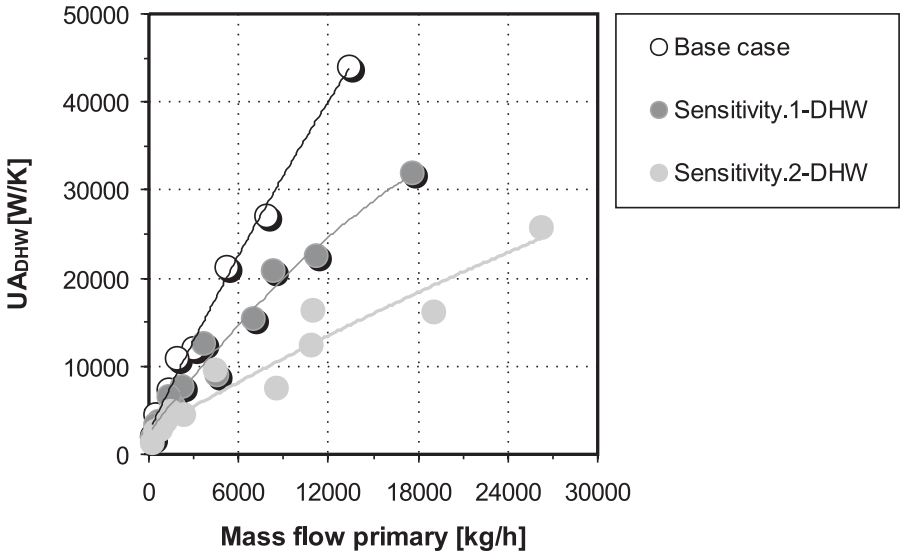

Figure 7.37: UA values assumed for the DHW heat exchangers as a function of the primary mass flow in case (1).

To investigate this, different heat exchangers for DHW preparation have been assumed (see Table 7.8). To ease comparison the UA value of the heat exchangers assumed is shown as referred to the base case (100%). Figure 7.37 shows graphically the variation of the UA values for DHW supply assumed here as a function of the primary side mass flow through the heat exchanger.

Figure 7.38 shows the variation of the total final energy and exergy required as a function of the UA value chosen for the heat exchanger as compared to the base case (100%). Table 7.9 shows primary side average supply and return temperatures and mass flow rates for each of

[23] i.e. including costs for the two separated pipe networks, pumps and DHW and SH heat exchangers.

Table 7.8: UA values, area, price and type of the heat exchangers for DHW supply assumed for the sensitivity analysis.

Case	UA compared to base case [%]	Area [m^2]	Heat exchanger type
Base case (1)	100	14.08	WP757-H90
Sensitivity.1-DHW	55	6.08	WP757-L40
Sensitivity.2-DHW	36	7.68	WP757-L50

the cases studied. Again, a correlation can be found between the final exergy efficiency and the primary side average return temperature from DHW supply.

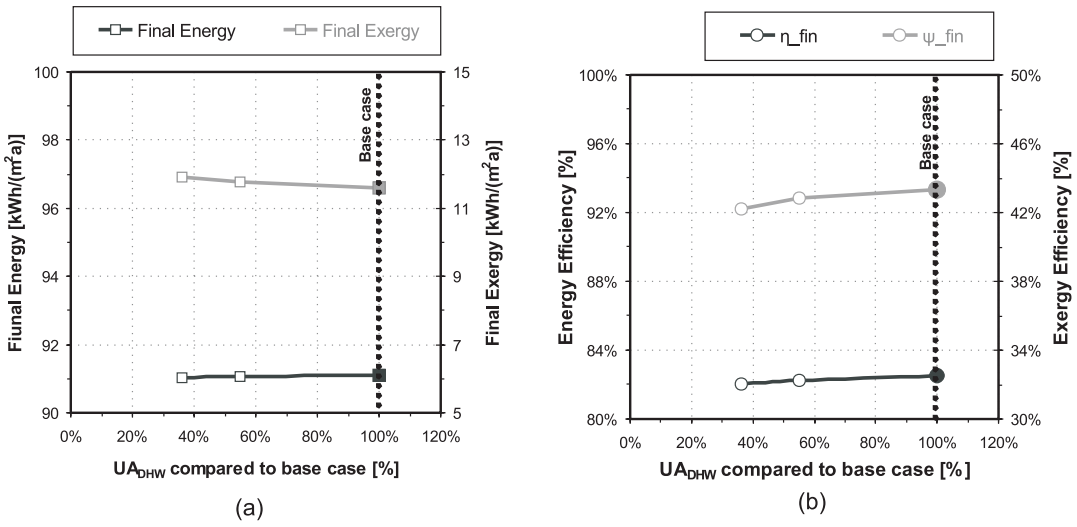

Figure 7.38: Final energy and exergy supply (a) and final energy and exergy efficiencies (b) for case (1) with different UA values chosen for the DHW heat exchanger. UA values in the X-axis are referred in percentage to the UA value of the DHW heat exchanger in the base case (100%).

Table 7.9: Mean values of the primary side inlet, return temperatures and required mass flows for the different UA values of the DHW heat exchanger analysed in this section. Average values of the thermal exergy efficiency for DHW supply, $\rangle\Psi_{th,DHW}\rangle$, and final exergy efficiencies for each case are also shown.

Case	$\rangle\theta_{ret,prim,DHW}\rangle$ [°C]	$\langle\theta_{in,prim,DHW}\rangle$ [°C]	$\langle\dot{m}_{prim,DHW}\rangle$ [kg/h]	$\langle\Psi_{th,DHW}\rangle$ [-]	Ψ_{fin} [-]
Base case (1)	44.27	58.06	1953.43	0.25	0.434
Sensitivity.1	47.79	58.06	2595.87	0.22	0.428
Sensitivity.2	52.81	58.04	5740.60	0.21	0.422

As expected, due to the lower magnitude of DHW supply as compared to space heating demands, sensitiveness of the results to variations in the UA value of the DHW heat exchanger is lower than for space heating supply. Reducing the UA value of the DHW heat exchanger to 36% that of the reference case causes merely a decrease of 1.2% in the final exergy efficiency.

7.3.4.4 Common and separate networks for space heating and DHW supply

Lower return temperatures achieved on case (1) and leading to a better exergy performance might be partly due to the sizing of the heat exchangers and to lower return temperatures on the secondary side due to:

- avoiding the mixing of return mass flows from the DHW and space heating supply circuits
- higher thermal losses in the distribution network

In this section the influence of having one or two secondary network for SH and DHW supply is checked. For this purpose, case (3) is build up by modifying the UA values of both heat exchangers in case (1), where two separated networks and heat exchangers are used for SH and DHW supply, and setting them identical to UA values for the single heat exchanger in case (0). Secondary distribution networks are operated in the same fashion in both cases. Thus, the only difference between cases (0) and (3) is having one or two separated secondary networks for SH and DHW supply.

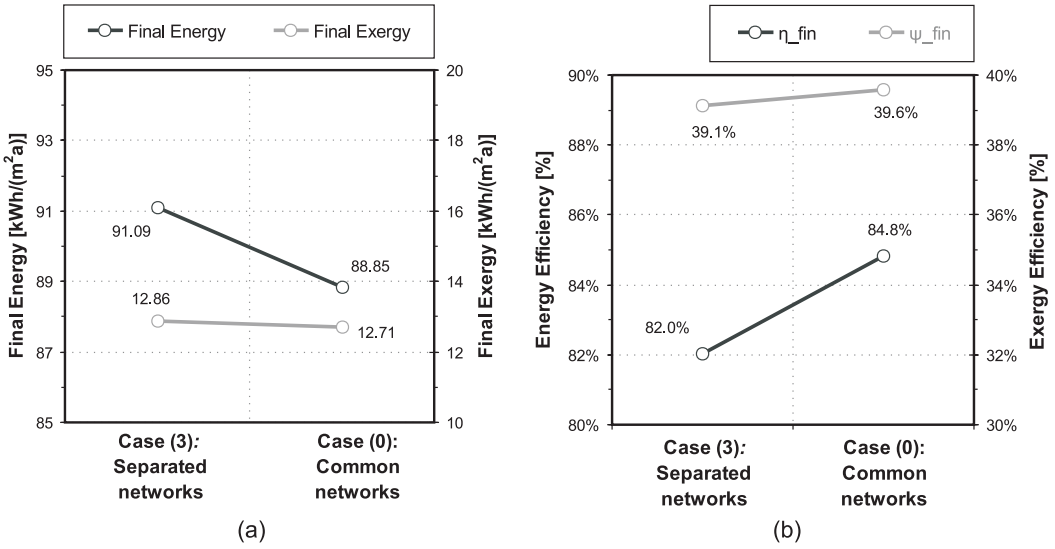

Figure 7.39: Final energy and exergy supply (a) and final energy and exergy efficiencies (b) for case (3) with two separated secondary networks for space heating and DHW supply and case (0) with a common network for supplying both energy demands.

The energy performance of the system with a common secondary network for supplying SH and DHW demands is significantly higher than if two separated networks are used: final energy supplied decreases in 2.23 kWh/m^{2}a and final energy efficiency increases by 2.8% (see Figure 7.39). Differences in the energy performance of both options are due to the higher thermal energy losses if two distribution networks are used instead of a single one.

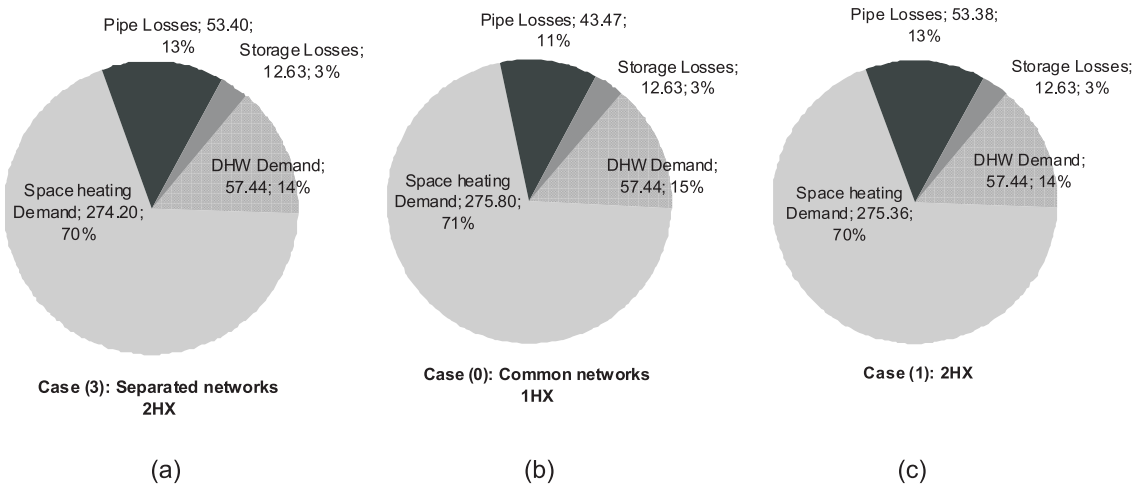

Figure 7.40: Energy demands and losses (in MWh/a) for the supply with separated (a) and common (b) networks for SH and DHW supply. In (a) and (b) the same UA value for the SH and DHW heat exchangers have been used. For completeness, energy demands and losses for option (1), i.e. with two separated networks and different UA value for SH supply (c), are shown.

Figure 7.40 shows that thermal losses for the case of two separated networks increase by 23%, and are very similar to those in option (1), where also two separated networks for SH and DHW supply are foreseen (see Figures 7.40 (a) and (c)). This results in a similar energy performance for both cases with separated networks for DHW and SH supply, i.e. option (1) and case (3), as it is shown in Table 7.10. Average operating conditions for systems (3) and option (0), i.e. with common and separated networks respectively but with the same heat exchanger, are very similar as it is shown in Table 7.10, resulting in a similar exergy performance (see Figure 7.39). Small differences in their exergy performance arise due to the different thermal energy losses, being however marginal as compared to its impact on the energy behaviour of the systems.

Table 7.10: Mean values of the primary side inlet, return temperatures and mass flows for combined SH and DHW supply with one separated network for each energy demand (case (3)) and with one common network for both demands (case (0)). Average values of the thermal exergy efficiency for combined space heating and DHW supply, $\langle \Psi_{th,tot} \rangle$ and final exergy efficiencies for each case are also shown.

Case	$\langle \theta_{ret,prim,tot} \rangle$ [°C]	$\langle \theta_{in,prim,tot} \rangle$ [°C]	$\langle \dot{m}_{prim,tot} \rangle$ [kg/h]	$\langle \Psi_{th,tot} \rangle$ [-]	Ψ_{fin} [-]	η_{fin} [-]
Case (3), Separated networks	42.29	57.70	3847.59	0.29	0.391	0.822
Case (0), 1HX Common networks	42.83	57.71	3928.47	0.30	0.396	0.848
Case (1), 2HX	37.88	57.70	2809.87	0.31	0.434	0.826

Hereby it is clearly shown that using one or two separated secondary side networks only has a significant influence on the energy performance of the systems. In turn, the improved exergy performance of option (1) is merely due to the more appropriate sizing of the heat

exchangers and not to the use of two separated secondary distribution networks.

7.3.4.5 Primary energy factors

In the following sections the sensitiveness of the energy and exergy performance of the district heating system studied to different primary energy factors for district heating is studied. Furthermore, the general expression of the parameter (quality factor) used in this thesis to evaluate the exergy of district heating is presented. Differences and main conclusions that can be gained from both parameters and analyses are also presented and the added value of combining both parameters is introduced and discussed.

Definitions of primary energy factors for district heat from CHP in the standards

As stated in section 2.7 exergy analysis is proposed here not as a substitute but as a complement to primary energy analysis. Results from primary energy analysis are strongly influenced by primary energy factors. Primary energy factors include the energy required for the conveyance, processing and transport of energy sources over the whole energy supply chain. Table A1 of the German standard DIN 18599-1 [2007] summarizes primary energy factors for different energy sources. It includes a default value for district heating from waste heat of co-generation systems of 0.7, corresponding to a district heating network with a share of 70% of CHP in the heat production. This default value might be used if not enough data for a more deatiled calculation are available.

Alternatively, Appendix A3.1 of [DIN 18599, 2007][24] defines a calculation method for primary energy factors for district heating from co-generation. In this calculation approach, primary energy factors for waste heat from co-generation systems are derived depending on several parameters describing the operation of the CHP unit and the heat production systems in the district heat network. Equation 7.2 shows the expression for calculating the primary energy factor of district heating. Figure 7.41 shows the variables and boundaries for calculating primary energy factors according to the standard DIN 18599 [2007].

$$f_{PE,DH} = \frac{\Sigma_i En_{fuel,in,DH,i} \cdot f_{PE,fuel,i} - En_{el,CHP} \cdot f_{PE,el}}{\Sigma_i Q_{out,DH,i}} \tag{7.2}$$

In equation 7.2 $En_{fuel,in,DH}$ represents the energy from all fuels supplied to the heat generators (*i*), i.e. heat plants or CHP units supplying the district heating network, $f_{PE,fuel,i}$ are the primary energy factors of the fuels used, $En_{el,CHP}$ is the electricity generated by the CHP unit, $f_{PE,el}$ is the primary energy factor for electricity according to the German electricity mix [DIN 18599-1, 2007] and $Q_{in,DH,i}$ is the total heat output from the district heating network measured at the heat exchangers providing energy demands to the buildings or users connected to the heat grid. Thermal losses in the heat distribution grid (primary side) are, thereby, regarded in

[24] In DIN 18599-100 (2009) corrections and amendments to the standards DIN 18599-1-10 are made. All corrections from this standard are taken into account here.

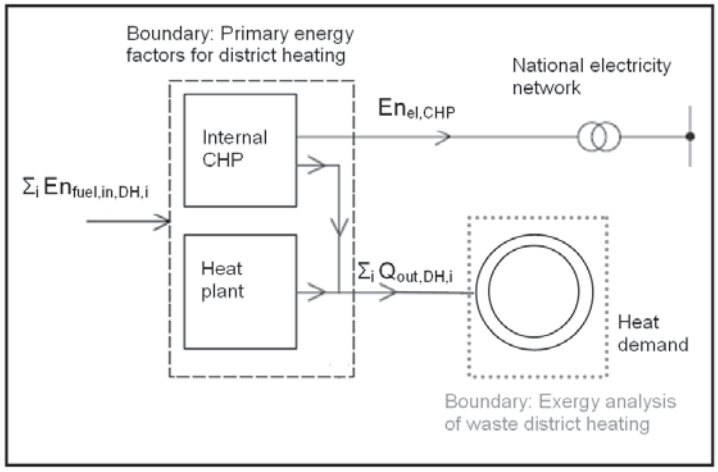

Figure 7.41: Variables and boundary for calculating primary energy factors for district heat from co-generation units (CHP) according to the standard DIN 18599 [2007] (translated and modified). The boundary for calculating exergy of waste district heat is also shown in the diagram.

the balance. Equation 7.3 shows the relation between the heat output from the grid and the total fuel input used for its supply $En_{fuel,in,DH}$. Thermal losses in the distribution network are characterized as a function of the energy efficiency of the heat network η_{HN}. If no other values are available the efficiency of the heat network η_{HN} can be assumed as 0.9. η_{HPl} and $\eta_{th,CHP}$ are the thermal efficiencies of heat generators and CHP units in the district heat systems. β represents the share of heat from the CHP plant in the heat distribution network.

$$En_{fuel,in,DH,i} = \frac{1}{\eta_{HN}} \cdot \left[\frac{Q_{out,DH,i} \cdot (1-\beta)}{\eta_{th,HPl}} + \frac{Q_{out,DH,i} \cdot \beta}{\eta_{th,CHP}} \right] \tag{7.3}$$

The electricity output from the CHP unit $En_{el,CHP}$ can be easily calculated as a function of the electric efficiency of the CHP unit and the total fuel input in the CHP, as shown in equation 7.4.

$$En_{el,CHP} = \frac{Q_{out,DH,i}}{\eta_{HN} \cdot \eta_{th,CHP}} \cdot \eta_{el,CHP} \tag{7.4}$$

Primary energy factors for district heat following equation 7.2 strongly depend on the electricity generated by the CHP units considered, i.e. on the electrical efficiency of the CHP units, as it is shown graphically in Figures 7.42 and 7.43. Primary energy factors for CHP units intend, thereby, to give insight on the electric efficiency of CHP units as compared to the German electricity mix. These factors are also very sensitive to the value of the primary energy factor for electricity from the German mix. Due to the high primary energy factor for electricity of 2.7, primary energy factors for district heat might even be negative[25] [Kühler, 2008] leading to confusing results. To avoid this in the standards it is stated that negative

[25] see Figure 7.43 in the following section.

values of primary energy factors for CHP units shall always be set to zero [DIN 18599-1, 2007].

General quality factors for district heat, $F_{Q,DH}$

The district heating cases analyzed above are supplied with waste heat. In this thesis, waste heat in district heating networks is evaluated as low temperature heat and its quality level, i.e. its exergy content, is evaluated accordingly as a function of its temperature level as shown in equation 7.5. The grey dotted line in Figure 7.41 shows the boundary regarded for exergy analysis of waste heat in district heat systems. It is clearly shown that with this approach the behaviour and performance of CHP units or heat plants in the district heat network are excluded from exergy analysis.

$$F_{Q,DH,waste} = \frac{1}{T_{in,prim} - T_{out,prim}} \cdot \left[(T_{in,prim} - T_{out,prim}) - T_0 \ln \frac{T_{in,prim}}{T_{out,prim}} \right] \tag{7.5}$$

However, in district heat systems waste heat from CHP units or industrial processes is often combined with heat from conventional heating plants. Equation 7.6 shows the general expression for calculating the quality of a district heat system where waste heat and thermal output from conventional heat plants are combined. The dotted grey boundary shown in Figure 7.41 would still be valid for the waste heat share. Additionally, the quality of fuels used in the heat plants is evaluated separately enhancing, thereby, the boundary for exergy analysis to the heat plants present in the network.

$$F_{Q,DH} = \beta \cdot F_{Q,DH,waste} + (1 - \beta) \cdot F_{Q,fuel} \tag{7.6}$$

The exergy of primary energy for district heat systems can be obtained, similarly as it is done for other energy systems, by multiplying the quality factor in equation 7.6 with the corresponding primary energy factors obtained as shown in equation 7.2.

It is important to remark that this exergy based parameter can be directly used to evaluated waste heat from other processes than co-generation, e.g. waste heat from industrial processes.

Sensitivity to primary energy factors for district heat, $f_{PE,DH}$

In this section, the sensitivity of results from primary energy and exergy analysis for district heating supply systems to different primary energy factors is presented.

Figure 7.42 shows primary energy and exergy input required for the district heat system studied[26] as a function of the primary energy factor assumed for district heating supply. Assuming 100% district waste heat supply[27] variations in the primary energy factors are due to different electric efficiencies of the CHP units supplying the network, as shown in the upper

[26] As in the rest of analyses included in section 7.3.4, option (1) is used as basis for the sensitivity analysis.
[27] i.e. parameter β in equations 7.3 and 7.6 is 1.

X-axis of Figure 7.42. To ease the comparison primary energy and exergy supply required for a decentralized supply with individual condensing boilers in each house are also shown. The efficiency of the heat distribution network η_{HN} has been assumed as 0.9.

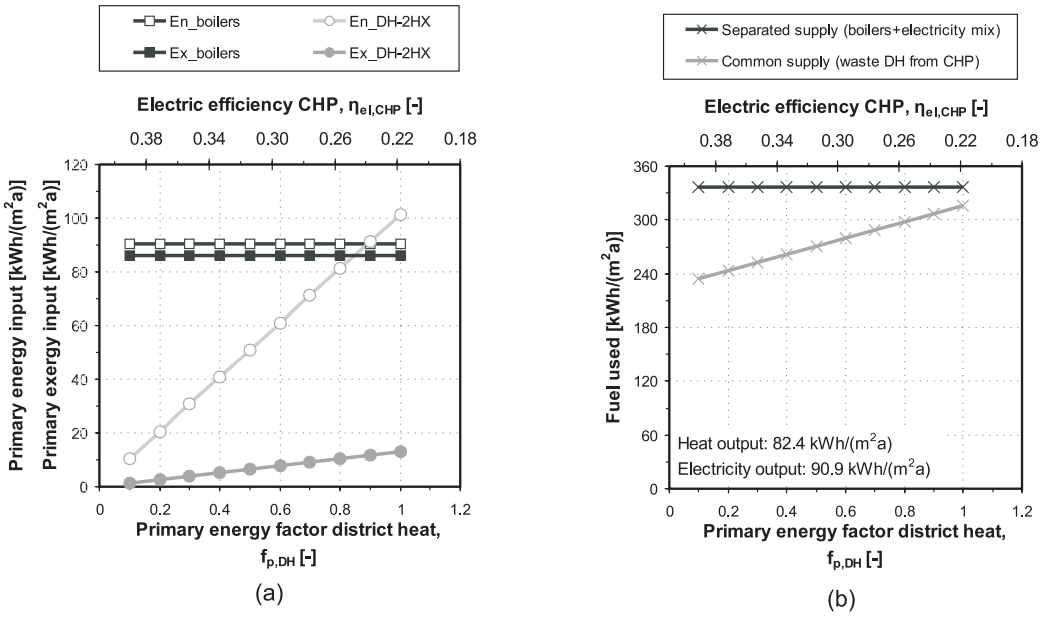

Figure 7.42: (a): Variation of the primary energy input *En_DH-2HX* and primary exergy input *Ex_DH-2HX* for a district heating system with different primary energy factors for district heating. For comparison, the primary energy *En_boilers* and primary exergy input *Ex_boilers* for a supply with individual condensing boilers in each single family house are shown; (b): Fuel used in the waste district heat supply from CHP units with different electric efficiencies (resulting in the different primary energy factors) and in a separated generation of heat via individual condensing boilers and the German electricity mix for electricity generation.

As expected, a strong and linear variation can be observed in the primary energy input for the district heating option *En_DH-2HX* as a function of the primary energy factors. Primary exergy input for the district heating system, obtained simply by multiplying the final exergy input times the primary energy factor, is also strongly influenced by the primary energy factors. However, it is remarkable that in terms of exergy analysis district heating supply from waste heat always shows a better performance than a decentralized supply with condensing boilers: primary exergy supply with waste district heat assuming a primary energy factor of 1 represents only 16% of the total primary exergy input with condensing boilers.

In turn, if primary energy factors are above 0.9[28], i.e CHP unit operates with low electrical efficiency, primary energy input is higher for the district heating option and a conventional supply with condensing boilers performs better. Primary energy factors try to promote high electrical efficiencies in CHP units. Low primary energy factors indicate that the electrical efficiency of the CHP unit is high, resulting in high electricity output able to substitute elec-

[28]This primary energy factor would correspond to a CHP operating at 24% electrical efficiency and 50% thermal efficiency.

tricity produced with the German electricity mix (i.e. the term $En_{el,CHP} \cdot f_{PE,el}$ in equation 7.2 increases). In turn, if the electric efficiency is low (below 26% in Figure 7.42) the substituted electricity is not high enough to compensate for the thermal losses present in the district heating network which would not be present in a dezentralized supply with individual boilers. In consequence, this last supply option seems more advantageous, i.e. shows lower primary energy input as the waste district heat supply.

Figure 7.42 (b) shows the fuel used for the electricity and heat supply assuming a separated supply with individual boilers for heat supply and the German electricity mix for electricity production and a common supply by means of waste district heat from CHP units with different electric efficiencies. Despite higher primary energy input for low electric efficiencies of CHP units, the fuel used for a combined supply is always lower than in the case of separated supply.

From an exergy perspective waste heat from a CHP unit, i.e. available heat at low temperature, always shows a significantly lower supply of exergy of primary energy than a heat supply with dezentralized individual boilers, independently of the electric efficiency of the CHP unit regarded. Thus, waste heat is always more suitable than fossil fuels for providing low exergy demands of SH and DHW supply in buildings. Firing fossil fuels in a CHP unit is always better than burning them in a boiler for producing heat, independently of the electrical efficiency of the CHP units used.

High electrical efficiencies are also desirable from an exergy point of view, since maximizing the high exergy output of a CHP (i.e. electricity) increases the exergy efficiency of the CHP unit [Kühler, 2008][29]. However, waste heat should not be punished for low electrical efficiencies. The performance of CHP units should be evaluated separately in detail with specific parameters and strategies for improving the electrical performance of CHP systems shall be elaborated, similarly as for any other component of the energy supply chain. A detailed discussion on energy and exergy methods for evaluating the performance of CHP units can be found in [Kühler, 2008].

Sensitivity of primary energy factors $f_{PE,DH}$ and quality factors $F_{Q,DH}$

In this section the sensitivity of primary energy factors (equation 7.2) and quality factors for district heat (equation 7.6) to different shares of waste heat in district heating supply and to different electrical efficiencies for the CHP units is presented. In this way, exergy analysis of the waste district heat system analyzed in section 7.3[30] can be extrapolated to district heat systems with different shares of waste heat and be related to different operating conditions of CHP units. This also allows highlighting main conclusions and added value from combined primary energy and exergy analysis for district heating systems.

[29] Additionally, higher electrical efficiency also increases the economic feasibility of these plants since the feed-in fee increases [BMU, 2009].

[30] i.e. with 100% waste heat

Figure 7.43 shows the variation of primary energy factors obtained according to equation 7.2, and of the quality factor for district heat (equation 7.6) as a function of the share of waste heat from co-generation plants in district heat supply. High shares of waste heat do not guarantee primary energy factors lower than those from a conventional supply with boilers (see the line corresponding to an electric efficiency of the CHP of 20%). For a given share of waste heat in district heat supply high electrical efficiencies ($\eta CHP,el$ in Figure 7.43) decrease primary energy factors significantly. Table 7.11 shows the main parameters assumed for this analysis. Under these assumptions, high electrical efficiency for the CHP unit (e.g. 45%) and high shares of waste heat (i.e. 90 to 100%) lead to negative primary energy factors.

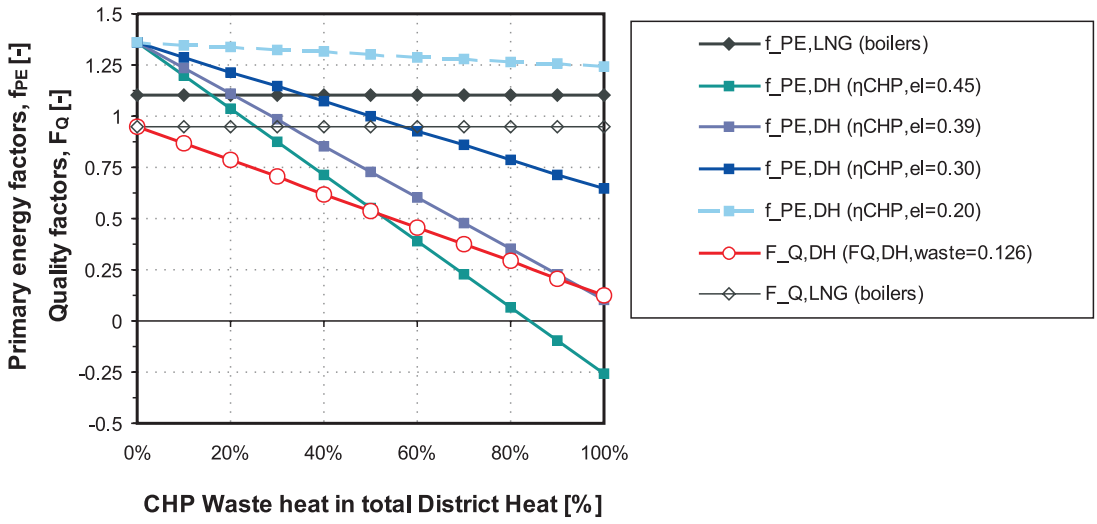

Figure 7.43: Variation of the primary energy factors *f_PE,DH* and quality factors for district heat *F_Q,DH* for a district heating system with different shares of waste heat in district heating supply and different electric efficiencies of CHP units. For comparison, the primary energy factor for a supply with individual condensing boilers in each single family house is also shown *f_PE,boilers*.

In turn, the quality factor proposed here for the evaluation of district heat $F_{Q,DH}$ (represented by the grey line with white dots in Figure 7.43) is independent from the electrical efficiency of the CHP units considered. This factor strongly decreases with higher shares of waste heat in district heat supply, i.e. as more energy is being supplied at low quality (i.e. low exergy) levels. It is also remarkable that as long as some share of waste heat is present in district heat supply, the quality factor proposed is always lower than that of a supply with condensing boilers (*F_Q,LNG (boilers)* in Figure 7.43). This indicates that direct use of high quality fuels in a combustion process for heat supply is always significantly less efficient from an exergy perspective than fueling them in CHP units. In other words, combustion processes for heat supply in buildings shall be substituted by waste heat.

Figures 7.44 (a) and (b) show the specific primary energy input and its associated exergy for different electrical efficiencies of the CHP unit and different shares of waste heat from the CHP in district heat supply. To ease the comparison primary energy input of a decentral-

Table 7.11: Main parameters assumed for calculating primary energy factors in Figure 7.43.

$f_{PE,fuel}$ [−]	$f_{PE,el}$ [−]	$\eta_{CHP,th}$ [−]	η_{HPl} [−]	η_{HN} [−]
1.1	2.7	0.5	0.9	0.9

ized supply with condensing boilers is also included in both diagrams. To avoid misleading results, and according to [DIN 18599-1, 2007], negative values of the primary energy factors have been set to zero.

Figure 7.44 (c) shows the fuel necessary for providing the same heat and electricity demands with a separated supply by means of condensing boilers and the German electricity mix and that required in a combined supply with different shares of CHP units, boilers and electricity mix. Heat and electricity demands assumed in all cases correspond to those provided with 100% district heat from CHP plants running with electrical and thermal efficiencies of 45% and 50% respectively[31]. It is shown that neither primary energy factors as defined in the standard [DIN 18599, 2007] nor quality factors proposed here give an indicator of the fuel used in common supply as compared to conventional separated supply.

Similarly as primary energy factors, primary energy input is very sensitive to the electrical energy efficiency of the CHP unit. The minimum share of waste heat from CHP units in the district heat supply necessary to make this system more favorable than a decentralized supply with condensing boilers varies greatly with the electrical efficiency of the CHP unit considered: with an electrical efficiency of 45% a share of around 25% in the district heating supply would be sufficient; with an electrical efficiency of 39% a share of 30% in the district heating supply would be enough; with an electrical efficiency of 30% a share of 50% would be required; with an electrical efficiency of 20% the decentralized supply with boilers would always be better.

From an exergy perspective, the minimum shares of district heat required to make district heat more favourable than decentralized supply with boilers are significantly lower. A 30% share of waste heat would be enough even for an electrical efficiency of the CHP units of 20%. This is due to the steep decrease of the quality of supplied energy as long as some share of waste heat (low temperature heat) is used to substitute direct combustion processes for heat supply in buildings.

The combined primary energy and exergy analysis shown in Figure 7.44 (b) allows highlighting the importance of increasing the use of waste heat for heat supply in buildings besides the importance of increasing the electrical efficiency of CHP units. However, as stated in the previous section, the electrical efficiency of CHP plants shall also be evaluated separately and efforts to improve it shall be conducted, similarly as it is done for any other energy supply system.

[31]The thermal and electrical demands provided in all cases amount 82.4 kWh/m^{2}a and 90.9 kWh/m^{2}a respectively, as shown in Figure 7.44.

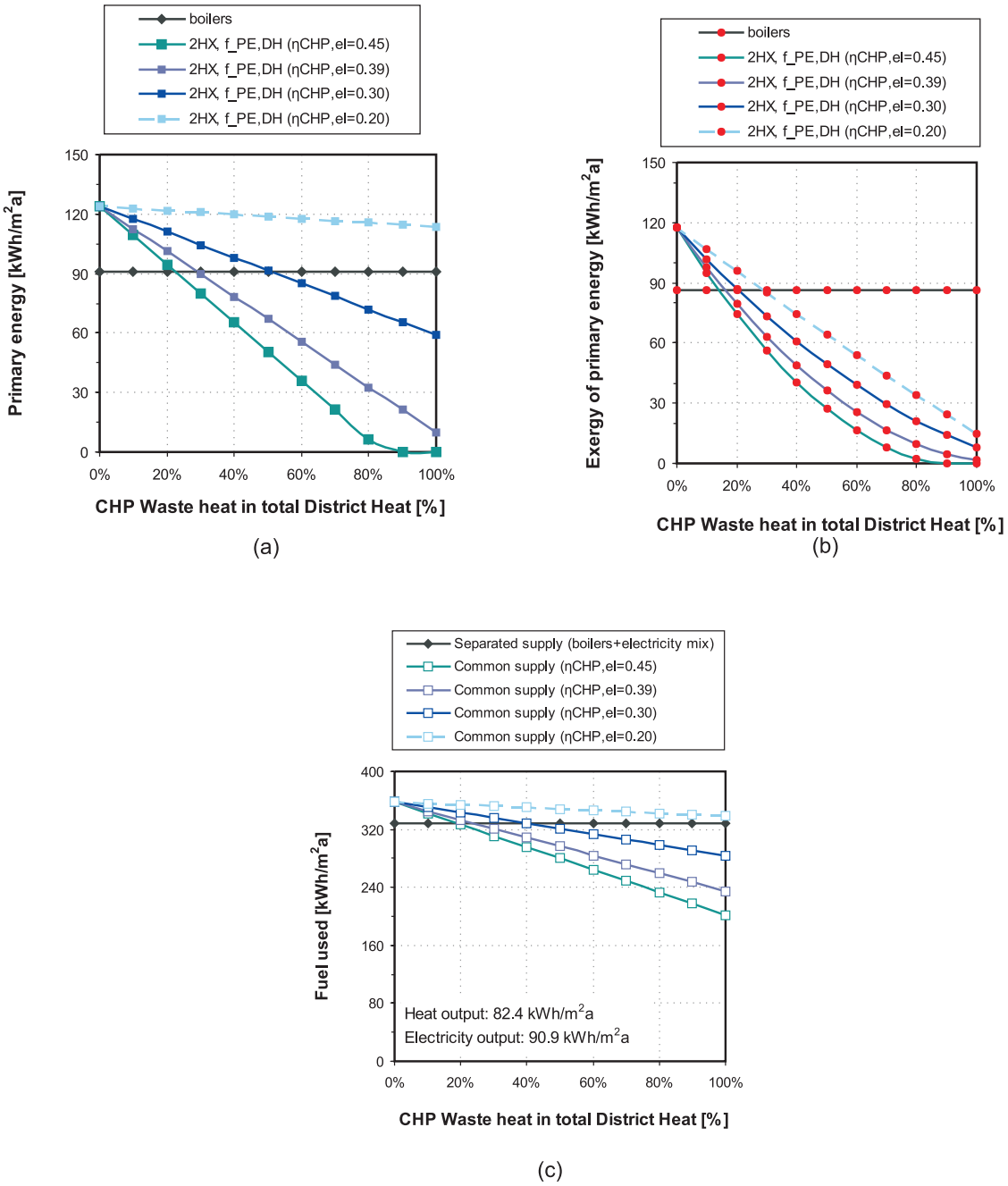

Figure 7.44: (a): Primary energy input for a district heating system as a function of the share of waste heat in district heat supply (in percentage) and of the electric efficiency assumed for CHP units providing waste heat in the network; (b): Exergy of primary energy input for district heat systems as a function of the share of waste heat in district heating supply (in percentage) and of the electric efficiency assumed for CHP units providing waste heat in the network. For comparison, primary energy and exergy supply required with individual condensing boilers in each single family house is shown in both diagrams; (c): Fuel used in a separated supply of electricity and heat demands with boilers and the electricity mix, and that of a combined supply with CHP units, boilers and electricity mix.

Temperature dependence of primary energy factors $f_{PE,DH}$ and quality factors $f_{Q,DH}$

The exergy-based parameter proposed here is not dependent on the electrical efficiency of the CHP units (see Figure 7.43). In turn, it depends on the temperature level of the district waste heat supplied (see equation 7.6). In Figure 7.45 (a) the variation of the proposed quality factor for different shares of waste heat in district heat supply is shown for three different sets of supply and return temperatures. Supply and return temperatures assumed in each case are given in Table 7.12.

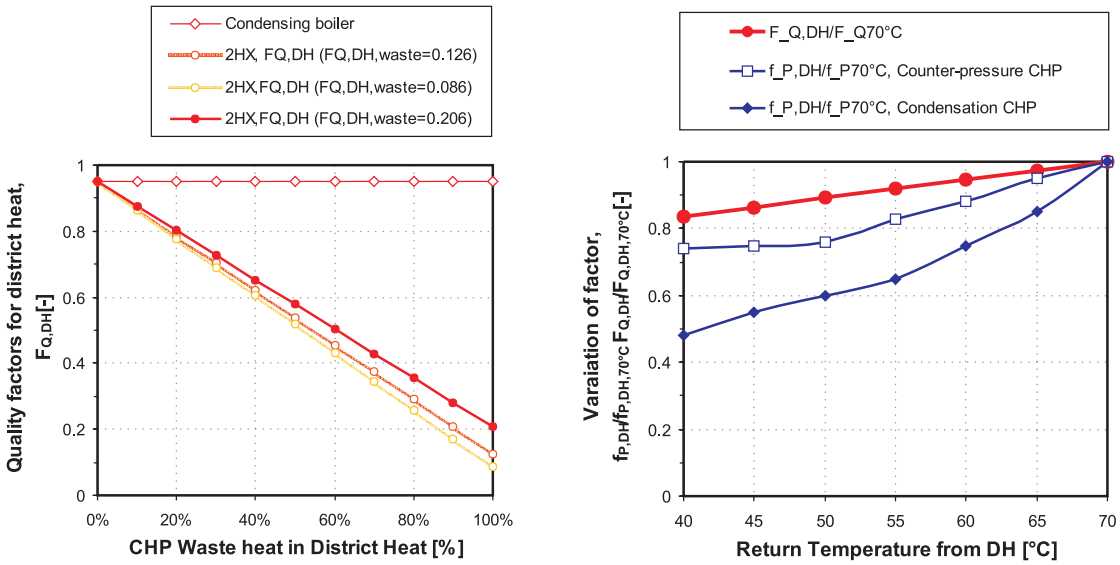

Figure 7.45: (a): Quality factors for three different sets of inlet and return temperatures in the primary side of district heat supply and for different shares of waste heat; (b): Variation of primary energy factors and quality factors for waste district heat as a function of the return temperature to the CHP plant. The variation of the primary energy factors is shown for two different types of CHP units, condensation and counter-pressure. Data for the curves showing the variation of primary energy factors is taken from [Wirths, 2008a].

Table 7.12: Inlet and return temperatures associated with the quality factors for district heat shown in Figure 7.45. Reference temperatures for exergy analysis θ_0 and resulting quality factors for the waste heat share $F_{Q,DH,waste}$ are shown.

Case	θ_0 [°C]	$\theta_{in,DH}$ [°C]	$\theta_{ret,DH}$ [°C]	$F_{Q,DH,waste}$ [–]
2HX, FQ,DH (FQ,DH,waste=0.206)	4.8	95	60	0.206
2HX, FQ,DH (FQ,DH,waste=0.126)	4.8	58	32	0.126
2HX, FQ,DH (FQ,DH,waste=0.086)	4.8	40	22	0.806

Primary energy factors do not depend directly on the temperature level at which district heat is provided (see equation 7.2). However, it is known that lower return temperatures on the district heat network allow achieving higher CHP coefficients[32] for the CHP units, thereby increasing the energy efficiency of such systems [Wirths, 2008]. Detailed assessments of the CHP operation at different return temperatures show that the amount of fuel used and the electricity and heat production of the plant are significantly and positively influenced by lower return temperatures from the district heat network. In consequence, a reduction in the primary energy factors associated with the operation of the plant can be found [Wirhts, 2008a]. Figure 7.45 (b) shows the variation of primary energy factors and the quality factor of waste heat from CHP plants for different return temperatures on the district heat network. A supply temperature of 95°C has been assumed in all cases. Data for the variation of primary energy factors have been taken from [Wirths, 2008a]. Despite the steeper decrease of primary energy factors, similar trends can be found for both parameters: lower return temperatures decrease the primary energy supplied as well as its quality.

However, such a detailed assessment of the power plant process is not possible for building planners and needs to be carried out by engineers from the power plant industry or local utility. In turn, quality factors can be easily and directly calculated by building engineers and planners as a function of the expected supply and return temperatures available and achievable in the district heat network for providing a certain building quarter.

Supplying district waste heat at lower temperature levels decreases primary energy and exergy inputs, thereby increasing the exergy efficiency of the heat supply. If all district heat is waste heat (100% share of waste heat) exergy efficiency of the energy supply can be greatly increased by reducing the temperature level of the energy supplied (from 0.27 to 0.63 for inlet/return temperatures of 95/60°C or 45/22°C, respectively).

The exergy based parameter can be directly calculated by building decision makers and helps them to identify the system design with better performance. In district energy systems for communities or neighbourhoods where waste heat from different processes at different temperature levels is available this parameter can help to pinpoint the most efficient supply option by promoting cascading and multiple use of thermal energy flows.

7.3.5 Improved building envelope

In this section the influence of improving the building envelope of the single family houses, i.e. reducing space heating demands, on the performance of the district heat supply is studied. For this aim, the insulation level of the base case (corresponding to a newly erected house complying with the standard EnEV 2009) has been increased to the level of a *KfW-Effizienzhaus 40* (KfW-EffH.40). The main details of both building envelopes can be found in Table 4.4. Additionally, a further building case with a space heating demand corresponding to a passive house is investigated (named *PassiveH* in the following). For this purpose, the KfW-EffH.40

[32] so-called *Stromkennzahlen* in German

building envelope and a balanced ventilation system with heat recovery are considered.

The air exchange rate due to infiltration in the *PassiveH* building case has been set to 0.06 h^{-1}. In turn, air changes per hour due to the ventilation unit are considered as 0.54 h^{-1}. A thermal effectiveness for the heat recovery unit of 85% is considered. For the three building standards supply option (1), i.e. with two separate heat exchangers for SH and DHW supply and the temperature profile for the DH pipe shown in Figure 4.7 (with temperatures between 50-65°C) are assumed.

Figure 7.46 shows final energy demands for the three building standards analyzed. The electricity required to power the fans in the ventilation unit has been estimated as 3.04 kWh/m^2a, corresponding to 116.6 W_{el}/kWh_{th}.

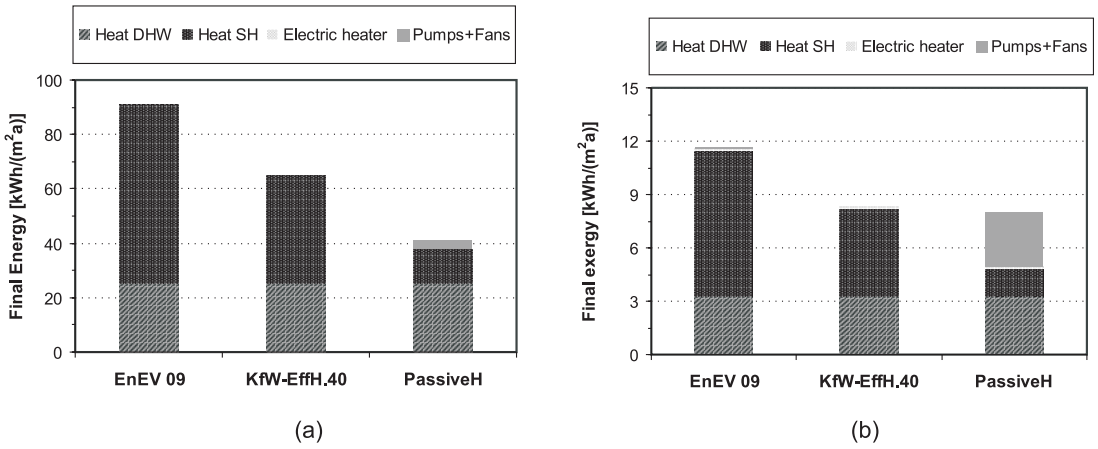

Figure 7.46: Final energy (a) and exergy (b) supplied in the three different options considered.

The great reduction in the space heating energy demand is evident and very beneficial in terms of energy supply, see Figure 7.46 (a). With the balanced ventilation unit, a reduction of 37% in the final energy input can be achieved as compared to the low energy house (KfW-EffH.40). However, final exergy input is only 4% lower than in the case of the KfW-EffH.40. The electricity demand required by the ventilation unit represents 38% of the total final exergy input. The reduction in the space heating demand is accomplished by means of a great high exergy input in the form of electricity for operating ventilation fans, i.e. electricity, which is a high exergy input, is being indirectly used for space heating purposes. As a result, in terms of final exergy, a passive house does not perform better than a KfW-EffH.40 if low temperature waste heat is available to supply the space heating demand.

Even in terms of primary energy the passive house is the best choice. The reduction in the thermal energy demand achieved by the ventilation unit is greater than the primary energy input of the electricity required as auxiliary energy for the fans of the ventilation unit (see Figure 7.47 (a)). However the passive house has the highest primary exergy input of the three cases investigated, as shown in Figure 7.47 (b). Any of the other two options, *EnEV 09* or

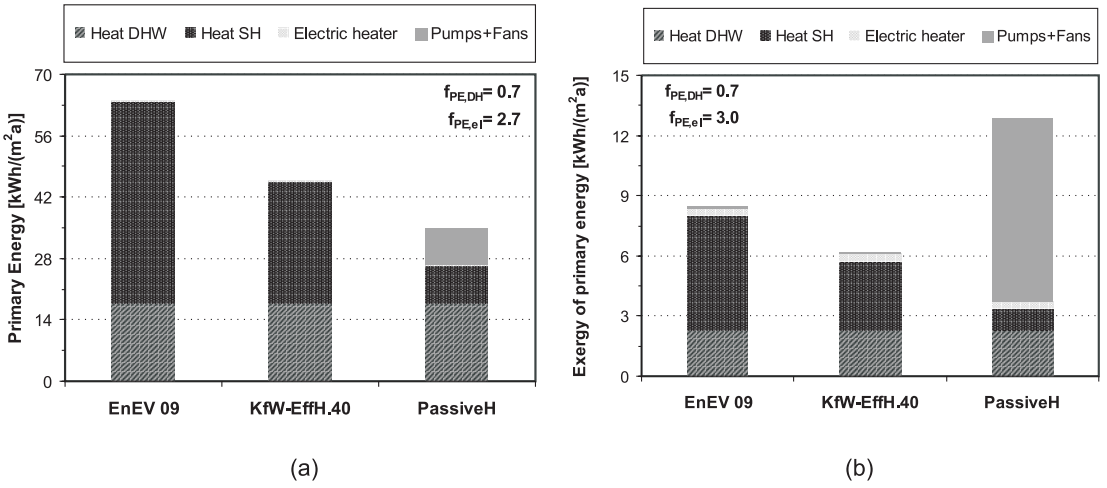

Figure 7.47: Primary energy (a) and exergy (b) supplied in the three different options considered. Primary energy factors assumed for district heat $f_{PE,DH}$ and electricity $f_{PE,el}$ are shown in the diagrams.

KfW-EffH.40, would allow making a more (exergy) efficient use of the available energy.

Low temperature waste heat available can be used for supplying space heating and DHW demands with great exergy efficiency saving the electricity for other high exergy applications.

This shows clearly that, if energy sources at low exergy levels are available, the reduction in the building´s energy demand is advantageous but not its minimization. Minimizing the space heating energy demand via a balanced ventilation unit with high efficiency heat recovery greatly increases the electricity demand, being not a suitable concept for an exergy efficient energy supply. As long as low exergy sources, i.e. low temperature heat is available, its use for heat supply in buildings shall be maximized avoiding the use of any other building equipment or technologies which require high exergy sources for their operation. Therefore, efforts for an efficient space heating and DHW supply in buildings should be conducted in two directions:

1. Improved building design, so that energy demands for space heating and DHW are reduced without any additional active system (e.g. ventilation unit)

2. Maximize the use of low temperature energy sources available

7.3.6 Accurateness of steady-state assessment

In the previous sections results from dynamic energy and exergy analysis were presented. Only in section 5.2.4.1 (chapter 5) results from steady state analysis of district heat supply are shown. Due to the sensitiveness of exergy flows for temperature ranges close to the reference environment it is expected that some degree of mismatching between steady state and dynamic analysis arises.

In the present section the accurateness of simplified steady state assessment for district heat supply of SH and DHW demands is closely investigated. Furthermore, the accurateness of steady state results presented in Figure 7.48[33] is also studied.

Figure 7.48 intends to depict the exergy performance of a district heating system under different operating conditions. It is helpful to get a first impression about possible improvements for appropriately designing the district heating system at the beginning of the design process. Thus, at this stage limited amount of data about the operation of the systems is available. It needs to be obtained with easily available data.

Exergy efficiencies represented by the different lines in Figure 7.48 are obtained applying equation 7.7. The expression for the steady state exergy demand is shown in equation 7.8. A first estimation of the average space heating $\langle Q_{dem,SH} \rangle$ and DHW $\langle Q_{dem,DHW} \rangle$ loads is necessary. Here, average values of the space heating and DHW loads are calculated from dynamic analysis. They have values of 76.43 kW and 9.54 kW, respectively. The total load for both demands amounts thus, 85.97 kW. In addition, absolute values of indoor comfort temperature T_r, required supply temperature for DHW $T_{sup,DHW}$ and cold net water temperature $T_{cw,DHW}$ are required. Here, 20°C are assumed as indoor comfort temperature, DHW supply temperature is considered as 50°C and cold network water temperature is assumed as 10°C.

$$\Psi_{stead} = \frac{Ex_{dem,SH+DHW,stead}}{Ex_{sup,SH+DHW,stead}} \tag{7.7}$$

$$\begin{aligned} Ex_{dem,SH+DHW,stead} = \langle Q_{dem,SH} \rangle \cdot \left(1 - \frac{T_0}{T_r}\right) + \frac{\langle Q_{dem,DHW} \rangle}{T_{supp,DHW} - T_{cw,DHW}} \\ \cdot \left[(T_{sup,DHW} - T_{cw,DHW}) - T_0 \cdot ln \left(\frac{T_{sup,DHW}}{T_{cw,DHW}} \right) \right] \end{aligned} \tag{7.8}$$

Exergy demands are calculated following equation 7.8. Equation 7.9 shows the expression for exergy supply, where $f_{ls,SH+DHW}$ represents the fraction of the energy demand corresponding to thermal losses in pipes and DHW storage tanks. Here, it is assumed to have a value of 0.16[34].

Varying supply and return temperatures the exergy supply at different mass flows, i.e. at different operating conditions, can be obtained. Following, the variation of the exergy efficiency for a given set of operating conditions is obtained, as shown by the grey lines in Figures 7.48 (a) and (b). In Figure 7.48 (a) mean outdoor air temperature during the heating period, i.e. 4.8°C, is assumed as reference. In Figure 7.48 (b) mean annual outdoor air temperature, i.e. 9.6°C, is taken as reference.

[33] Figure 7.48 (a) is the same as Figure 5.9 shown in chapter 5 and used to derive strategies for improved exergy performance of the district heat supply system.

[34] This value has been taken from the percentage of losses in case (1), which amount 13% for pipe losses and 3% from thermal energy losses in DHW tanks.

$$Ex_{sup,SH+DHW,stead} = \frac{\langle Q_{dem,SH+DHW} \rangle \cdot (1 + f_{ls,SH+DHW})}{T_{in,prim} - T_{ret,prim}} \cdot \left[(T_{in,prim} - T_{ret,prim}) - T_0 \cdot ln \left(\frac{T_{in,prim}}{T_{ret,prim}} \right) \right] \tag{7.9}$$

To check the accurateness of results from such a simplified steady state exergy analysis, final exergy efficiencies from dynamic analyses of the system are also shown in the diagram (equation 6.9). Values of the exergy efficiency obtained from dynamic analysis are represented by the grey (option (0), with one heat exchanger) and black (option (1), with two heat exchangers) dark filled squares. Average operating conditions from dynamic analysis for options (0) and (1) are shown in the grey and black rectangles above the diagrams. Values from steady state exergy efficiency for mean operating conditions of the systems are represented as white filled grey and black squares in the diagrams. Following, the difference between the white and dark filled squares shows the mismatching between steady state and dynamic assessment of the seasonal exergy efficiency for both options (0) and (1) respectively.

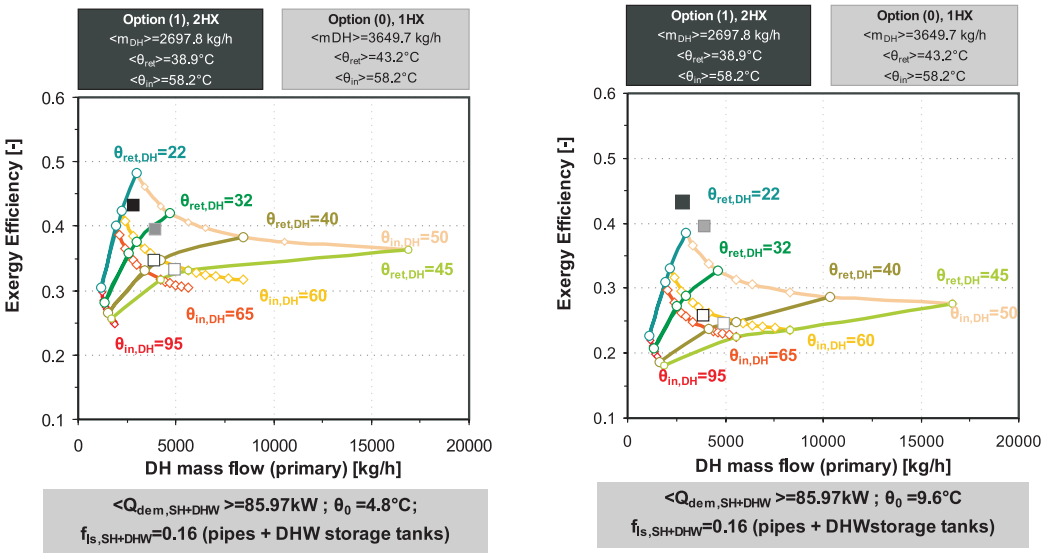

Figure 7.48: Lines represent steady state exergy efficiencies for different sets of average operating conditions (inlet, outlet temperatures and mass flows) for DHW and SH supply. Mean energy loads, fraction of thermal losses and reference temperatures assumed for steady state calculation are shown on the grey boxes below the diagrams. Dark filled squares represents seasonal exergy efficiency from dynamic analysis for the supply option with two heat exchangers and one heat exchanger respectively, i.e. options (1) and (0). Average operating conditions from dynamic analysis for each option are shown in the grey and black rectangles at the top of the diagrams. White filled squares represent steady state exergy efficiencies for the conditions shown in the rectangles. (a): average outdoor air temperature over the heating period is assumed as reference temperature; (b):average annual outdoor air temperature is assumed as reference temperature.

If mean outdoor air temperature during the heating period is taken as reference for steady state exergy analysis, i.e. Figure 7.48 (a), mismatching between dynamic seasonal exergy efficiency and values from steady state assessment amounts 19.9% for option (1) and 15.7% for option (0).

If, in turn, annual mean outdoor air temperature is taken as reference (Figure 7.48 (b)), mismatching increases to 40.3% and 37.6% for options (1) and (0), respectively. Since space heating is the biggest energy and exergy load, average outdoor air temperature during the heating period is a more representative value for a constant reference temperature for steady state analysis of thoses loads.

In any case, a similar trend can be found between dynamic exergy efficiencies for different operating conditions (black and grey filled squares) and steady state exergy efficiencies in Figures 7.48 (a) and (b). Thus, it can be concluded that such a simplified steady state analysis is suitable for showing the trend in the performance for different operating conditions of district heating systems for space heating and DHW supply. It can be very helpful in the first design steps of a district heating supply system. Absolute values for the exergy performance, however, are not shown accurately by such a simplified analysis.

7.3.6.1 Steady state assessment exergy demand, supply and performance

As stated in chapter 6, the final exergy efficiency of a system characterizes the seasonal exergy performance over the investigated period. In this section the accurateness of steady state estimations of this parameter, as well of the seasonal exergy demand and supply is investigated over a time frame of one year.

Steady state annual exergy supply and demand are estimated using annual energy demands and design inlet and return temperatures, as shown in Table 7.13.

Table 7.13: Main parameters assumed for steady state assessment of the exergy demand and supply.

	Units	(1) 2HX SH	(1) 2HX DHW	(0) 1HX SH+DHW
Energy demand	[kWh/(m^{2}a)]	62.5	13	75.5
$\theta_{in,prim}$	[°C]	50	50	50
$\theta_{ret,prim}$	[°C]	27	46	46
$\dot{m}_{prim}$	[kg/h]	6296	14000	14000

Results from steady state and dynamic exergy performance of the systems with one and two heat exchangers for district heat supply are shown in Figures 7.49 and 7.50, assuming reference temperatures for steady state exergy analysis corresponding to the average outdoor air temperature during the heating season (Figure 7.49) and annual average outdoor air temperature (Figure 7.50), respectively.

Disagreement between values for exergy supply and demand from steady state and dynamic assessment is higher than for the exergy efficiency of the systems (i.e. their seasonal performance). Greatest mismatching arises for the exergy demand amounting to 22% and

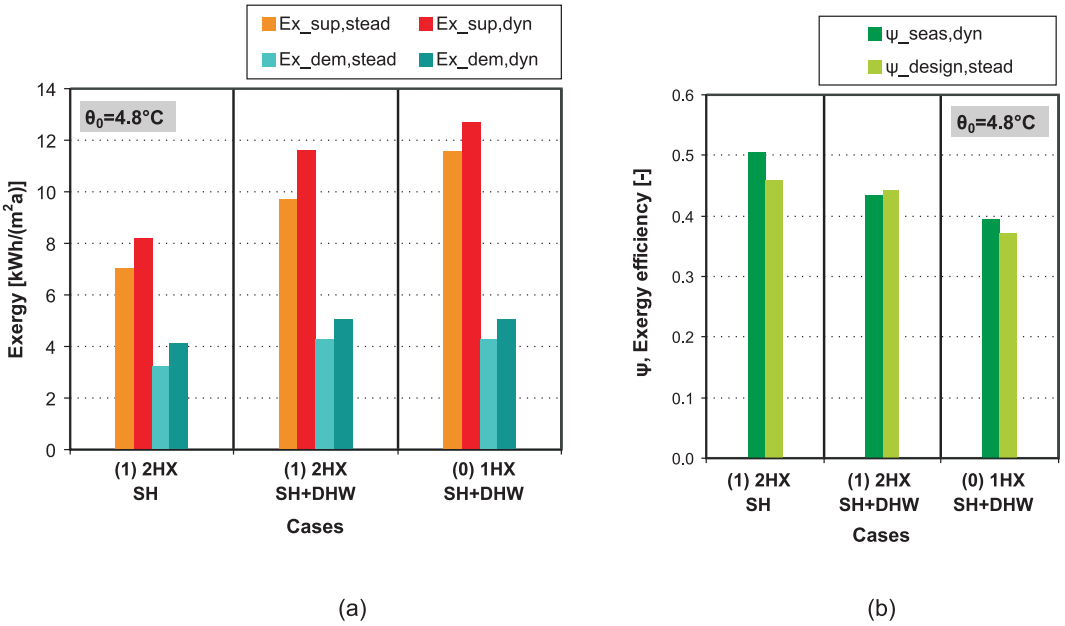

Figure 7.49: (a): Exergy demand and supplied resulting from dynamic exergy analysis and steady state analysis for case (1), labelled *(1) 2HX SH+DHW*, case (0), labelled *(0) 1HX SH+DHW*, and space heating supply for case (1), labelled *(1) 2HX SH*; (b): seasonal exergy efficiencies obtained from dynamic and steady state exergy analysis for the systems shown. For steady state assessment a constant reference temperature of 4.8°C corresponding to mean outdoor air temperature during the heating period is assumed.

46%, depending on whether the reference temperature for steady state assessment is taken as average value during the heating season or annual average. Thus, steady state exergy analysis does not allow an accurate estimation of the exergy demanded or supplied.

If the annual average outdoor air temperature is taken as reference for exergy analysis, greater mismatching between dynamic and steady state assessment can be found. This highlights the importance of choosing an appropriate reference temperature for steady state exergy assessment. For SH and DHW demands mean outdoor air temperature over the heating period can be regarded as a suitable reference temperature. This is coherent with results from previous research work [Torío and Schurig, 2009; Schmidt and Torío, 2009].

Despite mismatching in the absolute values of exergy supply, demand and efficiency, a similar trend can be found for results from dynamic and steady state exergy analysis. Therefore, steady state exergy analysis as performed here is a ressonable quick assessment method which might be used for first estimations and comparison of different options for district heat supply systems.

7.4 Comparison of district heat and solar thermal supply

In this section the exergy performance of the solar thermal and district heat supply systems studied above is compared. Their exergy performance can be compared since the same

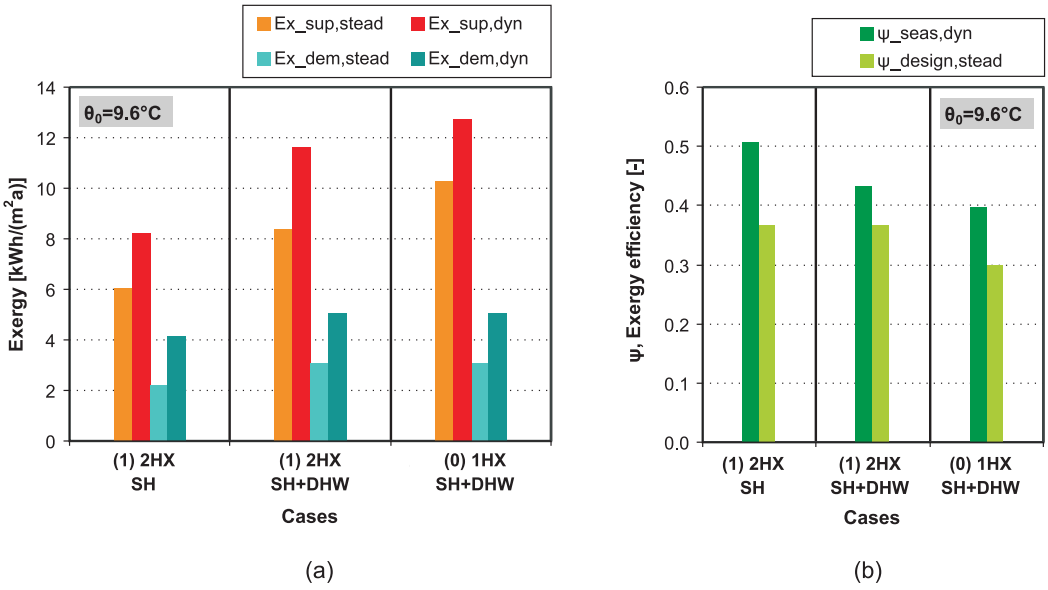

Figure 7.50: (a): Exergy demand and supplied resulting from dynamic exergy analysis and steady state analysis for case (1), labelled *(1) 2HX SH+DHW*, case (0), labelled *(0) 1HX SH+DHW* and space heating supply for case (1) *(1) 2HX SH*; (b): seasonal exergy efficiencies obtained from dynamic and steady state exergy analysis for the systems shown. For steady state assessment a constant reference temperature of 9.6°C corresponding to mean annual outdoor air temperature is assumed.

weather data has been used in both cases. Values of the exergy expenditure figures and exergy efficiencies are related to the energy and exergy demands of the systems, and thereby can be directly compared with each other.

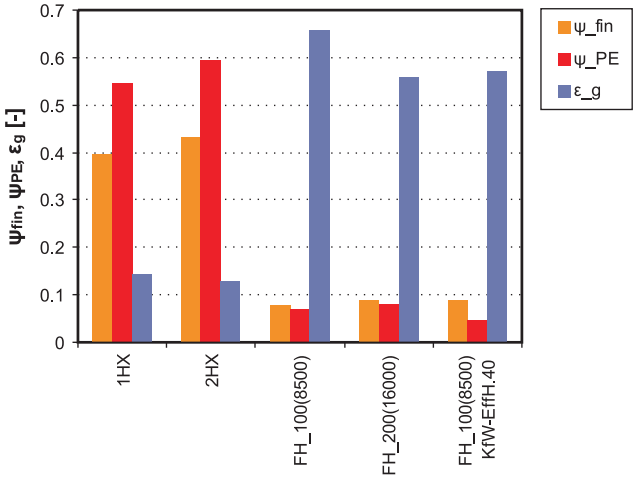

Figure 7.51: Exergy efficiencies and expenditure figures for selected cases of district heat and solar thermal supply.

Exergy expenditure figures are significantly higher for the solar thermal systems, as shown in Figure 7.51, indicating that a greater share of high-quality fuels is being used for the supply.

Following, exergy efficiencies for waste heat based district heat supply are always remarkably higher (around 6 times greater) than those achieved with solar thermal supply. Even in the case of high fractional energy savings ($f_{sav,ext}$=62% are achieved in the *FH_100(8500) KfW-EffH.40* case), exergy efficiencies are lower than 10%.

This highlights once more that the exergy performance of a system is strongly influenced by the high-quality inputs present in the supply. An exergy efficient supply can only happen if low temperature heat flows are directly used for covering thermal energy demands in buildings. Waste heat shows, thereby, a great potential for a more exergy efficient supply of those thermal demands in buildings.

Chapter 8

Conclusions and Outlook

8.1 Method for exergy analysis

An extensive literature review carried out as part of this thesis, shows that no scientific agreement can be found on a common method for performing exergy analysis of building energy systems. As part of this work, a method applicable for dynamic exergy analysis of sensible heating and cooling systems is derived and presented.

Different options for the reference environment for exergy analysis are introduced and their thermodynamic correctness and plausibility is discussed. Outdoor air surrounding the building is the only option totally complying with the thermodynamic definition of the reference environment and is, thus, proposed here as reference for exergy analysis. Dynamic exergy analysis can be performed using weather data for the given building location as reference.

In this thesis exergy analysis of different sensible heating systems is performed. For this purpose, an assessment of the thermal component of exergy suffices, i.e. temperature is the relevant property for defining the state of both the system and its reference environment. Pressure differences between indoor and outdoor air are irrelevant in the cases investigated, although might be relevant for exergy analysis of buildings with mechanical ventilation units. In turn, for latent cooling systems with humidity treatment chemical exergy flows need to be also regarded. Additionally, for exergy analysis on a building system level, the detailed and correct assessment of thermal radiant exergy is irrelevant, for it merely leads to a shift in the exergy losses within the different components of the energy supply chain, but does not influence the general performance of the building system. The exergy of thermal radiation can thus be estimated, instead, in a simplified way as a conductive-convective process.

Exergy analysis of direct solar systems is a controversial issue. To avoid physical inconsistencies found in the framework commonly applied for this purpose in the literature, a new boundary for the analysis of these systems has been developed and is applied in this thesis. The physical correctness and suitability of this approach has also been thoroughly discussed.

Steady-state exergy analysis of building systems can be performed for first estimations on the performance of the systems. For SH and DHW supply systems average outdoor air temperatures during the heating season shall be used as reference temperature. Results from steady-state exergy analysis of different building systems show a similar trend than those from detailed dynamic assessment. However, great mismatching in the absolute values with both methods can be found, making steady-state assessment unappropriate for an accurate evaluation and comparison of the systems.

The method presented here for dynamic exergy analysis is based on a quasi-steady state approach, i.e. storage phenomena are regarded dynamically in terms of energy but are not regarded separately in detail in exergy terms. Only for storage systems dynamic equations have been derived and applied. This is a reasonable simplification if exergy analysis is oriented to a system level, i.e. to compare the seasonal performance of different building systems. If the purpose is, instead, the optimization of the building construction or a particular component within the building system, storage phenomena need to be regarded in detail.

Finally, it is important to remark that exergy analysis gives insight on the thermodynamic performance of an energy system but does not give any information on its environmental performance or sustainability. Thus exergy analysis is proposed here as a complementary indicator to primary energy assessment and not as a substitute for it.

8.2 Applicability of exergy analysis

The exergy method is a scientifically correct approach for analyzing building energy systems, which allows evaluating all energy sources, renewable and fossil, on a common scientific basis. However, exergy analysis is strongly dominated by the high-quality fossil fuel input, similarly as conventional primary energy analysis. Thus, for energy systems with a great share of high quality energy sources in their supply, such as the solar systems analyzed here, conclusions from exergy analysis are always very similarly to those which can be gained from conventional energy analysis. These results can also be extrapolated to other energy systems with the same characteristics, such as heat pumps.

In turn, for energy systems with great shares of low exergy flows in their supply, exergy analysis provides further insight than mere primary energy assessment. This is the case of waste heat based district heating systems.

Exergy analysis is less sensitive to thermal energy losses in the distribution network than conventional energy analysis. Even if thermal energy losses would be several times greater than those found in conventionally sized and operated networks, exergy analysis would still favour waste district heat supply against other energy efficient supply systems implying great shares of high quality energy sources, e.g. condensing boilers. This is of particular importance

for evaluating low temperature district heat supply of an area with low energy demand density and shows the necessity of moving away from direct burning processes for supplying thermal energy demands in buildings. A supply by means of waste heat is several times more exergy efficient than a supply even with boilers and solar-combi systems with relatively high solar fractions (of 30-60%).

In turn, exergy analysis is more sensitive than energy analysis to high quality energy inputs present, i.e. pumping energy for operating the district heat network. To increase the thermodynamic performance of such systems, their pumping energy should be minimized, even at the expense of increasing distribution thermal energy losses. Exergy analysis might help, thus, to reconsider conventional sizing criteria for the distribution networks.

If low temperature waste heat is available, its use for supplying thermal energy demands in buildings should be maximized, avoiding the use of other (efficient) energy systems requiring high quality inputs for this purpose (such as balanced ventilation units with heat recovery).

A relatively simple parameter for characterizing the exergy performance of district heating systems with different shares of waste heat has been developed. It is shown that different boundaries are applicable for (conventional) primary energy and exergy analysis of waste district heating systems, excluding on the second the detailed analysis and performance of waste heat production units (e.g. CHPs). The boundary for exergy analysis only includes the heat plants present for the district heat shares which are not waste heat. Complex processes within CHP units in the district heat network are, thus, excluded from the exergy balance. Exergy analysis is, herewith, mainly focused on the building supply systems.

Primary energy factors for district heat are strongly influenced by the electric efficiency of CHP plants present in the network: higher electric efficiencies strongly reduce their value, leading to an improved energy performance of the system. In consequence, a separate supply with conventional systems such as boilers and the German electricity mix might look preferable as compared to a 100% waste heat supply from CHP units with low electric efficiencies.

The exergy based parameter proposed here is, in turn, not dependent on the electric efficiency of CHP units. Instead, it is greatly influenced by the share of waste heat and the temperature level of district heat supply: greater shares of waste heat drastically increase the exergy performance of district heat systems. Lower shares of waste heat than those pinpointed by primary energy analysis already make district heat systems more exergy efficient than a separate supply by conventional systems such as boilers and the German electricity mix. A 100% waste heat supply, even from CHP plants with low electric efficiencies, is always more exergy efficient than a separated supply with boilers and the electricity mix.

A combined primary energy and exergy analysis allows highlighting the importance of increasing the use of waste heat for heat supply in buildings, besides that of increasing the electrical efficiency of CHP units.

Additionally, lower return temperatures to the district heat network also increase significantly the exergy performance of the system. Results from detailed dynamic assessment of the investigated systems confirm this trend. Lower return temperatures increase the electric efficiency of CHP units in the district heat network, thereby increasing the efficiency of high quality fuels used.

Primary energy factors are only sensitive to return temperatures in the network if a detailed assessment of the complex processes within CHP plants in the network is performed. However, such a detailed assessment of the power plants is not possible for building planners and needs to be carried out by engineers from the power plant industry or local utility. In turn, the exergy based factor helps building planners and decision makers to identify the building system design leading to a greater overall performance without requiring a detailed assessment of the heat plants or CHP units in the district heat network.

Furthermore, the exergy-based factor can be applied to any type of waste heat, e.g. from

industrial processes, and is not limited to waste heat from CHP plants. In district energy systems for communities or neighbourhoods where waste heat from different processes at different temperature levels is available this parameter can help to pinpoint the most efficient supply option by promoting cascaded and multiple use of thermal energy flows.

8.3 Outlook

Exergy analysis seems to be a promising tool for the improvement and optimization of district heat supply systems. In the cases studied in this thesis only SH and DHW demands are regarded, greatly limiting possibilities for investigating a cascaded use of thermal energy flows and demands at different temperature levels. Future research applying this method to district heat and cold supply systems including different users (e.g. industries, office buildings, hospitals, etc.) and suppliers (e.g. CHP plants, industrial processes) is required to show the potential and importance of exergy assessment for distributed heat supply systems.

Due also to the constrain mentioned above, the only possibility of reducing return temperatures to the district heat network in the investigated systems was a separated supply of SH and DHW demands. It has been shown that this option is economically not viable with current financing schemes. Other cost structures, e.g. lower prices for district heat supply if lower return temperatures are achieved, could help financing additional costs required for such an exergy improved supply, improving thereby its economic aspects.

Bibliography

[AGFW, 2009] . *AGFW-Merkblatt FW526. Thermal reduction of legionella growth - implementation of DVGW working sheet W 551 in district heat supply*. Arbeitsgemeinschaft für Fernwärme, AGFW (2009).

[Alpuche et al., 2005] Alpuche M.G. et al.: *Exergy analysis of air cooling systems in buildings in hot humid climates*. Applied Thermal Engineering 25 (4) (2005), pp.507-517.

[Annex 37, 2003] *IEA ECBCS Annex 37: Low Exergy Systems for Heating and Cooling*. www.lowex.net

[Annex 49, 2010] *IEA ECBCS Annex 49: Low Exergy Systems for High-Performance Buildings and Communities*. www.annex49.com.

[Annex 49, 2010a] *Annex 49 pre-design Tool v.11*. www.annex49.com.

[Angelotti and Caputo, 2007] Angelotti A., Caputo P.: *The exergy approach for the evaluation of heating and cooling technologies: first results comparing steady-state and dynamic simulations*. Proceedings of the 2nd PALENC and 28th AIVC Conference, Vol.1, Crete Island, Greece (2007), pp.59-64.

[ASHRAE, 1993] . *Ashrae Handbook 1993: Fundamentals*. American Society of Heating, Refrigerating and Air Conditioning Engineers, Inc., Atlanta, United States, (1993).

[Badescu, 1998] Badescu V.: *Accurate upper bounds for the conversion efficiency of black-body radiation energy into work*. Physics Letters A 244 (1998), pp.31-34.

[Baehr, 2005] Baehr H.D.: *Thermodynamik. Grundlagen und technische Anwendungen*. 5 Ed. Springer Verlag, Berlin, Germany (2005).

[Bejan et al., 1996] Bejan A., Tsatsaronis G., Moran M.: *Thermal Design and Optimization*. John Wiley & Sons, New York, USA (1998).

[Bejan and Mamut, 1999] Bejan A., Mamut E. (Eds.): *Thermodynamic Optimization of Complex Energy Systems*. Kluwer Academic Publishers, The Netherlands (1999), pp.73-92.

[Bier, 2002] Bier W.: *Untersuchung von Gebäuden mit sehr niedrigem Heizwärmebedarf - validierte Modellierung zur thermischen Simulation*. Diploma thesis, University of Siegen (2002).

[BMU, 2009] *Begründung des EEG*. Bundesministerium für Umwelt, Naturschutz und Reaktorsicherheit BMU. Berlin, (2009).

[Boer et al., 2007] Boer D. et al.: *Exergy analysis of a solar absorption cooling system*. Proccedings of the 2nd OTTI International Conference in Solar Air-Conditioning, Tarragona, Spain.

[BUDERUS, 2007] *Katalog Teil 3 - Heizkörper und Zubehör - 2007/1*. BUDERUS, (2007).

[Candau, 2003] Candau Y.: *On the exergy of radiation*. Solar energy 75 (2003), pp.241-247.

[Chow et al., 2009] Chow T.T. et al.: *Energy and exergy analysis of photovoltaic-thermal collector with and without glass cover*. Applied Energy 86 (3) (2009), pp.310-316.

[Cornelissen, 1997] Cornelissen R.L.: *Thermodynamics and sustainable development - the use of exergy analysis and the reduction of irreversibility*. Doctoral Thesis, Technical University Twente, Enschede, the Netherlands, 1997..

[COSTeXergy, 2010] *C24:Analysis and Design of Innovative Systems for Low-EXergy in the Built Environment*. www.costexergy.eu.

[DIN V 4701-10, 2001] *DIN 4701-10: Energy Efficiency of Heating and Ventilation Systems in Buildings - Part 10: Heating, Domestic hot Water, Ventilation*. German National Standard. Berlin: Deutsches Institut für Normung (2001).

[DIN V 18599, 2007] *DIN 18599: Energy efficiency of buildings - Calculation of the net, final and primary energy demand for heating, cooling, ventilation, domestic hot water and lighting*. Deutsches Institut für Normung, DIN (2007).

[DIN V 18599-1, 2007] *DIN 18599 Part 1 - General balancing procedures, terms and definitions, zoning and evaluation of energy sources*. Deutsches Institut für Normung, DIN (2007).

[DIN V 18599-2, 2007] *DIN 18599 Part 2 - Net energy demand for heating and cooling of building zones*. Deutsches Institut für Normung, DIN (2007).

[DIN V 18599-10, 2007] *DIN 18599 Part 10 - Boundary conditions of use, climatic data*. Deutsches Institut für Normung, DIN (2007).

[DIN 12796-2, 2006] *DIN 12796: Thermal solar systems and components Part 2 - Test methods*. Deutsches Institut für Normung, DIN (2006).

[DIN EN 12831-1, 2008] *DIN EN 12831, Beiblatt 1: Heating systems in buildings - Method for calculation of the design heat load - National Annex NA*. Deutsches Institut für Normung, DIN (2008).

[DIN EN 1264-2, 1997] *DIN 1264-2: Floor heating, Systems and components - Part 2: Determination of the thermal output*. Deutsches Institut für Normung, DIN (1997).

[DIN EN 15251, 2007] *DIN EN 15251: Indoor environmental input parameters for design and assessment of energy performance of buildings addressing indoor air quality, thermal environment, lighting and acoustics*. Deutsches Institut für Normung, DIN (2007).

[DIN 4708, 1994] *DIN 4708: Zentrale Wassererwärmungsanlagen, Regeln zur Ermittlung des Wärmebedarfs zur Erwärmung von Trinkwasser in Wohngebäuden*. Deutsches Institut für Normung, DIN (1994).

[Dincer and Rosen, 2004] Dincer I., Rosen M.: *Effect of varying dead-state properties on energy and exergy analyses of thermal systems*. International Journal of Thermal Sciences 43 (2004), pp. 121-133.

[Dincer and Rosen, 2007] Dincer I., Rosen M.: *Exergy-Energy, Environment and Sustainable Development*. First Ed., Elsevier Publication, Oxford, UK, (2007).

[Dötsch and Bargel, 2009] Dötsch C., Bargel S. (2009). *Theoretische Betrachtung zur idealen Temperatur in Fernwärmenetzen auf Grundlage einer exergetischen Bewertung*. LowEx Symposium, Kassel, Germany, 2009.

[Drück and Hahne] Drück H., Hahne E.: *Test and comparison of hot water stores for solar combisystems*. Proceedings of Eurosun, Portoroz, Slovenia (1998), pp. (3.3)1-7.

[Duffie and Beckmann, 2006] Duffie J.A., Beckmann W.A.: *Solar engineering of thermal processes* Wiley Publications, 3rd Edition (2006).

[DVGW, 2004] *DVWG Arbeitsblat W 551: Trinkwassererwärmungs- und Trinkwasserleitungsanlagen; Technische Maßnahmen zur Verminderung des Legionellenwachstums; Planung, Errichtung, Betrieb und Sanierung von Trinkwasser-Installationen*. Deutscher Verband des Gas- und Wasserfaches e.V. (2004).

[EnEV, 2007] *EnEv: Verordnung zur Änderung der Energieeinsparverordnung*. Bundesanzeiger Verlag, April (2007).

[EnEV, 2009] *EnEv: Verordnung zur Änderung der Energieeinsparverordnung*. Bundesanzeiger Verlag, April (2009).

[EN ISO 13790, 2008] *Thermal performance of buildings. Calculation of energy use for space heating*. European Comitee for Standarization, (2008).

[EN ISO 7730, 2005] *Ergonomics of the thermal environment - Analytical determination and interpretation of thermal comfort using calculation of the PMV and PPD indices and local thermal comfort criteria*. European Comitee for Standarization, (2005).

[Esen et al., 2007] Esen H et al.: *EEnergy and exergy analysis of a ground-coupled heat pump system with two horizontal ground heat exchangers*. Building and Environment 42 (2007), pp.3606-3615.

[Erhorn et al., 2008] Erhorn H. et al.: *Energetische Potenziale im Gebäudebestand*. AFVEE Themen (2008), pp.54-58.

[Flamco, 2010] *Flamco Pufferspeicher PS/R: Flamco Wemefa Bruttopreisliste*. Flamco Wemefa, 01 (2010).

[Fink and Riva, 2004] Fink C., Riva R.: *Solar-supported heating networks in multi-storey residential buildings: A planning handbook with a holistic approach*. Arbeitsgemeinschaft Erneuerbare Energie - AEE (2004).

[Fink et al., 2007] Fink C. et al.: *MOSOL-NET: Entwicklung von modular erweitbaren tehcnischen Lösungen, die eine Wärmeversorgung von Neubaugebieten über solar unterstürzte Nahwärmenetze ermöglichen*. Arbeitsgemeinschaft Erneuerbare Energie - AEE, Gleisdorf (2007).

[Fitzner, 2008] Fitzner K.: *Raumklimatechnik, Band 2: Raumluft und Raumkühltechnik*. 16 Edition. Springer-Verlag, Berlin-Heidelberg (2008).

[Furbo et al., 2005] Furbo S. et al.: *Performance improvement by discharge from different levels in solar storage tanks* Solar Energy 79 (2005), pp. 431-439.

[Gassel, 1997] Gassel A.: *Beiträge zur Berechnung solarthermischer und exergieeffizienter Energiesysteme*. Doctoral thesis, TU Dresden, Germany (2008).

[GEA, 2009] *GEA BRAZED Select 2009.3*. GEA WTT GmbH, www.gea-phe.com (2009).

[GEA, 2010] *Angebot Nr. 100121-021 REV.0*. GEA WTT GmbH, (2010).

[Hauser, 2008] Hauser G.: *Energieeffizientes Bauen: Umsetzungsstrategien und Perspektiven*. AFVEE Themen (2008), pp.8-19.

[Hauser, 1997] Hauser G. *EnEV 2000 - Ein Konzeptvorschlag*. Internationaler Bauphysikkongreß, Bauphysik der Außenwände, Berlin (1997), pp.11-25.

[Heimrath, 2004] Heimrath R. *Optimierung und Vergleich solarthermischer Anlagen zur Raumwärmeversorgung für Mehrfamilienhäuser*. Doctoral Thesis, TU Graz, Austria (2004).

[Heimrath and Haller, 2007] Heimrath R., Haller M.: *Advanced storage concepts for solar and low energy buildings*. Report of IEA Solar Heating and Cooling programme - Task 32. Report A2 of Subtask A, May (2007).

[Henning, 2009] Henning H.M.: *Exergy analysis of solar cooling*. LowEx Symposium, Kassel, Germany, 28-29 October (2009).

[Hepbasli and Akdemir, 2004] Hepbasli A., Akdemir O.: *Energy and exergy analysis of a ground source heat pump system*. Energy Conversion and Management 45 (2004), pp.737-753

[Hepbasli and Tolga Balta, 2007] Hepbasli A., Tolga Balta M.: *A study on modelling and performance assessment of a heat pump system for utilizing low temperature geothermal resources in buildings*. Building and Environment 42 (2007), pp.3747-3756.

[Holst, 1996] Holst S.:. *TRNSYS - Models for Radiator Heating Systems*, Rev 23.4.96. Bayrisches Zentrum für angewandte Energieforschung e.V., Abteilung 4:Thermische Nutzung von Sonnenenergie (1996).

[Izquierdo Millán et al., 1996] Izquierdo Millán M., Hernández F., Martín E.: *Available solar exergy in absorption cooling process*. Solar Energy 56 (6), (1996), pp.505-511

[IWU, 2003] IWU (Ed.).: *Dokumentation: Deutsche Gebäudetypologie - Systematik und Datensätze*. Institut für Wohnen und Umwelt (IWU), (2003).

[IWU, 2007] IWU (Ed.).: *Basisdaten für Hochrechnungen mit der Deutschen Gebäudetypologie des IWU*. Institut für Wohnen und Umwelt (IWU), (2007).

[Jansen, 2009] Jansen S.: *Contribution to development of the method for dynamic exergy analysis of building systems as part of chapter 2 of the Final Annex 49 Guidebook*. Internal working report, (2009).

[Jansen, 2010] Jansen S., Woudstra N.: *Understanding the exergy of cold - theory and practical examples*. International Journal of Exergy IJEX, (2010).

[Jordan and Vajen, 2001] Jordan U., Vajen K. *Influence of the DHW Load on the Fractional Energy Savings: A Case Study of a Solar Combisystem with TRNSYS-Simulations*. Solar Energy, 69 (6), (2001), pp. 197-208.

[Jordan and Vajen, 2005] Jordan U., Vajen K. *DHWcalc: program to generate domestic hot water profiles iwth statistical means for user defined conditions*. Proceedings of the 8th ISES Solar World Congress, Orlando, United States (2005).

[Kaiser, 2009] Kaiser J.: *Temperature profile for district heating return pipe based on data from Städtische Werke in Kassel*. Internal working document, (2009).

[Khaliq and Kumar, 2007] Khaliq A., Kumar R.: *Exergy analysis of solar powered absorption refrigeration system using LiBr-H20 and NH3-H20 as working fluids*. Int. Journal of Exergy 4 (1), (2007) pp.1-18.

[Knudsen, 2002] Knudsen S. *Consumers influence on the thermal performance of small SDHW systems-Theoretical investigations*. Solar Energy, 73 (1), (2002), pp.33-42.

[Kühler, 2008] Kühler D.: *Beitrag der Kraft-Wärme-Kopplung zur rationellen Exergieversorgung von Gebäuden und Siedlungen - Vergleich unterschiedlicher Bewertungsmethoden*. Masterthesis, University of Kassel (2008).

[Manderfeld et al., 2008] Manderfeld et al.: *Leitungsgebundene Wärmeversorgung im ländlichen Raum: Handbuch zur Entscheidungsunterstützung - Fernwärme in der Fläche*. Wiss. Bericht, gefördert durch PtJ (2008).

[Marletta, 2008] Marletta L.: *Exergy analysis of solar cooling - a worked example*. Report for the IEA SHC Task 38, January 2008.

[Meggers, 2008] Meggers F.: *Exergy optimized wastewater heat recovery: minimizing losses and maximizing performance*. Proceedings of the 8^{th} International Conference for Enhanced Building Operations, Berlin (Germany), 20-22 October (2008).

[Meggers and Leibundgut, 2009] Meggers F., Leibundgut H.: *The Reference Environment: Redefining Exergy and Anergy for Buildings*. Proceedings of the ELCAS 2009 Symposium, Nysiros (Greece), 4-6 June (2009).

[Meteonorm, 2006] *Meteonorm, V 5*. Meteotest, Schweiz, 2008.

[Moran and Shapiro, 1998] Moran M.J., Shapiro H.N.: *Fundamentals of Engineering Thermodynamics*. 3^{rd} Edition, John Wiley & Sons, New York, USA (1998).

[Müller, 2009] Müller D.: *Research activities for PCM in building services equipment - an overview*. LowEx Symposium, Kassel, Germany, 28-29 October (2009).

[Nishikawa and Shukuya, 1999] Nishikawa R., Shukuya M.: *Numerical analysis on the production of cool exergy by making use of heat capacity of building envelopes*. Proceedings of the 6th International IBPSA Conference, Kyoto, Japan (1999), pp. 129-135.

[Olsen, 2008] Olsen P.K. et al.: *A new low temperature district heating system for low energy buildings*. The 11th International Symposium on district heating and cooling, Reykjavik (Iceland), 31 August - 2 September (2008).

[Olesen, 2002] Olesen B.: *Radiant floor heating in theory and practice*. ASHRAE Journal, July (2002).

[Oppermann, 2003] Oppermann J.: *Untersuchung der Sensitivität von Heizungs-Lüftungsanlagen in Niedrigenergiehäusern*. Doctoral thesis, University of Kassel (2003).

[Ozgener and Hepbasli, 2007] Ozgener O., Hepbasli A.: *Modeling and performance evaluation of a ground source (geothermal) heat pump system*. Energy and Building 39 (2007), pp.66-75.

[Perers and Bales, 2002] Perers B., Bales C.: *The reference building, the reference heating system*. Report of IEA Solar Heating and Cooling programme - Task 26-Solar combisystems, December (2002).

[Petela, 2003] Petela R.: *Exergy of undiluted thermal radiation*. Solar Energy 74 (2003), pp.469-488.

[Ptasinski et al., 2005] Ptasinski K., Prins M., Pierik A.: *EExergetic evaluation of biomass gasification*. Energy 30 (2005), pp.982-1002.

[Recknagel et al. 2007] Recknagel H., Sprenger E., Schramek E.R. *Taschenbuch für Heizung und Klimatechnik*. Oldenbourg Industrieverlag 07/08 (2007).

[Rosen, 2001] Rosen M.:*IThe exergy of stratified thermal energy storages*. Solar Energy 71 (3) (2001), pp.173-185.

[Rosen and Tang, 2008] Rosen M., Tang: *Improving steam power plant efficiency through exergy analysis: effects of altering excess combustion air and stack-gas temperature*. International Journal of Exergy 5 (2008) (1), pp.35-51.

[Sakulpipatsin, 2008] Sakulpipatsin P.: *Exergy efficient building design*. Doctoral Thesis, University of Delft, the Netherlands (2008).

[Seifert and Hoh, 2009] Seifert J., Hoh A.: *Dynamic exergetic evaluation methods*. LowEx Symposium, Kassel, Germany, 28-29 October (2009).

[Sencan et al., 2005] Sencan A., Yakut A., Kalogirou S.A.: *Exergy analysis of lithium bromide/water absorption systems*. Renewable Energy (30) (2005) pp.645-657.

[Schmidt, 2004] Schmidt D.: *Design of Low Exergy Buildings - Method and Pre-Design Tool*. The International Journal of Low Energy and Sustainable Buildings 3 (2004), pp.1-47.

[Schmidt and Torío, 2009] Schmidt D., Torío H. (Eds.): *Framework for exergy analysis on building and community level*. Mid-term report from IEA ECBCS Annex 49. www.annex49.com.

[Schmidt and Torío, 2010] Schmidt D., Torío H. (Eds.): *Final Guidebook of the IEA ECBCS Annex 49: Low Exergy Systems for High-Performance Buildings and Communities (full version)*. www.annex49.com.

[Schmidt et al., 2007] Schmidt D., Torío H., Sager C.: *Exergiebewertung für Gebäude*. Deutsche Klima-Kälte Tagung, Hannover, Germany, 2007.

[Schurig, 2010] Schurig M.: *Dynamische exergetische Bewertung eines Flächenkühlsystems*. Masterarbeit, University of Kassel, Germany (2010).

[Shariah and Löf, 1997] Shariah A. M., Löf G.: *Effects of Auxiliary Heater on Annual Performance of Thermosyphon Solar Water Heater Simulated under Variable Operating Conditions*. Solar Energy 60 (2), (1997) pp.119-126.

[Shukuya, 1996] M.: *Exergy-entropy process of passive solar heating and global environmental systems*. Solar Energy 58 (1-3) (1996), pp.25-32.

[Shukuya, 2009] Shukuya M.: *Exergy concept and its application to the built environment*. Building and Environment 44 (7) (2009), pp.1545-1550.

[Shukuya and Hammache, 2002] Shukuya M., Hammache A.: *Introduction to the concept of exergy - for a better understanding of low-temperature heating and high-temperature cooling systems*. VTT research notes 2158, Espoo, Finland (2002).

[Shukuya and Komuro, 1996] Shukuya M, Komuro D. *Exergy-entropy process of passive solar heating and global environmental systems*. Solar Energy 58 (1-3), (1996), pp.25-32.

[Sorensen, 2004] Sorensen B. *Renewable Energy: its physics, engineering, environmental impacts, economics and planning*. Elsevier Academic Press, London, UK (2004).

[StWerke, 2009] *Plan und Annahmen zur Versorgungskonzep*. Internal working document, Städtische Werke Kassel, Germany (2009).

[Szargut, 2005] Szargut J.: *The Exergy Method-Technical and Ecological Applications*. Renewable Wiley Interscience, 2005.

[Szargut and Styrylska, 1964] Szargut J., Styrylska T.: *Angenäherte Bestimmung der Exergie von Brennstoffen*. Zeitschrift für Energietechnik und Energiewirtschaft (BWK) 16 (12), (1964), pp.589-636.

[Torío and Schurig, 2009] Torío H., Schurig M.: *Stationäres exergetisches Bewertungsverfahren*. LowEx Symposium, Kassel, Germany, 2009.

[Torío and Schmidt, 2008] Torío H., Schmidt D.: *Exergetic assessment and contribution of solar energy systems to the energy performance of buildings*. Proceedings of the Nordic Symposium of Building Physics 2008, Copenhaguen, Denmark (2008) Vol. 2, pp.637-344.

[Torío et al., 2009] Torío H., Schmidt D., Angelotti A.: *Exergy analysis of renewable energy based climatisation systems for buildings*. Energy and Buildings 41 (2009), pp.8-19.

[Torío and Schmidt, 2010] Torío H., Schmidt D.: *Framework for analysis of solar energy systems in the built environment from an exergy perspective*. Renewable Energy 35 (2010), pp.2689-2697.

[TRNSYS, 2007] *A TRnsient SYstem Simulation program, version 16*. Solar Energy Laboratory, University of Winsconsin-Madison (2007).

[TRNSYS, 2007a] *A TRnsient SYstem Simulation program, version 16 - Volume 6: Multizone Building modeling with Type56 and TRNBuild*. Solar Energy Laboratory, University of Winsconsin-Madison (2007).

[Tsatsaronis, 1993] Tsatsaronis G.:*Thermoeconomic Analysis and Optimization of Energy Systems* Progress in Energy and Combustion Science 19 (1993), pp.227-257.

[UMSICHT, 2010] UMSICHT.*Das NahwärmeForum - das Informationsportal: Leitfaden*. www.nahwaerme-forum.de.

[Uponor, 2010] *Flexible, vorgedämmte Rohrsysteme, PE-Xa Hausansschlussleitungen und ProFuse Schuztmantelrohre fpr die Wärme und Gas-Wasserversorgung*. Uponor Versorgung, Preisliste 01/2010 D.

[Usemann, 2005] Usemann K.: *Energiesparende Gebäude und Anlagentechnik: Grundlagen, Auswirkungen, Probleme und Schwachstellen, Wege und Lösungen bei der Anwendung der EnEV*. Springer Verlag, Berlin - Heidelberg, Germany (2005).

[VDI 2067, 2000] *VDI 2067: Wirtschaftlichkeit gebäudetechnischer Anlagen, Grundlagen und Kostenberechnung*. Verein Deutsche Ingenieure (VDI), Düsseldorf, Germany (1999).

[Wagner, 2007] . *RATIOfresch 800 - Frischwasserstation: Technische Information / Montageanleitung*. Wagner& Co. GmbH (2010).

[Wall and Gong, 2001] Wall G., Gong M.: *On exergy and sustainable development - Part 1: Conditions and concepts*. Exergy, an International Journal, 1 (3) (2001), pp.128-145.

[Weiss, 2003] Weiss W. (Ed.):*Solar Heating Systems for Houses, A Design Handbook For Solar Combisystems*, Solar Heating and Cooling Executive Committee of the IEA, James & James Ltd. 8-12 Camden High Street, London, UK, (2003).

[Wepfer et al., 1979] Wepfer W.J., Gaggioli R.A., Obert E.F.: *Proper evaluation of available energy for HVAC*. ASHRAE Transactions (1979) 85 (1) pp.214-230.

[Wepfer and Gaggioli, 1980] Wepfer W.J., Gaggioli R.A.: *Reference Datums for Available Energy*. In: American Chemical Society, Symposium on Theoretical and Applied Thermodynamics (1980), pp. 77-92.

[Wirths, 2008] Wirths A. *Einfluss der Netzrücklauftemperatur auf die Effizienz von Fernwärmesystemen*. 13 Dresdner Fernwärmekolloquium, September (2008).

[Wirths, 2008a] Wirths A. *Wärmeversorgung aus dem Netzrücklauf - Stand der Technik und Perspektive für die Netzverdichtung*. 1 Fernwärmekolloquium Gießen, February (2008).

[Wright et al., 2002] Wright S. E. et al.: *The exergy flux of radiative heat transfer for the special case of blackbody radiation*. Exergy, an International Journal 2 (2002), pp. 24-33.

[Wilo, 2010] . *Wilo-Select Online*. www.wilo-select.com.

[Xiaowu and Ben, 2005] Xiaowu W., Ben H.: *Exergy analysis of domestic-scale solar water heaters*. Renewable and Sustainable Energy Reviews 9 (2005), pp.638-645.

[Zaß et al., 2008] Zaß K. et al.:*Vergleich verschiedener Maßnahmen zur Ertragssteigerung von solarthermischen Kombianlagen* Tagungsbericht 18th Symposium Thermische Solarenergie, Staffelstein, 23-25 April (2008).

[ZUB, 2009] ZUB: *Geometrie des Einfamilienhauses*. Internal working report, Zentrum für Umweltbewusstes Bauen (ZUB), (2009).

Nomenclature

A	[m^2]	Area
c	[kJ/(kgK)]	Specific heat capacity
En	[J]	Energy
Ex	[J]	Exergy
$\dot{En}$	[W]	Energy rate, power
$\dot{Ex}$	[W]	Exergy rate, power
F_Q	[-]	Quality factor
H	[m]	Height
$H_T{}'$	[$W/(m^2K)$]	Specific heat transmission coefficient
m	[kg]	Mass
$\dot{m}$	[kg/h]	Mass flow rate
P	[J]	Electric energy demand
p	[Pa]	Pressure
Q	[J]	Heat
S	[J/K]	Entropy
T	[K]	Absolute temperature
t	[s]	Time
V	[l]	Volume
v	[m/s]	Velocity
< >	-	Average value

Greek characters

Δ	[-]	Increment, variation
ε	[-]	Exergy expenditure figure
ϵ	[-]	Emissivity
η	[-]	Energy efficiency
Ψ	[-]	Exergy efficiency
θ	[°C]	Temperature
σ	[$W/(m^2K^4)$]	Stephan-Boltzmann constant

Subscripts

0	Reference state
a	Air
active	Active
amplit	Amplitude
ave	Average
aux	Auxiliary
b	Building
boil	Boiler
ce	Emission
ch	Charging process
CHP	Combined heat and power
coll	Collector
cons	Consumed
cont	Content
cw	Cold water
d	Distribution
dem	Demand
des	Desired
DH	District heating
DHW	Domestic hot water
disch	Discharge process
dyn	Dynamic
el	Electric, electricity
eq	Equivalent
env	Envelope
ext	Extended
FH	Floor heating
fin	Final
fuel	Fuel
g	Generation
h	Heating; heater
HHV	Higher heating value
HN	Heat (distribution) network
HP	Heating period
HPl	Heat plant
Hx	Heat exchanger
i	Component
in	Inlet

irrev	Irreversibilities
LMTD	Logarithmic mean temperature difference
ls	Losses
max	Maximum
mech	Mechanical
op	Operative
out	Outlet
ove	Overall
overh	Overheating
p	Constant pressure
PE	Primary energy
prim	Primary side
pump	Pump
q-stead	Quasi steady state
r	Room air
rad	Radiation
ret	Return
s	Storage
sav	Savings
seas	Seasonal
sens	Sensor
sec	Secondary side
SH	Space heating
simple	Simple
sol	Solar
stead	Steady state
sto	Stored
sup	Supply
surf	Surface
surr	Surroundings
th	Thermal
w	Water
wall	Wall

Acronyms

CHP	Combined heat and power
DH	District heating
DHW	Domestic hot water
MFH	Multi-family house
LNG	Liquefied natural gas
SFH	Single-family house
SH	Space heating
SHC	Space heating and cooling
w.	With
wo.	Without

Appendix A

Assumptions for modeling

A.1 Geometry of buildings analyzed

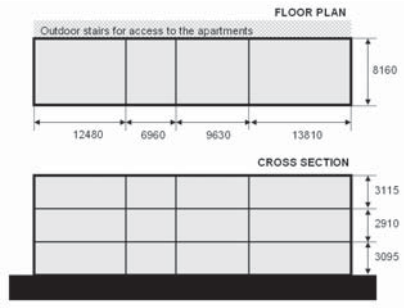

Figure A.1: Geometry of the MFH considered. Values are given in milimeters.

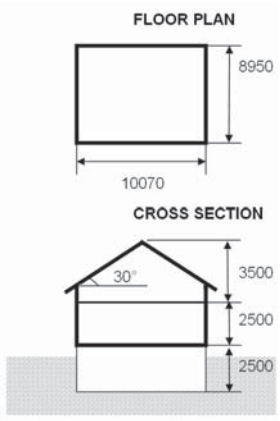

Figure A.2: Geometry of the SFH considered. Values are given in millimeters. The thick black lines represent the envelope of the building and enclose the thermal zones simulated.

A.2 General assumptions for DHW Draw off profiles

Table A.1: Assumptions for the generation of the yearly detailed draw-off profiles on a 3-minute timescale.

	Category A short draw-off	Category B medium draw-off	Category C Bath	Category D Shower
Mean mass flow, [l/h]	20	120	2400	800
Mean volume per draw-off, [l]	1	6	120	40
Mean number of draw-offs per day, [-]	28	12	0.166	2
Proportion in daily consumption, [%]	14	36	10	40

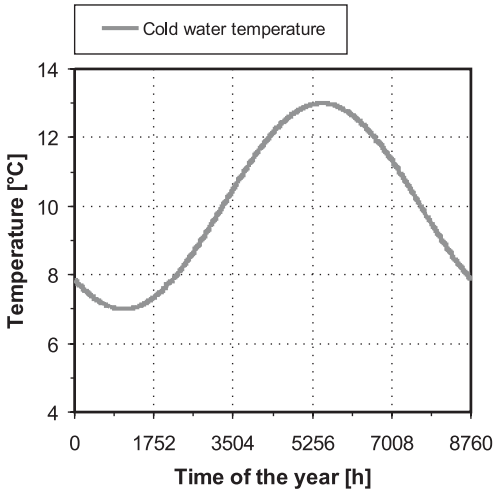

Figure A.3: Seasonal yearly variation of the cold water temperature for the net assumed here, in accordance with the Standard DIN EN 12976-2 (2000).

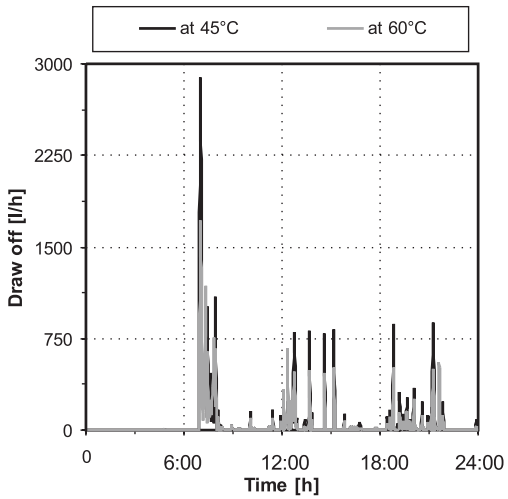

Figure A.4: Draw off profiles in l/h for one day assuming supply temperatures of 45°C and 60°C respectivley.

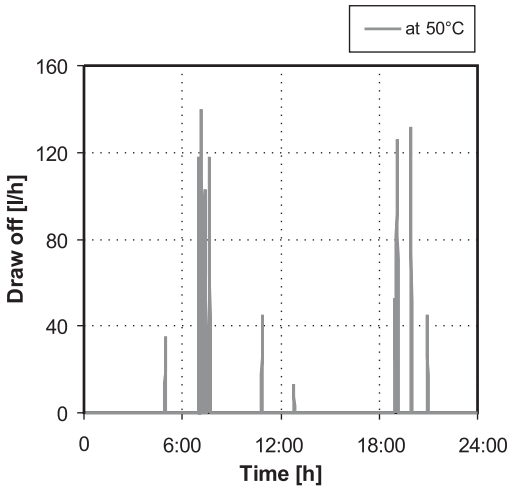

Figure A.5: Draw off profiles in l/h for one day and for each single family house assuming a supply temperature of 50°C.

A.3 Detailed layout, lengths and diameter of pipes for SH supply

A.3.1 Multifamily house

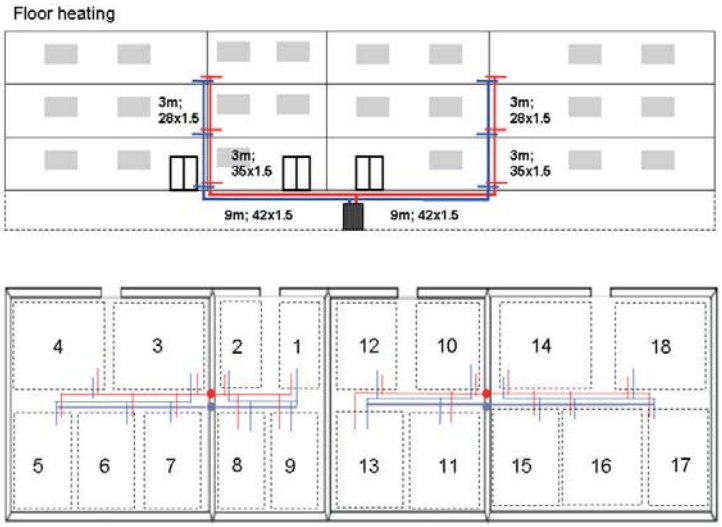

Figure A.6: Layout of the supply (black) and return (light grey) pipes for space heating supply with floor heating. Pipe lengths given refer to each of the supply and return pipes separately, and not to the total of both. Numerated squares represent the different floor heating circuits in one floor of the MFH. Dotted light grey lines in the floor section represent the inverted return pipe for each half of the floor area. Light grey and black dots represent the junction with the common vertical supply and return pipes.

Table A.2: Pipe diameter and length for each of the floor heating systems in one floor of the multi-family dwelling represented Figure .

	Diameter	Length [m]		Diameter	Length [m]
to 1	0.5	15x1	from 1	0.5	15x1
to 2	0.5	22x1	from 2	5	22x1
to 3	0.5	28x1.2	from 3	0.5	15x1
to 4	3	18x1	from 4	2	22x1
to 5	2	15x1	from 5	10	28x1.2
to 6	3	22x1	from 6	3	22x1
to 7	0.5	22x1	from 7	3	18x1
to 8	0.5	22x1	from 8	3.5	18x1
to 9	3.5	18x1	from 9	0.5	22x1
to 10	0.5	22x1	from 10	0.5	15x1
to 11	0.5	22x1	from 11	6	18x1
to 12	6	18x1	from 12	0.5	15x1
to 13	0.5	15x1	from 13	7.5	22x1
to 14	0.5	28x1.2	from 14	0.5	15x1
to 15	0.5	22x1	from 15	0.5	18x1
to 16	0.5	22x1	from 16	7	22x1
to 17	7	18x1	from 17	0.5	22x1
to 18	0.5	15x1	from 1	8.5	28x1.2

A.3.2 Single family house

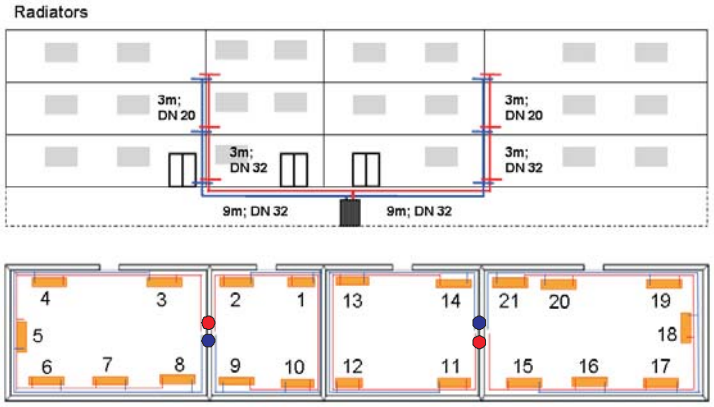

Figure A.7: Layout of the supply (black) and return (light grey) pipes for space heating supply with radiators. Pipe lengths given refer to each of the supply and return pipes separately, and not to the total of both. Radiators are represented as lined boxes. Black and light grey dots represent the junction with the common vertical supply and return pipes.

Table A.3: Pipe diameter and length for each of the radiators in one floor of the multi-family dwelling represented Figure .

	Diameter	Length [m]		Diameter	Length [m]
to 1	4	DN 15	from 1	10	DN 10
to 2	5	DN 15	from 2	5	DN 10
to 3	5	DN 20	from 3	6	DN 10
to 4	6	DN 15	from 4	2	DN 10
to 5	2	DN 15	from 5	7	DN 15
to 6	5	DN 15	from 6	5	DN 15
to 7	5	DN 10	from 7	5	DN 15
to 8	8	DN 10	from 8	6	DN 20
to 9	5	DN 10	from 9	6	DN 15
to 10	4	DN 10	from 10	5	DN 15
to 11	5	DN 15	from 11	7.5	DN 10
to 12	7.5	DN 15	from 12	8	DN 10
to 13	8	DN 10	from 13	7.5	DN 15
to 14	7.5	DN 10	from 14	5	DN 15
to 15	6	DN 20	from 15	5	DN 10
to 16	5	DN 15	from 16	5	DN 10
to 17	5	DN 15	from 17	5	DN 15
to 18	5	DN 15	from 18	6	DN 15
to 19	6	DN 10	from 19	10	DN 15
to 20	5	DN 10	from 20	5.5	DN 20
to 21	5	DN 10	from 21	5	DN 20

A.4 Detailed layout, lengths and diameter of pipes for district heat supply

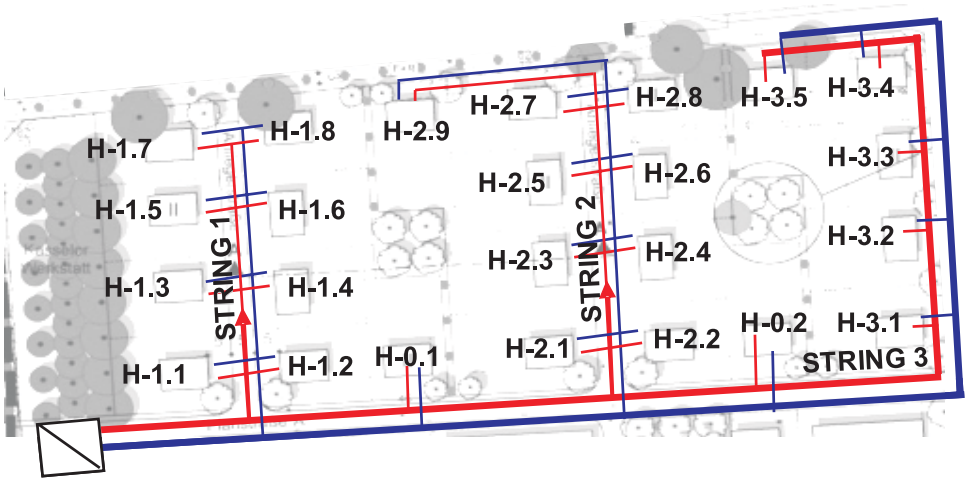

Figure A.8: Layout of the supply and return pipes of the local heat network for district heat supply. Thick lines represent the most unfavorable circuit (to string 3) used for sizing the pumps in the circuit. The crossed square at the left lower corner of the diagram represents the heat exchanger separating the local heat network from the district heating pipe.

In Table A.4 the nominal diameter (DN) of the pipes in the local heat networks for the two maximum fluid velocities in the pipes chosen as sizing criteria and for different hydraulic configurations investigated in this thesis are shown. Different hydraulic configurations correspond to a common supply of SH and DHW demands with one single heat exchanger, labeled as *SH+DHW* in Table A.4. Pipe diameters for the configurations with a separate network and heat exchanger for the supply of SH and DHW demands are also shown (labeled as *SH* and *DHW* respectively). In the column labelled *SH cascaded* pipe diameters are shown for the space heating supply network assuming a cascaded supply of SH demands after supplying DHW demands. The details of the different hydraulic configurations are explained in detail in chapter 5.

Table A.4: Pipe diameter and length regarded for the local heat distribution network represented in Figure A.8. *SH+DHW* labels pipes for district heat supply of DHW and SH demands together, i.e. with only one heat exchanger and heat network for both uses; networks for a separate supply of DHW and SH are labeled accordingly, i.e. *SH* and *DHW* respectively. *SH cascaded* shows the pipes in the network for cascaded supply of the SH demands.

		v_{max} = 2.5 m/s	v_{max} = 1 m/s			
Pipes to and from	Length [m]	SH+DHW	SH+DHW	DHW	SH	SH cascaded
string 1	10	DN 65	DN 100	DN 50	DN 50	DN 100
H-0.1	12	DN 50	DN 80	DN 40	DN 40	DN 80
H-1.1 and H-1.2	7	DN 40	DN 65	DN 32	DN 32	DN 65
H-1.3 and H-1.4	7	DN 32	DN 50	DN 32	DN 32	DN 50
H-1.5 and H-1.6	7	DN 32	DN 50	DN 25	DN 25	DN 50
H-1.7 and H-1.8	7	DN 25	DN 32	DN 20	DN 20	DN 32
H-2.1 and H-2.2	7	DN 40	DN 50	DN 32	DN 32	DN 50
H-2.3 and H-2.4	7	DN 40	DN 50	DN 32	DN 32	DN 50
H-2.5 and H-2.6	7	DN 32	DN 50	DN 32	DN 32	DN 50
H-2.7 and H-2.8	7	DN 32	DN 40	DN 25	DN 25	DN 40
H-2.9	5	DN 20	DN 25	DN 20	DN 20	DN 25
string 2	15	DN 50	DN 80	DN 40	DN 40	DN 80
H-0.2	11	DN 32	DN 50	DN 32	DN 32	DN 65
H-3.1	11	DN 32	DN 50	DN 32	DN 32	DN 50
H-3.2	7	DN 32	DN 50	DN 25	DN 25	DN 50
H-3.3	7	DN 32	DN 40	DN 25	DN 25	DN 40
H-3.4	7	DN 25	DN 32	DN 20	DN 20	DN 32
H-3.5	14	DN 20	DN 25	DN 20	DN 20	DN 25

A.5 Parameters for sizing space heating systems

Table A.5: Main parameters for the design and sizing of radiator heating system in the multi-family dwelling with the two building envelopes studied, MFH-07 and MFH-KfW-EffH.40. The chosen radiator type in the case of MFH-07 corresponds to the flat radiator Logatrend-VK Type 22 with 600 mm height. For the building with increased insulation level (MFH-KfW-EffH.40) the radiator Logatrend-VK Type 22 with a height of 400 mm is chosen.

	Unit	MFH-07	MFH-MFH-KfW-EffH.40
Q_{design}	kW/store	21.28	11.54
ΔT_{design}	K	10	10
$Q_{design,55/45/20}$	W/radiator	1052	578
Min. Nr. of radiators per store	-	20.2	20.0
Nr. of radiators per store	-	21	21
Area of one radiator	m^2	0.72	0.36
Heating power	W/m	876	643
Mass flow per radiator	kg/(h radiator)	90.40	49.70
Radiator exponent, n_{rads}	-	1.33	1.30

Table A.6: Values for the parameters used for defining the active layers in TRNSYS.

Parameter	Unit	Value
Pipe spacing	[m]	0.2
Pipe outside diameter	[m]	0.02
Pipe wall thickness	[m]	0.002
Pipe wall conductivity	[W/(mK)]	0.35

A.6 Parameters for sizing auxiliary storage volume in the solar thermal systems

Table A.7: Parameters and variables for estimating the auxiliary storage volume required for the building with radiators and conventional building shell (MFH-07). *The names of the variables and subindexes are not in accordance with DIN 4708 (1994) and (Fink and Riva, 2004) but have been translated to English.

Parameter*	Unit	Value	Parameter*	Unit	Value
$Q_{tot,SH}$	[kW]	63.8	ΔT_{SH}	K	20
$Q_{180,SH}$	[kWh/3h]	148.3	ΔT_{DHW}	K	55
$Q_{SH,apart}$	[kW]	5.3	ΔT_{boil}	K	30
Q_{DHW}	[kW]	177.3	Q_{boil}	[kW]	110
$V_{SH,180}$	[litres at 65°C]	8249.4	$V_{SH,red}$	[litres at 65°C]	191.7
V_{SH}	[litres at 65°C]	8057.7	V_{DHW}	[litres at 65°C]	2232.2
V_{aux}	[litres at 65°C]	906.3			

A.7 Overview of solar systems investigated

Table A.8: Overview of the cases analyzed for the solar thermal system shown in Figure 7.19.

Case	Collector Area [m^2]	Storage Volume [m^3]	Emission System [-]	Building Envelope [-]
RADS	100	8.5	Radiators with night setback	MFH-07
FH	100	8.5	Floor heating with night setback	MFH-07
RADS wo. setback	100	8.5	Radiators without night setback	MFH-07
FH wo. setback	100	8.5	Floor heating without night setback	MFH-07
RADS_200(8500)	200	8.5	Radiators with night setback	MFH-07
FH_200(8500)	200	8.5	Floor heating with night setback	MFH-07
RADS_200(16000)	200	16	Radiators with night setback	MFH-07
FH_200(16000)	200	16	Floor heating with night setback	MFH-07
RADS (KfW-EffH.40)	100	8.5	Radiators with night setback	KfW-EffH.40
FH (KfW-EffH.40)	100	8.5	Floor heating with night setback	KfW-EffH.40

Appendix B

Operation of the systems

B.1 Multi-family house

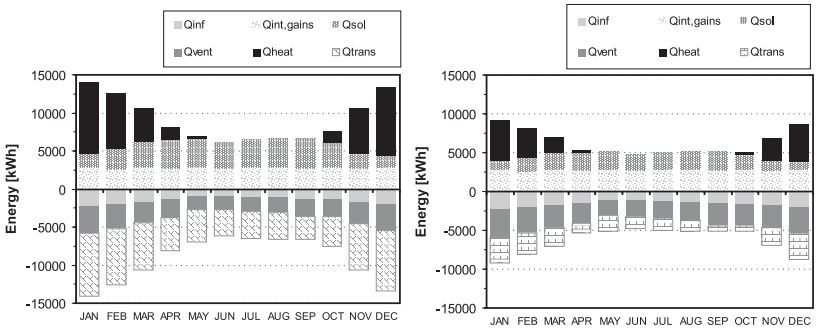

Figure B.1: (a): Energy balances for the building envelope and space heating demand in the multi-family dwelling with standard building envelope (MFH-07). (b): Energy balances for the building envelope and space heating demand in the multi-family dwelling with improved building envelope (MFH-KfW-EffH.40).

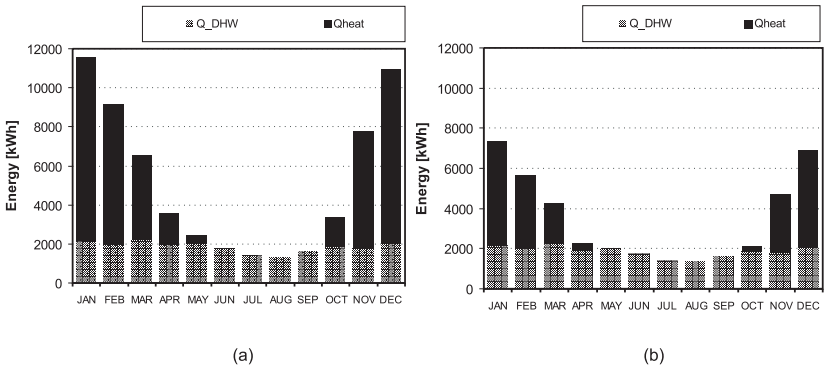

Figure B.2: (a): Monthly space heating and DHW demands in the multi-family dwelling with standard building envelope (MFH). (b): Monthly space heating and DHW demands in the multi-family dwelling with improved building envelope (MFH-KfW-EffH.40).

B.2 Single-family house

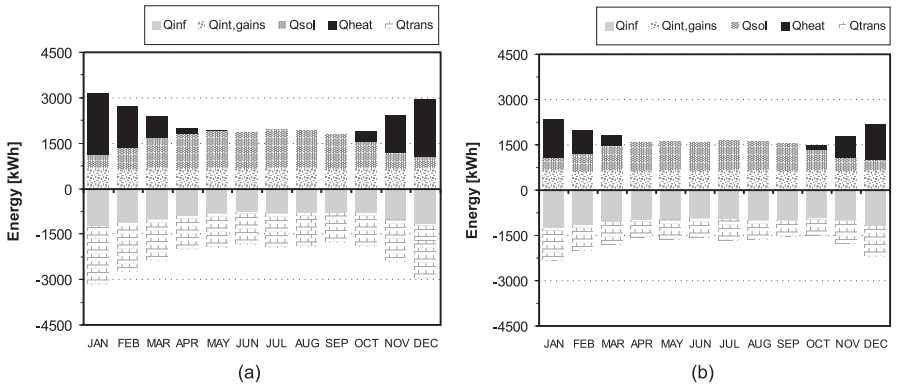

Figure B.3: (a): Energy balances for the building envelope and space heating demand in the single family house with standard building envelope (SFH-09).(b): Energy balances for the building envelope and space heating demand in the single family house with improved building envelope (SFH-KfW-EffH.40).

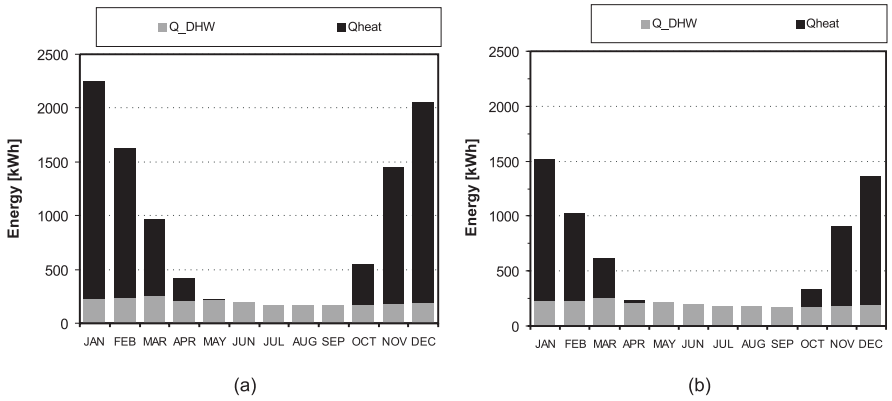

Figure B.4: (a): Monthly values of space heating and DHW energy loads for the single family house with EnEV 2009 building shell (SFH-09); (b):Monthly values of space heating and DHW energy loads for the single family house with KfW-EffH.40 building shell (SFH-KfW-EffH.40).

FORSCHUNGSERGEBNISSE AUS DER BAUPHYSIK BAND 11

Growing concerns on environmental problems related to current energy use have emphasized the importance of „energy-saving measures“ and the necessity for an increased efficiency in all forms of energy utilization. Being responsible for around 40% of the final energy use in Germany, buildings are major contributors to energy related problems and a sector where a more rational and efficient energy use is absolutely necessary.

By showing the thermodynamic efficiency of an energy system, exergy analysis is expected to be a valuable tool for developing and designing more efficient energy supply systems in buildings, similarly as it has contributed to raise the efficiency of power plants. In this thesis, the usability and added value of exergy analysis applied to different building energy systems is investigated. Exergy analysis is, herefore, compared to conventional primary energy assessment and the different results and conclusions obtained from both methods are thoroughly studied and discussed.

ISBN 978-3-8396-0452-6